Investigation of the neurotoxic and neurodegenerative effects of engineered nanomaterials

Inaugural-Dissertation

zur Erlangung des Doktorgrades der Mathematisch-Naturwissenschaftlichen Fakultät der Heinrich-Heine-Universität Düsseldorf

vorgelegt von

Adriana Sofranko
aus Belgrad

Düsseldorf, Oktober 2021

Aus dem IUF – Leibniz-Institut für umweltmedizinische Forschung.

Herausgegeben und gedruckt mit freundlicher Genehmigung der Mathematisch-Naturwissenschaftlichen Fakultät der Heinrich-Heine-Universität Düsseldorf.

Erstbetreuer: Prof. Dr. med. Jean Krutmann, IUF
Mentor: Prof. Dr. rer. nat. Dieter Willbold, HHU
Co-Betreuer: Dr. Roel Schins, IUF

Tag der mündlichen Prüfung in deutscher Sprache:

„Das Problem zu erkennen ist wichtiger, als die Lösung zu erkennen, denn die genaue Darstellung des Problems führt zur Lösung.“

Albert Einstein

Table of contents

Danksagung

Mein besonderer Dank gilt meinem Doktorvater Prof. Dr. Jean Krutmann für die Begutachtung, Betreuung und die Möglichkeit, an diesem interessanten und aktuellen Thema am IUF zu forschen und zu meinem Doktorthema zu machen. Weiterhin danke ich meinem Zweitgutachter Prof. Dr. Dieter Willbold für die Begutachtung dieser Arbeit und darüber hinaus für seine überragende Expertise auf dem Gebiet der Alzheimer-Forschung.

Großer Dank gilt auch Dr. Roel Schins, in dessen Arbeitsgruppe für Partikelforschung ich diese Arbeit angefertigt habe. Ich danke für die offene und herzliche Art, die stets offene Tür für alle Belange, die fachliche Betreuung, die vielen hilfreichen Diskussionen und die Anleitung zur wissenschaftlichen Selbstständigkeit. Ich möchte mich auch bei allen Kolleg*innen und Co-Autor*innen des binationalen Forschungsprojekts und darüber hinaus für die biologische, toxikologische, mathematische und physikalische Expertise, die gute Zusammenarbeit und die wertvollen Beiträge für die Erstellung und Veröffentlichung der Manuskripte.

Des Weiteren möchte ich Dr. Tina Wahle, für die besondere Unterstützung und Einführung in die Alzheimer-Forschung bedanken. Was haben wir viel Zeit in der Tieranlage verbracht… Besonders im Sommer konnte es in voller Montur ziemlich anstrengend sein, aber mit dir was es angenehm und aus einem Leid wurde Leidenschaft und Spaß! Danke auch an Dr. Catrin Albrecht für ihre besondere Unterstützung und Lehre in der Versuchstierhaltung, Tierschutz, im Antragsverfahren, aber auch für die konstruktiven Gespräche darüber hinaus.

Vielen Dank auch an all meine Kollegen der Arbeitsgruppe, Mathias Busch, Dr. Angela Kämpfer, Gerrit Bredeck, Dr. Eleonora Scarcello, Dr. Julia Kolling und Dr. Waluree Thongkam, die mir Wegbegleiter waren und zu Freunden geworden sind. Danken möchte ich auch Isabel Masson, Andrea Boltendahl und Christel Weishaupt für ihre tolle technische und experimentelle Unterstützung. Danke für die nette Atmosphäre und die inspirierenden Gespräche!

Zu guter Letzt, möchte ich meiner Familie und meinen Freunden für ihre Unterstützung, Geduld und Verständnis danken.

Abbreviations and symbols

°C	degree Celsius
µl	microliter
AD	Alzheimer's Disease
Ag	silver
AICD	APP intracellular domain
AP	activator protein
APH	anterior pharynx-defective
APOE	apolipoprotein E
APP	amyloid precursor protein
Aß	amyloid beta
BACE	β-site APP-cleaving enzyme
BBB	blood-brain-barrier
BCA	bicinchoninic acid assay
CAT	catalase
CB	cerebellum
Ce	cerium
CeO_2	cerium oxide
CNS	central nervous system
CTX	cortex
CTF	carboxy-terminal fragments
DNA	deoxyribonucleic acid
ELISA	enzyme-linked-immunosorbent assay
FAD	familiar Alzheimer disease
FCS	fetal calf serum
g	gram
GFAP	glial fibrillary acidic protein
GSH	glutathione
GSSG	glutathione disulfide
GPx	glutathione peroxidase
h	hour
HC	hippocampus
HE	haematoxylin-eosin
IBA	ionized calcium binding adaptor molecule
IGF	insulin-like growth factor

IL	interleukin
i.p.	Intraperitoneal
i.v.	intravenous
l	litre
m	molar
MAPK	mitogen activated protein kinase
mg	milligrams
min	minutes
ml	millilitre
mm	millimetre
mM	millimolar
nm	nanometer
NF-κB	nuclear factor-κB
NM	nanomaterial
NO	nitric oxygen
NP	nanoparticle
PBS	phosphate buffered saline
PEN-2	presenilin enhancer-2
PFA	paraformaldehyde
PI	protease inhibitor
PM	particulate matter
PS	presenilin
Rpm	revolutions per minute
RIVM	National Institute for Public Health and the Environment
ROS	reactive oxygen species
s	seconds
SiO_2	silicon dioxide
SOD	superoxide dismutase
TGF	transforming growth factor
Ti	titanium dioxide
TNF	tumor necrosis factor
V	volt

Summary

Growing evidence indicates that nanomaterials (NMs) might translocate to the brain and may cause neurotoxicity by induction of oxidative stress, neuroinflammation, disturbed neurotransmitter homeostasis and even may initiate and progress neurodegenerative diseases like Alzheimer's disease (AD). Compared to toxicity in the lung and other secondary target organs, relatively little is known about the brain as a target organ for NMs induced neurotoxicity. It is mostly unknown whether NMs might contribute to neurotoxicity or the initiation of AD, especially regarding the type, dosing, and exposure route. Currently, the neurotoxic and neurodegenerative potential of NMs is focusing on inhalation studies due to the identification of pathways of NMs translocation from the respiratory tract to the brain. However, because of its widespread use in numerous consumer products like in the food sector and its potential to cause neurotoxicity through indirect effects, e.g., the gut-brain axis, there is an increasing need in further toxicological research to address the safety of NMs following more realistic oral exposure scenarios.

Thus, in the first experimental study, neurotoxic endpoints were investigated following subacute dietary oral exposure to TiO_2 and Ag NMs, including a 2-week post-exposure period in male and female C57BL/6J mice. We observed NM-specific and sex-related differences in neurotoxicity. Decreased motor coordination and increased tyrosine kinase activity were observed exclusively in Ag NM exposed female mice. In the second experimental study, the potential of dietary fed CeO_2 and SiO_2 NMs to cause neurotoxicity and progress the pathogenesis of AD was tested. While exposure to both NMs did not result in the progression of AD-related pathology, we could surprisingly demonstrate that subchronic dietary exposure to 1% CeO_2 significantly inhibited amyloid plaque formation in the hippocampus and improved motor function in 5xFAD mice. A third experimental subacute inhalation study using CeO2 NMs coated with different amounts of Zr (0 %, 27% and 78%) was performed to evaluate the influence of different redox activities on AD-related pathology. Here, inhalation to CeO_2 did neither aggravate nor inhibit amyloid plaque formation in 5xFAD mice. However, exposure to the highest Zr-doped CeO_2 initiated motor performance changes in the 5xFAD and ApoE-/- mice and neuroinflammation in C57BL/6J mice.

The studies performed in the present thesis provide novel insight into the importance of the chemical composition and redox state of NMs and disease susceptibility in terms of neurotoxicity. They also demonstrate the need to use more realistic exposure scenarios and to include both sexes in future NM neurotoxicity studies.

Zusammenfassung

Immer mehr Hinweise deuten darauf hin, dass Nanomaterialien (NM) in das Gehirn translozieren und durch Induktion von oxidativem Stress, Neuroinflammation, gestörter Neurotransmitter-Homöostase Neurotoxizität verursachen und sogar neurodegenerative Erkrankungen wie die Alzheimer-Krankheit (AK) auslösen und vorantreiben können. Im Vergleich zur Toxizität in der Lunge und anderen sekundären Zielorganen ist relativ wenig über das Gehirn als Zielorgan für NM-induzierte Neurotoxizität bekannt. Es ist weitgehend unbekannt, ob NM zur Neurotoxizität oder zur Initiierung von AK beitragen können, insbesondere in Bezug auf Art, Dosierung und Expositionsweg. Derzeit konzentriert sich das neurotoxische und neurodegenerative Potenzial von NM auf Inhalationsstudien basierend auf der Identifizierung von NM-Translokationswegen über die Atemwege ins Gehirn. Aufgrund der weit verbreiteten Verwendung von NM in zahlreichen Konsumgütern, z. B. im Lebensmittelsektor, und ihres Potenzials, durch indirekte Wirkungen, z. B. über die Darm-Hirn-Achse, Neurotoxizität zu verursachen, besteht ein zunehmender Bedarf an weiterer toxikologischer Forschung, um die Sicherheit von NM nach realistischeren oralen Expositionsszenarien zu untersuchen.

In einer ersten experimentellen Studie wurden daher neurotoxische Endpunkte nach subakuter oraler Exposition einschließlich einer zweiwöchigen Nachexpositionsphase gegenüber TiO_2 und Ag-NM über die Nahrung in männlichen und weiblichen C57BL/6J-Mäusen untersucht. Wir identifizierten NM-spezifische und geschlechtsspezifische Unterschiede in der Neurotoxizität. Eine verminderte motorische Koordination und eine erhöhte Tyrosinkinase-Aktivität wurden ausschließlich bei Ag-NM-exponierten weiblichen Mäusen beobachtet. In einer zweiten experimentellen Studie wurde das Potenzial von mit der Nahrung zugeführten CeO_2- und SiO_2-NM, Neurotoxizität zu verursachen und die Pathogenese von AK zu fördern untersucht. Während die Exposition gegenüber beiden NM nicht zu einem Fortschreiten der AK-bedingten Pathologie führte, konnten wir überraschenderweise zeigen, dass eine subchronische diätetische Exposition gegenüber 1% CeO_2 die Bildung von Amyloid-Plaques im Hippocampus signifikant hemmte und die Motorik von 5xFAD-Mäusen verbesserte. Um den Einfluss unterschiedlicher Redox-Aktivitäten auf die AK-bedingte Pathologie zu untersuchen, wurde eine dritte subakute Inhalationsstudie unter Verwendung von CeO_2 NM, die mit unterschiedlichen Mengen an Zr (0 %, 27 % und 78 %) beschichtet wurden, durchgeführt. Hier hatten CeO_2 NM keinen Einfluss auf die Bildung von Amyloid-Plaques in 5xFAD-Mäusen. Allerdings führte die Exposition mit dem höchsten Zr-dotierten CeO_2 NM zu einer Veränderung der motorischen Leistung in 5xFAD- und $ApoE^{-/-}$- und zu einer Neuroinflammation in C57BL/6J-Mäusen.

Die in dieser Arbeit durchgeführten Studien liefern neue Erkenntnisse über die Bedeutung der chemischen Zusammensetzung und des Redoxzustands von NM und der Krankheitsanfälligkeit im Hinblick auf die Neurotoxizität. Sie zeigen auch die Notwendigkeit, realistischere Expositionsszenarien zu berücksichtigen und beide Geschlechter in zukünftige NM-Neurotoxizitätsstudien einzubeziehen.

1 General Introduction

1.1 Engineered nanomaterials

1.1.1 Characteristics of engineered nanomaterials

NMs are defined as engineered or natural materials in the nanoscale of 1–100 nm in at least one dimension, like the one-dimensional nano-sheets (for instance graphene), the two-dimensional nanotubes, or the three-dimensional nanoparticles [1, 2]. NMs have a large surface area which is exponentially increasing with decreasing NM size [3]. The smaller the NM, the greater the surface area and thereby the chemical reactivity to interact with surrounding materials. Next to the size, other physicochemical properties like surface hydrophobicity, chemical composition and shape affect its reactivity [4]. Particles in the nanosize range also occur naturally in the environment, e.g., as combustion-derived nanoparticles with heterogeneous sizes, chemistry, and material and physio-chemical properties. While for industrial and medical applications, NMs are manufactured or engineered to generate monodispersed NMs with controlled sizes, material and physio-chemical properties [1, 3]. NMs are categorized according to their chemical composition into carbon-based NMs, organic-based NMs (such as dendrimers, micelles, liposomes), inorganic-based NMs (such as metal and metal-oxide NMs, e.g., Ag, TiO_2, SiO_2, CeO_2) and composite-based NMs, which are combined with other materials in more complex structures [1]. Due to their beneficial properties, NMs are increasingly used for industrial applications, in consumer products like food, cosmetics and in medical applications as therapeutic agents, for early diagnostic or for drug delivery [5, 6]. Nevertheless, the extensive use of NMs in daily-use products and the continuous exposure to combustion-derived nanoparticles like diesel engine exhaust particles may also cause adverse health effects [7].

Exposure to NMs usually occurs through inhalation, dermal absorption, ingestion, or intravenous injection, whereby the different exposure routes might affect its bioavailability and cause different adverse effects. For inhalation, dermal and oral exposures, unlike i.v. injections, NMs have to cross biological barriers to reach systemic targets, which might lead to lower bioavailability [8, 9]. It is hard to estimate exact dose-response curves of NMs compared to other chemical substances due to their unique properties to agglomerate at higher concentrations [10], to form corona shells when interacting with surrounding biomolecules such as proteins, lipids and sugars dependent on its environment [8, 11] and their tendency to “age” at different conditions during storage and time [12]. All of these NM characteristics may result in changes in their physicochemical properties and size which furthermore impact their cellular uptake [13], their interactions with other biomolecules and receptors and thus their toxicity in general (see Figure 1.1) [12, 13].

The central toxicity mechanisms of NMs are induced through membrane damage, the release of toxic ions and the generation of reactive oxygen species (ROS) that can cause oxidative stress, leading to DNA, protein or lipid oxidation [14, 15]. These processes have been demonstrated as critical toxic mechanisms of ultrafine particles in ambient air pollution like combustion-derived particles from diesel engine exhaust [16].

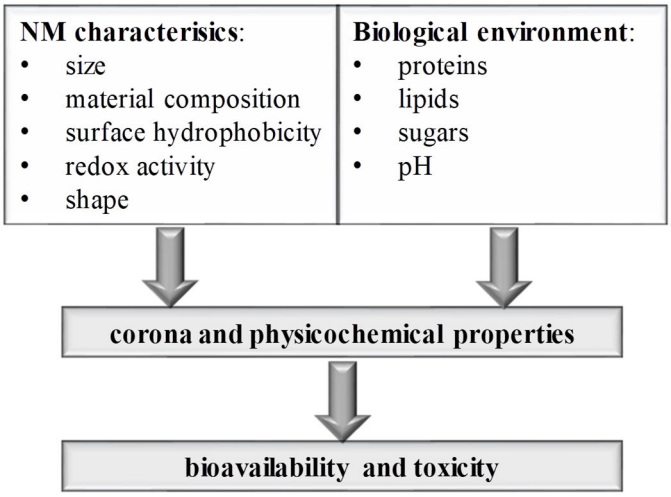

Figure 1.1. Characteristics of nanomaterials (NMs) in biological environments. NMs have unique properties to form corona shells when interacting with surrounding biomolecules such as proteins, lipids and sugars dependent on their biological environment. These interactions may result in changes in size and other physicochemical properties like surface hydrophobicity, redox activity, and shape, impacting their bioavailability and toxicity in general.

1.1.2 Exposure routes of engineered nanomaterials to the adult brain

NMs may reach the brain via various possible routes of exposure and translocation pathways. These principle routes are schematically shown in Figure 1.2. Through any route of exposure, NMs can reach the brain through the BBB when reaching the blood circulation. The BBB is a highly selective semipermeable structural barrier that preserves brain homeostasis by regulating ion and molecular transport to the brain and further prevents neurotoxic substances from translocating to and damaging the brain [17]. The BBB is formed by endothelial cells, connecting tight junctions and surrounding astrocytes and pericytes [18]. Pericytes are covered around the membrane and are responsible for tight junction formation, which connects endothelial cells. Tight junction proteins, like zonula occludens (ZO)-1 and ZO-2 and occludin, claudin-1, -3 and -5, regulate the diffusion of free radicals ions and hydrophilic molecules and targeted signalling [18]. Due to the selectivity of the tight junctions, paracellular pathway and passive transmembrane diffusion through the BBB are only possible for small lipophilic molecules (<400-500 Da) or small gas molecules like CO_2 and O_2 [19]. Other molecules such

as amino acids, nutrients and nucleosides pass through the BBB by specific receptor-mediated transcytosis or adsorptive-mediated transcytosis [19, 20]. NMs can pass the BBB and are therefore increasingly used as drug carriers. The ability and pathway of which NMs may enter the central nervous system (CNS) depend on their size and other physicochemical properties, such as chemical composition, shape and charge [21]. Small NMs coated with definite peptides or lipids could be delivered through the BBB via endocytosis or passive diffusion [22], but most NMs pass the endothelial barrier by specific receptor- and unspecific adsorptive-mediated transcytosis [23]. Especially in pharmacology for drug delivery purposes, NM surfaces can be functionalized with specific surface changes to improve BBB passage of these NMs loaded with the specific drug [21].

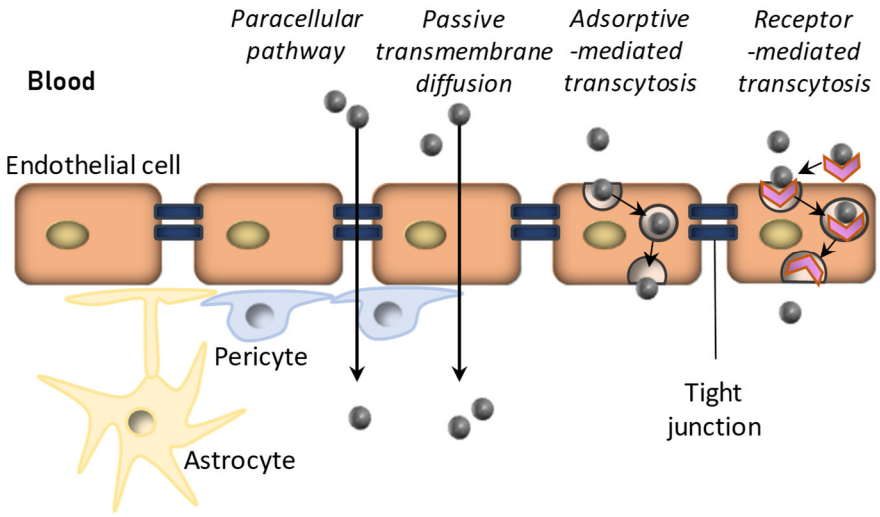

Figure 1.2: Blood-brain-barrier (BBB) structure and possible nanomaterial (NM)-passage mechanisms. The BBB is formed by tight junctions, endothelial cells, pericytes and astrocytes. Due to the selectivity of the tight junctions, paracellular pathway and passive transmembrane diffusion through the BBB are only possible for small lipid-based NMs. The other NMs pass through the BBB by specific adsorptive-mediated transcytosis or specific receptor-mediated transcytosis.

One mechanism of NM translocation to the brain is through the nose-to-brain (or olfactory) pathway, bypassing the BBB (see Figure 1.3). This route of translocation has emerged as an important route of exposure to the brain [3, 24, 25]. Oberdorster and colleagues were the first who could demonstrate direct translocation via the olfactory pathway of inhaled combustion-derived NMs [26]. The delivery of NMs through the epithelium of the nasal mucosa to the olfactory bulb using nerve pathways and subsequent to other parts of the brain has been reviewed by Boyes and Thriel [25]. This intraneural delivery route is strongly size-dependent and small NMs or lipophilic molecules can be transported via the various passage mechanisms including passive diffusion more easily to different parts of the brain [25, 27, 28]. Researchers observed that intranasal instilled TiO_2 NMs were first translocated to the olfactory bulb and

further to the hippocampus on the second day of post-exposure. Over time, the Ti content migrated under the diffusion mechanism to the cerebral cortex and cerebellum and continuously increased in every brain region [29]. However, extracellular transport by entering blood or lymphatic vessels through intercellular clefts of the nasal cavity may also occur [28]. Moreover, exposure through the intranasal route may lead to higher bioavailability of NMs compared to other routes of exposure where NMs have to cross several biological barriers. Upon inhalation, a considerable amount of the NMs will be removed from the respiratory tract by mucociliary clearance or by macrophages, while the remaining fraction may reach the brain through sensory neuronal pathways or translocation from the alveoli into the blood, whereby they have to cross the air-blood barrier and subsequently the BBB [24, 27, 30]. Whereas after ingestion of NMs present in food or beverages, or following the mucociliary clearance from the lung, the NMs have to cross additional physical barriers like the gastric and intestinal fluids with changing pH conditions, the mucus barrier and the epithelial cells of the intestine to get into the blood circulation and subsequent pass the BBB to reach the brain [31, 32].

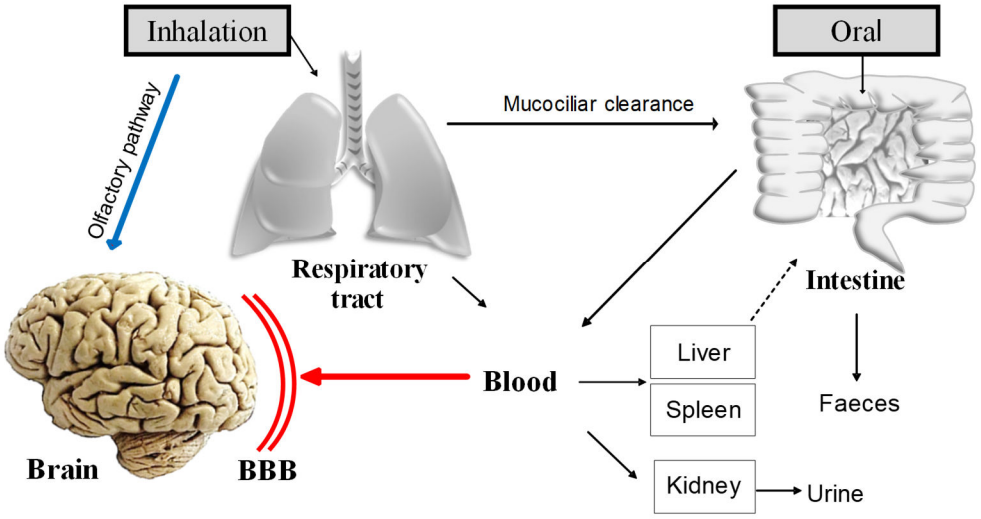

Figure 1.3. Exposure routes of nanomaterials (NMs) to the adult brain. Translocation of airborne NMs to the brain may occur upon nasal deposition through the olfactory pathway bypassing the blood-brain barrier (BBB). NMs that deposit in more distal regions of the respiratory tract or NMs that are ingested need to translocate into the bloodstream and subsequently pass the BBB in order to enter the brain parenchyma. Translocation of NMs into the blood circulation will also lead to potential accumulation in other organs such as the liver, spleen and kidney. Excretion of NMs is mainly via faeces or urine.

Yokel et al. [33] published a review about the ability of metal-based NMs (nanoceria, nanogold, nanosilica, nanotitania, and nanoiron) following i.v. injection and described that less than 0.1% of the applied dose could be detected in the brain of the treated animals. Even if i.p. or i.v. injections of NMs do not represent normal and non-medical human exposure routes and NM content in the brain may be even lower following more realistic exposure routes; the ability of

NM to accumulate in specific brain regions may cause adverse neurotoxic effects over time [25, 34]. Also, neuropathological changes might be possible through indirect effects where NMs do not have to cross the BBB or translocate along nerves into the brain. Recent studies on ingested NMs effects on the microbiota-gut-brain axis have come more in focus and gained interest in the context of neuropathological changes, including alterations of the BBB structure and permeability [35, 36]. During pathological brain conditions, such as neurodegenerative diseases like AD, BBB disruption is well described (reviewed in [20]). Several studies indicated that BBB disruption might also be the result of NM exposure and goes along with alterations of permeability and structure of the BBB and furthermore has been related to decreased expression of the tight junction proteins [37-39].

1.1.3 **Impact of engineered nanomaterials on oxidative stress**

The brain is a highly energy-demanding organ and uses nearly 20% of the total oxygen (O_2) consumption [40]. Molecular O_2 is essential for all aerobic organisms to support ATP synthesis in mitochondria, but incomplete reduction results in the production of highly reactive superoxide anion ($O_2^{\cdot-}$), hydroxyl ($^{\cdot}OH$), or hydrogen peroxide (H_2O_2), which classified as reactive oxygen species (ROS) [41]. These ROS can lead to oxidative stress if redox balance is impaired, whether through an increase in ROS levels or a decrease in antioxidant defence mechanisms. Finally, these ROS may induce lipid, DNA and/or protein oxidation, calcium and/or glutamate dysregulation resulting in structural changes, dysfunction or loss of activity of various molecules until cell death [42, 43]. The brain is susceptible to oxidative stress based on its high oxygen consumption, high amounts of easily oxidable polyunsaturated fatty acids and high amounts of metals like iron and copper, which can generate ROS in their redox-active state, but in turn, relatively low levels of antioxidants [43, 44]. Furthermore, oxidative damage of neurons is generally irreversible because of insufficient self-repair mechanisms and since they are non-dividing in most parts of the adult brain and thus, cannot be replaced [43].

Induction of oxidative stress leading to activation of antioxidant defence and inflammation upon NM exposure is well recognised as a central mechanism of toxicity in the lungs of NMs after inhalation [45] and following other exposure routes in various cell types *in vitro* and *in vivo* (reviewed by [14, 46-48]). Intracellular antioxidant defence mechanisms include enzymes, like glutathione peroxidase (GPx), catalase (CAT) or superoxide dismutase (SOD) and other antioxidants, like glutathione (GSH), coenzyme Q10, vitamin C (ascorbic acid) or vitamin E (α-tocopherol), which either scavenge ROS directly or initiate other detoxification mechanisms

[49, 50]. The primary mechanism of NMs inducing oxidative stress is either direct, through the production of ROS or indirect, as a result of the depletion of antioxidants. ROS can be enhanced directly from NMs when free radicals and oxidants bind to its surface or due to metal-ion release of metallic NMs, which subsequently can react via Fenton-type or Haber Weiss-type reactions generating highly toxic hydroxyl radicals [42, 47, 51]. Besides being self-oxidative, NMs can activate enzyme systems within the cell which are key producers of radical superoxide by one-electron reduction of molecular oxygen, such as xanthine oxidase, cytochrome P450 or NADPH oxidase [52]. Furthermore, NMs can disturb mitochondrial functions and ATP production by disrupting the membrane permeability or the electron transport chain [47, 53], resulting in increased ROS levels and therefore oxidative stress. Also, it has been shown that NMs can modulate the enzyme activities of CAT, GPx and SOD or modulate GSH into its oxidized version glutathione disulfide (GSSG) [47, 53, 54]. GSH is a potent free-radical scavenger and a key player in maintaining the cellular redox balance. Decreased levels of GSH, increased levels of GSSG and a decreased ratio of its reduced and oxidized form (GSH/GSSG) can be measured upon NM-induced oxidative stress [55].

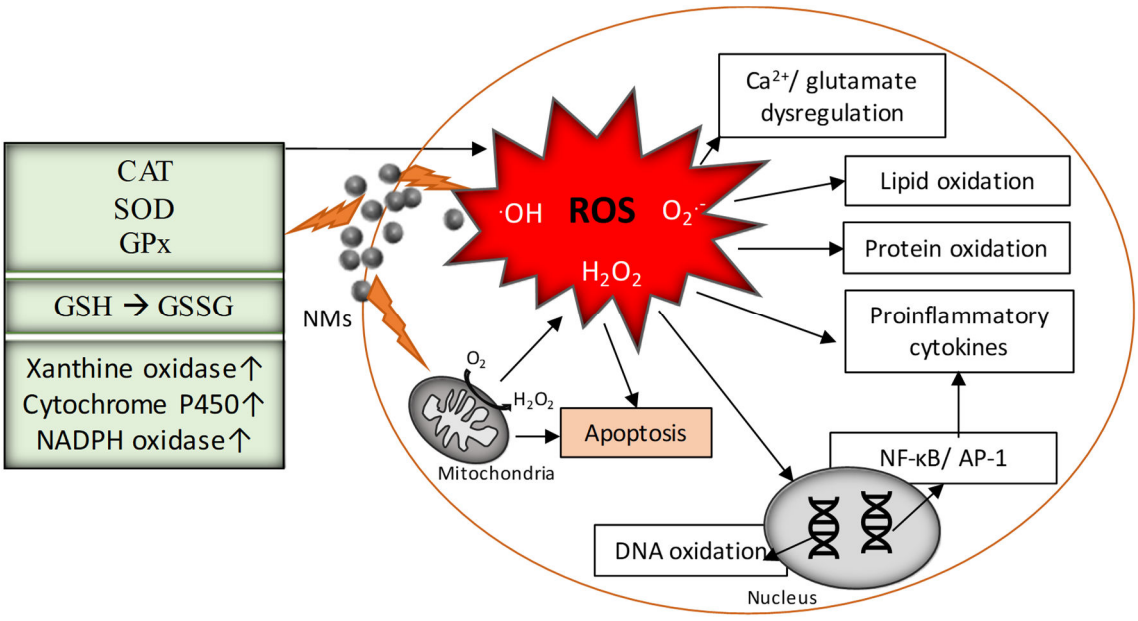

Figure 1.4: Impact of engineered nanomaterials (NMs) on oxidative stress. Superoxide anion ($O_2^{\cdot-}$), hydrogen peroxide (H_2O_2) and hydroxyl ($^{\cdot}OH$) are highly reactive and classified as reactive oxygen species (ROS). The primary mechanism of NMs inducing oxidative stress is either through direct production of ROS, resulting from the (catalytically) reactive physicochemical properties of the particle surfaces, or indirect through the disruption of mitochondrial functions, or the activation of xanthine oxidase, cytochrome P450 or NADPH oxidase. In addition, oxidative stress may result from the degradation or impaired (re)generation of antioxidant enzyme activities such as catalase (CAT), superoxide dismutase (SOD) and glutathione peroxidase (GPx), or the reduction of glutathione (GSH) into its oxidized form glutathione disulfide (GSSG). The increased levels of ROS may induce calcium and/or glutamate dysregulation, lipid, DNA and/or protein oxidation and furthermore may activate signalling pathways like the nuclear transcription factor-κB (NF-κB) and activator protein 1 (AP-1) leading to proinflammatory cytokine expression. Finally, oxidative stress may lead to cell death through apoptosis.

Moreover, ROS can act as a second messenger and activate various signal pathways involved in important physiological and pathophysiological processes, including inflammation, embryogenesis and organ developments such as proliferation and apoptosis [56, 57]. It has been demonstrated that ROS activates the nuclear transcription factor-κB (NF-κB) and activator protein 1 (AP-1) signalling pathways, which modulates gene expression for the mentioned pathophysiological processes and further the expression of proinflammatory cytokines and chemokines [57, 58]. Finally, oxidative stress may lead to apoptotic cell death, e.g., through mitochondrial or lipid peroxidation mediated activation of pro-apototic factors [59, 60]. The main mechanism of NMs inducing oxidative stress is summarized in Figure 1.4.

Various studies provide hints for a correlation between specific types of NMs, on neurotoxicity and induction of oxidative stress, such as TiO_2 and Ag, which are the most widely used metal-based NMs in numerous consumer applications and products [61, 62]. The primary mechanism of neurotoxicity induced by NMs is usually through the generation of ROS that induces oxidative stress, activation of signalling pathways and subsequent release of proinflammatory cytokines causing neuroinflammation, which finally may lead to neuronal cell death mainly through apoptotic mechanisms [48, 57, 58, 63, 64]. In rodent studies, exposure to TiO_2 NMs resulted in deposition of Ti in the brain [65, 66] and/or increased levels of oxidative stress [65-69] and neuroinflammatory markers [66] and/or changes in AChE activity [68]. Also, Ag NMs were found to translocate to the brain [70, 71], and/or increased levels of oxidative stress [70, 72, 73] and neuroinflammatory markers [71] and/or induced apoptosis [71] and/or cognitive impairment [70, 74]. SiO_2 NMs are one of the most prevalent components of airborne pollutants and are widely used in the industry, e.g., as an anti-caking agent in the food industry, listed in Europe as food additive E551 [75, 76]. SiO_2 NMs were found to translocate to the brain and induce neurotoxicity after intranasal instillation in rats [77]. This accumulation increased levels of ROS while inhibiting antioxidant enzyme activities, decreased GSH levels and increased expression of apoptosis genes and proteins [77]. Although oxidative stress has been demonstrated to be involved in the neurotoxicity of these metallic NMs, the exact mechanism remains unclear.

1.1.4 **Impact of engineered nanomaterials on neuroinflammation**

Neuroinflammation is defined as an inflammatory response to infection, toxic metabolites, oxidative stress or diseases in the CNS. The CNS is composed of neurons and glial cells. The ratio of glial to neuronal cells in the whole brain is about 1:1 but varies between different brain

regions [78]. Astrocytes, oligodendrocytes, and microglia are the most prevalent types of glial cells in the brain and function primarily as physical support for neurons in the regulation of their homeostasis (water, neurotransmitter, metabolites) and in pathological conditions maintaining of tissue damage [78, 79].

Microglia

Microglia account for about 10% of glial cells and can become activated in terms of pathological conditions, e.g., to respond to toxic metabolites or proteins such as Aβ, infectious pathogens or NMs [78, 80-82]. Active microglia undergo a variety of structural changes to transform and migrate towards the injured part. They phagocytose foreign materials, release growth factors for the healing of neurons or secrete proinflammatory cytokines like interleukin (IL)-1β, IL-6 and tumor necrosis factor (TNF)-α or radicals like nitric oxide (NO) to recruit leukocytes or more microglia to proliferate to this part of the brain [80, 83-85]. The release of growth factors (e.g., insulin-like growth factor 1 (IGF-1)) and the release of proinflammatory cytokines, in turn, is regulated by anti-inflammatory cytokines like IL-10, IL-4 and transforming growth factor-β (TGF-β), which is known to suppress proinflammatory cytokine release [85, 86]. In general, microglial activation and expression of proinflammatory cytokines are intended to be neuroprotective but strong stimuli or chronic, persistent activation can contribute to apoptotic cell death and neurodegeneration with manifesting pathological changes such as cognitive deficits [60, 80, 82, 87].

Astrocytes

Astrocytes are the most abudant glial cells in the mammalian brain [78]. Astrocytes are structural components of the BBB and are involved in various physiological processes regulating the blood flow, synaptic plasticity, neurogenesis, and the homeostasis of water, neurotransmitter and other metabolites [79, 88-90]. The glial fibrillary acidic protein (GFAP) is the main protein of the intermediate filaments in astrocyte cytoplasm, and upregulation or rearrangement of GFAP indicates reactive astrogliosis as it is shown in response to pathological conditions [89, 91]. Similar to microglia, astrocytes are under normal physiological conditions neuroprotective but depending on the type and duration of pathological stimuli, they can initiate a neuroinflammatory response and release harmful proinflammatory cytokines or NO [85].

There are various studies providing a link between NM exposure and neuroinflammatory response. Activated microglia are characterised by an increased expression of the ionized calcium-binding adaptor molecule 1 (IBA-1), and it has been demonstrated that these activated

cells are capable to uptake NMs and subsequent secrete proinflammatory cytokines [92-94]. Equivalent to microglia, the activation of astrocytes could be demonstrated in rat brains following TiO_2 NM exposure, revealed by an increased expression GFAP [95]. The release of proinflammatory cytokines is mainly regulated through NF-κB as well as mitogen-activated protein kinase (MAPK) signal pathways, which were found to be activated in response to NM exposure [37, 96-98]. Although these investigations clearly show that NM exposure is linked to neuroinflammation, it remains unclear whether neuroinflammation is the primary response to direct NM brain interactions or the secondary response to NM-induced oxidative stress or systemic inflammation [39, 48, 99]. Most researchers suggest oxidative stress as the prime mechanism, which is supported by studies showing that neuroinflammation in rodents is induced mainly through ROS-mediated pathways [39, 48, 66], and by studies showing that antioxidant treatment can reduce neuroinflammation [48]. Anyhow, oxidative stress and neuroinflammation are closely linked to each other. In response to oxidative stress mediators, glial cells can release proinflammatory cytokines as well as ROS [100].

1.2 Alzheimer´s Disease

Neurodegenerative processes related to the CNS are defined as slow and progressive neuropathological conditions in which neurons might lose their structure and function due to misfolded and aggregated proteins [101] until neuronal cell death by apoptosis [102]. These processes are central features of neurodegenerative diseases which can cause problems with movement (called ataxias) or cognition (called dementias). Dementia is the fifth leading cause of death globally, affecting 40–50 million people worldwide, and this number is estimated to double every 20 years [103-105]. Alzheimer's disease (AD) forms with 60-80% the majority of dementia cases [60, 106]. AD is characterized by an extensive apoptosis-associated neuronal loss in brain regions such as cortex, hippocampus, and cerebellum that control cognition, memory, movement and emotion [60]. Histopathological presence of neurofibrillary tangles and amyloid plaques, surrounded by glial cells, are the most prominent hallmarks of the disease and are present before cognitive deficits are observed [107, 108]. Amyloid plaques consist mainly of Amyloid β- (Aβ)40 and 42 proteins that are derived from proteolytic processing of the amyloid precursor protein (APP) [109, 110]. Amyloid deposition starts in poorly myelinated areas of the basal neocortex, extensions into the hippocampus and finally spreads in all cortical areas [111].

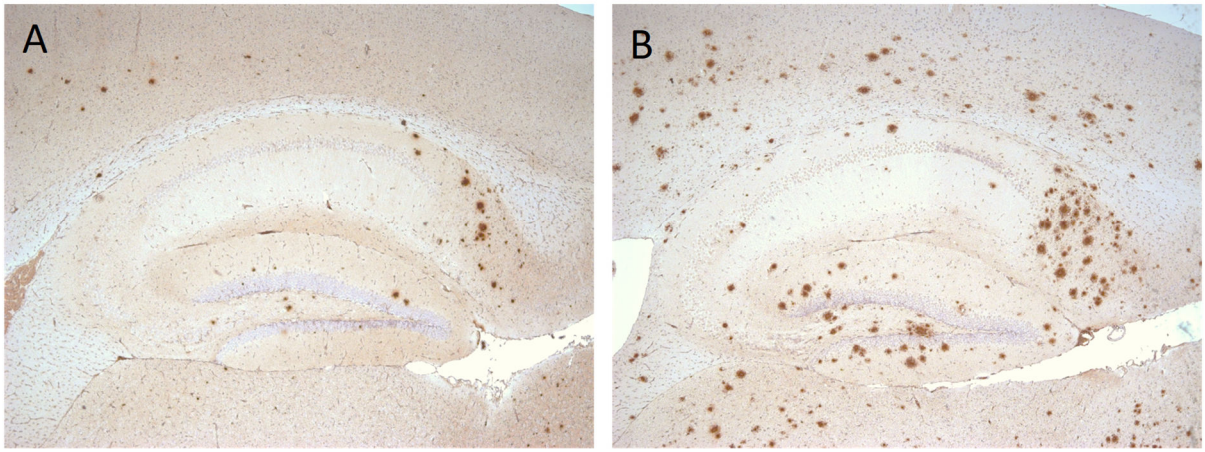

Figure 1.5: Amyloid deposition in 5xFAD mouse model of Alzheimer´s disease (AD). Amyloid depositions in 5xFAD mice. Parasagittal sections of the hippocampus from 3 (A) and 5 (B) month old 5xFAD mice were stained with Aβ42 antibodies and counterstained with hematoxylin. 5xFAD mice rapidly develop amyloid deposition, beginning in the deep cortex and subiculum, which then spreads further into other brain regions at older ages.

To study cellular and molecular mechanisms of the initiation and progression as well as to test potential therapeutic or preventive strategies of the disease, various mouse models of AD have been developed. One of the investigated mouse models express 5 familiar AD (5xFAD) mutations in human APP (Swedish (K670N/M671L), London (V717I) and Florida (I716V))

and PS1 (M146L, L286V) and therefore develop early and rapidly spreading amyloid depositions, starting in the cortex and subiculum at the age of about two months (see Figure 1.5)[112].

1.2.1 The proteolytic processing of the Amyloid precursor protein

The amyloid cascade hypothesis suggests that excessive levels of Aβ monomers in the brain could lead to aggregation into toxic Aβ oligomers and further to fibril structures which initiate brain damages leading to AD [113-115]. Aβ is one fragment among others that results from proteolytic processing of APP. APP is a type I transmembrane protein expressed in many types of mammalian cells and concentrated in the synapses of neurons [116]. APP is proteolytically processed sequentially by two pathways into various fragments, including Aβ (see Figure 1.6) [117, 118].

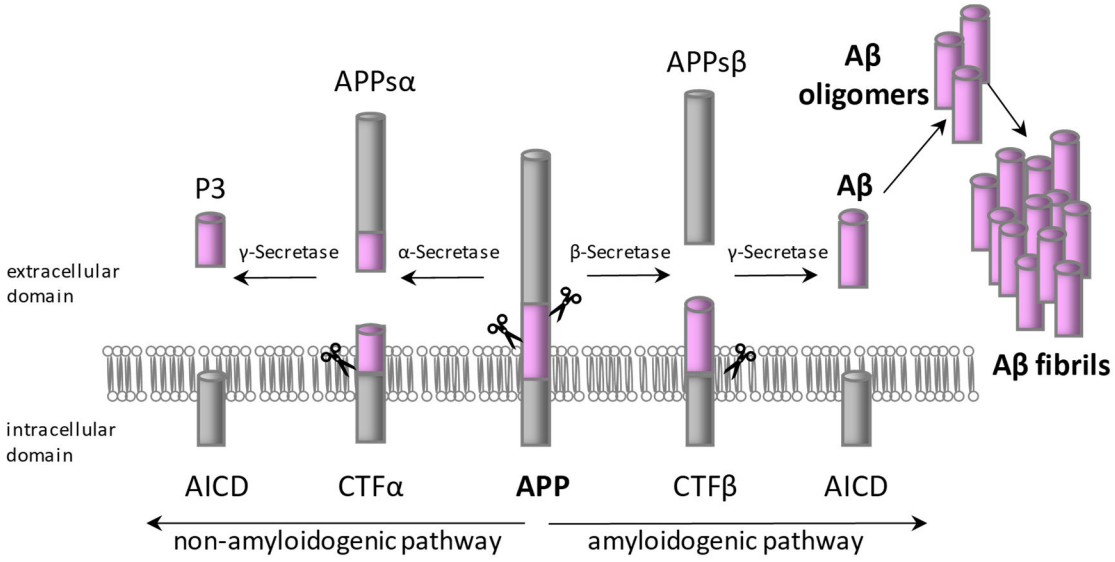

Figure 1.6: Proteolytic processing of the β-Amyloid precursor protein (APP)
In the non-amyloidogenic pathway, APP is cleaved by α-secretase to release its extracellular fragment APPsα and to generate the membrane-bound fragment APP CTFα, which is subsequently cleaved by γ-secretase, to release the p3 fragment in the extracellular space. In the amyloidogenic pathway, β-secretase cleavage of APP resulted in the APPsβ extracellular release and the membrane-bound APP CTFβ, which is subsequently cleaved by γ-secretase resulting in the release of Aβ protein. In the extracellular space, Aβ can aggregate to oligomers and fibrillogenic structures, forming amyloid plaques.

1.2.1.1 Amyloidogenic pathway

Aβ is generated in the amyloidogenic pathway by successive processing of APP. First, APP is cleaved by β-secretase to release the soluble fragment APPsβ in the extracellular environment, followed by subsequent cleavage of the left membrane-bound APP CTFβ fragment by γ-secretase resulting in APP intracellular domain (AICD) and Aβ generation [119]. Depending

on the exact cleavage location of γ-secretase, 38- to 43- amino acid long Aβ peptides are processed, from which Aβ40 peptides are the most predominant in healthy adults followed by the primary aggregation-prone Aβ42 peptide [120]. The β-secretase (β-site APP-cleaving enzyme 1) BACE1 is a type I transmembrane protein [121]. As BACE1 concentration and activity are increased in AD brains, inhibition of BACE1 for slowing down Aβ production in early AD was the focus of many clinical trials [122, 123]. However, several clinical trials failed, perhaps due to insufficient understanding of BACE1 and APPsβ physiology [123]. The γ-secretase is a membrane-bound hetero-tetrameric protein complex of presenilin (PS1/2), presenilin enhancer-2 (PEN-2), nicastrin and anterior pharynx-defective-1 (APH-1) with presenilin as the proteolytic component, housing the catalytic domain [118, 124, 125]. Mutations in the genes encoding presenilin cause early-onset familial AD with an increase in the ratio of Aβ42/40 [126]. Inhibition of γ-secretase has been the focus for AD drug discovery. However, most clinical trials failed mainly due to severe side effects and toxicity, probably due to inhibition of other γ-secretase substrates, such as the highly conserved Notch signalling pathway, which plays a substantial role in many essential regulatory mechanisms [122, 127]. Next to APP and Notch, more than 150 γ-secretase substrates have been identified to date (reviewed in [128].

1.2.1.2 Non-amyloidogenic pathway

In the non-amyloidogenic pathway, APP is cleaved by α-secretase to produce its extracellular fragment APPsα. The membrane-bound fragment APP CTFα is further cleaved by γ-secretase, resulting in the release of the non-toxic 3 kDa fragment called p3 into the intracellular space [129]. The α-secretases belong to the ADAM ('a disintegrin and metalloprotease domain') family, which requires a zinc co-factor for activity [130]. ADAM10 is suggested as the physiology relevant α-secretase, as RNAi-mediated knockdown completely suppressed α-cleavage of APP *in vitro* [131]. Upregulation of ADAM10 in an AD transgenic mouse model decreased formation of Aβ peptides and reduced deposition in plaques while secretion of APPsα increased [132]. Unlike APPsβ, APPsα has neuroprotective functions, either through protecting neurons against Aβ induced oxidative damage [133, 134] or through reducing Aβ generation by inhibiting β-secretase activity [135]. Thus, shifting the amyloidogenic towards the non-amyloidogenic pathway by increasing the activity of ADAM10 could be promising as a therapeutic for decreasing Aβ generation in AD. However, ADAM10 is involved in various other physiological processes, and thus, further research is necessary [136, 137].

1.2.2 **Oxidative stress and neuroinflammation in Alzheimer´s disease**

The initiation of AD is mainly sporadic (>95%) and the cause is not fully identified and considered to be multifactorial. Only a small percentage (<5%) of known AD cases is associated with mutations in the genes for APP and/or PS1/2 [118, 138]. The main risk factor considered for AD is age: approximately 3% of people age 65-74 and 49% of people age 75 or older [139]. Besides age, the main other unmodifiable risk factor for AD is a genetic polymorphism in the APOE gene encoding for apolipoprotein E [140]. The remaining AD causality is associated with various etiological factors that include fat diet, smoking, lack of physical exercise, infections, systemic inflammation, pesticides, some neurotoxic metals like lead, arsenic and aluminium, as well as particulate air pollution and metal-based NMs [141-143]. The mechanisms of how environmental factors are presumed to generate higher Aβ levels could be mediated through an increase in APP production, modulation of the proteolytic processing of APP by increasing the activity of BACE1 and γ-secretase activity or expression or a decreased degradation of Aβ [141, 144]. Aβ-degrading enzymes, such as neprilysin, have the ability to degrade Aβ and could be positively influenced by exercise [141]. The mechanism by which the environmental factors produce excess Aβ is mainly associated with oxidative stress and inflammatory responses in the brain (see Figure 1.7) [87, 145, 146]. However, more research is needed to identify the exact molecular mechanism, which could help find risk factors based on their molecular response.

1.2.2.1 Oxidative stress and AD

Many discovered risk factors of AD promote oxidative stress, indicating that it might play a primary role in AD initiation and progression [145]. Mitochondrial oxidative DNA damage is one of the earliest procedures in AD pathogenesis and is detectable before amyloid plaque deposition. Research indicates that Aβ causes mitochondrial DNA oxidation resulting in mitochondrial structural changes and mitochondrial dysfunction [147]. Indeed, oxidative stress and Aβ are closely linked because oxidants increase Aβ production [148] and Aβ generates ROS itself [149]. Brain regions with high levels of Aβ, like the hippocampus and cortex, have been associated with increased oxidative stress [149]. Redox-active metals in the brain, like zinc, iron or copper, can bind Aβ and are involved in the production of ROS, leading to oxidative stress [150, 151]. Furthermore, the imbalance of these metals in AD patients is closely related to amyloid plaque formation containing high metal concentrations [152]. Erroneous deposition of these metals in the brain can promote Aβ overproduction and/or bind to Aβ inducing oligomer formation and thus modulate the aggregation process [151]. Furthermore,

oxidative stress can promote Aβ overproduction by upregulating BACE1 and γ-secretase expression and activity [153]. Perhaps the most convincing evidence that oxidative stress and neurodegenerative diseases are linked to each other is the efficiency of antioxidants to decrease behavioural impairments, markers of oxidative stress and even Aβ in *in vitro* and *in vivo* studies (reviewed in [148]). In clinical trials however, efficiency of antioxidant treatment was not consistent [148].

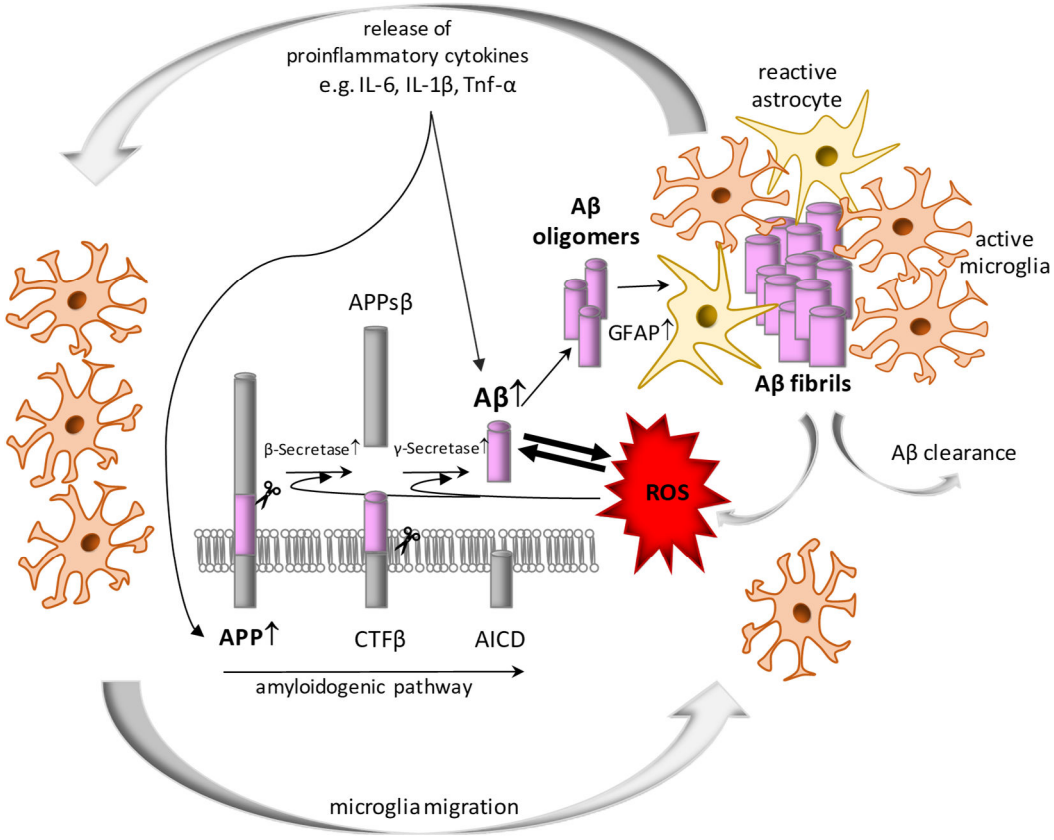

Figure 1.7: Oxidative stress and neuroinflammation in Alzheimer's disease (AD)
The mechanism by which environmental factors are hypothesised to promote amyloid plaque formation is considered to be associated with oxidative stress and inflammatory responses. Oxidative stress and Amyloid-β (Aβ) are closely linked because Aβ can generate reactive oxygen species (ROS) itself, and ROS can increase Aβ production by affecting the amyloidogenic pathway and upregulating β-secretase (BACE1) and/or γ-secretase expression and/or activity. Amyloid plaques with surrounding astrocytes and microglia are key hallmarks of the disease. While on the one hand, microglia have neuroprotective effects due to Aβ clearance, persistence interactions with amyloid plaques can lead on the other hand to proinflammatory cytokine and ROS formation: Proinflammatory cytokines can cause further accelerate amyloid formation by increasing the expression levels of APP and by affecting the amyloidogenic processing, leading to increased Aβ production.

1.2.2.2 Neuroinflammation and AD

Research indicates that in addition to oxidative stress, inflammation can also contribute to AD pathology [87, 146]. AD is associated with amyloid plaques with surrounding astrocytes and microglia [80]. The function of microglial cells in AD pathology is controversial. On the one hand, they can be neuroprotective by Aβ clearance, but on the other hand, persistent interactions

with Aβ can lead to ROS and proinflammatory cytokine release, causing further spreading of amyloid pathology and finally leading to neuronal loss [80]. Indeed, cytokines can impact the expression levels of APP and regulate APP processing by affecting amyloidogenic processing, Aβ production and/or plaque formation [146]. Moreover, there is an increasing concern on the microbiota-gut-brain axis role in connection to nutrient factors and the risk for AD, which is associated mainly via systemic inflammatory response [154].

1.2.3 **Impact of nanomaterials on the initiation and progression of Alzheimer´s disease**

1.2.3.1 Ambient air pollution as a risk factor for AD

The WHO currently estimates that eight million people die due to ambient and household air pollution every year [155]. Air pollution is closely related to adverse effects on human health and an increased risk for cardiovascular and pulmonary diseases, cancer and pneumonia [155]. Furthermore, air pollution has also been explicitly linked with dementia and AD [156, 157]. Air pollution consists of particulate matter (PM), organic compounds and gases such as carbon monoxide (CO), nitrogen dioxide (NO_2) and ozone (O_3) [158]. PM is comprised of solid or liquid particles and is characterised by its aerodynamic diameters and classified as PM_{10} (diameter ≤ 10μm) or $PM_{2.5}$ (diameter ≤2.5μm). Long-term exposure to traffic-related PM has been demonstrated to impair cognitive function in older women in a dose-dependent relation [156]. The results of a recent meta-analysis including over 10 million adults suggested that exposure to increased levels of $PM_{2.5}$ is significantly associated with AD [157]. Pioneering studies from Calderon-Carciduenas and co-workers demonstrated that residents of highly polluted cities had a significantly higher accumulation of Aβ42 as well as increased neuroinflammation compared to inhabitants in low air pollution cities [159]. The working group recently stated that in Mexico City, AD initiation and progression starts in childhood, which was confirmed in more than 99% of 134 subsequent autopsies of residents under the age of 30 years [160]. Mexico City is one of the most polluted cities with $PM_{2.5}$ values above the maximum recommended by the WHO, and brain examinations of every Mexico City resident showed accumulation of combustion-derived and highly oxidable nanoparticles [160, 161]. These findings suggest that combustion-derived nanoparticles from car engines (e.g., from diesel engine exhaust) may initiate and progress AD and have become a topic of investigation in various experimental studies in rodents [162-165].

1.2.3.2 NMs as a risk factor for AD?

Up to now, the impact of engineered NMs on the initiation and progression of AD has not been studied sufficiently. Recently it has been demonstrated in an *in vitro* study that exposure to copper oxide (CuO) NM contributes to cellular apoptosis, oxidative stress and increased Aβ levels in human neuroblastic cells [166]. In a related study, Ag NM were found to increase Aβ levels in murine neuroblastoma cells, and the mechanism was found to through inflammatory - mediated increased expression of APP and decreased neprilysin expression, leading to decreased Aβ degradation [167]. Only a few studies provide hints for a correlation between silica (SiO_2) and cerium dioxide (CeO_2) and the AD initiation and progression. In a study with murine neuroblastoma cells, SiO_2 NMs caused ROS to release and evaluated levels of Aβ due to the upregulation of APP and the downregulation of the Aβ degrading enzyme neprilysin [168]. Furthermore, You and colleagues could demonstrate that intranasal instillation of SiO_2 NM in male mice resulted in cognitive impairment and caused neurodegeneration-like pathology, including neuroinflammation, increased tau phosphorylation and neuronal loss [98]. Figure 1.8 summarizes the mechanisms of how etiological factors and especially NMs are presumed to generate higher Aβ levels.

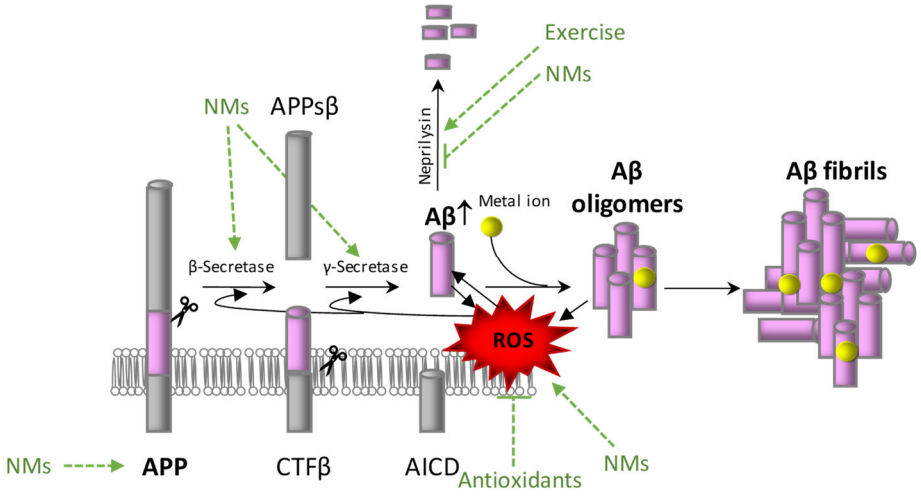

Figure 1.8: Impact of nanomaterials (NMs) on the initiation and progression of Alzheimer's disease (AD)
The impact of NMs on the initiation and progression of AD has been associated with increased oxidative stress, leading to increased Aβ levels. NMs have been found to increase Aβ levels through increased expression of APP by affecting the amyloidogenic pathway and upregulating β-secretase (BACE1) and/or γ-secretase expression and/or activity and decreased neprilysin expression. Neprilysin is an Aβ degrading enzyme and can be positively influenced by exercise leading to decreased Aβ, which can be further be achieved by antioxidants. Furthermore, deposition of redox-active metals, which may be released from metallic NMs, can bind to Aβ inducing oligomer formation and thus modulate amyloid plaque formation.

1.2.3.3 NMs in the prevention and treatment of AD?

While there is concern about the toxicity of NMs, there have also been tremendous research efforts in the field of nanomedicine to develop and use NM-based strategies for the early diagnosis, prevention or treatment of diseases. Often this involves a sophisticated synthesis of complex NMs with functionalised surfaces or hybrid materials [169-172]. In recent years, such nanomedical approaches have also focused on their early diagnostic capabilities and their potential to prevent or treat neurodegenerative diseases, including AD [170, 173-176]. Among the various NMs, CeO_2 has emerged as particularly interesting. While adverse effects of CeO_2 NMs have been reported in several toxicological studies, there has also been a rapidly growing number of studies that indicate beneficial effects of this specific NM. Ce is a rare lanthanide series element and exists in two chemical redox states, Ce^{3+} (fully reduced) and Ce^{4+} (fully oxidized). Due to its ability to alternate between the two redox states, Ce particles are often used as catalysts, e.g., for CO oxidation and the reduction of NOx in combustion engines or as sun protection in UV resistant coatings [177, 178]. In the nanoparticle form, cerium is bound to oxygen and based on its redox state (= the ratio of Ce^{3+}/Ce^{4+}) and oxygen vacancies, CeO_2 NMs can scavenge numerous free radicals and reduce oxidative stress [179] or even induce oxidative stress [180]. Several reports suggested that cerium in the 3+ state enhanced toxicity [180]. Indeed, CeO_2 NM with relatively higher Ce^{3+} levels mimic SOD activities and increase cytotoxic H_2O_2 levels [181], while CeO_2 NM with higher Ce^{4+} mimic CAT enzymatic activities, converting the toxic H_2O_2 to O_2 [182]. However, there appeared to be a range of Ce^{3+} content, around 30%, which produced the best general antioxidant activity and no toxicity [8, 180]. It has been shown that the stability and redox activity of CeO_2 NMs can be modulated by doping with zirconium (Zr) [183, 184]. While other antioxidants are destroyed in the process of scavenging free radicals, CeO_2 NMs have a unique regenerative redox-active matrix, allowing repetitive free radical interactions [8]. This feature may be promising in the treatment of several diseases due to handling sufficient levels of free radicals without high and repetitive dosing [8]. In a mouse model of Parkinson's disease, i.p. injection of CeO_2 was able to protect neurons against ROS-induced damage by decreasing apoptosis and even improved motor dysfunctions [185]. In another study, Ce in the shell of multifunctional magnetite/ceria NMs could successfully reduce ROS generation during Aβ cleansing treatment in a mouse model of AD [186]. In addition, CeO_2 NMs treatment in rats for 28 days could effectively counteract oxidative stress mediated neurotoxic effects [187]. Taken together, CeO_2 represents a particularly interesting type of NM to address effects of on neurotoxicity and on neurogenerative diseases including AD in relation to different routes of exposure.

1.3 Aim and Outline of the Thesis

Growing evidence indicates that NMs might translocate to the brain and may cause neurotoxicity or neurodegeneration by induction of oxidative stress, neuroinflammation and disturbed neurotransmitter homeostasis [33, 63, 188, 189]. Compared to toxicity in the lung and toxicity in other secondary target organs like the liver or spleen, the neurotoxic and neurodegenerative potential of NMs has not been studied sufficiently. Thus, further toxicological research on the brain as a target organ for NMs is needed. Moreover, any degenerative process related to the brain might result in protein structural changes [101] until cell death [102], which are central features of Alzheimer's disease (AD) [60]. AD is mostly of sporadic nature and is associated with various etiological factors like systemic inflammation, heavy metals, as well as particulate air pollution [143, 190]. However, many factors are still not identified, and it is mostly unknown whether and how NMs might contribute to the initiation of AD, especially in regard of type, dosing and exposure route. Neurotoxicity studies focused on inhalation studies based on identification of NM-translocation via the olfactory pathway [27]. However, it is still not fully understood whether certain NMs enter the brain in sufficient quantities to cause neurotoxic effects directly or whether NMs cause neurotoxicity indirectly through, for example, systemic inflammation. Moreover, there is an increasing concern for NM-induced neurotoxicity following oral exposure. Here also, it is not well investigated whether enough NMs can translocate from the intestine into the blood and then across the BBB to cause neurotoxicity directly or whether oral exposure to NMs has adverse effects indirectly through the (microbiota-)gut-brain axis mechanisms [35, 36]. Moreover, the few available long-term studies that have addressed neurotoxic effects of NMs after oral exposure typically used the non-physiological administration procedure of repeated oral gavage. Consequently, there is an urgent need for further oral exposure studies with NMs, that also consider realistic human exposure scenarios by avoiding artificial oral gavage bolus effects.

The **aim of this thesis** was to determine if repeated exposure to four of the most widely used engineered NMs, i.e., Ag, TiO_2, SiO_2 and CeO_2, causes neurotoxicity in general or promotes the development and progression of AD following inhalation or dietary exposure. Therefore, neurotoxic effects were either investigated in mice following controlled repeated nose-only inhalation to aerosolised NMs, or upon long-term *ad libitum* oral exposure to NMs incorporated into mouse food pellets. The anticipated novel insights could contribute to risk assessment by identifying relevant endpoints in the field of nanotoxicology and, furthermore, to support the grouping of NMs in terms of exposure route and toxicity.

The thesis incorporates the following research objectives:

1. The first research objective of the thesis (described in **Chapter 2**) was to investigate sex-dependent effects of subacute dietary oral exposure to TiO_2 and Ag NMs on neurotoxic endpoints, including behaviour in male and female C57BL/6J mice. The study was designed in alignment with recommendations of the OECD TG 424 guideline for neurotoxicity testing in rodents [191]. The endpoints measured in this study included a broad spectrum of neurobehavioural tests, markers of neuroinflammation, oxidative stress and BBB disruption. In addition, tyrosine and serine/threonine protein kinases activity were investigated in the brains using peptide microarrays.

2. The second objective (**Chapter 3**) was to determine the effects of subacute and subchronic dietary oral exposure to CeO_2 and SiO_2 NMs on neurodegenerative endpoints and on the progression of AD-related pathology in 5xFAD mice and their C57BL/6J littermates. Increased levels of amyloid-β (Aβ) peptides in the brain aggregating to amyloid plaques are a major hallmark of the disease. 5xFAD mice rapidly accumulate massive Aβ42 levels and display amyloid deposition and gliosis by expressing a total of five familial AD mutations in human APP and PS1 [112]. Only female mice were used because of higher sensitivity in β-amyloidogenesis to stress responses [192].

3. The third objective (**Chapter 4**) was to evaluate the effects of NMs and their redox activity on the progression of neurodegenerative endpoints in C57BL/6J, 5xFAD and $ApoE^{-/-}$ mice following subacute inhalation exposure to CeO_2 NMs. The role of the redox activity was studied by applying CeO_2 NMs coated with varying amounts of Zr. The study was conducted based on findings that free radicals and oxidative stress play a prominent role in the pathology of the disease (reviewed in [148]). In addition to 5xFAD mice, apolipoprotein E-deficient ($ApoE^{-/-}$) mice were included in this inhalation exposure studies (1) because of findings that genetic polymorphism in the APOE gene is a risk factor for developing AD and (2) to test whether their compromised BBB might increase the susceptibility of NM-induced effects [140, 193]. The key endpoints measured in both studies included behaviour tests, histopathological evaluation of amyloid-plaque formation and gliosis, expression levels of Aβ, and markers of neuroinflammation and oxidative stress.

1.4 References

1. Jeevanandam, J., et al., *Review on nanoparticles and nanostructured materials: history, sources, toxicity and regulations.* Beilstein journal of nanotechnology, 2018. **9**: p. 1050-1074.
2. Borm, P., et al., *Research Strategies for Safety Evaluation of Nanomaterials, Part V: Role of Dissolution in Biological Fate and Effects of Nanoscale Particles.* Toxicological Sciences, 2006. **90**(1): p. 23-32.
3. Oberdörster, G., E. Oberdörster, and J. Oberdörster, *Nanotoxicology: an emerging discipline evolving from studies of ultrafine particles.* Environmental health perspectives, 2005. **113**(7): p. 823-839.
4. Jiang, J., et al., *Does Nanoparticle Activity Depend upon Size and Crystal Phase?* Nanotoxicology, 2008. **2**(1): p. 33-42.
5. Singh, R. and J.W. Lillard, *Nanoparticle-based targeted drug delivery.* Experimental and Molecular Pathology, 2009. **86**(3): p. 215-223.
6. Khan FA, A.D., Alomari M, Almofty SA, *Impact of nanoparticles on neuron biology: current research trends.* Int J Nanomedicine., 2018. **13:2767-2776**.
7. Donaldson, K., et al., *Combustion-derived nanoparticles: a review of their toxicology following inhalation exposure.* Particle and fibre toxicology, 2005. **2**: p. 10-10.
8. Rzigalinski, B.A., C.S. Carfagna, and M. Ehrich, *Cerium oxide nanoparticles in neuroprotection and considerations for efficacy and safety.* Wiley interdisciplinary reviews. Nanomedicine and nanobiotechnology, 2017. **9**(4): p. 10.1002/wnan.1444.
9. Riediker, M., et al., *Particle toxicology and health - where are we?* Particle and fibre toxicology, 2019. **16**(1): p. 19-19.
10. Yang, Y., et al., *Particle agglomeration and properties of nanofluids.* Journal of Nanoparticle Research, 2012. **14**(5): p. 852.
11. Lynch, I., et al., *Nanoscience and the environment.* Frontiers of nanoscience, 2014. **7**: p. 127-156.
12. Izak-Nau, E., et al., *Impact of storage conditions and storage time on silver nanoparticles' physicochemical properties and implications for their biological effects.* Rsc Advances, 2015. **5**(102): p. 84172-84185.
13. Huk, A., et al., *Is the toxic potential of nanosilver dependent on its size?* Part Fibre Toxicol, 2014. **11**: p. 65.
14. Unfried, K., et al., *Cellular responses to nanoparticles: Target structures and mechanisms.* Nanotoxicology, 2007. **1**(1): p. 52-71.
15. Buchman, J.T., et al., *Understanding Nanoparticle Toxicity Mechanisms To Inform Redesign Strategies To Reduce Environmental Impact.* Accounts of Chemical Research, 2019. **52**(6): p. 1632-1642.
16. Stone, V., et al., *Nanomaterials Versus Ambient Ultrafine Particles: An Opportunity to Exchange Toxicology Knowledge.* Environ Health Perspect, 2017. **125**(10): p. 106002.
17. Hawkins, B.T. and T.P. Davis, *The Blood-Brain Barrier/Neurovascular Unit in Health and Disease.* Pharmacological Reviews, 2005. **57**(2): p. 173.
18. Abbott, N.J., et al., *Structure and function of the blood–brain barrier.* Neurobiology of Disease, 2010. **37**(1): p. 13-25.
19. Pardridge, W.M., *Targeted delivery of protein and gene medicines through the blood-brain barrier.* Clin Pharmacol Ther, 2015. **97**(4): p. 347-61.
20. Sweeney, M.D., A.P. Sagare, and B.V. Zlokovic, *Blood–brain barrier breakdown in Alzheimer disease and other neurodegenerative disorders.* Nature Reviews Neurology, 2018. **14**(3): p. 133-150.
21. Lombardo, S.M., et al., *Key for crossing the BBB with nanoparticles: the rational design.* Beilstein Journal of Nanotechnology, 2020. **11**: p. 866-883.

22. Kreuter, J., *Influence of the Surface Properties on Nanoparticle-Mediated Transport of Drugs to the Brain.* Journal of Nanoscience and Nanotechnology, 2004. **4**(5): p. 484-488.
23. Hervé, F., N. Ghinea, and J.-M. Scherrmann, *CNS delivery via adsorptive transcytosis.* The AAPS journal, 2008. **10**(3): p. 455-472.
24. Heusinkveld, H.J., et al., *Neurodegenerative and neurological disorders by small inhaled particles.* NeuroToxicology, 2016. **56**: p. 94-106.
25. Boyes, W.K. and C. van Thriel, *Neurotoxicology of Nanomaterials.* Chemical research in toxicology, 2020. **33**(5): p. 1121-1144.
26. Oberdorster, G., et al., *Translocation of inhaled ultrafine particles to the brain.* Inhal Toxicol, 2004. **16**(6-7): p. 437-45.
27. Oberdörster, G., A. Elder, and A. Rinderknecht, *Nanoparticles and the brain: cause for concern?* Journal of nanoscience and nanotechnology, 2009. **9**(8): p. 4996-5007.
28. Lochhead, J.J. and R.G. Thorne, *Intranasal delivery of biologics to the central nervous system.* Adv Drug Deliv Rev, 2012. **64**(7): p. 614-28.
29. Wang, J., et al., *Time-dependent translocation and potential impairment on central nervous system by intranasally instilled TiO2 nanoparticles.* Toxicology, 2008. **254**(1): p. 82-90.
30. Elder, A. and G. Oberdörster, *Translocation and effects of ultrafine particles outside of the lung.* Clin Occup Environ Med, 2006. **5**(4): p. 785-96.
31. Oberdörster, G., E. Oberdörster, and J. Oberdörster, *Concepts of nanoparticle dose metric and response metric.* Environ Health Perspect, 2007. **115**(6): p. A290.
32. Kreyling, W.G., et al., *Age-Dependent Rat Lung Deposition Patterns of Inhaled 20 Nanometer Gold Nanoparticles and their Quantitative Biokinetics in Adult Rats.* ACS Nano, 2018. **12**(8): p. 7771-7790.
33. Yokel, R., E. Grulke, and R. MacPhail, *Metal-based nanoparticle interactions with the nervous system: the challenge of brain entry and the risk of retention in the organism.* Wiley Interdiscip Rev Nanomed Nanobiotechnol, 2013. **5**(4): p. 346-73.
34. van der Zande, M., et al., *Distribution, Elimination, and Toxicity of Silver Nanoparticles and Silver Ions in Rats after 28-Day Oral Exposure.* ACS Nano, 2012. **6**(8): p. 7427-7442.
35. Hu, L., et al., *High Salt Elicits Brain Inflammation and Cognitive Dysfunction, Accompanied by Alternations in the Gut Microbiota and Decreased SCFA Production.* J Alzheimers Dis, 2020. **77**(2): p. 629-640.
36. Morais, L.H., H.L.t. Schreiber, and S.K. Mazmanian, *The gut microbiota-brain axis in behaviour and brain disorders.* Nat Rev Microbiol, 2021. **19**(4): p. 241-255.
37. Xu, L., et al., *Silver nanoparticles induce tight junction disruption and astrocyte neurotoxicity in a rat blood-brain barrier primary triple coculture model.* International journal of nanomedicine, 2015. **10**: p. 6105-6118.
38. Chen, I.C., et al., *Influence of silver and titanium dioxide nanoparticles on in vitro blood-brain barrier permeability.* Environmental Toxicology and Pharmacology, 2016. **47**: p. 108-118.
39. Liu, X., B. Sui, and J. Sun, *Blood-brain barrier dysfunction induced by silica NPs in vitro and in vivo: Involvement of oxidative stress and Rho-kinase/JNK signaling pathways.* Biomaterials, 2017. **121**: p. 64-82.
40. Magistretti, Pierre J. and I. Allaman, *A Cellular Perspective on Brain Energy Metabolism and Functional Imaging.* Neuron, 2015. **86**(4): p. 883-901.
41. D'Autréaux, B. and M.B. Toledano, *ROS as signalling molecules: mechanisms that generate specificity in ROS homeostasis.* Nature Reviews Molecular Cell Biology, 2007. **8**(10): p. 813-824.

42. Knaapen, A.M., et al., *Inhaled particles and lung cancer. Part A: Mechanisms.* International Journal of Cancer, 2004. **109**(6): p. 799-809.
43. Wang, X. and E.K. Michaelis, *Selective neuronal vulnerability to oxidative stress in the brain.* Frontiers in aging neuroscience, 2010. **2**: p. 12-12.
44. Cobley, J.N., M.L. Fiorello, and D.M. Bailey, *13 reasons why the brain is susceptible to oxidative stress.* Redox Biology, 2018. **15**: p. 490-503.
45. Li, N., T. Xia, and A.E. Nel, *The role of oxidative stress in ambient particulate matter-induced lung diseases and its implications in the toxicity of engineered nanoparticles.* Free Radic Biol Med, 2008. **44**(9): p. 1689-99.
46. Mendoza, R.P. and J.M. Brown, *Engineered nanomaterials and oxidative stress: current understanding and future challenges.* Current opinion in toxicology, 2019. **13**: p. 74-80.
47. Manke, A., L. Wang, and Y. Rojanasakul, *Mechanisms of nanoparticle-induced oxidative stress and toxicity.* BioMed research international, 2013. **2013**: p. 942916-942916.
48. Song, B., et al., *Is Neurotoxicity of Metallic Nanoparticles the Cascades of Oxidative Stress?* Nanoscale research letters, 2016. **11**(1): p. 291-291.
49. Matés, J.M., *Effects of antioxidant enzymes in the molecular control of reactive oxygen species toxicology.* Toxicology, 2000. **153**(1): p. 83-104.
50. Kurutas, E.B., *The importance of antioxidants which play the role in cellular response against oxidative/nitrosative stress: current state.* Nutrition journal, 2016. **15**(1): p. 71-71.
51. Miller, C.J., A.L. Rose, and T.D. Waite, *Importance of Iron Complexation for Fenton-Mediated Hydroxyl Radical Production at Circumneutral pH.* Frontiers in Marine Science, 2016. **3**(134).
52. Masoud, R., et al., *Titanium Dioxide Nanoparticles Increase Superoxide Anion Production by Acting on NADPH Oxidase.* PloS one, 2015. **10**(12): p. e0144829-e0144829.
53. Flores-López, L.Z., H. Espinoza-Gómez, and R. Somanathan, *Silver nanoparticles: Electron transfer, reactive oxygen species, oxidative stress, beneficial and toxicological effects. Mini review.* Journal of Applied Toxicology, 2019. **39**(1): p. 16-26.
54. Fenoglio, I., et al., *The oxidation of glutathione by cobalt/tungsten carbide contributes to hard metal-induced oxidative stress.* Free Radic Res, 2008. **42**(8): p. 437-745.
55. Chen, Z., et al., *Tissue-specific oxidative stress and element distribution after oral exposure to titanium dioxide nanoparticles in rats.* Nanoscale, 2020. **12**(38): p. 20033-20046.
56. Hensley, K., et al., *Reactive oxygen species, cell signaling, and cell injury.* Free Radic Biol Med, 2000. **28**(10): p. 1456-62.
57. Lingappan, K., *NF-κB in Oxidative Stress.* Current opinion in toxicology, 2018. **7**: p. 81-86.
58. Lin, C.-C., et al., *Carbon Monoxide Releasing Molecule-2-Upregulated ROS-Dependent Heme Oxygenase-1 Axis Suppresses Lipopolysaccharide-Induced Airway Inflammation.* International journal of molecular sciences, 2019. **20**(13): p. 3157.
59. Mohammadinejad, R., et al., *Necrotic, apoptotic and autophagic cell fates triggered by nanoparticles.* Autophagy, 2019. **15**(1): p. 4-33.
60. Sharma, V.K., et al., *Apoptotic Pathways and Alzheimer's Disease: Probing Therapeutic Potential.* Neurochemical Research, 2021.
61. Vance, M.E., et al., *Nanotechnology in the real world: Redeveloping the nanomaterial consumer products inventory.* Beilstein journal of nanotechnology, 2015. **6**: p. 1769-1780.

62. FAO/WHO, *FAO/WHO expert meeting on the application of nanotechnologies in the food and agriculture sectors: potential food safety implications: meeting report. Rome. 130 pp.* 2010.
63. Bencsik, A., P. Lestaevel, and I. Guseva Canu, *Nano- and neurotoxicology: An emerging discipline.* Progress in Neurobiology, 2018. **160**: p. 45-63.
64. Teleanu, D.M., et al., *Neurotoxicity of Nanomaterials: An Up-to-Date Overview.* Nanomaterials (Basel, Switzerland), 2019. **9**(1): p. 96.
65. Hu, R., et al., *Molecular mechanism of hippocampal apoptosis of mice following exposure to titanium dioxide nanoparticles.* J Hazard Mater, 2011. **191**(1-3): p. 32-40.
66. Meena, R., S. Kumar, and R. Paulraj, *Titanium oxide (TiO2) nanoparticles in induction of apoptosis and inflammatory response in brain.* Journal of Nanoparticle Research, 2015. **17**(1): p. 49.
67. Yin, J., et al., *Aerosol inhalation exposure study of respiratory toxicity induced by 20 nm anatase titanium dioxide nanoparticles.* Toxicology Research, 2014. **3**(5): p. 367-374.
68. Jeon, Y.-M., S.-K. Park, and M.-Y. Lee, *Toxicoproteomic identification of TiO2 nanoparticle-induced protein expression changes in mouse brain.* Animal Cells and Systems, 2011. **15**(2): p. 107-114.
69. Zhang, R., et al., *Acute toxicity study of the interaction between titanium dioxide nanoparticles and lead acetate in mice.* Environmental Toxicology and Pharmacology, 2010. **30**(1): p. 52-60.
70. Davenport, L.L., et al., *Systemic and behavioral effects of intranasal administration of silver nanoparticles.* Neurotoxicology and teratology, 2015. **51**: p. 68-76.
71. Dan, M., et al., *Silver Nanoparticle Exposure Induces Neurotoxicity in the Rat Hippocampus Without Increasing the Blood-Brain Barrier Permeability.* J Biomed Nanotechnol, 2018. **14**(7): p. 1330-1338.
72. Rahman, M.F., et al., *Expression of genes related to oxidative stress in the mouse brain after exposure to silver-25 nanoparticles.* Toxicol Lett, 2009. **187**(1): p. 15-21.
73. Skalska, J., B. Dabrowska-Bouta, and L. Struzynska, *Oxidative stress in rat brain but not in liver following oral administration of a low dose of nanoparticulate silver.* Food Chem Toxicol, 2016. **97**: p. 307-315.
74. Greish, K., et al., *The Effect of Silver Nanoparticles on Learning, Memory and Social Interaction in BALB/C Mice.* International journal of environmental research and public health, 2019. **16**(1): p. 148.
75. Additives, E.Panel o.F., et al., *Re-evaluation of silicon dioxide (E 551) as a food additive.* EFSA Journal, 2018. **16**(1): p. e05088.
76. Murugadoss, S., et al., *Toxicology of silica nanoparticles: an update.* Arch Toxicol, 2017. **91**(9): p. 2967-3010.
77. Parveen, A., et al., *Silica nanoparticles mediated neuronal cell death in corpus striatum of rat brain: implication of mitochondrial, endoplasmic reticulum and oxidative stress.* Journal of Nanoparticle Research, 2014. **16**(11): p. 2664.
78. Verkhratsky, A., et al., *The Concept of Neuroglia.* Advances in experimental medicine and biology, 2019. **1175**: p. 1-13.
79. Jäkel, S. and L. Dimou, *Glial Cells and Their Function in the Adult Brain: A Journey through the History of Their Ablation.* Frontiers in Cellular Neuroscience, 2017. **11**(24).
80. Hickman, S., et al., *Microglia in neurodegeneration.* Nature neuroscience, 2018. **21**(10): p. 1359-1369.
81. Carroll, J.A. and B. Chesebro, *Neuroinflammation, Microglia, and Cell-Association during Prion Disease.* Viruses, 2019. **11**(1).
82. Wu, T. and M. Tang, *The inflammatory response to silver and titanium dioxide nanoparticles in the central nervous system.* Nanomedicine, 2017. **13**(2): p. 233-249.

83. Zhou, H., et al., *A requirement for microglial TLR4 in leukocyte recruitment into brain in response to lipopolysaccharide.* J Immunol, 2006. **177**(11): p. 8103-10.
84. Block, M.L., L. Zecca, and J.-S. Hong, *Microglia-mediated neurotoxicity: uncovering the molecular mechanisms.* Nature Reviews Neuroscience, 2007. **8**(1): p. 57-69.
85. Liddelow, S.A. and B.A. Barres, *Reactive Astrocytes: Production, Function, and Therapeutic Potential.* Immunity, 2017. **46**(6): p. 957-967.
86. Zhao, W., et al., *Protective effects of an anti-inflammatory cytokine, interleukin-4, on motoneuron toxicity induced by activated microglia.* J Neurochem, 2006. **99**(4): p. 1176-87.
87. Kwon, H.S. and S.-H. Koh, *Neuroinflammation in neurodegenerative disorders: the roles of microglia and astrocytes.* Translational neurodegeneration, 2020. **9**(1): p. 42-42.
88. Sofroniew, M.V. and H.V. Vinters, *Astrocytes: biology and pathology.* Acta neuropathologica, 2010. **119**(1): p. 7-35.
89. Zhou, B., Y.-X. Zuo, and R.-T. Jiang, *Astrocyte morphology: Diversity, plasticity, and role in neurological diseases.* CNS neuroscience & therapeutics, 2019. **25**(6): p. 665-673.
90. Zhou, Y., et al., *Dual roles of astrocytes in plasticity and reconstruction after traumatic brain injury.* Cell communication and signaling : CCS, 2020. **18**(1): p. 62-62.
91. Li, D., et al., *Neurochemical regulation of the expression and function of glial fibrillary acidic protein in astrocytes.* Glia, 2020. **68**(5): p. 878-897.
92. Levesque, S., et al., *Diesel exhaust activates and primes microglia: air pollution, neuroinflammation, and regulation of dopaminergic neurotoxicity.* Environmental health perspectives, 2011. **119**(8): p. 1149-1155.
93. De Astis, S., et al., *Nanostructured TiO2 surfaces promote polarized activation of microglia, but not astrocytes, toward a proinflammatory profile.* Nanoscale, 2013. **5**(22): p. 10963-10974.
94. Zhang, F., et al., *Microglial migration and interactions with dendrimer nanoparticles are altered in the presence of neuroinflammation.* Journal of Neuroinflammation, 2016. **13**(1): p. 65.
95. Grissa, I., et al., *The effect of titanium dioxide nanoparticles on neuroinflammation response in rat brain.* Environmental Science and Pollution Research, 2016. **23**(20): p. 20205-20213.
96. Guerra, R., et al., *Exposure to inhaled particulate matter activates early markers of oxidative stress, inflammation and unfolded protein response in rat striatum.* Toxicology letters, 2013. **222**(2): p. 146-154.
97. Ze, Y., et al., *TiO2 Nanoparticles Induced Hippocampal Neuroinflammation in Mice.* PLOS ONE, 2014. **9**(3): p. e92230.
98. You, R., et al., *Silica nanoparticles induce neurodegeneration-like changes in behavior, neuropathology, and affect synapse through MAPK activation.* Particle and fibre toxicology, 2018. **15**(1): p. 28-28.
99. Hampel, R., et al., *Long-term effects of elemental composition of particulate matter on inflammatory blood markers in European cohorts.* Environ Int, 2015. **82**: p. 76-84.
100. Block, M.L., *Modulating mighty microglia.* Nature Chemical Biology, 2014. **10**: p. 988.
101. Rubinsztein, D.C., *The roles of intracellular protein-degradation pathways in neurodegeneration.* Nature, 2006. **443**(7113): p. 780-6.
102. Bredesen, D.E., R.V. Rao, and P. Mehlen, *Cell death in the nervous system.* Nature, 2006. **443**(7113): p. 796-802.
103. Prince, M.J., et al., *World Alzheimer Report 2015-The Global Impact of Dementia: An analysis of prevalence, incidence, cost and trends.* 2015.

104. Wu, Y.T., et al., *The changing prevalence and incidence of dementia over time - current evidence.* Nat Rev Neurol, 2017. **13**(6): p. 327-339.
105. Nichols, E., et al., *Global, regional, and national burden of Alzheimer's disease and other dementias, 1990–2016: a systematic analysis for the Global Burden of Disease Study 2016.* The Lancet Neurology, 2019. **18**(1): p. 88-106.
106. *2020 Alzheimer's disease facts and figures.* Alzheimer's & Dementia, 2020. **16**(3): p. 391-460.
107. Masters, C.L. and K. Beyreuther, *Alzheimer's disease: molecular basis of structural lesions.* Brain Pathol, 1991. **1**(4): p. 226-7.
108. Selkoe, D.J., *Alzheimer's disease results from the cerebral accumulation and cytotoxicity of amyloid beta-protein.* J Alzheimers Dis, 2001. **3**(1): p. 75-80.
109. Alzheimer, A., et al., *An English translation of Alzheimer's 1907 paper, "Uber eine eigenartige Erkankung der Hirnrinde".* Clin Anat, 1995. **8**(6): p. 429-31.
110. DeTure, M.A. and D.W. Dickson, *The neuropathological diagnosis of Alzheimer's disease.* Molecular neurodegeneration, 2019. **14**(1): p. 32-32.
111. Braak, H. and E. Braak, *Frequency of Stages of Alzheimer-Related Lesions in Different Age Categories.* Neurobiology of Aging, 1997. **18**(4): p. 351-357.
112. Oakley, H., et al., *Intraneuronal beta-amyloid aggregates, neurodegeneration, and neuron loss in transgenic mice with five familial Alzheimer's disease mutations: potential factors in amyloid plaque formation.* J Neurosci, 2006. **26**(40): p. 10129-40.
113. van Groen, T., et al., *The Aβ oligomer eliminating D-enantiomeric peptide RD2 improves cognition without changing plaque pathology.* Scientific reports, 2017. **7**(1): p. 16275-16275.
114. Hardy, J.A. and G.A. Higgins, *Alzheimer's disease: the amyloid cascade hypothesis.* Science, 1992. **256**(5054): p. 184-5.
115. Gremer, L., et al., *Fibril structure of amyloid-β(1-42) by cryo-electron microscopy.* Science (New York, N.Y.), 2017. **358**(6359): p. 116-119.
116. Kim, T.W., et al., *Selective localization of amyloid precursor-like protein 1 in the cerebral cortex postsynaptic density.* Brain Res Mol Brain Res, 1995. **32**(1): p. 36-44.
117. Selkoe, D.J., *The cell biology of beta-amyloid precursor protein and presenilin in Alzheimer's disease.* Trends Cell Biol, 1998. **8**(11): p. 447-53.
118. Zhang, Y.-w., et al., *APP processing in Alzheimer's disease.* Molecular brain, 2011. **4**: p. 3-3.
119. Steiner, H., R. Fluhrer, and C. Haass, *Intramembrane proteolysis by gamma-secretase.* The Journal of biological chemistry, 2008. **283**(44): p. 29627-29631.
120. Michno, W., et al., *Refining the amyloid β peptide and oligomer fingerprint ambiguities in Alzheimer's disease: Mass spectrometric molecular characterization in brain, cerebrospinal fluid, blood, and plasma.* Journal of Neurochemistry, 2021. **159**(2): p. 234-257.
121. Vassar, R., et al., *Beta-secretase cleavage of Alzheimer's amyloid precursor protein by the transmembrane aspartic protease BACE.* Science, 1999. **286**(5440): p. 735-41.
122. Zhao, J., et al., *Targeting Amyloidogenic Processing of APP in Alzheimer's Disease.* Frontiers in Molecular Neuroscience, 2020. **13**(137).
123. Hampel, H., et al., *The β-Secretase BACE1 in Alzheimer's Disease.* Biological psychiatry, 2021. **89**(8): p. 745-756.
124. Wolfe, M.S., *The gamma-secretase complex: membrane-embedded proteolytic ensemble.* Biochemistry, 2006. **45**(26): p. 7931-9.
125. Wolfe, M.S., et al., *Two transmembrane aspartates in presenilin-1 required for presenilin endoproteolysis and gamma-secretase activity.* Nature, 1999. **398**(6727): p. 513-7.

126. Wolfe, M.S., *When loss is gain: reduced presenilin proteolytic function leads to increased Abeta42/Abeta40. Talking Point on the role of presenilin mutations in Alzheimer disease.* EMBO Rep, 2007. **8**(2): p. 136-40.
127. Bray, S.J., *Notch signalling in context.* Nature Reviews Molecular Cell Biology, 2016. **17**(11): p. 722-735.
128. Güner, G. and S.F. Lichtenthaler, *The substrate repertoire of γ-secretase/presenilin.* Seminars in Cell & Developmental Biology, 2020. **105**: p. 27-42.
129. Haass, C. and D.J. Selkoe, *Cellular processing of beta-amyloid precursor protein and the genesis of amyloid beta-peptide.* Cell, 1993. **75**(6): p. 1039-42.
130. Naus, S., et al., *Identification of candidate substrates for ectodomain shedding by the metalloprotease-disintegrin ADAM8.* Biol Chem, 2006. **387**(3): p. 337-46.
131. Kuhn, P.H., et al., *ADAM10 is the physiologically relevant, constitutive alpha-secretase of the amyloid precursor protein in primary neurons.* Embo j, 2010. **29**(17): p. 3020-32.
132. Postina, R., et al., *A disintegrin-metalloproteinase prevents amyloid plaque formation and hippocampal defects in an Alzheimer disease mouse model.* J Clin Invest, 2004. **113**(10): p. 1456-64.
133. Goodman, Y. and M.P. Mattson, *Secreted forms of beta-amyloid precursor protein protect hippocampal neurons against amyloid beta-peptide-induced oxidative injury.* Exp Neurol, 1994. **128**(1): p. 1-12.
134. Gralle, M., M.G. Botelho, and F.S. Wouters, *Neuroprotective secreted amyloid precursor protein acts by disrupting amyloid precursor protein dimers.* J Biol Chem, 2009. **284**(22): p. 15016-25.
135. Obregon, D., et al., *Soluble amyloid precursor protein-α modulates β-secretase activity and amyloid-β generation.* Nat Commun, 2012. **3**: p. 777.
136. Wetzel, S., L. Seipold, and P. Saftig, *The metalloproteinase ADAM10: A useful therapeutic target?* Biochimica et Biophysica Acta (BBA) - Molecular Cell Research, 2017. **1864**(11, Part B): p. 2071-2081.
137. Manzine, P.R., et al., *ADAM10 in Alzheimer's disease: Pharmacological modulation by natural compounds and its role as a peripheral marker.* Biomedicine & Pharmacotherapy, 2019. **113**: p. 108661.
138. Goate, A., et al., *Segregation of a missense mutation in the amyloid precursor protein gene with familial Alzheimer's disease.* Nature, 1991. **349**(6311): p. 704-6.
139. Hebert, L.E., et al., *Alzheimer disease in the United States (2010-2050) estimated using the 2010 census.* Neurology, 2013. **80**(19): p. 1778-83.
140. Verghese, P.B., J.M. Castellano, and D.M. Holtzman, *Apolipoprotein E in Alzheimer's disease and other neurological disorders.* The Lancet Neurology, 2011. **10**(3): p. 241-252.
141. Chin-Chan, M., J. Navarro-Yepes, and B. Quintanilla-Vega, *Environmental pollutants as risk factors for neurodegenerative disorders: Alzheimer and Parkinson diseases.* Frontiers in cellular neuroscience, 2015. **9**: p. 124-124.
142. Calderón-Garcidueñas, L., et al., *Early Alzheimer's and Parkinson's Disease Pathology in Urban Children: Friend versus Foe Responses—It Is Time to Face the Evidence.* BioMed Research International, 2013. **2013**: p. 161687.
143. Serrano-Pozo, A. and J.H. Growdon, *Is Alzheimer's Disease Risk Modifiable?* Journal of Alzheimer's disease : JAD, 2019. **67**(3): p. 795-819.
144. Rahman, M.A., et al., *Exposure to Environmental Arsenic and Emerging Risk of Alzheimer's Disease: Perspective Mechanisms, Management Strategy, and Future Directions.* Toxics, 2021. **9**(8): p. 188.

145. Akanji, M.A., et al., *Redox Homeostasis and Prospects for Therapeutic Targeting in Neurodegenerative Disorders.* Oxidative medicine and cellular longevity, 2021. **2021**: p. 9971885-9971885.
146. Domingues, C., O.A.B. da Cruz E Silva, and A.G. Henriques, *Impact of Cytokines and Chemokines on Alzheimer's Disease Neuropathological Hallmarks.* Current Alzheimer research, 2017. **14**(8): p. 870-882.
147. Tobore, T.O., *On the central role of mitochondria dysfunction and oxidative stress in Alzheimer's disease.* Neurological Sciences, 2019. **40**(8): p. 1527-1540.
148. Ionescu-Tucker, A. and C.W. Cotman, *Emerging roles of oxidative stress in brain aging and Alzheimer's disease.* Neurobiology of Aging, 2021. **107**: p. 86-95.
149. Butterfield, D.A. and D. Boyd-Kimball, *Oxidative Stress, Amyloid-β Peptide, and Altered Key Molecular Pathways in the Pathogenesis and Progression of Alzheimer's Disease.* Journal of Alzheimer's disease : JAD, 2018. **62**(3): p. 1345-1367.
150. Cheignon, C., et al., *Oxidative stress and the amyloid beta peptide in Alzheimer's disease.* Redox Biology, 2018. **14**: p. 450-464.
151. Wang, L., et al., *Current understanding of metal ions in the pathogenesis of Alzheimer's disease.* Translational Neurodegeneration, 2020. **9**(1): p. 10.
152. Lovell, M.A., et al., *Copper, iron and zinc in Alzheimer's disease senile plaques.* Journal of the Neurological Sciences, 1998. **158**(1): p. 47-52.
153. Guglielmotto, M., et al., *The up-regulation of BACE1 mediated by hypoxia and ischemic injury: role of oxidative stress and HIF1alpha.* J Neurochem, 2009. **108**(4): p. 1045-56.
154. Romanenko, M., et al., *Nutrition, Gut Microbiota, and Alzheimer's Disease.* Frontiers in psychiatry, 2021. **12**: p. 712673-712673.
155. WHO, *Air pollution.* 2021.
156. Ranft, U., et al., *Long-term exposure to traffic-related particulate matter impairs cognitive function in the elderly.* Environ Res, 2009. **109**(8): p. 1004-11.
157. Fu, P. and K.K.L. Yung, *Air Pollution and Alzheimer's Disease: A Systematic Review and Meta-Analysis.* Journal of Alzheimer's Disease, 2020. **77**: p. 701-714.
158. Møller, P., et al., *Role of oxidative damage in toxicity of particulates.* Free Radic Res, 2010. **44**(1): p. 1-46.
159. Calderón-Garcidueñas, L., et al., *Brain inflammation and Alzheimer's-like pathology in individuals exposed to severe air pollution.* Toxicol Pathol, 2004. **32**(6): p. 650-8.
160. Calderón-Garcidueñas, L., et al., *Alzheimer disease starts in childhood in polluted Metropolitan Mexico City. A major health crisis in progress.* Environmental Research, 2020. **183**: p. 109137.
161. Calderón-Garcidueñas, L., et al., *Reduced repressive epigenetic marks, increased DNA damage and Alzheimer's disease hallmarks in the brain of humans and mice exposed to particulate urban air pollution.* Environmental Research, 2020. **183**: p. 109226.
162. Gerlofs-Nijland, M.E., et al., *Effect of prolonged exposure to diesel engine exhaust on proinflammatory markers in different regions of the rat brain.* Part Fibre Toxicol, 2010. **7**: p. 12.
163. van Berlo, D., et al., *Comparative evaluation of the effects of short-term inhalation exposure to diesel engine exhaust on rat lung and brain.* Archives of toxicology, 2010. **84**(7): p. 553-562.
164. Hullmann, M., et al., *Diesel engine exhaust accelerates plaque formation in a mouse model of Alzheimer's disease.* Particle and Fibre Toxicology, 2017. **14**: p. 35.
165. Levesque, S., et al., *Air pollution & the brain: Subchronic diesel exhaust exposure causes neuroinflammation and elevates early markers of neurodegenerative disease.* Journal of neuroinflammation, 2011. **8**: p. 105-105.

166. Shi, Y., A.R. Pilozzi, and X. Huang, *Exposure of CuO Nanoparticles Contributes to Cellular Apoptosis, Redox Stress, and Alzheimer's Aβ Amyloidosis.* International journal of environmental research and public health, 2020. **17**(3): p. 1005.
167. Huang, C.-L., et al., *Silver nanoparticles affect on gene expression of inflammatory and neurodegenerative responses in mouse brain neural cells.* Environmental Research, 2015. **136**: p. 253-263.
168. Yang, X., et al., *Uptake of silica nanoparticles: neurotoxicity and Alzheimer-like pathology in human SK-N-SH and mouse neuro2a neuroblastoma cells.* Toxicol Lett, 2014. **229**(1): p. 240-9.
169. Sims, C.M., et al., *Redox-active nanomaterials for nanomedicine applications.* Nanoscale, 2017. **9**(40): p. 15226-15251.
170. Eleftheriadou, D., et al., *Redox-Responsive Nanobiomaterials-Based Therapeutics for Neurodegenerative Diseases.* Small, 2020. **16**(43): p. e1907308.
171. Su, H., et al., *Potential applications and human biosafety of nanomaterials used in nanomedicine.* J Appl Toxicol, 2018. **38**(1): p. 3-24.
172. Agwa, M.M. and S. Sabra, *Lactoferrin coated or conjugated nanomaterials as an active targeting approach in nanomedicine.* Int J Biol Macromol, 2021. **167**: p. 1527-1543.
173. Sriramoju, B., R.K. Kanwar, and J.R. Kanwar, *Nanomedicine based nanoparticles for neurological disorders.* Curr Med Chem, 2014. **21**(36): p. 4154-68.
174. Manek, E., F. Darvas, and G.A. Petroianu, *Use of Biodegradable, Chitosan-Based Nanoparticles in the Treatment of Alzheimer's Disease.* Molecules, 2020. **25**(20).
175. Yavarpour-Bali, H., M. Ghasemi-Kasman, and M. Pirzadeh, *Curcumin-loaded nanoparticles: a novel therapeutic strategy in treatment of central nervous system disorders.* Int J Nanomedicine, 2019. **14**: p. 4449-4460.
176. Hülsemann, M., et al., *Biofunctionalized Silica Nanoparticles: Standards in Amyloid-β Oligomer-Based Diagnosis of Alzheimer's Disease.* J Alzheimers Dis, 2016. **54**(1): p. 79-88.
177. Yao, H.C. and Y.F.Y. Yao, *Ceria in automotive exhaust catalysts: I. Oxygen storage.* Journal of Catalysis, 1984. **86**(2): p. 254-265.
178. Dahle, J.T. and Y. Arai, *Environmental geochemistry of cerium: applications and toxicology of cerium oxide nanoparticles.* Int J Environ Res Public Health, 2015. **12**(2): p. 1253-78.
179. Estevez, A.Y., et al., *Neuroprotective mechanisms of cerium oxide nanoparticles in a mouse hippocampal brain slice model of ischemia.* Free Radic Biol Med, 2011. **51**(6): p. 1155-63.
180. Pulido-Reyes, G., et al., *Untangling the biological effects of cerium oxide nanoparticles: the role of surface valence states.* Scientific Reports, 2015. **5**(1): p. 15613.
181. Heckert, E.G., et al., *The role of cerium redox state in the SOD mimetic activity of nanoceria.* Biomaterials, 2008. **29**(18): p. 2705-9.
182. Pirmohamed, T., et al., *Nanoceria exhibit redox state-dependent catalase mimetic activity.* Chem Commun (Camb), 2010. **46**(16): p. 2736-8.
183. Rodriguez, J.A., et al., *Properties of CeO2 and Ce1-xZrxO2 Nanoparticles: X-ray Absorption Near-Edge Spectroscopy, Density Functional, and Time-Resolved X-ray Diffraction Studies.* The Journal of Physical Chemistry B, 2003. **107**(15): p. 3535-3543.
184. Tsai, Y.Y., et al., *Reactive oxygen species scavenging properties of ZrO2-CeO2 solid solution nanoparticles.* Nanomedicine (Lond), 2008. **3**(5): p. 637-45.
185. Hegazy, M.A., et al., *Cerium oxide nanoparticles could ameliorate behavioral and neurochemical impairments in 6-hydroxydopamine induced Parkinson's disease in rats.* Neurochemistry International, 2017. **108**: p. 361-371.

186. Kim, D., H.J. Kwon, and T. Hyeon, *Magnetite/Ceria Nanoparticle Assemblies for Extracorporeal Cleansing of Amyloid-β in Alzheimer's Disease.* Advanced Materials, 2019. **31**(19): p. 1807965.
187. Elshony, N., et al., *Ameliorative Role of Cerium Oxide Nanoparticles Against Fipronil Impact on Brain Function, Oxidative Stress, and Apoptotic Cascades in Albino Rats.* Frontiers in neuroscience, 2021. **15**: p. 651471-651471.
188. Wu, J., et al., *Neurotoxicity of Silica Nanoparticles: Brain Localization and Dopaminergic Neurons Damage Pathways.* ACS Nano, 2011. **5**(6): p. 4476-4489.
189. Liu, Y., et al., *Oxidative stress and acute changes in murine brain tissues after nasal instillation of copper particles with different sizes.* J Nanosci Nanotechnol, 2014. **14**(6): p. 4534-40.
190. Calderon-Garciduenas, L., et al., *Air Pollution, Combustion and Friction Derived Nanoparticles, and Alzheimer's Disease in Urban Children and Young Adults.* J Alzheimers Dis, 2019. **70**(2): p. 343-360.
191. OECD, *Test No. 424: Neurotoxicity Study in Rodents*. 1997.
192. Devi, L., et al., *Sex- and brain region-specific acceleration of beta-amyloidogenesis following behavioral stress in a mouse model of Alzheimer's disease.* Mol Brain, 2010. **3**: p. 34.
193. Methia, N., et al., *ApoE deficiency compromises the blood brain barrier especially after injury.* Mol Med, 2001. **7**(12): p. 810-5.

2 Evaluation of the neurotoxic effects of engineered nanomaterials in C57BL/6J mice in 28-day oral exposure studies

Adriana Sofranko[1], Tina Wahle[1], Harm J. Heusinkveld[2], Burkhard Stahlmecke[3], Michail Dronov[3], Dirk Pijnenburg[4], Riet Hilhorst[4], Karsten Lamann[5,6], Catrin Albrecht[1], Roel P.F. Schins[1]

[1]IUF - Leibniz Research Institute for Environmental Medicine, Düsseldorf, Germany; [2]National Institute for Public Health and the Environment (RIVM), Bilthoven, The Netherlands; [3]Institute for Energy and Environmental Technology e.V. (IUTA), Duisburg, Germany; [4]PamGene International B.V., 's-Hertogenbosch, The Netherlands; [5]Tascon GmbH, Münster, Germany; [6]University of Münster, Institute of Inorganic and Analytical Chemistry, Münster, Germany

Neurotoxicology. 2021 May, 84:155-171
Doi: 10.1016/j.neuro.2021.03.005

Author contribution: The author of this dissertation was involved in the design and planning of the *in vivo* study, handled and weighed the mice in the animal facility during the whole study, performed behaviour tests, neuroinflammation, oxidative stress and BBB integrity analyses, processed and shipped brain (tissue) sections from mice for ICP-MS, ToF-SIMS and LA analyses, wrote the manuscript, made the graphs and discussed the results. Relative contribution: about 70%.

2.1 Abstract

In recent years, concerns have emerged about the potential neurotoxic effects of engineered nanomaterials (NMs). Titanium dioxide and silver are among the most widely used types of metallic NMs. We have investigated the effects of these NMs on behaviour and neuropathology in male and female C57BL/6J mice following 28-day oral exposure with or without a 14-day post-exposure recovery. The mice were fed *ad libitum* with food pellets dosed with 10 mg/g TiO_2, 2 mg/g polyvinylpyrrolidone-coated Ag or control pellets. Behaviour was evaluated by X-maze, open field, string suspension and rotarod tests. Histological alterations were analysed by immunohistochemistry and brain tissue homogenates were investigated for markers of oxidative stress, inflammation and blood-brain barrier disruption. Effects of the NMs on tyrosine and serine/threonine protein kinase activity in mouse brains were investigated by measuring kinase activity on peptide microarrays.

Markers of inflammation, oxidative stress and blood-brain barrier integrity were not significantly affected in the male and female mice following exposure to Ag or TiO_2. Both types of NMs also revealed no consistent significant treatment-related effects on anxiety and cognition. However, in the Ag NM exposed mice altered motor performance effects were observed by the rotarod test that differed between sexes. At 1-week post-exposure, a diminished performance in this test was observed exclusively in the female animals. Cortex tissues of female mice also showed a pronounced increase in tyrosine kinase activity following 28 days oral exposure to Ag NM. A subsequent Inductively Coupled Plasma - Mass Spectrometry (ICP-MS) based toxicokinetic study in female mice revealed a rapid and persistent accumulation of Ag in various internal organs including liver, kidney, spleen and the brain up to 4 weeks post-exposure. In conclusion, our study demonstrated that subacute exposure to foodborne TiO_2 and Ag NMs does not cause substantial neuropathological changes in mice. However, the toxicokinetic and specific toxicodynamic findings indicate that long-term exposures to Ag NM can cause neurotoxicity, possibly in a sex-dependent manner.

Key words: silver, TiO_2, 28-day oral, neurobehavioural testing, kinase activity, peptide microarray

2.2 Introduction

The widespread use of engineered metallic nanomaterials (NMs) in various consumer products has led to a growing concern about their adverse effects on human health. Depending on their physico-chemical properties (e.g. size, agglomeration, surface reactivity) and their route of exposure (e.g. inhalation, ingestion, dermal exposure, intravenous application), NMs may be

absorbed into the body and distributed to different secondary target organs and tissues (Oberdörster *et al.* 2005). In recent years, there has been increasing interest in the investigation of the central nervous system (CNS) as target organ for NMs (Boyes *et al.* 2012; Boyes and van Thriel 2020). Initial awareness of the potential adverse effects of nanosize particles on the CNS came with a study that demonstrated translocation of ultrafine particles into the brains of rats upon short-term inhalation exposure (Oberdörster *et al.* 2004). Since then, several rodent inhalation studies have provided support for the effects of nanoparticles on the brain and, thereby, revealed a mechanistic link to epidemiological studies that show an association between exposure to ambient air pollution particles and neurological diseases (reviewed by (Heusinkveld *et al.* 2016)). While inhalation represents the primary exposure route for ambient (nanosize) particles as well as for many bulk-manufactured NMs in occupational settings, oral exposure to NMs has also become a topic of increasing investigation. Concerns about the adverse health effects of ingested NMs, including neurotoxicity, have emerged with the growing number of applications in nanomedicine and, in particular, the food sector where NMs are used e.g. as food additives or in food packaging (Bouwmeester *et al.* 2009; Sohal *et al.* 2018).

For inhalation exposure, the translocation of NMs via the olfactory nerve into the brain has emerged as an important exposure route (Heusinkveld *et al.* 2016; Oberdörster *et al.* 2005). However, for ingested NMs, brain targeting of these particulate entities or their dissolved compounds requires the translocation from the gastrointestinal tract into the circulation and subsequent passage of the blood-brain barrier (BBB). Absorption from the gastrointestinal tract has been shown for various NMs, including silver (Ag) and titanium dioxide (TiO_2) (Geraets *et al.* 2014; Kreyling *et al.* 2017; Lee *et al.* 2019; Wang *et al.* 2007; Boudreau *et al.* 2016; Loeschner *et al.* 2011; van der Zande *et al.* 2012). Furthermore, crossing of the BBB and accumulation into the CNS has been suggested for Ag and TiO_2 in several studies that applied intravenous or oral administration (Kreyling *et al.* 2017; Lee *et al.* 2019; Fabian *et al.* 2008; Disdier *et al.* 2015; Loeschner *et al.* 2011; Recordati *et al.* 2015; van der Zande *et al.* 2012). Ag and TiO_2 have also been reported to disrupt the BBB integrity (Trickler *et al.* 2010; Brun *et al.* 2012; Xu *et al.* 2015).

The main mechanisms whereby NMs can cause neurotoxicity in the CNS are thought to be through the induction of oxidative stress and inflammation (Feng *et al.* 2015; Song *et al.* 2016; Boyes and van Thriel 2020). Because of its high content of polyunsaturated fatty acids and low concentrations of antioxidants and antioxidant enzymes, the brain is more sensitive to oxidative stress than other tissues (Valko *et al.* 2007; Oberdörster *et al.* 2009; Islam 2017).

Indeed, increased levels of the lipid peroxidation marker malondialdehyde (MDA) and changes in the glutathione antioxidant defense system have been shown in the brain but not in the liver of rats after repeated oral gavage application of Ag NM (Skalska *et al.* 2016).

Despite the increasing number of neurotoxicological studies on metallic NMs, their role in neuroinflammation has not yet been well understood. It is suggested to result from their ability to activate microglia and astrocytes. Activation of these glial cell types results in secretion of mediators triggering neuronal repair or the release of proinflammatory cytokines and ROS, resulting in neuroinflammation (Mayer *et al.* 2013). Increased expression of the glial fibrillary acidic protein (GFAP), which is expressed in astrocytes (Sofroniew and Vinters 2010), and ionized calcium-binding adapter molecule 1 (IBA-1), which is expressed upon activation of microglia (Kovacs 2017) are therefore recognised as important markers of neuroinflammation. In response to exposure to NMs, microglia cells have been shown to enhance the release of proinflammatory cytokines, whereas astrocytes prefer to increase the production of anti-inflammatory factors (Wu and Tang 2017). The acute innate pro-inflammatory cytokines tumour necrosis factor α (TNF-α), interleukin 1β (IL-1β) and IL-6 are all regulated by mitogen activated protein kinase (MAPK) signalling pathway (Wu and Tang 2017). These serine-threonine protein kinases regulate cellular activities including proliferation, differentiation, apoptosis or survival and inflammation (Kim and Choi 2015). Tyrosine kinases represent another type of protein kinase that regulate the majority of cellular pathways as well. They can be subdivided into the receptor tyrosine kinases which have extra-cellular ligand-binding domains and the cytoplasmic (i.e. nonreceptor) tyrosine kinases (Shah *et al.* 2018). Altered activities of protein kinase signalling pathways have been implicated in the pathology of diverse human diseases including cancer and neurodegeneration (Dhillon *et al.* 2007; Rosenberger *et al.* 2016) .

In this study, we investigated the potential neurotoxic effects of two different types of NMs in male and female C57BL/6J mice in a 28-day oral repeated exposure design including a 14-day post-exposure recovery period. We choose TiO_2 and Ag since these are widely used metal based NMs in numerous consumer applications and products (Vance *et al.* 2015; FAO/WHO 2010). Oral exposure studies with NMs in rodents predominantly have used gavage as the method of their administration. However, while this bolus application procedure ensures a precise dosimetry, it poorly represents the way in which humans may typically be exposed. Accordingly, in our present study, we explored the effects of the TiO_2 and Ag NMs by their incorporation into the mouse feed pellets. The aim of our study was to explore the effects of repeated oral exposures to these NMs on neurobehaviour and expression of markers of

oxidative stress, inflammation and blood-brain-barrier disruption, with specific evaluation of sex-specificity of treatment-related changes. Effects of the NMs on tyrosine and serine/threonine protein kinases activity were investigated using peptide microarrays.

2.3 Materials and Methods

2.3.1 Nanomaterials.

For this study, we used TiO_2-P25 (JRC reference nanomaterial NM105) and 0.2% polyvinylpyrrolidone (PVP) coated Ag (Sigma-Aldrich, USA: #576832-5G, Lot #MKBX3387V). Scanning electron microscopy (SEM) imaging of the NMs was performed to determine the morphology, size distribution and primary particle size of the specific batch of the NMs that were used in our study. The size distribution of the TiO_2 NM displayed a mean size of 26.2 nm ± 10.7 nm and a nearly spherical particle morphology. The mode diameter obtained by a fit using a lognormal size distribution has a value of d_{mode} = 21.0 nm with σ = 1.39. The Ag NM showed a spherical morphology as well. The mean size of the Ag NM was determined to be 40.2 ± 17.6 nm and the mode diameter has a value of d_{mode} = 32.0 nm with σ = 1.40.

2.3.2 Study design.

Female and male C57Bl/6J mice were purchased from Janvier Labs in Le Genest-Saint-Isle, France at the age of 5 weeks. The mice were housed under standard conditions with a sequence of 12 h light and 12 h dark artificial lighting and access to food and water *ad libitum*. Two independent studies were performed, a toxicodynamic and a subsequent toxicokinetic study. In the design of the toxicodynamic study, 10 mice per sex and treatment group for the behaviour tests was chosen to align with the recommendations of the OECD TG 424 (OECD 1997). By combining the two NMs treatments in this study only one control group was required, thus reducing the number of mice in compliance with animal research ethical guidelines. In addition, we assumed for the toxicokinetic study that there would be no major sex-specific effects on distribution and therefore selected only one sex in our animal application. All mice were handled according to guidelines of the Society for Laboratory Animals Science (GV-SOLAS). The studies were approved by the Landesamt für Natur, Umwelt und Verbraucherschutz (LANUV) (Ref.nr.84-02.04.2017.A338). The toxicodynamic study was designed using 10 female and 10 male mice per treatment group (i.e. control, TiO_2 and Ag) and time point, referred to as substudy I (i.e. 28 days oral exposure) and substudy II (i.e. 28 days exposure followed by 14 days recovery), as shown in Figure 2.1. For these investigations, the mice were randomised

and acclimated in groups of 5 animals per cage at least one week before starting the exposure. The oral exposures were started at an age of six weeks.

The mice were fed with 1% TiO_2 or 0.2% Ag NMs (w/w) incorporated into the feed pellets *ad libitum* for 28 days with or without a subsequent 14 days post-exposure recovery period. The amount of TiO_2 introduced in the feed equals its maximum permitted percentage as feed additive by the US Food and Drug Administration (FDA 2020). For Ag NM the lower dose was selected because of the intrinsic higher oral toxicity as observed with this NM in comparison to TiO_2, for instance, in sub-chronic oral gavage studies in rats (Kim *et al.* 2010; Heo *et al.* 2020). Based on an estimated daily feed consumption of 4 g and average body weight of 20 g this results in a daily intake of about 2 g/kg bodyweight (BW) for TiO_2 and 0.4 g/kg BW for the Ag NMs. The feed pellets were prepared and provided by ssniff GmbH, Soest, Germany. Appropriate dosing of the NMs was verified by Inductively Coupled Plasma - Mass Spectrometry (ICP-MS) analysis and additional RFA (x-ray fluorescence analysis) investigations. Furthermore, the presence of NMs was confirmed using SEM/EDS (Scanning Electron Microscopy/ Energy Dispersive X-Ray Spectroscopy) spectrum investigation (see Supplementary Material - S1). Mice of the control groups (and all mice during the post-exposure period) received pellets from the same batch of feed without the added NMs.

.

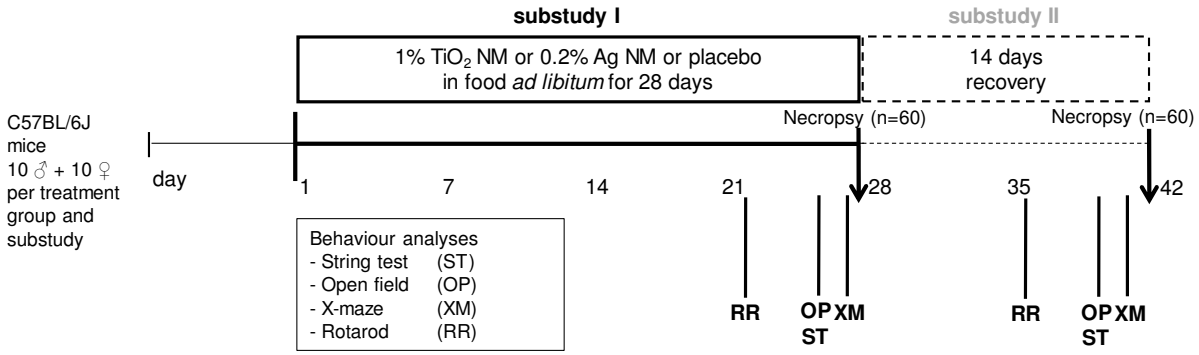

Figure 2.1. Neurotoxicity study design. About six weeks old male and female C57BL/6J mice were exposed to 1% TiO_2 or 0.2% Ag nanomaterials (NMs) in feed pellets *ad libitum* for 28 days (substudy I) or for 28 days followed by a 14 days post exposure recovery period (substudy II). Motor function, learning and memory were determined in a series of behaviour tests performed in the weeks before the necropsies, as follows for the respective substudies: The rotarod test (RR) was performed on exposure day 21 and post-exposure day 7, the open field (OP) and string test (ST) were both performed on exposure day 24 and postexposure day 12, and the X-maze test (XM) was performed on exposure day 27 and post exposure day 13. Markers of neuroinflammation, oxidative stress, blood-brain barrier integrity as well as kinase activity were determined in the brains of the mice after necropsy.

Behaviour studies were performed in the weeks before the sacrifice, to evaluate the potential effects of the NMs on motor function, anxiety, learning and memory. The string test was applied to evaluate grip strength and agility, the rotarod test was used to assess motor performance and skill learning, the X-maze test allowed for the evaluation of spatial working memory and the

open field test was included to assess for anxiety. At the time points of sacrifice, body weights were determined, the mouse brains were then dissected for immunohistochemical, biochemical and kinase activity analyses. Liver, kidney and spleen were isolated and weighed. The design of this study is shown in Figure 2.1.

2.3.3 **Design of the toxicokinetic study.**

An independent toxicokinetic study was performed to assess the availability of the NMs from the food pellets and translocation from the intestine. Therefore, inductively Coupled Plasma - Mass Spectrometry (ICP-MS) was used to evaluate the distribution of Ti or Ag in the mice at various time points during and post-exposure in the small intestine, blood, brain, liver, kidney and spleen. This additional kinetic study was designed according to the scheme shown in Figure 2.2, and performed in only one sex (female mice) due to animal ethical reasons. One week before exposure start, the mice were randomised and acclimated in groups of 6 animals per cage. At the start of the study, the C57BL/6J mice were about 6 weeks old and were fed with the feed pellets dosed with 1% TiO_2 or 0.2% Ag NMs or control feed. For the toxicokinetic analysis, three animals per treatment group and time point were sacrificed as indicated in Figure 2.2. For the 1-day exposure time point of this kinetic study, a group of additional mice was exposed in parallel via the method of oral gavage administration at equivalent (estimated) dose. Accordingly, the mice were treated either with 40 mg TiO_2 NM, 8 mg Ag NM or H_2O (vehicle) by single gavage (400 µl) (n=3 per treatment group) and sacrificed after 24 hours for comparative toxicokinetic analysis.

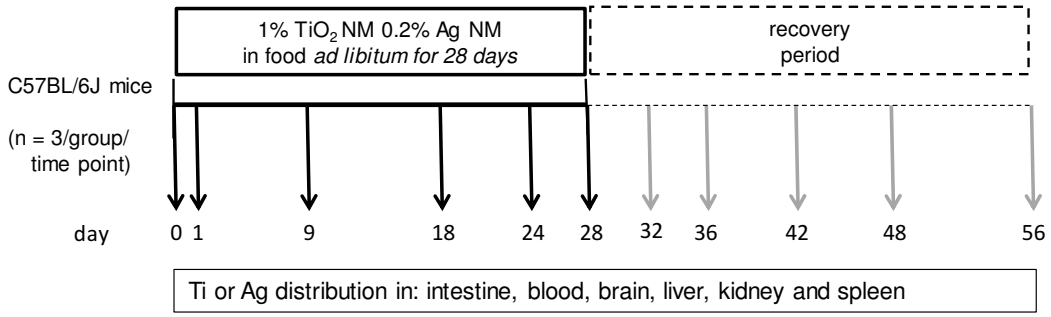

Figure 2.2. Study design kinetic study. About six weeks old female C57BL/6J mice were exposed to 1% TiO_2 or 0.2% Ag nanomaterials (NMs) in feed pellets *ad libitum* for up to 28 days and a subsequent post-exposure period up to 28 days (i.e. n=3 per time treatment and time point). The distribution of Ti and Ag was assessed at the specified time points by Inductively Coupled Plasma – Mass Spectrometry (ICP-MS) in the small intestine, blood, brain, liver, kidney and spleen.

2.3.4 **Behavioural tests.**

The behaviour tests in the 28 days and the 42 days substudies were performed, respectively, during the last week of the exposure period and in the second week of the recovery period. The

specific test days for the various tests are indicated in Figure 2.1. In alignment with animal ethics, requirements and routine of our animal facility all behaviour tasks were performed during daytime, i.e. during the resting phase of the animals. Motor function of the mice was tested using the string test and the rotarod test. The rotarod test (Ugo Basile, Italy) evaluates motor performance and motor skill learning, as follows: The mice were trained to run on the horizontal rotating rod with accelerating speed from 5 to 40 rpm during a 300 sec testing trial, which was repeated three times in one day. The increase in performance over time during the multiple testing trials is defined as skill learning (Buitrago *et al.* 2004). The string test is used to test grip strength and agility in rodents (Miquel and Blasco 1978). Therefore, a 3 mm cotton string 50 cm was suspended between two platforms constructed of plastic (9 cm x 15 cm) placed above two vertical poles at a height of 40 cm (Jawhar *et al.* 2012). The mice were permitted to grasp the middle of the string with their forepaws and then immediately released allowing the mice to escape to one of the platforms. A rating system from 0 to 7 was used to rate the agility of each mouse during a 60 seconds trial; adapted from (Moran *et al.* 1995) with the following modifications: 0, unable to hang on the string; 1, hangs only by forepaws; 2, attempting to climb the string; 3, climbing the string with four paws successfully; 4, moving laterally along the string; 5, tries to escape to one of the platforms; 6, falls while escaping to one of the platforms; 7, escaping to one of the platforms at the end of the string.

To reflect spatial working memory by spontaneous alternation behaviour, an X-maze task (in a 90-degree angle plastic X-maze with arm sizes: 30 cm length, 8 cm width and 15 cm height) was performed during 5 min test sessions and constructed according to X-maze used in Jawhar and colleagues (Jawhar *et al.* 2012). Spontaneous alternation is based on the natural behaviour of rodents to explore new environments and thus to rotate in the entries of the arms. Alternation was defined as successive entries into the four arms in repeated quadruple sets (Jawhar *et al.* 2012). A decreased spontaneous alternation is indicative of impaired spatial working memory.

The open field test (Noldus, the Netherlands) is commonly used to assess anxiety (Hall and Ballachey 1932). Therefore, the mice were placed in the middle of the field with 50 cm x 50 cm surface area and walls to prevent the mice from escaping. The behavioural parameters registered during a 5 min session were the ratio of time spent in the central part (20 cm x 20 cm) versus total time to assess anxiety.

All behaviour setups were cleaned between trials with 70% ethanol to avoid odour distraction. A dedicated infrared video camera setup with associated software (EthoVision XT 11, Noldus) was used to record the behaviour tests and facilitate the analyses.

2.3.5 **Dissection and tissue preparations.**

Mice were sacrificed by cervical dislocation, followed by decapitation. The right brain hemispheres of the mice were stored in 4% PFA for later processing for immunohistochemistry as descried below. All left hemispheres were rapidly dissected into five parts: cortex (CTX), hippocampus (HC), olfactory bulb (OLF), cerebellum (CB) and midbrain (MB), and snap frozen in liquid nitrogen and stored at -80°C until further processing. The applied dissection protocol for investigations of brain tissues was included in the animal ethics applications to obtain approval and used in previous studies (Hullmann *et al.* 2017; Wahle *et al.* 2020). For the current study we focused on investigating the regions that are deemed most relevant. The kinase analyses were performed in the cortical tissues to compare this with parallel *in vitro* studies that were performed in primary cortical cultures in the framework of the collaborative project in which the current study was embedded (InnoSysTox/N3rvousSystem). For IBA-1 and GFAP we selected regions in association with the immunohistochemistry analysis. Because of the limited availability of the cortex tissues per mouse, midbrains were considered of relevance for the oxidative stress markers MDA and GSH. The small intestine and colon were removed, flushed, opened, weighed and snap frozen in liquid nitrogen and stored at -80°C until further processing or rolled and embedded in 4% PFA. Organs including liver, kidney, spleen and intestine were removed, weighed and snap frozen in liquid nitrogen and stored at -80°C until further processing or embedded in 4% PFA. For the toxicokinetic analysis (see Figure 2.2), whole blood, intestines, liver, kidneys, spleens and brains were collected and weighed. Intestines were flushed and opened before weighing. All organs except the blood were immediately snap-frozen in liquid nitrogen and stored at -80°C until further processing for ICP-MS analysis.

2.3.6 **Immunostaining of paraffin-embedded brain tissue sections.**

After sacrificing the mice and careful dissection of the brains, the right hemispheres were fixed in 4% buffered formalin at 4°C for a minimum of 24 hours for the subsequent cutting in 4-5 µm paraffin-embedded sections on glass. Neuropathological changes are often present before behavioural changes occur. Therefore, we stained hippocampus and cortex for glial fibrillary acidic protein (GFAP) and ionized calcium-binding adapter molecule 1 (IBA-1) as well-established markers of neuroinflammation (Sofroniew and Vinters 2010; Kovacs 2017; Li *et al.* 2020). For the immunostaining the paraffin sections were deparaffinized in xylene and rehydrated in a series of ethanol baths (100%, 95%, 70%). To block endogenous peroxidases, sections were pre-treated with 0.3% H_2O_2 in 0.01 M PBS. Antigen retrieval was generated by boiling slices in 10 mM citrate buffer. A solution of 5% normal goat serum (NGS) in 0.01 M

PBS was used to block unspecific antigens. Slices were incubated in primary antibody GFAP (Cat No. Z0334, Dako; dilution 1:2000) and IBA-1 (Cat No. GTX100042, GeneTex; dilution 1:500) in 5% NGS in 0.01 M PBS overnight at 4°C. Next day the sections were washed and incubated 45 min at room temperature with biotinylated secondary antibody, diluted 1:1000 in 0.01 M PBS and 5% NGS. Staining was visualized using the avidin/biotin- complex-method (ABC) by Vectastain kit. Treatment with diaminobenzidine (DAB) as chromogen resulted in a brown colour. The counterstaining was performed with Hematoxylin and led to a blue staining of the nucleus. Light microscope images from cortex and hippocampus were taken with a Zeiss Axiophot microscope equipped with AxioCam MRc (Carl Zeiss, Jena, Germany). Analyses were performed using image analysis software (ZEN2011, Zeiss) in cortex and hippocampus at 200x magnification in defined regions of interest. For cortex, we have chosen the cortical layer 5 of the frontal lobe and for the hippocampus the CA1 region. The image analyses software uses a colour deconvolution algorithm to count the number of pixels that have strong immunoreactivity (i.e. brown colour indicating positive staining of the respective antibodies). The output represents the percentage of positive staining relative to the total area of the cortex or hippocampus and is defined as GFAP load for positive stained astrocytes and IBA-1 load for positive stained microglia.

2.3.7 **Western blotting analyses.**

For the analysis of protein levels and expression, the brain tissues were homogenized in ~8 volumes of ice-cold PBS in a potter tissue grinder. The homogenate was centrifuged in a microcentrifuge for 45 min at 12500 rpm and 4°C. The amount of protein in the supernatant was evaluated with the BCA kit (Thermo) according to the manufacturer's protocol. The samples were prepared with equal amounts of protein (40 µg) and loaded on a 4-12% precast NUPAGE gel (Invitrogen) and were separated at 180 V in a Mini-PROTEAN II tank (BIO-RAD). After electrophoresis, the proteins were blotted on a 0.45 µm pore diameter nitrocellulose transfer membrane (Whatman, Schleicher & Schuell) at 250 mA for 45 min in a Mini Trans-Blot tank (BIO-RAD). The membrane was blocked with 5% milk in PBS-T (0.01 M PBS and 0.05 % Tween-20) for 60 min. Subsequently, the membrane was incubated with the primary antibody GFAP (Cat No. ab7260, Abcam, 1:2000), IBA-1 (Cat No. GTX100042, Gentex, 1:500), Claudin-5 (Cat No. 35-2500, Invitrogen, 1:1000), Occludin (Clone OC-3F10, Cat No. 33-1500, Invitrogen, 1:1000) and ZO-1 (Cat No. 61-7300, Invitrogen, 1:2000) overnight at 4°C. Next day the membrane was washed with PBS-T and was incubated 1 h at room temperature with the HRP conjugated secondary antibody and washed again 5 times with PBS-T. For the detection of the proteins, the ECL solutions were applied (GE Healthcare) and

the visualization was performed with the FluorChem 8900 (Biozym, Hessisch Oldendorf). Quantification of protein expression was evaluated using the ImageJ software (National Institutes of Health, Bethesda, USA).

2.3.8 **Oxidative stress markers MDA and GSH.**

Oxidative stress, resulting from the disruption of the pro- and antioxidant balance in cells and tissues has been proposed as a key mechanism of the toxicity of NMs. Accordingly, the levels of MDA and GSH were determined in the mouse brains. The amount of MDA was evaluated with a commercial kit (Sigma-Aldrich) according to the manufacturers' protocol. This assay determines lipid peroxidation by the reaction of MDA with thiobarbituric acid (TBA) to form a colorimetric product, proportional to the MDA present. Samples were analysed using a microplate spectrophotometer (Multiskan GO, Thermo) at a wavelength of 532 nm. The amount of total glutathione (GSH) was evaluated in brain tissues after homogenization in cold 100 mM phosphate buffer (pH 6.8), containing 0.1 mM EDTA. After centrifugation (10,000g, 15 min, 4°C) the supernatants were deproteinized with an equal volume of 10 % metaphosphoric acid and thereafter with a solution of 4 M triethanolamine to increase the pH of the sample. This assay is based on the catalytic reaction of GSH with 5,5'-dithio-bis-(2-nitrobenzoic acid) (DTNB, also named as Ellman's reagent) that forms the yellow derivate 5-thionitrobenzoic acid (TNB) with a maximal absorbance at 412 nm. Samples were analysed at 30 second intervals for a total of 3 minutes using a multimode plate reader (Infinite 200PRO, Tecan). The concentration of total glutathione was expressed as nmol GSH per mg of protein. The amount of protein in the supernatant was evaluated with the BCA kit (Thermo) according to the manufacturer's protocol.

2.3.9 **Cytokine ELISAs.**

The concentrations of the proinflammatory cytokines IL-6 (Cat No. M6000B, R&D Systems), IL-1β (Cat No. MLB00C, R&D Systems) and TNF-α (Cat No. MTA00B, R&D Systems) in cortex brain homogenates were determined by mouse quantikine ELISA kits (R&D Systems, Minneapolis, USA). Briefly, brain cortex tissue was homogenized in 400 µL of lysis buffer (1xPBS, 1% Triton X-100 and complete protease inhibitor cocktail tablet (Roche)). The homogenates were centrifuged at 14,000 rpm at 4°C for 15 minutes and the supernatant was immediately transferred and used for cytokine detection. Total protein concentrations in supernatants of the cortex homogenates were evaluated by BCA kit according to the manufactures protocol (Thermo).

2.3.10 **Kinase activity assay on peptide microarray.**

Tissue sections of fresh frozen brain cortex of mice sacrificed at day 28 day (substudy I) were extracted on ice for 30 min in 65 µl of Mammalian Protein Extraction Reagent (M-PER, Thermo), supplemented with Halt Protease inhibitor cocktail (1:100, Thermo) and Halt Phosphatase inhibitor cocktail (1:100, Thermo Fischer Scientific), followed by centrifugation for 15 min at 16000xg. The supernatants were aliquoted, flash frozen and stored at -80ºC till use. Protein concentration was determined with the Pierce™ Coomassie Plus (Bradford) Assay Kit (Thermo Fischer Scientific). Protein tyrosine kinase (PTK) and serine/threonine kinase (STK) activity was determined in duplicate (technical replicates) for 10 mice per treatment (5 female, 5 male) on tyrosine and serine/threonine peptide microarrays, according to the standard protocols of the manufacturer (PamGene International BV, 's-Hertogenbosch, The Netherlands) (Hilhorst *et al.* 2013; Chirumamilla *et al.* 2019). These peptide microarrays comprise 195 and 142 consensus peptide substrates covalently coupled to the tyrosine kinase and serine/threonine microarrays respectively, to assess activity of the protein kinases. For the determination of tyrosine kinase activity 5 µg of protein was used per array, for the serine/threonine kinase activity 1 µg, in 40 µl of kinase assay buffer, supplemented with 400 µM ATP and antibodies for detection of phosphorylated peptides. Peptide phosphorylation was captured with a CCD camera. Signals on these images were quantified with BioNavigator software (PamGene International BV, 's-Hertogenbosch, The Netherlands). The same software package was used for data visualisation and statistical analysis. For each peptide spot the local background around that spot was subtracted from the signal intensity in the spot. For PTK, the 163 peptides that showed kinetics (statistically significant ($p<0.05$) increase of signal in time) on at least 5% of the arrays were included in the analysis. For STK, 81 peptides that had nominal CV (Coëfficient of variation) <0.5 were retained for analysis. The CV was calculated per peptide with a 2-component error fit model using overall mean as input. Values were ^{2}log transformed for visualization. Technical replicates were averaged prior to statistical analysis. Treatment related effects vs control were analysed using one-way analysis of variance (ANOVA) followed by Dunnett's post hoc evaluation. The proportion of expected false discoveries among a set of significant peptides that result from performing multiple hypothesis tests in parallel was determined using the Benjamini-Hochberg method (Benjamini and Hochberg 1995). Upstream kinase analysis was performed as described by (Chirumamilla *et al.* 2019). Results were projected on the kinome tree using KinMap (Eid *et al.* 2017).

2.3.11 **ICP-MS analysis**

ICP-MS was used to assess uptake and translocation kinetics of the NMs based on elemental analysis of Ag and Ti (see Figure 2.2). The analysis of a first selection of tissue samples from the NMs-treated mice, and control tissue samples that were spiked with different amounts of both NMs, revealed that no reliable measurements could be made for TiO_2 due to analytical difficulties. The method of Ti detection in rodent tissues described in an inter-laboratory comparison study (Krystek *et al.* 2014) revealed that concentrations below 4 µg/g showed too high variance to allow its statistically reliable quantitative determination in the given tissues. For this reason, the digestion was exclusively optimized for the quantitative determination of Ag in tissues using the method described by Loeschner and colleagues (Loeschner *et al.* 2011). The ICP-MS analysis of Ag in small intestine, blood, liver, spleen, kidney and brain were performed as described by McGillicuddy and colleagues (McGillicuddy *et al.* 2017). Briefly, the samples were prepared by using microwave digestion with nitric acid. After the addition of hydrochloric acid, the solutions were examined by ICP-MS (iCAP-Q, Thermo Fisher Scientific).

2.3.12 **Statistical analysis.**

The design of the toxicodynamic study included 10 mice per sex and treatment group. No data could be generated in any of the behaviour tests for 1 male control mouse (not delivered by supplier at study start) and 1 male TiO_2 exposed mouse (died during exposure, not considered related to the treatment) for the 42 days sub-study. Moreover, the string suspension test for the 42 days subgroup was only performed for 5 female mice (instead of 10) for all three treatment groups. Immunohistological and biochemical analyses were determined for the number of animals as indicated in the figure legends. All data are shown as mean and standard error of mean (SEM), unless specified otherwise. Treatment related effects were analysed using one-way analysis of variance (ANOVA) followed by Dunnett's post hoc evaluation of control groups versus NMs-treated groups. For the evaluation of ordinal data, the Kruskal-Wallis test with Dunn-Bonferroni post hoc analysis was used. Sex-specific effects of control mice were analysed by Student's t-test or Mann-Whitney U-test in the case of ordinal data. Analysis were performed using SPSS statistics, Version 25 IBM Corporation, USA). Statistical analysis of the kinase data was performed with BioNavigator software as described in section 2.10.

2.4 Results

2.4.1 Effects of oral exposure to TiO_2 and Ag NMs on body and organ weights

The body weights of the mice were determined prior to the first oral exposure as well as on days 28 and 42 (i.e. on day 14 of the exposure recovery period). Organ weights were determined at sacrifice days 28 and 42. Results are shown in Table 2.1. As can be seen in the table, there were no obvious treatment related effects on body organ weights in the mice. In the male mice of substudy II (recovery groups), kidney weights/g body weight were lower for the TiO_2 fed male mice compared to corresponding controls. Treatment related differences in absolute organ weights were not observed in either of the substudies (data not shown).

Table 2.1. Body and organ weights of the male and female mice following 28-day oral exposure to TiO_2 (1%) or Ag (0.2%) NMs (substudy I) and at 14-day post-exposure recovery (substudy II).

Sub-study	Day	Gender	Treatment	Body weight (g)		Body weight gain[a] (g)		Liver (mg/g)		Spleen (mg/g)		Kidney (mg/g)	
I	28	male	control	27.4	±1.1	5.7	±0.8	47.2	±2.1	2.8	±0.4	6.0	±0.4
			TiO_2 1%	27.8	±1.4	6.1	±1.0	50.1	±3.4	2.8	±0.4	6.0	±0.6
			Ag 0.2%	27.8	±2.2	5.9	±1.4	49.6	±8.3	2.5	±0.3	5.8	±0.4
		female	control	20.2	±0.8	2.9	±0.5	47.6	±3.4	3.5	±0.3	5.9	±0.5
			TiO_2 1%	20.6	±1.0	3.2	±0.4	47.9	±4.5	3.4	±0.6	5.8	±0.4
			Ag 0.2%	20.7	±1.0	3.3	±0.5	47.1	±2.3	3.5	±0.3	5.6	±0.4
II	28 + 14	male	control	28.7	±1.7	7.2	±1.1	50.1	±2.0	2.7	±0.3	6.6	±0.4
			TiO_2 1%	29.7	±1.4	7.6	±1.5	51.7	±2.7	2.7	±0.4	6.0*	±0.3
			Ag 0.2%	29.0	±1.2	7.3	±0.9	51.0	±1.7	2.7	±0.3	6.2	±0.6
		female	control	21.4	±1.3	4.4	±0.6	46.4	±5.8	3.4	±0.5	5.9	±0.3
			TiO_2 1%	22.2	±0.7	4.8	±0.9	48.2	±4.0	3.5	±0.3	5.9	±0.5
			Ag 0.2%	21.9	±0.9	4.7	±0.5	50.1	±3.6	3.3	±0.1	5.8	±0.3

[a] Body weight gain at time interval between exposures start and sacrifice, *$p<0.05$ (ANOVA with Dunnett's multiple comparison test).

2.4.2 Effects on mouse behaviour

The mice were subjected to the string test, the rotarod test, the X-maze test and the open field test during exposure to the NMs (substudy I) or during the exposure recovery period (substudy II), respectively. This battery of tests revealed no significant treatment-related differences in male and female mice in relation to the exposure to the distinct NMs, with the exception of motor coordination effects (see Figure 2.3).

No significant treatment-related effects were observed in the open field task, the X-maze task, and the string suspension task for both NMs in either of the substudies. In the string suspension test, the performance of the TiO_2 exposed male mice tended to be higher than the performance of the untreated control group during the 28 days exposure period, but this difference was not statistically significant (Fig. 2.3E). However, it should be pointed out that the control male mice of the 28 days exposure showed a low performance score in comparison to the females at this time point ($p<0.05$, Fig. 2.3E) as well as in comparison to the control mice of both sexes at the recovery time point of analysis (Fig. 2.3F). Interestingly, the male and female control mice for the 28-day exposure also showed significant differences in the relative time spent in the center of the open field test (Fig. 2.3A), and special working memory, as identified with the X-maze task (Fig. 2.3C).

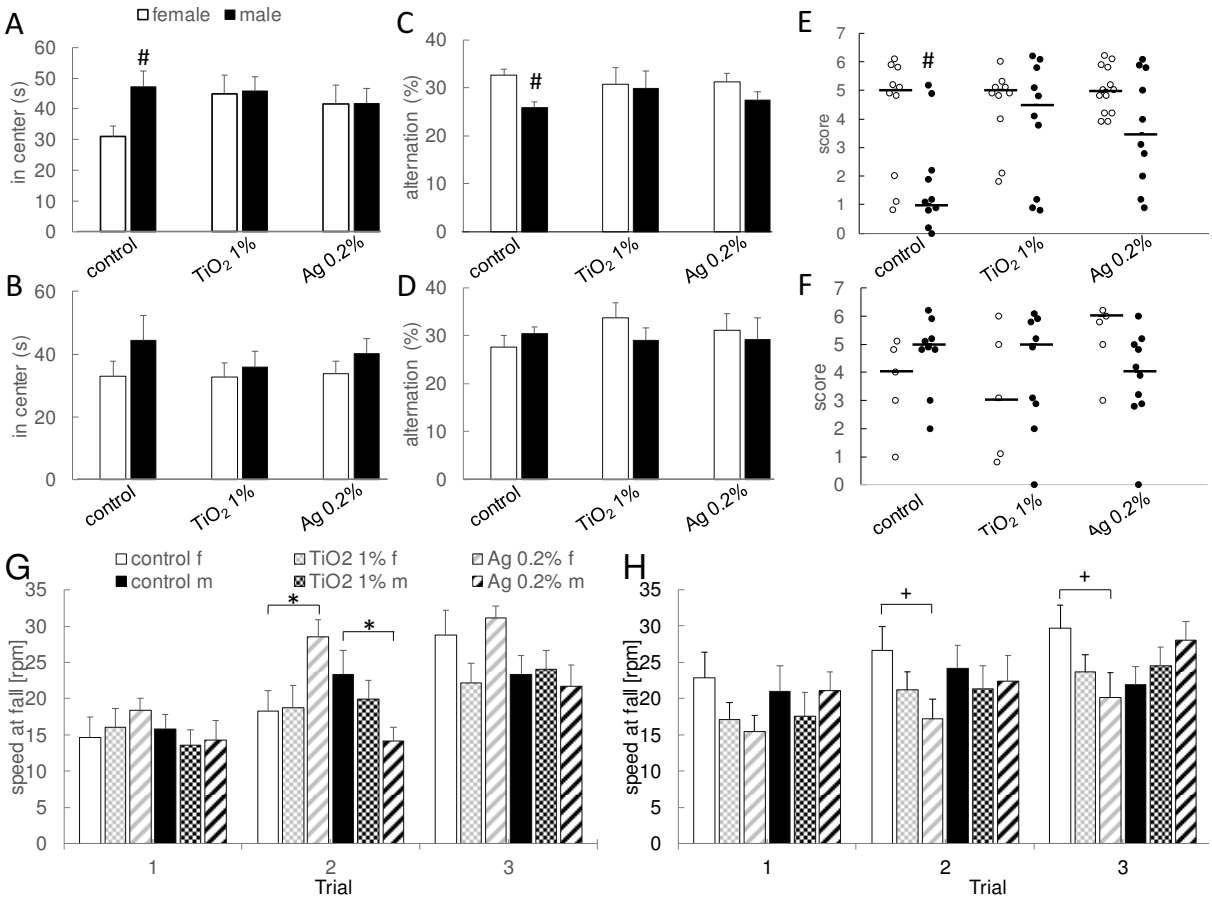

Figure 2.3. Behaviour task performance in mice following oral exposure exposure to TiO_2 or Ag nanomaterials. The graphs indicate center duration in the open field task (A, B); % alternation in the X-maze task (C, D); the string suspension task score (E, F), speed in rpm at fall in the rotarod test (G, H) during the 28- day exposure period (A, C, E, G; substudy I) and during the 14-day recovery period (B, D, F and H; substudy II). Data represent mean ± SEM for the open field task, X-maze task and rotarod test. String suspension task score data are indicated as scatterplots The $^{\#}$ indicates a significant difference ($p<0.05$) between female and male groups (Student's t-test for the open field and X-maze tasks; Mann-Whitney test for the string suspension task); The (borderline) differences in effects between the indicated treatment groups of the same sex are indicated by $^{*}p<0.05$ and $^{+}p<0.06$ (ANOVA with Dunnett's multiple comparison test) for the rotarod test. Treatment related effects for the string suspension task results were evaluated by the nonparametric Kruskal-Wallis test followed by Dunn-Bonferroni post hoc evaluation.

In the rotarod tests, significant effects were observed exclusively for the Ag NM. As expected, this test revealed that performance increased during the multiple trials in the control animals (Fig. 2.3G and 2.3H). Performance in this test during the 28 days exposure period in trial 2 was significantly increased in the female mice and, in contrast, significantly decreased in the male mice exposed to the Ag NM, in comparison to the mice of the respective untreated control groups (Fig. 2.3G). Effects were not observed in both other trials and the 3-trials average did not reveal significant treatment-related effects. During the 14 days recovery period, the performance in the rotarod test was not affected in the male mice and also not increased for the Ag NM exposed female animals. On the contrary, at post-exposure follow-up performance tended to be diminished ($p<0.06$) for the Ag NM treated female mice for trial 2 as well as for trial 3 (Fig 2.3H). In fact, for the female mice in all three trials the same trend was observed, which was also verified by the statistical significance of the three trials' average of the speed at fall (ANOVA/Dunnett, $p<0.05$).

2.4.3 **Effects on neuroinflammation**

Immunohistochemical analysis revealed that the 28-day repeated exposures to both types of NMs had no effect on astrocyte morphology and expression of GFAP in the female (see Fig. 2.4A, C, D) and the male mice (see Fig. 2.4B, C, D) when comparing the different treatments with the respective untreated control groups. This finding was independently confirmed using Western blotting of the brain tissues (see Fig. 2.4E, F). Western blot analysis of mouse brain homogenates at 14 days post-exposure recovery also revealed no delayed treatment related effect (Fig. 2.4G, H). In alignment with the GFAP analysis, also for IBA-1 no treatment related effects were observed (Figure 2.5). No marked changes were observed in the morphology of microglia and the expression of IBA-1 in male and female mice after 28-days of exposure, as measured by immunohistochemistry (Fig. 2.5A, B, C, D) and Western blotting (Fig. 2.5E, F). Expression changes were also not observed after 14 days exposure recovery (Fig. 2.5G, H).

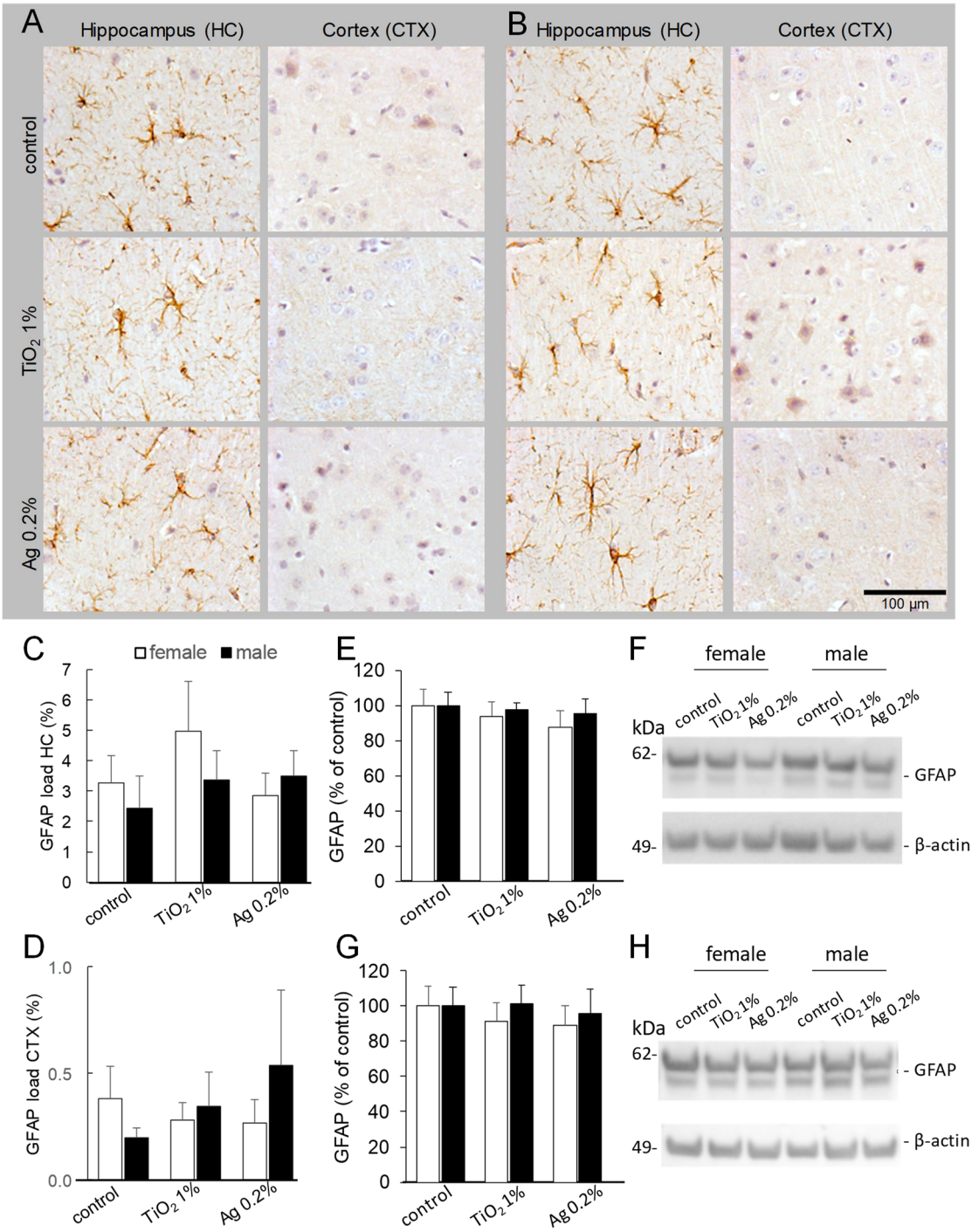

Figure 2.4. GFAP expression in female and male C57BL/6J mice after oral exposure to the different nanomaterials. Representative pictures (200-fold microscopic magnification) of glial fibrillary acidic protein (GFAP) (brown staining) in hippocampus (Rosenberger *et al.* 2016) and cortex (CTX) of female (A) and male (B) C57BL/6J mice exposed orally to 1% TiO_2 and 0.2% Ag in feed pellets *ad libitum* for 28 days. For quantification, GFAP load was determined using image analysis software and calculated as the percentage area occupied by GFAP immunostaining in HC (C) and CTX (D). GFAP was also visualized by western blot using FluorChem Imager for mice after 28 days exposure (F) as well as after 14 days recovery from the 28-days exposure (H). Total GFAP expression was detected in CTX and normalized to the respective control sample (E, 28 days; G, 28 days + 14 days recovery). Data represent mean ± SEM for n=5-7 mice per group.

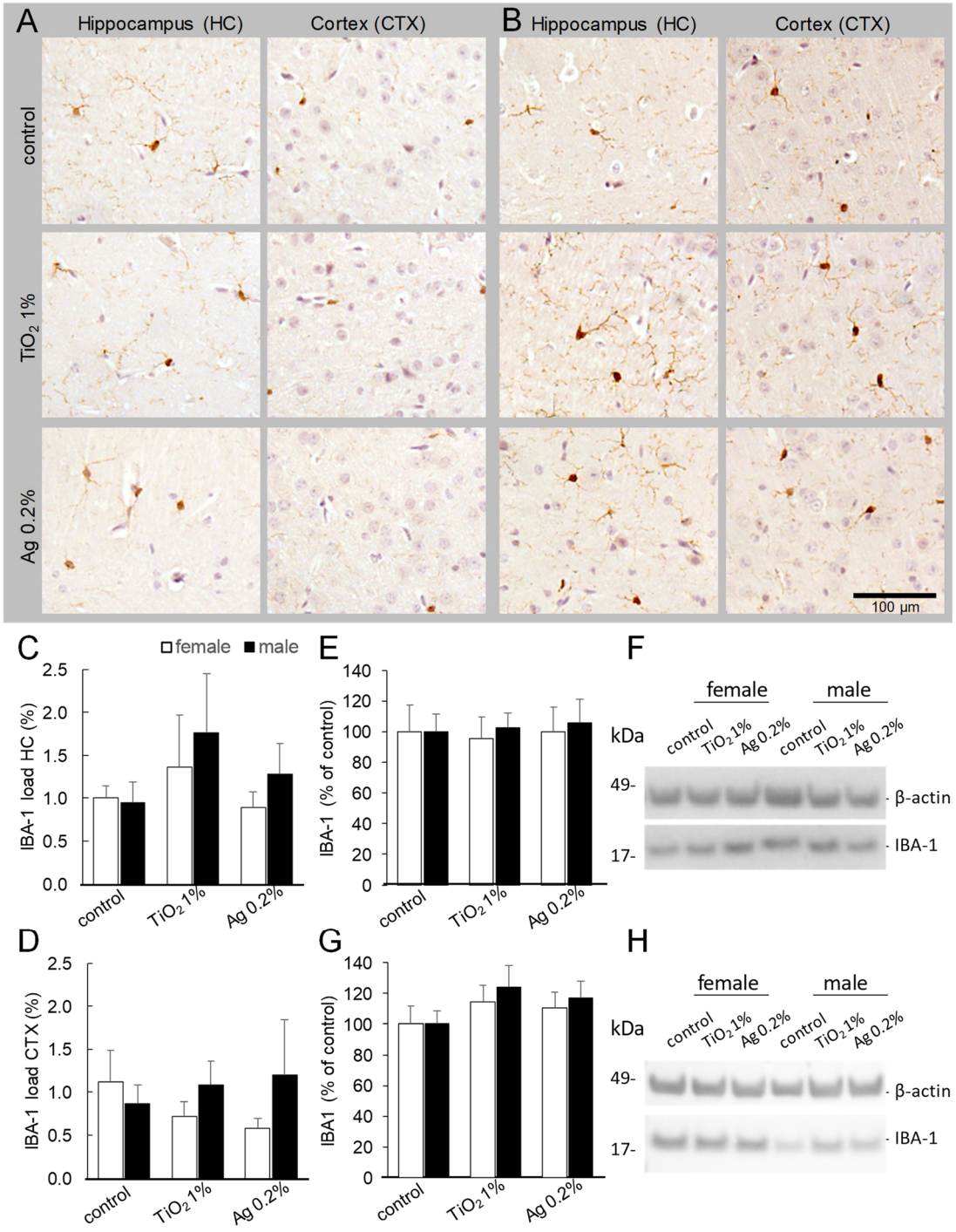

Figure 2.5. IBA-1 expression in female and male C57BL/6J mice after oral exposure to the different nanomaterials. Representative pictures (200-fold microscopic magnification) of ionized calcium-binding adapter molecule 1 (IBA-1) (brown staining) in hippocampus (Rosenberger *et al.* 2016) and cortex (CTX) of female (A) and male (B) C57BL/6J mice exposed orally to 1% TiO_2 and 0.2% Ag in feed pellets *ad libitum* for 28 days. For quantification, IBA-1 load was determined using image analysis software and calculated as the percentage area occupied by IBA-1 immunostaining in HC (C) CTX (D). IBA-1 was also visualized by western blot using FluorChem Imager for mice after 28 days exposure (F) as well as after 14 days recovery from the 28-days exposure (H). Total IBA-1 expression was detected in CTX and normalized to the respective control sample (E, 28 days; G, 28 days + 14 days recovery). Data represent mean ± SEM for n=5-7 mice per group.

To further explore the potential effects of the NMs on neuroinflammation, the protein levels of the pro-inflammatory cytokines IL-6 and IL-1β and TNF-α were evaluated in mouse cortex immediately after exposure as well as at the 14 days exposure recovery time point. As can be seen in Figure 2.6, the oral exposure to the NMs for 28 days in feed pellets *ad libitum* revealed no significant treatment related differences in tissue levels of IL-6 and IL-1β. Levels of TNF-α were below detection limit for all treatment groups after 28 days as well as at post-exposure recovery. Thus, the NMs did not cause (persistent) inflammatory responses in the mice brains following the oral exposures.

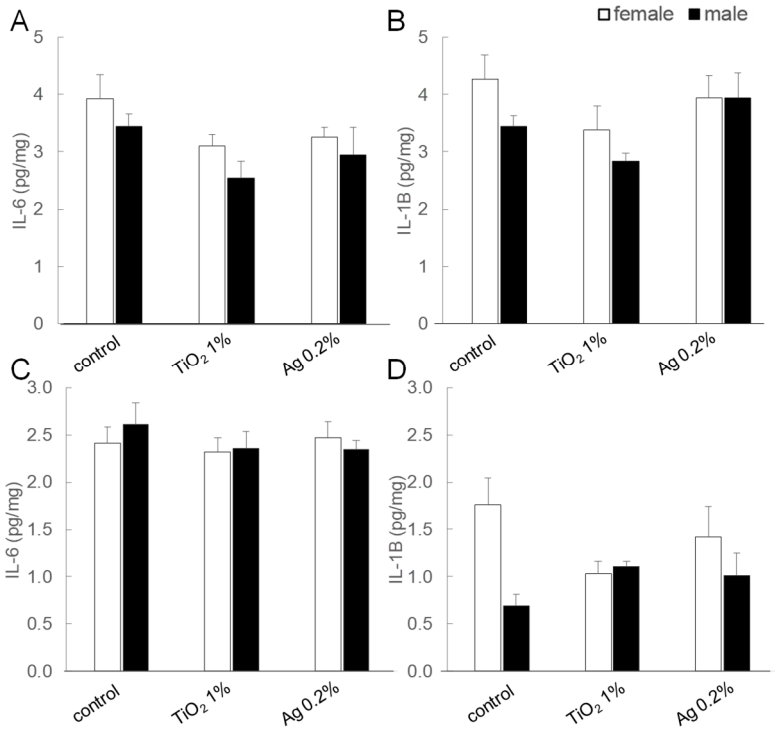

Figure 2.6. Proinflammatory cytokines in cortex of female and male C57BL/6J mice following oral exposure to TiO_2 or Ag nanomaterials. Concentrations of IL-6 (A, C) and IL-1β (B, D) in mouse cortex were analysed by ELISA after 28 days exposure (A, B) as well as after 14 days recovery from a 28 days exposure (C, D). Data are represented as mean ± SEM of n = 5 mice per group.

2.4.4 **Effects on oxidative stress in mouse brain**

We tested the levels of MDA and GSH in the brains of the mice following 28 days of exposure (see Figure 2.7). Both stress markers tended to be higher in control males than in control females although this effect was not statistically significant. No significant treatment related effects were observed in the male or female mice, indicating that the repeated oral exposures to the respective NMs did not result in marked oxidative stress in the brains.

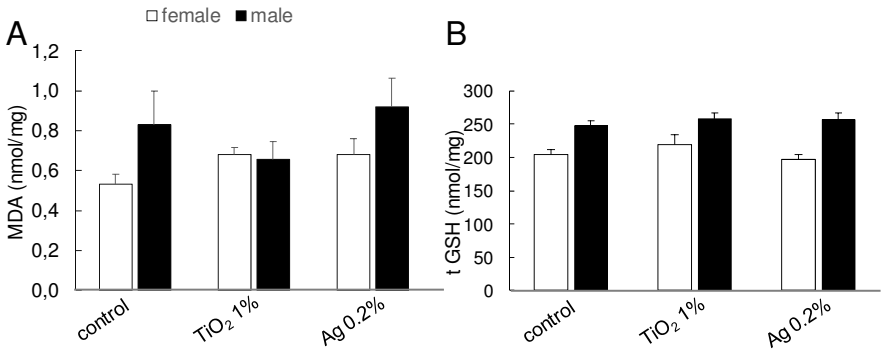

Figure 2.7. Malondialdehyde (MDA) concentrations (A) and total glutathione concentrations (GSH) (B) in midbrain of female and male C57BL/6J mice following 28 days oral exposure exposure to TiO_2 or Ag nanomaterials. Data represent mean ± SEM, of n = 5 mice per group.

2.4.5 **Effects on blood brain barrier integrity**

To study the potential adverse impact of the oral exposures to TiO_2 and Ag NMs on blood-brain barrier (BBB) of the male and female mice, we determined the expression of the tight junction proteins, claudin-5, occludin and ZO-1 in midbrain lysates by Western blot analyses (Figure 2.8). Both types of NMs did not significantly affect the expression of claudin-5 (Fig. 2.8A), occludin (Fig. 2.8B) or ZO-1 (Fig. 2.8C) suggesting that the oral exposures to the respective NMs did not cause an impairment of BBB integrity.

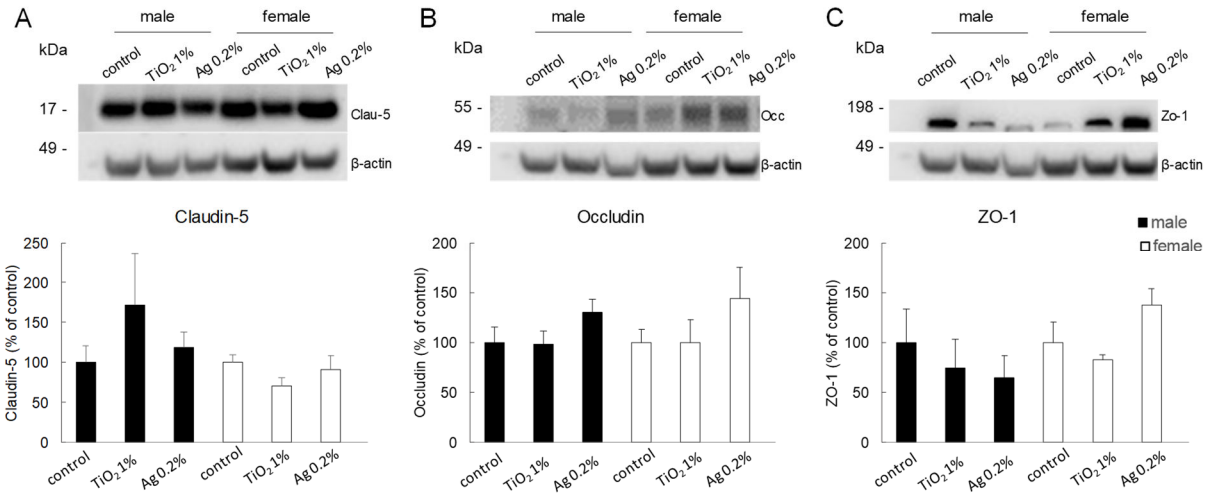

Figure 2.8. Blood-brain barrier (BBB) integrity markers in midbrain of female and male C57BL/6J mice following 28 days oral exposure to TiO_2 or Ag nanomaterials. Claudin-5 (A), Occludin (B) and ZO-1 (C) in midbrain of the mice was visualised by western blot. Data were normalized for β-actin expression as a loading control and expressed as fold change. Values represent mean ± SEM for n = 5 mice per group.

2.4.6 **Kinase screening**

Kinase activity assays were performed in cortical tissues of the 28 days exposed male and female mice, 5 per treatment group. A first analysis of the kinase activity encompassed the

comparison of the median signals per sample (Fig. 2.9A). Within the control groups of the males, PTK activity, but not STK activity showed a large biological variation. Treatments effects vs controls were compared for males and, females separately and combined (Table 2.2).

Table 2.2. Comparison of protein kinase activity of treated animals vs. controls per gender and combined. Each treatment group contained 5 animals. Difference expressed as number of peptides with p<0.05 and p<0.01 as well as the False Discovery Rate.

			Male + Female		**Male**		**Female**	
			# peptides	FDR	# peptides	FDR	# peptides	FDR
Ag	PTK	p<0.05	5	0.521	2	0.995	29	0.208
		p<0.01	0		0		1	0.208
	STK	p<0.05	8	0.294	4	0.482	1	0.890
		p<0.01	1	0.294	0		0	
TiO_2	PTK	p<0.05	4	0.710	1	0.541	2	0.996
		p<0.01	0		0		0	
	STK	p<0.05	1	0.966	1	0.977	0	
		p<0.01	0		0		0	

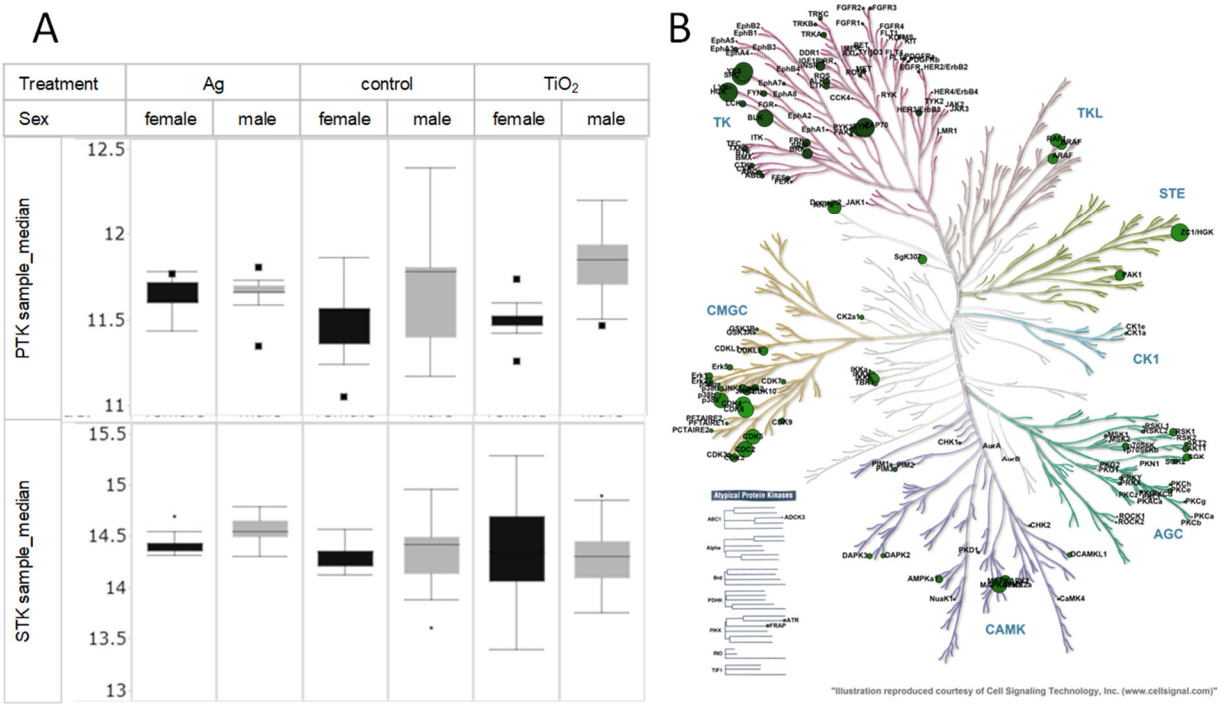

Figure 2.9. Kinase screening in cortex of female and male C57BL/6J mice following oral exposure to TiO_2 or Ag nanomaterials. (A) Protein tyrosine kinase (PTK) and serine/threonine kinase (STK) activity was determined in cortical tissue on tyrosine and serine/threonine peptide microarrays. Median signals of all peptides for each sample were calculated and represented in box plots. (B) Results of upstream kinase analysis for the effect of exposure of male and female mice to Ag NM are projected on the kinome tree (courtesy Cell Signalling Technology). A brighter colour indicates higher significance**.** Treatment related effects vs. control were analysed using one-way analysis of variance (ANOVA) followed by Dunnett's post hoc evaluation. Values represent mean ± SD for n = 5 mice per sex and group.

Treatment had hardly any effect on STK activity, for the number of peptides with $p<0.05$ is limited and the likelihood of the peptides being false positives is high. The table shows differential effects of Ag treatment on PTK activity between males and females. Comparison of Ag treated animals with controls revealed a large effect on PTK activity in females but not in males, caused by the large biological variation in the control male mice (Fig. 2.9A). To gain insight in kinases that could be activated by the treatments, we performed upstream kinase analysis as described in (Chirumamilla *et al.* 2019). For both the females alone and combined with males, activity of ZAP70, SYK and Src family kinases was suggested to be increased upon exposure to Ag NM (Fig. 2.9B). When comparing differential upstream kinase activity in males and females exposed to TiO_2, males were suggested to have increased activity of these same kinases.

2.4.7 **Distribution analysis of Ag by ICP-MS**

For the mice that were treated with the Ag NM in the feed pellets, the results of the ICP-MS analysis are shown in Figure 2.10. The supplementary file S2 (Table S2-1), shows the Ag concentration in the various investigated tissues at the 24 h time for Ag NM fed mice in comparison to mice that were treated by single oral gavage. Among the Ag NM treated mice, the average concentrations of Ag detected in all investigated tissues tended to be markedly higher in the animals that were exposed via the feed pellets compared to those that were gavaged (see Table S2-1). Differences were most pronounced for the intestine, followed by liver and spleen, athough it should be emphasized that considerable variations in accumulation of Ag were observed between the animals from both exposure groups. For the brain an average 2-fold difference was observed for the gavage versus the feed application. Figure 2.10 shows the concentration of Ag over the course of the 28-days of exposure via feed pellets followed subsequent 28-days post-exposure interval. During the exposure period, high levels of Ag were measured in the small intestine, and increasing Ag levels were also detected in blood from exposure day 1, suggestive of a rapid uptake of the Ag NM via this barrier organ following oral exposure. The high variations seen among the different animals and time points may be explained by age-dependent, inter-individual differences in feeding behaviour, resulting in different daily exposures. However, this could not be verified in our study, in the absence of ethical approval for individual (metabolic cage) housing of the mice. A rapid decline in Ag concentrations in blood and small intestine was observed post exposure. Accumulation of Ag was also observed in liver, kidney, spleen and brain during the 28 days feeding period. Concentrations in liver and spleen were higher than in kidney, and the lowest levels were

observed for the brain. Importantly, in contrast to the observations in the blood, the silver seemed to persist for the studied period in the brain and other organs except the intestine.

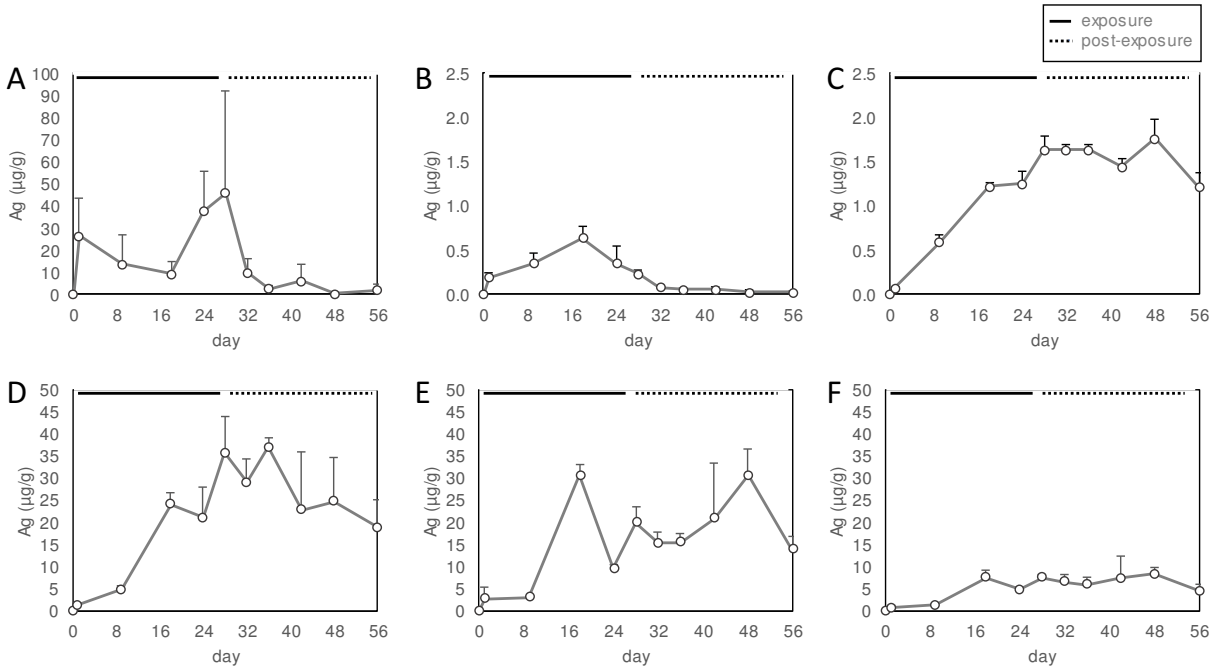

Figure 2.10. Inductively Coupled Plasma - Mass Spectrometry (ICP-MS) analyses of Ag in different tissues at different time points. Ag concentrations were determined at the indicated time points in small intestine (A), blood (B), brain (C), liver (D), spleen (E) and kidney (F) of female C57BL/6J mice over the 28-day oral exposure period to Ag nanomaterial and a subsequent 28-day recovery period.

To further evaluate the observed accumulation of the Ag in the brain, cryo-fixed brain tissue from a 28-days fed mouse was analysed by a complementary, independent analytical approach, i.e. using Time-of-Flight Secondary Ion Mass Spectrometry (ToF-SIMS) and Laser Ablation – Inductively Coupled Plasma – Mass Spectrometry (LA-ICP-MS). Results are shown in supplementary file S3. The results of these analyses revealed a clear marked spatial distribution of Ag in the brain, thus also confirming its accumulation in mouse brain upon exposure to foodborne Ag NM.

2.5 Discussion

Contrasting data have been reported in literature regarding the neurotoxicity of NMs following oral exposure. In this study we examined the effects of two widely applied metallic NMs, i.e. TiO_2 and Ag in male and female C57BL/6J mice in a 28-day oral exposure study with or without a 14-day post-exposure recovery period. TiO_2 and Ag are used in various consumer applications (Hadrup and Lam 2014; Munger *et al.* 2014; Shakeel *et al.* 2016; Gajbhiye and Sakharwade 2016; Rai and Shegokar 2017). In the food sector, Ag NMs are used because of their antimicrobial and anti-odorant properties in food and water as well as in food packaging

materials (FAO/WHO 2010; Hadrup and Lam 2014; Gunawan *et al.* 2017; Gaillet and Rouanet 2015; Azeredo *et al.* 2019). Likewise, TiO_2 finds application in food packaging as UV-blocker and antimicrobial agent (Chawengkijwanich and Hayata 2008; Bodaghi *et al.* 2013; FAO/WHO 2010). Regarding its addition to food and beverages, TiO_2 is known in the EU as food additive E171 and typically represents particles in a wide size-distribution of which only a portion is nanoscale. The specific NMs used in our study were selected in view of their applications and use in previous toxicological investigations. PVP-coated Ag represents a widely used type of nanosilver and the specific material was used previously in an *in vivo* oral exposure study to address effects on the microbiome (van den Brule *et al.* 2016). The P25 used here represents one of the earliest and most investigated types of TiO_2 materials in toxicology, albeit mostly regarding inhalation exposure (Oberdörster *et al.* 2005; Shi *et al.* 2013). It should be emphasized that P25 is not being considered as food additive and thus not equal to food-grade TiO_2 (i.e. E171).

In our present study, general clinical signs, body weight changes, organ weights and macroscopic findings were examined, but no major treatment-related toxicological findings were observed. The one exception was observed for the TiO_2 fed male mice in substudy II (i.e. 14 days exposure recovery group) in which a reduced kidney weight per kg. body weight was found. Such an effect was not observed in the TiO_2 exposed male mice of substudy I (i.e. 28-days exposure group), nor in the TiO_2 exposed female animals of both substudies. We also found no treatment related differences in absolute organ weights, including kidney (data not shown). Adverse health concerns related to long term oral exposure to TiO_2 are currently mainly discussed for liver and intestine, although the relevance of other organs including spleen and kidney has also been postulated in a literature review by Brand *et al.* (Brand *et al.* 2020). Recent 28-days and 90-days oral gavage studies with P25 TiO_2 in rats, performed according to OECD TG 407 and TG 408 respectively, found no systemic toxicological effects up to 1 g/kg bw/day (Heo *et al.* 2020). While changes in whole body and (relative) organ weights were absent for any of the Ag NM treated groups in our study, Kim *et al.* observed body weight decreases in male rats following a 13 weeks repeated gavage study with Ag nanoparticles at a dose of 0.5 g/kg bw/day (Kim *et al.* 2010) The authors also reported an effect on rat liver, identified by histopathology as minimal bile duct hyperplasia. While another toxicity study in mice with Ag nanoparticles at a single oral dose of 5 g/kg, in accordance with OECD TG 425, revealed neither significant haematological and clinical changes nor histopathology findings in various organs including liver and kidney after 1, 7 and 14 days (Maneewattanapinyo *et al.* 2011).

Our current studies did not reveal major neuropathological changes in the male and female mice for the TiO_2 and Ag NMs. In the brains, we did not detect significant treatment-related changes in conventional markers of oxidative stress, neuroinflammation or BBB disruption. The results from the behavioural test battery revealed absence of alterations in anxiety or cognition (i.e. spatial working memory). However, we did observe alterations in motor performance as well as some effect on cortical kinase activities, which were both NM specific and sex-specific.

A battery of behaviour tasks was used in this study to explore neurological effects of the NMs. It is important to consider that the mice were housed without inverted light conditions and behaviour tasks were performed during daytime, while such testing is considered more suitable during the active phase for these night-active species (Beeler *et al.* 2006). Thus, apart from the aforementioned differences in administration and dosimetry, this may have further influenced the results of behavioural outcomes when compared with other studies that perform behaviour during activity phase. However, as all mouse groups were tested under those identical conditions, potential NM-treatment effects could be captured. Moreover, our current results can be directly compared to the findings from previous studies in which behavioural changes were studied in response to inhalation exposures that are routinely performed during resting phase. As such, we were recently able to identify effects of repeated inhalation exposures to diesel-engine exhaust and cerium dioxide NMs on behaviour in a mouse model of Alzheimer's disease (Hullmann *et al.* 2017; Wahle *et al.* 2020). In our current oral exposure study, for the TiO_2 NM, no significant adverse effects were observed in any of the tests.

With the Ag NM, significant effects were observed solely in the rotarod test. For the 28-day exposure (i.e. substudy I), effects were found exclusively in one out of the three test runs (i.e. trial 2, performed on day 21 of the exposure). Interestingly, effects were opposite between the female and male mice in this for this test run, possibly indicating a sex-dependent response to the Ag NM exposures. However, when averaged over the three trails the differences were not significant, suggesting that the effects at the second trial may have been caused by chance. In contrast, at the post-exposure analyses (i.e. substudy II), motor performance impairments were consistent for the Ag exposed female mice in all three rotarod trials and significant for the 3-trials average. This indicates a delayed sex-specific effect for Ag NM, i.e. observed after 7 days of recovery from the 28-day repeated oral exposure (see Figure 2.3). The contrasting effects seen in the rotarod test for the Ag NM exposed female mice in the two substudies may relate to a delayed response to this nanomaterial and/or to differences in cumulative exposure, which were respectively 21 days (substudy I) and 28 days plus 7 post-exposure days (substudy

II). Other investigators have reported findings that indeed support a role of Ag NMs exposure on impairment in motor function. Yin *et al.* showed impairment of motor coordination and locomotor activity in rats after 14 weeks intranasal instillation to Ag NM (Yin *et al.* 2015). Greish *et al.* reported impairment in motor functions along with impairment in exploratory activity and learning following injection of Ag NM (Greish *et al.* 2019). So far, only few studies have identified sex-specificity of neurotoxic effects of NMs. Ghaderi and colleagues have shown adverse effects on neurobehavioural development regarding cognitive behaviour with greater susceptibility of female offspring upon subcutaneous injection of Ag NM in pregnant mice (Ghaderi *et al.* 2015). Similarly, while no adverse effect of TiO_2 NM were found in our present study, in a TiO_2 inhalation exposure study with time-mated mice more pronounced behaviour impairments were observed in female offspring compared to male offspring (Hougaard *et al.* 2010).

In association with the currently observed motor impairment effects, with the use of ICP-MS we could demonstrate a rapid and persistent accumulation of Ag in the mouse brains (as well as in liver, kidney and spleen) up to 4 weeks post-exposure. At this time point, Ag was also still detectable in blood and the intestine although the decline in their concentrations with cessation of exposure was obvious. In line with our Ag ICP-MS findings, Van der Zande *et al.* showed accumulation of Ag in the rat brain after oral exposure to PVP-coated Ag NM (90 mg/kg BW) (van der Zande *et al.* 2012). In 28-day exposed male rats, they found that Ag was cleared from most organs after 8 weeks post-dosing, except for the brain and testis (van der Zande *et al.* 2012) indicative of the potential higher vulnerability of these target tissues. Skalska *et al.* showed Ag in brains of Wistar rats after gavage exposure at even lower concentrations, i.e. 0.2 mg/kg BW (Skalska *et al.* 2015). Similar to this study outcome, Park *et al.* showed Ag in mouse brain after 14 days exposure by gavage application to Ag NM of different size at a daily dose of 1 mg/kg BW. The largest size particles did not lead to detectable Ag levels, indicating a size dependency of translocation from the intestine up to the brain (Park *et al.* 2010). Our ICP-MS results demonstrate translocation of Ag into the brain following exposure to foodborne Ag NMs, albeit this technique cannot provide a distinction between Ag in nanosized versus non-particulate (ionic) form and also cannot confirm the extent of actual crossing of the BBB of silver (nanoparticles). Interestingly, however, we were also able to localize Ag in specific brain regions by LA-ICP-MS analyses (Supplement S3), where the BBB may be comprised of a more fenestrated endothelial layer (Abbott *et al.* 2010). To our opinion, this complementary technique provides a promising approach in future toxicokinetic and toxicodynamic studies with NMs, for the investigation of brain region specificity of

accumulation and potentially associated neurotoxic responses. Notably, the effects observed in our study in females could at least in part also be the result of sex-specific differences in Ag accumulation. Indeed, Kim *et al.* noted a two-fold increase in Ag content in female kidneys compared to male kidneys of rats following a 90-day orally exposure regime (Kim *et al.* 2010). In another 90-days oral gavage study, significant higher accumulation of Ag was demonstrated in various organs of female rats, most notably in kidney, liver, jejunum, and colon (Boudreau *et al.* 2016). Unfortunately, we were not able to verify such sex-dependent accumulation behaviour in the mouse brains. Because of animal ethical restrictions, our kinetics study was a-priori designed for one mouse sex only (i.e. females, in association with the observed behavioural effects).

Although we could not determine Ti in the mouse organs of our toxicokinetic study, we can assume that the translocated amount for the TiO_2 NM will be minimal, especially to the brain. In the inter-laboratory comparison study by Krystek and colleagues Ti contents in the order of magnitude of 100 µg/g tissue were reported for liver and spleen, 14 days after a single intravenous (i.v.) administration of TiO_2 NM at a dose of about 10 mg/kg body weight (Krystek *et al.* 2014). However, the Ti contents that were measured by the four participating laboratories in the brains of the same animals merely ranged from less than 0.1 to 0.6 µg/g, even though the i.v. application bypasses the intestinal barrier. An oral toxicokinetic study in rats at doses up to 1 g/kg/day revealed no significant increases in Ti levels in liver, spleen, kidney and brain tissues following 13 weeks repeated gavage application (Cho *et al.* 2013). Yet, the fundamental ability of TiO_2 NM to cross the gastro-intestinal barrier and reach the brain following oral exposure was demonstrated in landmark investigations by Kreyling and colleagues (Kreyling *et al.* 2017). Using radiolabelled ^{48}V- TiO_2, a content of 0.36 ng/g brain tissue could be detected in rats, 7 days after a single oesophageal instillation dose of 30 - 80 µg/kg body weight. Most importantly, however, no consistent treatment-related brain effects were observed for the TiO_2 NM in present study, irrespective of whether or not significant concentrations could have accumulated in the brain.

As for the toxicity of NMs in general (Unfried *et al.* 2007), oxidative stress and inflammation have been implicated as main underlying mechanisms for their neurotoxicity (Feng *et al.* 2015; Song *et al.* 2016; Boyes and van Thriel 2020). Adverse effects of NMs in the CNS have been linked to their ability to activate glia cells and to disrupt the BBB (Sharma *et al.* 2010; Li and Martin 2017; Gao and Jiang 2017). Direct interactions of NMs with microglia have been implicated in their activation and subsequent release of ROS and pro-inflammatory cytokines like IL-1β, IL-6 and TNF-α, which can cause neuroinflammation, and finally, through

apoptotic mechanisms, trigger the death of surrounding neurons (Block and Hong 2005; Lull and Block 2010). The findings of our present study are not in support of such cascade of mechanisms. Immunostaining for IBA-1 and GFAP in brain remained unchanged after oral exposure to both types of NMs when compared with the untreated control group. Protein expression of IBA-1 and GFAP in cortex homogenates, analysed by Western blot, also did not show treatment related differences, both at 28 days and at 14 days post exposure. Moreover, at both time points, levels of IL-1β, IL-6 and TNF-α were not increased. Together, these data are indicative of absence of delayed neuroinflammatory responses. Moreover, the mouse brains in our study also did not display treatment-related changes in the oxidative stress markers MDA and GSH. This is also in contrast with the study by Skalska *et al.* in which oxidative stress reponses were found in rats after repeated application of Ag NM by oral gavage (Skalska *et al.* 2016) . Finally, we did not find significant changes in the protein levels of the tight junction proteins claudin-5, occludin and ZO-1 as indicators of BBB disruptive effects. In contrast to our findings, Xu *et al.* described marked BBB disintegration by Ag NM in rats following upon a 2-week exposure via intragastric administration at 1 mg/kg and 10 mg/kg BW doses (Xu *et al.* 2015). Increased penetration and disrupted tight junction proteins (i.e. claudin-5 and ZO-1) has also been shown for Ag and TiO_2 NMs in an *in vitro* BBB model represented by a co-culture of endothelial and astrocyte-like cells (Chen *et al.* 2016). However, Dabrowska-Bouta *et al.* observed an increased expression of tight junction proteins claudin-5, ZO-1, and occludin in rat over a 2-week oral treatment with Ag NM (Dabrowska-Bouta *et al.* 2018).

Taken together our findings suggest that the locomotor impairment effects observed in the mice that were fed with the Ag NM containing feed pellets are not mediated by marked oxidative stress or neuroinflammation, and also do not involve BBB integrity changes. Thereupon, we also investigated the brain tissues for more subtle molecular changes that could explain for the observed sex-specific motor function changes, by looking at serine/threonine and tyrosine protein kinases activity. The analyses indicated that the NMs have no effects on serine/threonine kinase activity. In contrast, the female mice showed an increased tyrosine kinase activity after exposure to Ag NM, whereas this was not seen in males. An upstream kinase analysis was performed, to generate hypotheses for kinases that are differentially active. This indicated that the oral exposure to Ag NM triggers increased signalling via receptor tyrosine kinases and canonical pathways. The upstream kinase analysis indicated increased activity of Zap 70, SYK and Src family kinases. Five members of the Src family (SFKs) are expressed in the mammalian brain, i.e. Src, Fyn, Lyn, Yes, and Lck (Salter and Kalia 2004). Especially Src and Fyn are involved in the regulation of neuronal excitability and activity

(Groveman *et al.* 2012). Activated SFKs can induce tyrosine phosphorylation of N-methyl-d-aspartate (NMDA) receptors (Grosshans and Browning 2001). NMDA receptors are permeable to ions such as Na+ and K+ and Ca^{2+}, and are blocked in a voltage-dependent manner by Mg^{2+} (MacDonald *et al.* 1982). Furthermore, NMDAs are co-receptors for glutamate as well (Salter and Pitcher 2012). Interactions between dopamine and glutamate in the prefrontal cortex are known to be essential for motor, behavioural and cognitive functions (Castner and Williams 2007; Mittal and Eddy 2013). Excessive stimulation of glutamate receptors causes excitotoxicity leading to motor neurodegenerative diseases e.g., ischemia, Huntington's disease, and amyotrophic lateral sclerosis (ALS) (Foran and Trotti 2009) and decreased motor coordination as evaluated by rotarod test in a mouse model of excitotoxicity (Saliba *et al.* 2017). *In vitro* investigations could demonstrate that the neurotoxic effect induced by Ag NM is partially mediated by the glutamatergic NMDA receptor followed by calcium imbalance (Ziemińska *et al.* 2014). *In vivo* studies in female rats even found that Ag NM and ionic silver increased the dopamine concentration in the brain following 28 days of oral administration (Hadrup *et al.* 2012).

To the best of our knowledge, the results of our study are the first to show an effect of Ag NM oral exposure in feed pellets regarding tyrosine kinase activity in mouse brain. Our data indicate that Ag may have an effect on motor coordination by increasing tyrosine kinase activities, especially Src. However, further research is necessary to unravel the underlying molecular mechanisms whereby Ag NMs may trigger increased tyrosine kinase activity and cause motor impairment. Herein, also the observed sex-specificity should be addressed.

Finally, the outcomes of our study are to be addressed in association with route, dose and method of exposure. Our study design involved *ad libitum* exposures to feed pellets dosed with 1% (w/w) TiO_2 and 0.2% PVP-coated Ag, which implicates an estimated daily intake of 2000 mg/kg/BW and 400 mg/kg/BW for TiO_2 and Ag, respectively. Although data concerning neurotoxicity after oral exposure already exists for TiO_2 NMs (Hu *et al.* 2010; Shrivastava *et al.* 2014; Shakeel *et al.* 2016) as well as Ag NMs (Hadrup and Lam 2014; Skalska *et al.* 2015; Ghaderi *et al.* 2015; Skalska *et al.* 2016; Garcia *et al.* 2016; Cameron *et al.* 2018) this merely involves the 'artificial' bolus administration by gavage. In our study, we applied comparatively high concentrations of both types of NMs. Major differences in exposure kinetics and associated effects can be anticipated to result from multiple repeated forced gavage instillations versus an *ad libitum* exposure via food intake. Indeed, already for a single gavage we observed marked contrasts in Ag content in various organs of the mice, including brain, when compared to those that were exposed via the feed pellets. Our design considers physiological conditions

that are of known importance for the investigation of nanomaterials in view of their complex intrinsic physicochemical properties (e.g. size, agglomeration behaviour, solubility). By application of the NMs in the food pellets, also their interactions with, and availability from the food matrix are addressed as well as the role of digestion processes and gastrointestinal passage duration. When extrapolated to human diet, the 1% w/w content of the TiO_2 in the mice feed pellets represents a realistic amount. The US Food and Drug Administration (USFDA) allows its use as food additive in case its weight does not exceed 1% of overall food weight (FDA 2020); the EU allows *quantum satis* levels of TiO_2 in most foodstuffs (Jovanović 2015). For the Ag NM we applied a five-fold lower amount in the feed pellets, because of the intrinsic higher toxicity of this NM when compared with TiO_2. While also allowed *quantum satis* as food additive in the EU (i.e. E 174), it finds more selective applications such as coating of confectionary, decoration and filling and in spirit drinks (Additives and Nutrient Sources added to 2016). However, in relation to its antimicrobial properties there is concern about its growing use in food packaging and release into the food matrix (Gaillet and Rouanet 2015; Azeredo *et al.* 2019).

In the present study, no adverse neurotoxic effects were observed for TiO_2 whereas Ag NM at 0.2 % w/w content in the mice feed pellets revealed altered motor performance and increase in tyrosine kinase activity changes. Together with the observed persistence of Ag in the mouse brains, this justifies further evaluation of foodborne Ag NM at lower exposure scenario.

Conclusions

We investigated the neurotoxicity of TiO_2 and Ag NMs, applied in food pellets, in male and female C57BL/6J mice in a 28-day oral exposure study with or without a 14-day post-exposure recovery period. No major neuropathological changes regarding neuroinflammation in biochemical and immunohistochemical analyses could be observed and behavioural changes in anxiety and cognition were absent. However, in the Ag NM exposed mice motor performance effects were observed by the rotarod test that differed between sexes. The female mice that were exposed to Ag NM for 28 days, showed a consistent diminished motor coordination and increased cortical activity of specific tyrosine kinases. Female mice that were exclusively investigated in a subsequent toxicokinetic study also revealed whole brain levels of Ag that steadily increased during the 28 days of exposure and persisted up to 4 weeks post-exposure. Our study demonstrates that subacute exposure to foodborne TiO_2 and Ag NMs does not cause marked neurotoxicity in mice. However, our toxicokinetic and specific toxicodynamic findings

with Ag NMs indicate that long-term oral exposures to this nanomaterial may cause adverse effects on the central nervous system in a sex-dependent manner. Further dose-dependent investigations with nanosilver regarding this route and type of exposure are justified.

Acknowledgements

The work leading to these results has received funding from the German Federal Ministry of Education and Research (BMBF/InnoSysTox-Verbund, Grant number: FKZ 031L0020A). We thank Isabelle Masson, Gabriele Wick and Petra Gross (IUF) for technical support. We also thank Uwe Karst (Institute of Inorganic and Analytical Chemistry, University of Münster) as well as Daniel Breitenstein and Birgit Hagenhoff (both Tascon GmbH) for equipment support and advice on the ToF-SIMS and LA-ICP-MS analyses.

2.6 Supplementary Material

2.6.1 S1- Analysis of nanoparticle content and distribution within feed pellets

The nominal nanoparticle content of the feed pellets was investigated by ICP-MS analysis (iCAP™ Q from Thermo Scientific) and additional RFA (x-ray fluorescence analysis conducted with a Shimadzu EDX-7000P analyser) investigations. Both methods confirmed the nominal values for the feed pellets (0.2 weight-% for Ag and 1 weight-% for TiO_2). Since these measurements are not conclusive with regard to the distribution of the particles within the feed matrix, scanning electron microscopy in conjunction with energy dispersive x-ray analysis was applied to assess the distribution of the additive particles within the feed pellets, again on pellets spiked with the highest concentration of NP. The investigations were conducted by using a JEOL 7500F (JEOL (Germany) GmbH) and a Tescan CLARA RISE (Tescan GmbH, Dortmund, Germany) high-resolution scanning electron microscope both with a nominal resolution below 2 nm. The results were obtained by applying different acceleration voltages between 2 kV (in gentle-beam mode) and 15 kV for EDS analysis. X-ray analysis was conducted using an EDAX Apollo XL detector.

The SEM images were obtained using backscattered electrons, which yield a better material contrast, thus emphasizing metallic parts of the scanned area. Representative images are shown in Figures S1-I an S1-II. The images show a quasi-homogeneous distribution of nanoparticles on the surface of the feed pellet ingredients (e.g. single grains) with the added nanoparticles, especially for the TiO_2 particles which were added at higher mass concentration in the pellets (i.e. 1 % w/w) in comparison to the Ag NM (i.e. 0.2% w/w). The TiO_2-NP mainly appear as single nanoparticles and also as smaller agglomerates. The Ag-NP appear as single particles and mainly as smaller agglomerates, again distributed over the feed pellet ingredients, as can be seen in the SEM images. At lower magnification, showing larger parts of the pellets no areas were observed with highly agglomerated NPs thus confirming the good dispersion of the NPs within the feed matrix.

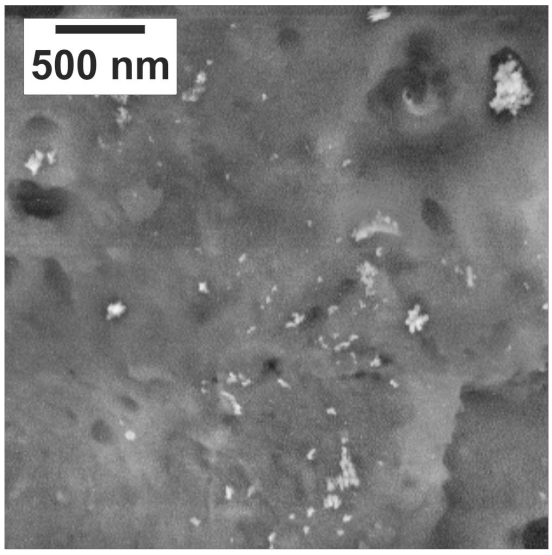

Figure S1-I. Representative SEM micrograph of TiO_2-spiked feed pellet. The NP present mainly as single particles and small agglomerates are well distributed over the surface.

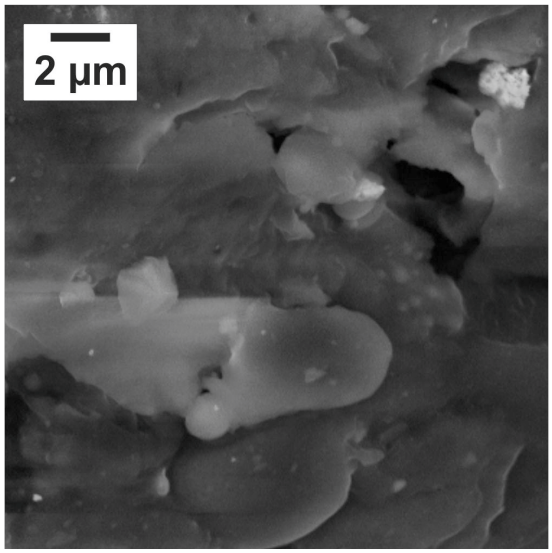

Figure S1-II: Representative SEM micrograph of Ag-spiked feed pellet. The NP present mainly as small agglomerates are well distributed over the surface.

2.6.2 S2- Comparative Inductively Coupled Plasma - Mass Spectrometry (ICP-MS) analyses of Ag in different tissues following exposure via feed pellets or oral gavage.

Table S2-I. Comparative Inductively Coupled Plasma - Mass Spectrometry (ICP-MS) analyses of Ag concentrations (µg/g) in different tissues following exposure via feed pellets or oral gavage. The concentrations of Ag were determined in various organs including the brain of female C57BL/6J mice at 24 h following a single oral gavage administration of Ag NMs (8 mg/400 µl H_2O) or vehicle (400 µl H_2O) as well as following 24 h feeding with pellets containing 0.2% Ag NMs or control feed pellets.

	gavage				feed			
	control		Ag		control		Ag	
small intestine	≤ 0.004#		0.03	± 0.01	≤ 0.001#		30.00	± 20.00
blood	≤ 0.001#		0.01	± 0.01	≤ 0.005#		0.20	± 0.05
brain	≤ 0.004#		0.04	± 0.04	*n.d.*		0.08	± 0.01
liver	0.040	± 0.020	0.05	± 0.02	0.007	± 0.002	1.00	± 0.40
kidney	0.010	± 0.003	0.04	± 0.02	0.006	± 0.001	0.60	± 0.50
spleen	*n.d.*		0.08	± 0.07	*n.d.*		3.00	± 3.00

Values represent mean ± SD for n = 3 mice per group. # Ag levels only above detection limit for 1 out of the 3 analysed mice for the corresponding tissue; n.d. = Ag levels below detection limit in all 3 mice for the corresponding tissue.

2.6.3 S3- Time-of-Flight Secondary Ion Mass Spectrometry and Laser Ablation – Inductively Coupled Plasma – Mass Spectrometry analysis of Ag in mouse brain tissue.

After sacrificing the mice, right brain hemispheres of female C57BL/6J mice fed during 28-days with Ag NMs in feed pellets (0.2% w/w) were dissected for cryo-sectioning. After removal of the brain, it was immediately stored in 4% buffered formalin at 4°C for a minimum of 24 hours for the subsequent placement in 25% sucrose solution in 1xPBS until tissue sinks and subsequently tissue was frozen in dry-iced cold isopentane and stored at -80°C until further cutting of 20 µm thick tissue sections on glass using a Leica CM3050 S cryostat (Leica Biosystems, Germany).

The Laser Ablation – Inductively Coupled Plasma – Mass Spectrometry (LA-ICP-MS) analysis was performed using an LSX 213 G2+ laser system (CETAC Technologies, Omaha, USA) which was equipped with a 2-volume HelEx II cell connected via Tygon tubing to an ICPMS-2030 (Shimadzu, Kyoto, Japan). With a spot size of 25 µm samples were ablated via line-by-line scan using a scan speed of 50 µm/s and 800 mL/min He as transport gas. Data evaluation for the LA-ICP-MS imaging data sets was performed using the in-house developed software Imajar (Robin Schmid, University of Münster, Münster, Germany).

The Time-of-Flight Secondary Ion MassSpectrometry (ToF-SIMS) analyses were conducted after evacuation of the sample chamber (to 1x10-6 mbar) at ambient temperature.

Analyses were performed using a TOF.SIMS5 instrument (IONTOF, Münster, Germany) in the dual-beam 3D analysis mode. The primary ion beam was Bi1+ with a target current of 0.8 pA, and a field of view of 500 x 500 µm². Analysis was performed in sawtooth rastering mode with 512 x 512 pixels. (Dose density: 8.5 x 1013 cm-2). A 1000 eV O2 sputter beam with a current of 250 nA on an area of 1000 x 1000 µm² was used for depth profiling, respectively. The applied ion-dose density was 9.3 x 1017 ions/cm². Profiling was carried out in the non-interlaced mode. The reproducibility of the data was studied by replicate analyses (two replicates of Ag-rich and two replicates of Ag-poor areas) on the same sample performed in the same manner. Data evaluation for the ToF-SIMS 3D imaging data sets was done with the IONTOF Surface Lab 7.1 evaluation software (Münster, Germany).

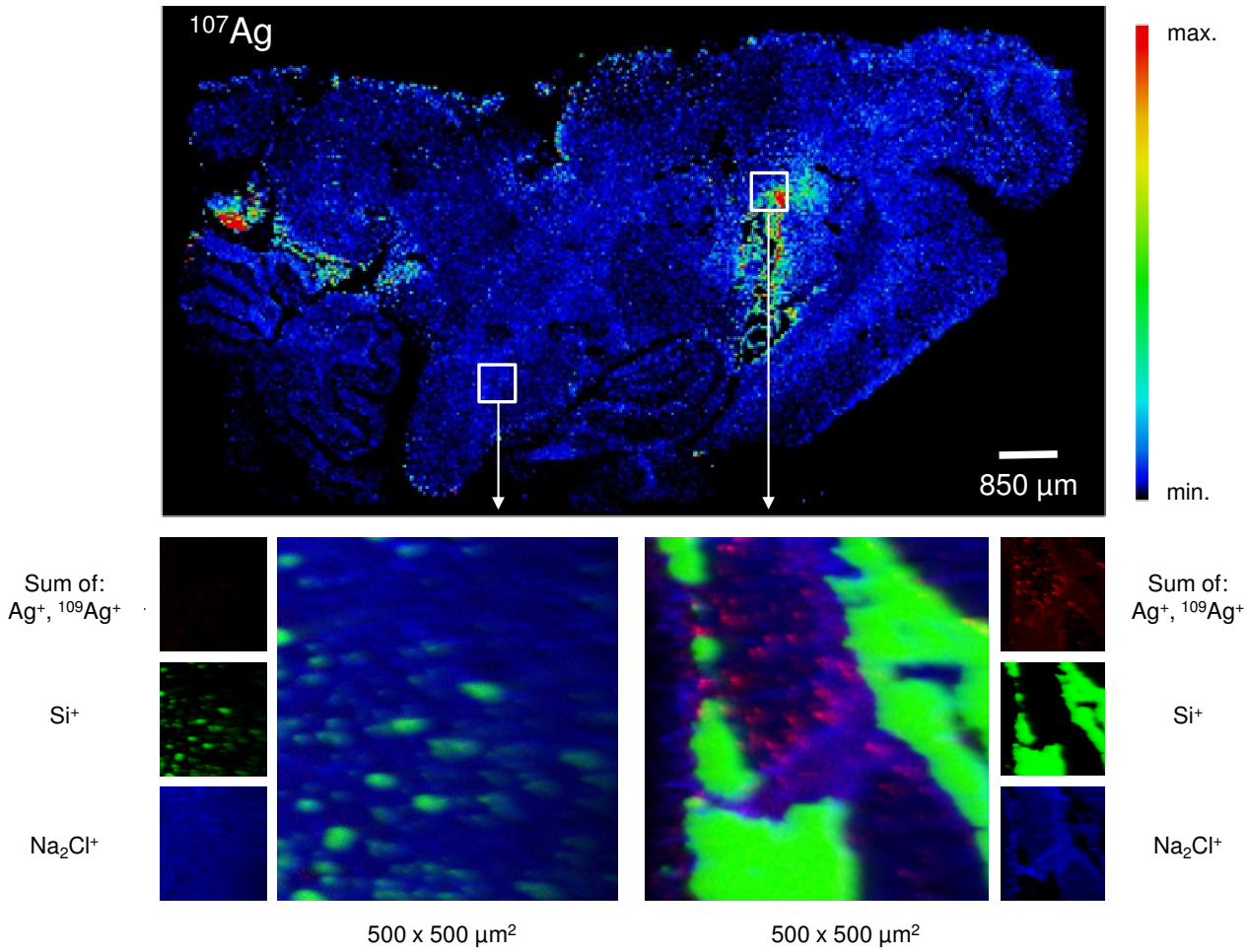

Figure S3-I. LA-ICP-MS (top) and ToF-SIMS (bottom) analyses of the brain. LA-ICP-MS was performed on the complete brain section revealing the lateral distribution of ^{107}Ag (top). A detailed analysis on the Ag enriched area (bottom, right) as well as on an Ag free area (bottom, left) was performed by ToF-SIMS on a subsequent tissue section. With the ToF-SIMS detail analysis ^{107}Ag was detected within the tissue (Na_2Cl^+) but not in the area of the glass-substrate (Si^+).

2.7 References

Abbott, N. Joan, Adjanie A. K. Patabendige, Diana E. M. Dolman, Siti R. Yusof, and David J. Begley. 2010. 'Structure and function of the blood–brain barrier', *Neurobiology of disease*, 37: 13-25.

Additives, Efsa Panel on Food, and Food Nutrient Sources added to. 2016. 'Scientific opinion on the re-evaluation of silver (E 174) as food additive', *EFSA Journal*, 14: 4364.

Azeredo, Henriette M. C., Caio G. Otoni, Daniel S. Corrêa, Odílio B. G. Assis, Márcia R. de Moura, and Luiz Henrique C. Mattoso. 2019. 'Nanostructured Antimicrobials in Food Packaging—Recent Advances', *Biotechnology Journal*, 14: 1900068.

Beeler, J. A., B. Prendergast, and X. Zhuang. 2006. 'Low amplitude entrainment of mice and the impact of circadian phase on behavior tests', *Physiol Behav*, 87: 870-80.

Benjamini, Yoav, and Yosef Hochberg. 1995. 'Controlling the False Discovery Rate: A Practical and Powerful Approach to Multiple Testing', *Journal of the Royal Statistical Society. Series B (Methodological)*, 57: 289-300.

Block, Michelle L., and Jau-Shyong Hong. 2005. 'Microglia and inflammation-mediated neurodegeneration: Multiple triggers with a common mechanism', *Progress in Neurobiology*, 76: 77-98.

Bodaghi, Hojatollah, Younes Mostofi, Abdolrasul Oromiehie, Zabihollah Zamani, Babak Ghanbarzadeh, Cristina Costad, Amalia Conte, and Matteo Nobile. 2013. 'Evaluation of the photocatalytic antimicrobial effects of a TiO2 nanocomposite food packaging film by in vitro and in vivo tests', *Food Science and Technology*, 50: 702-06.

Boudreau, Mary D., Mohammed S. Imam, Angel M. Paredes, Matthew S. Bryant, Candice K. Cunningham, Robert P. Felton, Margie Y. Jones, Kelly J. Davis, and Greg R. Olson. 2016. 'Differential Effects of Silver Nanoparticles and Silver Ions on Tissue Accumulation, Distribution, and Toxicity in the Sprague Dawley Rat Following Daily Oral Gavage Administration for 13 Weeks', *Toxicol Sci*, 150: 131-60.

Bouwmeester, Hans, Susan Dekkers, Maryvon Y. Noordam, Werner I. Hagens, Astrid S. Bulder, Cees de Heer, Sandra E. C. G. ten Voorde, Susan W. P. Wijnhoven, Hans J. P. Marvin, and Adriënne J. A. M. Sips. 2009. 'Review of health safety aspects of nanotechnologies in food production', *Regulatory Toxicology and Pharmacology*, 53: 52-62.

Boyes, William K., Rui Chen, Chunying Chen, and Robert A. Yokel. 2012. 'The neurotoxic potential of engineered nanomaterials', *NeuroToxicology*, 33: 902-10.

Boyes, William K., and Christoph van Thriel. 2020. 'Neurotoxicology of Nanomaterials', *Chemical Research in Toxicology*, 33: 1121-44.

Brand, Walter, Ruud J. B. Peters, Hedwig M. Braakhuis, Lidka Maślankiewicz, and Agnes G. Oomen. 2020. 'Possible effects of titanium dioxide particles on human liver, intestinal tissue, spleen and kidney after oral exposure', *Nanotoxicology*, 14: 985-1007.

Brun, Emilie, Marie Carrière, and Aloïse Mabondzo. 2012. 'In vitro evidence of dysregulation of blood–brain barrier function after acute and repeated/long-term exposure to TiO2 nanoparticles', *Biomaterials*, 33: 886-96.

Buitrago, Manuel M., Jörg B. Schulz, Johannes Dichgans, and Andreas R. Luft. 2004. 'Short and long-term motor skill learning in an accelerated rotarod training paradigm', *Neurobiology of Learning and Memory*, 81: 211-16.

Cameron, Shana J., Farah Hosseinian, and William G. Willmore. 2018. 'A Current Overview of the Biological and Cellular Effects of Nanosilver', *International Journal of Molecular Sciences*, 19: 2030.

Castner, S. A., and G. V. Williams. 2007. 'Tuning the engine of cognition: a focus on NMDA/D1 receptor interactions in prefrontal cortex', *Brain Cogn*, 63: 94-122.

Chawengkijwanich, C., and Y. Hayata. 2008. 'Development of TiO2 powder-coated food packaging film and its ability to inactivate Escherichia coli in vitro and in actual tests', *Int J Food Microbiol*, 123: 288-92.

Chen, I. C., I. L. Hsiao, H. C. Lin, C. H. Wu, C. Y. Chuang, and Y. J. Huang. 2016. 'Influence of silver and titanium dioxide nanoparticles on in vitro blood-brain barrier permeability', *Environ Toxicol Pharmacol*, 47: 108-18.

Chirumamilla, C. S., Mhut Fazil, C. Perez-Novo, S. Rangarajan, R. de Wijn, P. Ramireddy, N. K. Verma, and W. Vanden Berghe. 2019. 'Profiling Activity of Cellular Kinases in Migrating T-Cells', *Methods in molecular biology (Clifton, N.J.)*, 1930: 99-113.

Cho, Wan-Seob, Byeong-Cheol Kang, Jong Kwon Lee, Jayoung Jeong, Jeong-Hwan Che, and Seung Hyeok Seok. 2013. 'Comparative absorption, distribution, and excretion of titanium dioxide and zinc oxide nanoparticles after repeated oral administration', *Part Fibre Toxicol*, 10: 9.

Dabrowska-Bouta, B., G. Sulkowski, M. Frontczak-Baniewicz, J. Skalska, M. Salek, J. Orzelska-Gorka, and L. Struzynska. 2018. 'Ultrastructural and biochemical features of cerebral microvessels of adult rat subjected to a low dose of silver nanoparticles', *Toxicology*, 408: 31-38.

Dhillon, A. S., S. Hagan, O. Rath, and W. Kolch. 2007. 'MAP kinase signalling pathways in cancer', *Oncogene*, 26: 3279-90.

Disdier, C., J. Devoy, A. Cosnefroy, M. Chalansonnet, N. Herlin-Boime, E. Brun, A. Lund, and A. Mabondzo. 2015. 'Tissue biodistribution of intravenously administrated titanium dioxide nanoparticles revealed blood-brain barrier clearance and brain inflammation in rat', *Part Fibre Toxicol*, 12: 27.

Eid, Sameh, Samo Turk, Andrea Volkamer, Friedrich Rippmann, and Simone Fulle. 2017. 'KinMap: a web-based tool for interactive navigation through human kinome data', *BMC Bioinformatics*, 18.

Fabian, Eric, Robert Landsiedel, Lan Ma-Hock, Karin Wiench, Wendel Wohlleben, and Ben van Ravenzwaay. 2008. 'Tissue distribution and toxicity of intravenously administered titanium dioxide nanoparticles in rats', *Archives of toxicology*, 82: 151-57.

FAO/WHO. 2010. 'FAO/WHO expert meeting on the application of nanotechnologies in the food and agriculture sectors: potential food safety implications: meeting report. Rome. 130 pp'.

FDA. 2020. "Title 21 - Food and Drugs, Part 73: LISTING OF COLOR ADDITIVES EXEMPT FROM CERTIFICATION." In, edited by U. S. Food and Drug Administration, 447-48. https://www.govinfo.gov/content/pkg/CFR-2020-title21-vol1/pdf/CFR-2020-title21-vol1-sec73-575.pdf.

Feng, X., A. Chen, Y. Zhang, J. Wang, L. Shao, and L. Wei. 2015. 'Central nervous system toxicity of metallic nanoparticles', *Int J Nanomedicine*, 10: 4321-40.

Foran, Emily, and Davide Trotti. 2009. 'Glutamate transporters and the excitotoxic path to motor neuron degeneration in amyotrophic lateral sclerosis', *Antioxidants & Redox Signaling*, 11: 1587-602.

Gaillet, Sylvie, and Jean-Max Rouanet. 2015. 'Silver nanoparticles: Their potential toxic effects after oral exposure and underlying mechanisms – A review', *Food and Chemical Toxicology*, 77: 58-63.

Gajbhiye, Swati, and Satish Sakharwade. 2016. 'Silver nanoparticles in cosmetics', *Journal of Cosmetics, Dermatological Sciences and Applications*, 6: 48.

Gao, H., and X. Jiang. 2017. 'Introduction and Overview.' in Xinguo Jiang and Huile Gao (eds.), *Neurotoxicity of Nanomaterials and Nanomedicine* (Academic Press).

Garcia, T., D. Lafuente, J. Blanco, D. J. Sanchez, J. J. Sirvent, J. L. Domingo, and M. Gomez. 2016. 'Oral subchronic exposure to silver nanoparticles in rats', *Food Chem Toxicol*, 92: 177-87.

Geraets, Liesbeth, Agnes G. Oomen, Petra Krystek, Nicklas R. Jacobsen, Håkan Wallin, Michel Laurentie, Henny W. Verharen, Esther F. A. Brandon, and Wim H. de Jong. 2014. 'Tissue distribution and elimination after oral and intravenous administration of different titanium dioxide nanoparticles in rats', *Part Fibre Toxicol*, 11: 30-30.

Ghaderi, Shahab, Seyed Reza Fatemi Tabatabaei, Hossein Najafzadeh Varzi, and Masome Rashno. 2015. 'Induced adverse effects of prenatal exposure to silver nanoparticles on neurobehavioral development of offspring of mice', *The Journal of Toxicological Sciences*, 40: 263-75.

Greish, Khaled, Abdulelah Abdullah Alqahtani, Abdulla Falah Alotaibi, Ahmed Mohamed Abdulla, Aysha Tariq Bukelly, Fanar Mohammed Alsobyani, Ghazi Hamad Alharbi, Israa Saeed Alkiyumi, Majed Mutlaq Aldawish, Turki Fahad Alshahrani, Valeria Pittalà, Sebastien Taurin, and Amer Kamal. 2019. 'The Effect of Silver Nanoparticles on Learning, Memory and Social Interaction in BALB/C Mice', *International journal of environmental research and public health*, 16: 148.

Grosshans, D. R., and M. D. Browning. 2001. 'Protein kinase C activation induces tyrosine phosphorylation of the NR2A and NR2B subunits of the NMDA receptor', *J Neurochem*, 76: 737-44.

Groveman, Bradley R., Shuang Feng, Xiao-Qian Fang, Melissa Pflueger, Shuang-Xiu Lin, Ewa A. Bienkiewicz, and XianMin Yu. 2012. 'The regulation of N-methyl-d-aspartate receptors by Src kinase', *The FEBS Journal*, 279: 20-28.

Gunawan, C., C. P. Marquis, R. Amal, G. A. Sotiriou, S. A. Rice, and E. J. Harry. 2017. 'Widespread and Indiscriminate Nanosilver Use: Genuine Potential for Microbial Resistance', *ACS Nano*, 11: 3438-45.

Hadrup, Niels, and Henrik R. Lam. 2014. 'Oral toxicity of silver ions, silver nanoparticles and colloidal silver – A review', *Regulatory Toxicology and Pharmacology*, 68: 1-7.

Hadrup, Niels, Katrin Loeschner, Alicja Mortensen, Anoop K. Sharma, Klaus Qvortrup, Erik H. Larsen, and Henrik R. Lam. 2012. 'The similar neurotoxic effects of nanoparticulate and ionic silver in vivo and in vitro', *NeuroToxicology*, 33: 416-23.

Hall, Calvin S., and Egerton L. Ballachey. 1932. *A study of the rat's behavior in a field; a contribution to method in comparative psychology* ([Univ. of California Press]: [Berkeley]).

Heo, Min Beom, Minjeong Kwak, Kyu Sup An, Hye Jin Kim, Hyeon Yeol Ryu, So Min Lee, Kyung Seuk Song, In Young Kim, Ji-Hwan Kwon, and Tae Geol Lee. 2020. 'Oral toxicity of titanium dioxide P25 at repeated dose 28-day and 90-day in rats', *Part Fibre Toxicol*, 17: 34.

Heusinkveld, Harm J., Tina Wahle, Arezoo Campbell, Remco H. S. Westerink, Lang Tran, Helinor Johnston, Vicki Stone, Flemming R. Cassee, and Roel P. F. Schins. 2016. 'Neurodegenerative and neurological disorders by small inhaled particles', *NeuroToxicology*, 56: 94-106.

Hilhorst, Riet, Liesbeth Houkes, Monique Mommersteeg, Joyce Musch, Adriënne van den Berg, and Rob Ruijtenbeek. 2013. 'Peptide microarrays for profiling of serine/threonine kinase activity of recombinant kinases and lysates of cells and tissue samples', *Methods in molecular biology (Clifton, N.J.)*, 977: 259-71.

Hougaard, Karin S., Petra Jackson, Keld A. Jensen, Jens J. Sloth, Katrin Löschner, Erik H. Larsen, Renie K. Birkedal, Anni Vibenholt, Anne-Mette Z. Boisen, Håkan Wallin, and Ulla Vogel. 2010. 'Effects of prenatal exposure to surface-coated nanosized titanium dioxide (UV-Titan). A study in mice', *Part Fibre Toxicol*, 7: 16-16.

Hu, R., X. Gong, Y. Duan, N. Li, Y. Che, Y. Cui, M. Zhou, C. Liu, H. Wang, and F. Hong. 2010. 'Neurotoxicological effects and the impairment of spatial recognition memory in mice caused by exposure to TiO2 nanoparticles', *Biomaterials*, 31: 8043-50.

Hullmann, Maja, Catrin Albrecht, Damiën van Berlo, Miriam E. Gerlofs-Nijland, Tina Wahle, Agnes W. Boots, Jean Krutmann, Flemming R. Cassee, Thomas A. Bayer, and Roel P. F. Schins. 2017. 'Diesel engine exhaust accelerates plaque formation in a mouse model of Alzheimer's disease', *Part Fibre Toxicol*, 14: 35.

Islam, M. T. 2017. 'Oxidative stress and mitochondrial dysfunction-linked neurodegenerative disorders', *Neurol Res*, 39: 73-82.

Jawhar, S., A. Trawicka, C. Jenneckens, T. A. Bayer, and O. Wirths. 2012. 'Motor deficits, neuron loss, and reduced anxiety coinciding with axonal degeneration and intraneuronal Abeta aggregation in the 5XFAD mouse model of Alzheimer's disease', *Neurobiol Aging*, 33: 196.e29-40.

Jovanović, Boris. 2015. 'Critical review of public health regulations of titanium dioxide, a human food additive', *Integrated Environmental Assessment and Management*, 11: 10-20.

Kim, E. K., and E. J. Choi. 2015. 'Compromised MAPK signaling in human diseases: an update', *Arch Toxicol*, 89: 867-82.

Kim, Yong Soon, Moon Yong Song, Jung Duck Park, Kyung Seuk Song, Hyeon Ryol Ryu, Yong Hyun Chung, Hee Kyung Chang, Ji Hyun Lee, Kyung Hui Oh, Bruce J. Kelman, In Koo Hwang, and Il Je Yu. 2010. 'Subchronic oral toxicity of silver nanoparticles', *Part Fibre Toxicol*, 7: 20-20.

Kovacs, G. G. 2017. 'Cellular reactions of the central nervous system', *Handb Clin Neurol*, 145: 13-23.

Kreyling, Wolfgang G., Uwe Holzwarth, Carsten Schleh, Ján Kozempel, Alexander Wenk, Nadine Haberl, Stephanie Hirn, Martin Schäffler, Jens Lipka, Manuela Semmler-Behnke, and Neil Gibson. 2017. 'Quantitative biokinetics of titanium dioxide nanoparticles after oral application in rats: Part 2', *Nanotoxicology*, 11: 443-53.

Krystek, P., J. Tentschert, Y. Nia, B. Trouiller, L. Noël, M. E. Goetz, A. Papin, A. Luch, T. Guérin, and W. H. de Jong. 2014. 'Method development and inter-laboratory comparison about the determination of titanium from titanium dioxide nanoparticles in tissues by inductively coupled plasma mass spectrometry', *Anal Bioanal Chem*, 406: 3853-61.

Lee, Jinsoo, Ji-Seong Jeong, Sang Yun Kim, Min-Kyu Park, Sung-Deuk Choi, Un-Jung Kim, Kwangsik Park, Eun Ju Jeong, Sang-Yoon Nam, and Wook-Joon Yu. 2019. 'Titanium dioxide nanoparticles oral exposure to pregnant rats and its distribution', *Part Fibre Toxicol*, 16: 31-31.

Li, Dongyang, Xiaoyu Liu, Tianming Liu, Haitao Liu, Li Tong, Shuwei Jia, and Yu-Feng Wang. 2020. 'Neurochemical regulation of the expression and function of glial fibrillary acidic protein in astrocytes', *Glia*, 68: 878-97.

Li, J., and F. L. Martin. 2017. 'Chapter 4 - Current Perspective on Nanomaterial-Induced Adverse Effects: Neurotoxicity as a Case Example.' in Xinguo Jiang and Huile Gao (eds.), *Neurotoxicity of Nanomaterials and Nanomedicine* (Academic Press).

Loeschner, Katrin, Niels Hadrup, Klaus Qvortrup, Agnete Larsen, Xueyun Gao, Ulla Vogel, Alicja Mortensen, Henrik Rye Lam, and Erik H. Larsen. 2011. 'Distribution of silver in rats following 28 days of repeated oral exposure to silver nanoparticles or silver acetate', *Part Fibre Toxicol*, 8: 18-18.

Lull, Melinda E., and Michelle L. Block. 2010. 'Microglial activation and chronic neurodegeneration', *Neurotherapeutics : the journal of the American Society for Experimental NeuroTherapeutics*, 7: 354-65.

MacDonald, J. F., A. V. Porietis, and J. M. Wojtowicz. 1982. 'L-Aspartic acid induces a region of negative slope conductance in the current-voltage relationship of cultured spinal cord neurons', *Brain Res*, 237: 248-53.

Maneewattanapinyo, Pattwat, Wijit Banlunara, Chuchaat Thammacharoen, Sanong Ekgasit, and Theerayuth Kaewamatawong. 2011. 'An Evaluation of Acute Toxicity of Colloidal Silver Nanoparticles', *Journal of Veterinary Medical Science*, 73: 1417-23.

Mayer, Cynthia L., Bertrand R. Huber, and Elaine Peskind. 2013. 'Traumatic brain injury, neuroinflammation, and post-traumatic headaches', *Headache*, 53: 1523-30.

McGillicuddy, E., I. Murray, S. Kavanagh, L. Morrison, A. Fogarty, M. Cormican, P. Dockery, M. Prendergast, N. Rowan, and D. Morris. 2017. 'Silver nanoparticles in the environment: Sources, detection and ecotoxicology', *Science of The Total Environment*, 575: 231-46.

Miquel, Jaime, and Margarita Blasco. 1978. 'A simple technique for evaluation of vitality loss in aging mice, by testing their muscular coordination and vigor', *Experimental Gerontology*, 13: 389-96.

Mittal, Sumeer K., and Clare Eddy. 2013. 'The role of dopamine and glutamate modulation in Huntington disease', *Behavioural neurology*, 26: 255-63.

Moran, P. M., L. S. Higgins, B. Cordell, and P. C. Moser. 1995. 'Age-related learning deficits in transgenic mice expressing the 751-amino acid isoform of human beta-amyloid precursor protein', *Proc Natl Acad Sci U S A*, 92: 5341-5.

Munger, Mark A., Przemyslaw Radwanski, Greg C. Hadlock, Greg Stoddard, Akram Shaaban, Jonathan Falconer, David W. Grainger, and Cassandra E. Deering-Rice. 2014. 'In vivo human time-exposure study of orally dosed commercial silver nanoparticles', *Nanomedicine : nanotechnology, biology, and medicine*, 10: 1-9.

Oberdörster, G., Z. Sharp, V. Atudorei, A. Elder, R. Gelein, W. Kreyling, and C. Cox. 2004. 'Translocation of inhaled ultrafine particles to the brain', *Inhal Toxicol*, 16: 437-45.

Oberdörster, Günter, Alison Elder, and Amber Rinderknecht. 2009. 'Nanoparticles and the brain: cause for concern?', *J Nanosci Nanotechnol*, 9: 4996-5007.

Oberdörster, Günter, Eva Oberdörster, and Jan Oberdörster. 2005. 'Nanotoxicology: an emerging discipline evolving from studies of ultrafine particles', *Environmental Health Perspectives*, 113: 823-39.

OECD. 1997. *Test No. 424: Neurotoxicity Study in Rodents*.

Park, E. J., E. Bae, J. Yi, Y. Kim, K. Choi, S. H. Lee, J. Yoon, B. C. Lee, and K. Park. 2010. 'Repeated-dose toxicity and inflammatory responses in mice by oral administration of silver nanoparticles', *Environ Toxicol Pharmacol*, 30: 162-8.

Rai, Mahendra, and Ranjita Shegokar. 2017. 'Metal Nanoparticles in Pharma.', *n. pag. Crossref. Web.*

Recordati, Camilla, Marcella De Maglie, Silvia Bianchessi, Simona Argentiere, Claudia Cella, Silvana Mattiello, Francesco Cubadda, Federica Aureli, Marilena D'Amato, Andrea Raggi, Cristina Lenardi, Paolo Milani, and Eugenio Scanziani. 2015. 'Tissue distribution and acute toxicity of silver after single intravenous administration in mice: nano-specific and size-dependent effects', *Part Fibre Toxicol*, 13: 12.

Rosenberger, Andrea F. N., Tjado H. J. Morrema, Wouter H. Gerritsen, Elise S. van Haastert, Hripsime Snkhchyan, Riet Hilhorst, Annemieke J. M. Rozemuller, Philip Scheltens, Saskia M. van der Vies, and Jeroen J. M. Hoozemans. 2016. 'Increased occurrence of protein kinase CK2 in astrocytes in Alzheimer's disease pathology', *J Neuroinflammation*, 13: 4-4.

Saliba, Soraya Wilke, Erica Leandro Marciano Vieira, Rebeca Priscila de Melo Santos, Eduardo Candelario-Jalil, Bernd L. Fiebich, Luciene Bruno Vieira, Antonio Lucio Teixeira, and Antonio Carlos Pinheiro de Oliveira. 2017. 'Neuroprotective effects of intrastriatal injection of rapamycin in a mouse model of excitotoxicity induced by quinolinic acid', *J Neuroinflammation*, 14: 25-25.

Salter, M. W., and L. V. Kalia. 2004. 'Src kinases: a hub for NMDA receptor regulation', *Nat Rev Neurosci*, 5: 317-28.

Salter, Michael W., and Graham M. Pitcher. 2012. 'Dysregulated Src upregulation of NMDA receptor activity: a common link in chronic pain and schizophrenia', *The FEBS Journal*, 279: 2-11.

Shah, Neel H., Jeanine F. Amacher, Laura M. Nocka, and John Kuriyan. 2018. 'The Src module: an ancient scaffold in the evolution of cytoplasmic tyrosine kinases', *Critical reviews in biochemistry and molecular biology*, 53: 535-63.

Shakeel, Muhammad, Farhat Jabeen, Samina Shabbir, Muhammad Saleem Asghar, Muhammad Saleem Khan, and Abdul Shakoor Chaudhry. 2016. 'Toxicity of Nano-Titanium Dioxide (TiO2-NP) Through Various Routes of Exposure: a Review', *Biological Trace Element Research*, 172: 1-36.

Sharma, Hari Shanker, Saber Hussain, John Schlager, Syed F. Ali, and Aruna Sharma. 2010. "Influence of Nanoparticles on Blood–Brain Barrier Permeability and Brain Edema Formation in Rats." In *Brain Edema XIV*, edited by Zbigniew Czernicki, Alexander Baethmann, Umeo Ito, Yoichi Katayama, Toshihiko Kuroiwa and David Mendelow, 359-64. Vienna: Springer Vienna.

Shi, Hongbo, Ruth Magaye, Vincent Castranova, and Jinshun Zhao. 2013. 'Titanium dioxide nanoparticles: a review of current toxicological data', *Part Fibre Toxicol*, 10: 15.

Shrivastava, R., S. Raza, A. Yadav, P. Kushwaha, and S. J. Flora. 2014. 'Effects of sub-acute exposure to TiO2, ZnO and Al2O3 nanoparticles on oxidative stress and histological changes in mouse liver and brain', *Drug Chem Toxicol*, 37: 336-47.

Skalska, J., B. Dabrowska-Bouta, and L. Struzynska. 2016. 'Oxidative stress in rat brain but not in liver following oral administration of a low dose of nanoparticulate silver', *Food Chem Toxicol*, 97: 307-15.

Skalska, J., M. Frontczak-Baniewicz, and L. Struzynska. 2015. 'Synaptic degeneration in rat brain after prolonged oral exposure to silver nanoparticles', *NeuroToxicology*, 46: 145-54.

Sofroniew, Michael V., and Harry V. Vinters. 2010. 'Astrocytes: biology and pathology', *Acta Neuropathol*, 119: 7-35.

Sohal, Ikjot Singh, Kevin S. O'Fallon, Peter Gaines, Philip Demokritou, and Dhimiter Bello. 2018. 'Ingested engineered nanomaterials: state of science in nanotoxicity testing and future research needs', *Part Fibre Toxicol*, 15: 29.

Song, Bin, YanLi Zhang, Jia Liu, XiaoLi Feng, Ting Zhou, and LongQuan Shao. 2016. 'Is Neurotoxicity of Metallic Nanoparticles the Cascades of Oxidative Stress?', *Nanoscale Res Lett*, 11: 291-91.

Trickler, W. J., S. M. Lantz, R. C. Murdock, A. M. Schrand, B. L. Robinson, G. D. Newport, J. J. Schlager, S. J. Oldenburg, M. G. Paule, W. Slikker, Jr., S. M. Hussain, and S. F. Ali. 2010. 'Silver nanoparticle induced blood-brain barrier inflammation and increased permeability in primary rat brain microvessel endothelial cells', *Toxicol Sci*, 118: 160-70.

Unfried, Klaus, Catrin Albrecht, Lars-Oliver Klotz, Anna Von Mikecz, Susanne Grether-Beck, and Roel P. F. Schins. 2007. 'Cellular responses to nanoparticles: Target structures and mechanisms', *Nanotoxicology*, 1: 52-71.

Valko, M., D. Leibfritz, J. Moncol, M. T. Cronin, M. Mazur, and J. Telser. 2007. 'Free radicals and antioxidants in normal physiological functions and human disease', *Int J Biochem Cell Biol*, 39: 44-84.

van den Brule, Sybille, Jérôme Ambroise, Hélène Lecloux, Clément Levard, Romain Soulas, Pieter-Jan De Temmerman, Mihaly Palmai-Pallag, Etienne Marbaix, and Dominique Lison. 2016. "Dietary silver nanoparticles can disturb the gut microbiota in mice." In *Part Fibre Toxicol*, 38.

van der Zande, Meike, Rob J. Vandebriel, Elke Van Doren, Evelien Kramer, Zahira Herrera Rivera, Cecilia S. Serrano-Rojero, Eric R. Gremmer, Jan Mast, Ruud J. B. Peters, Peter

C. H. Hollman, Peter J. M. Hendriksen, Hans J. P. Marvin, Ad A. C. M. Peijnenburg, and Hans Bouwmeester. 2012. 'Distribution, Elimination, and Toxicity of Silver Nanoparticles and Silver Ions in Rats after 28-Day Oral Exposure', *ACS Nano*, 6: 7427-42.

Vance, Marina E., Todd Kuiken, Eric P. Vejerano, Sean P. McGinnis, Michael F. Hochella, Jr., David Rejeski, and Matthew S. Hull. 2015. 'Nanotechnology in the real world: Redeveloping the nanomaterial consumer products inventory', *Beilstein Journal of Nanotechnology*, 6: 1769-80.

Wahle, Tina, Adriana Sofranko, Susan Dekkers, Mark R. Miller, Harm J. Heusinkveld, Catrin Albrecht, Flemming R. Cassee, and Roel P. F. Schins. 2020. 'Evaluation of neurological effects of cerium dioxide nanoparticles doped with different amounts of zirconium following inhalation exposure in mouse models of Alzheimer's and vascular disease', *Neurochemistry International*, 138: 104755.

Wang, Jiangxue, Guoqiang Zhou, Chunying Chen, Hongwei Yu, Tiancheng Wang, Yongmei Ma, Guang Jia, Yuxi Gao, Bai Li, Jin Sun, Yufeng Li, Fang Jiao, Yuliang Zhao, and Zhifang Chai. 2007. 'Acute toxicity and biodistribution of different sized titanium dioxide particles in mice after oral administration', *Toxicol Lett*, 168: 176-85.

Wu, Tianshu, and Meng Tang. 2017. 'The inflammatory response to silver and titanium dioxide nanoparticles in the central nervous system', *Nanomedicine*, 13: 233-49.

Xu, Liming, Mo Dan, Anliang Shao, Xiang Cheng, Cuiping Zhang, Robert A. Yokel, Taro Takemura, Nobutaka Hanagata, Masami Niwa, and Daisuke Watanabe. 2015. 'Silver nanoparticles induce tight junction disruption and astrocyte neurotoxicity in a rat blood-brain barrier primary triple coculture model', *Int J Nanomedicine*, 10: 6105-18.

Yin, Nuoya, Yang Zhang, Zhaojun Yun, Qian Liu, Guangbo Qu, Qunfang Zhou, Ligang Hu, and Guibin Jiang. 2015. 'Silver nanoparticle exposure induces rat motor dysfunction through decrease in expression of calcium channel protein in cerebellum', *Toxicol Lett*, 237: 112-20.

Ziemińska, Elżbieta, Aleksandra Stafiej, and Lidia Strużyńska. 2014. 'The role of the glutamatergic NMDA receptor in nanosilver-evoked neurotoxicity in primary cultures of cerebellar granule cells', *Toxicology*, 315: 38-4

3 Effects of subchronic dietary exposure to the engineered nanomaterials SiO_2 and CeO_2 in C57BL/6J and 5xFAD Alzheimer model mice: CeO_2 reduces amyloid plaque burden

Adriana Sofranko[1], Tina Wahle[1], Julia Kolling[1], Harm J. Heusinkveld[1,2], Burkhard Stahlmecke[3], Martin Rosenbruch[4], Catrin Albrecht[1], Roel P.F. Schins[1]

[1]IUF - Leibniz Research Institute for Environmental Medicine, Düsseldorf, Germany; [2]National Institute for Public Health and the Environment (RIVM), Bilthoven, The Netherlands; [3]Institute for Energy and Environmental Technology e.V. (IUTA), Duisburg, Germany; [4]Heinrich- Heine University, Düsseldorf, Germany.

Manuscript submitted to Particle and Fibre Toxicology.

Author contribution: The author of this dissertation was involved in weighing and handling of the mice in the animal facility during the whole study, performed behaviour tests, analysed immunohistochemical plaque burden, performed Aβ analyses as well as neuroinflammation and oxidative stress marker analyses, wrote the manuscript, made the graphs and discussed the results. Relative contribution: about 50%.

Already performed, analysed, discussed and published in the master thesis of the author of this dissertation: X-maze, string suspension and open field test, Amyloid plaque burden in 5xFAD mice.

3.1 Abstract

Background: There is an increasing concern about the neurotoxicity of engineered nanomaterials (NMs). To investigate the effects of subchronic oral exposures to SiO_2 and CeO_2 NMs on Alzheimer's disease (AD)-like pathology, 5xFAD transgenic mice and their C57BL/6J littermates were fed *ad libitum* for 3 or 14 weeks with control food pellets, or pellets dosed with these respective NMs at 0.1% or 1% (w/w). Behaviour effects were evaluated by X-maze, string suspension, balance beam and open field tests. Brains were analysed for plaque load, beta-amyloid peptide levels, markers of oxidative stress and neuroinflammation.

Results: No marked behavioural impairments were observed in the mice exposed to SiO_2 or CeO_2 and neither treatment resulted in accelerated plaque formation, increased oxidative stress or inflammation. In contrast, the 5xFAD mice exposed to 1% CeO_2 for 14 weeks showed significantly lower hippocampal Aβ plaque load and improved locomotor activity compared to the corresponding controls.

Conclusions: The findings from present study suggest that long-term oral exposure to SiO_2 or CeO_2 NMs has no neurotoxic and AD-promoting effects. The reduced plaque burden observed in the mice following dietary CeO_2 exposure warrants further investigation to establish the underlying mechanism as well as the feasibility of this physiological administration method.

Keywords: Amorphous silica, nanoceria, subchronic oral exposure study, neurobehavioral testing, neurotoxicity, Alzheimer's Disease

3.2 Introduction

The development and steady introduction of new engineered nanomaterials (NMs) to the market has raised awareness about potential adverse health effects resulting from long-term exposures. The health risk concerns for NMs originated from inhalation toxicology studies that could substantiate the role of ultrafine particles in the epidemiological link between ambient air pollution exposure and cardiopulmonary diseases (reviewed by [1]). Likewise, the awareness about potential adverse effects of NMs on the central nervous system came from inhalation studies in more recent years. Neuroinflammatory, neurotoxicological and neurodegenerative effects observed by inhaled ultrafine particles and NMs in these toxicological studies provided experimental support to the growing number of epidemiological studies that showed associations between particulate air pollution exposure and neurological diseases [2, 3].

Specific concern has risen that long-term exposure to particulate air pollution could contribute to the pathogenesis of Alzheimer's disease (AD) the most common neurodegenerative disease in the world [3, 4, 5]. A major neuropathological hallmark of AD is the generation of hydrophobic Amyloid-β peptide (Aβ) containing plaques resulting from the sequential proteolysis of the amyloid precursor protein (APP) by β- and γ-secretase enzymes (reviewed in [6, 7]). Although the exact mechanisms of initiation and progression of AD are still incompletely understood, it has been suggested that specific NMs may be involved due to their ability to disrupt Aβ homeostasis, resulting from reactive oxygen species generation (ROS) and oxidative stress, in similarity with other environmental factors like specific neurotoxic metals and some pesticides [8, 9, 10, 11].

With the growing evidence for a role of inhaled nanoparticles in AD, there is also an increasing debate regarding the neurotoxicity and potential AD-promoting effects of ingested NMs. Indeed, neurotoxic effects in mice have been reported following oral exposure to NMs composed of silver [12, 13, 14], zinc oxide [15, 16], titanium dioxide [17] and iron oxide [18]. However, to the best of our knowledge it has not yet been investigated if long-term oral exposure to NMs can promote the development and progression of AD. Therefore, the main goal of our study was to address if subchronic oral exposure to NMs can accelerate hallmarks of Alzheimer-like pathology in mice. For this purpose, we selected amorphous SiO_2 (SAS) and CeO_2 NMs ("nanoceria"), representing two of the most widely used and investigated types of nanoparticles.

SiO_2 is extensively used in chemistry, agriculture and consumer products, including cosmetics [19, 20, 21]. In the food sector, it finds application as anti-caking agent in powdered food products and is listed in Europe as food additive E551 [22]. CeO_2 NMs are used as well in various commercial and industrial applications, e.g., as catalyst, ultraviolet-filter [23] and as fuel additive to improve combustion [24]. They are also increasingly promoted in agricultural applications [25, 26]. Although CeO_2 NMs are not used as food additive, accumulation in agricultural crops and trophic transfer have been reported [27, 28]. Furthermore, as an additive to diesel and gasoline fuels, it can be inhaled following its emission with exhaust gases [29, 30] and a substantial fraction of this can subsequently reach the gastrointestinal tract following mucociliary clearance and swallowing [31, 32, 33]. Finally, because of the coexistence of Ce^{3+} and Ce^{4+} in nanosized CeO_2 and its resulting unique redox-active properties, nanoceria has also received rapidly growing attention in biomedical and pharmaceutical applications that include oral administration strategies [34, 35].

For our present investigations, the SiO_2 and CeO_2 NMs were incorporated into mouse feed pellets at 1% and 0.1% weight/weight (w/w) concentrations. The highest dose of the NMs in the pellets was selected on the basis of the amount of SiO_2 that should not be exceeded in food applications, i.e. 2%, according to the US Food and Drug Administration (US FDA 2021). For the investigation of neurotoxicity and AD-like pathology, female heterozygous 5xFAD mice [36, 37] and their female nontransgenic C57BL/6J littermates were fed *ad libitum* during 3 or 14 weeks with the various NM-dosed or control pellets. In the 3rd and 14th week of exposure neurotoxicity was assessed by a series of behavioural tests, while specific effects on AD-like pathology were evaluated in the 5xFAD mice by evaluation of plaque load, Aβ-peptide levels and markers of oxidative stress and neuroinflammation. General toxicity beyond the brain was concurrently assessed by analysis of body weight gain as well as gross examinations, weight and histopathological analyses of specific organs.

3.3 Materials and Methods

3.3.1 **Nanomaterials.**

The CeO_2 JRC reference nanomaterial NM-212 was purchased from the Fraunhofer Institute for Molecular Biology and Applied Ecology (IME, Schmallenberg, Germany). The amorphous fumed SiO_2 NM sample was obtained from Sigma-Aldrich, Munich, Germany (#S5130). The characteristics of the pristine NMs were determined by scanning electron microscopy (SEM). The CeO_2 NMs had a mean size of 35.4 nm ± 17 nm and displayed a nearly spherical particle morphology. The analysis of the SiO_2 revealed a spherical morphology with a mean size of 12.9 ± 4.9 nm.

3.3.2 **Study design.**

The oral exposure studies were performed in heterozygous 5xFAD mice and their nontransgenic C57BL/6J littermates. The 5xFAD mouse model carries five familial AD mutations and is characterized by an early onset of AD-related pathology: the double Swedish mutation (K670N/M671L), which is responsible for the enhanced amyloid production, and mutations which are responsible for altered amyloid precursor protein processing leading to a higher ratio of the more amyloidogenic Aβ production such as the Florida (I716V) and London (V717I) mutations in APP and the mutant presenilin 1 (M146L + L286V) with neuronal expression driven by the neuron-specific mouse Thy-1 promoter [36]. Amyloid deposition starts in the deep layers of the cortex and subiculum at 2 months of age, while memory and motor deficits become detectable from 4 to 6 months of age [36, 37]. The mice were handled

according to guidelines of the Society for Laboratory Animals Science (GV-SOLAS) and were housed under standard conditions with access to food and water *ad libitum*. Lighting was artificial with a sequence of 12 hours light and 12 hours dark. The study was approved by the Landesamt für Natur, Umwelt und Verbraucherschutz (LANUV, NRW, Germany; Ref. no. 84-02.04.2013.A443). Nine weeks old female 5xFAD and female C57BL/6J littermates were exposed *ad libitum* for 3 or 14 weeks to feed pellets that were loaded with 0.1% or 1% (w/w) SiO_2 NM or CeO_2, or to control feed pellets (**Figure 3.7**). The study was designed with n=160 mice, i.e. for the respective sub-studies n=50 5xFAD mice (n=10 per treatment group) and n=30 WT mice (n=6 per treatment group). One 5xFAD mouse (0.1% SiO_2 exposed) died in the first week of exposure and thus were excluded from all analyses. Moreover, in the 3-week sub-study one WT mouse exposed to 1% SiO_2 was inappropriately labelled as 5xFAD mouse, whereas in the 14-week study one control 5xFAD mouse was inappropriately classified as WT animal. The study design is shown in Figure 3.7. The feed pellets were prepared and provided by ssniff GmbH, Soest, Germany. **Figure S1** shows representative SEM images of the SiO_2 and CeO_2 NMs within prepared feed pellets and by comparison of the pristine NMs (see also 5.1). One week prior to study start mice were randomized according to age and body weight. During the weeks before dissection, behavioural studies were performed to assess for effects on anxiety, motor performance and spatial working memory. Following sacrifice, brain tissues were collected as well as further organs for analyses as described below.

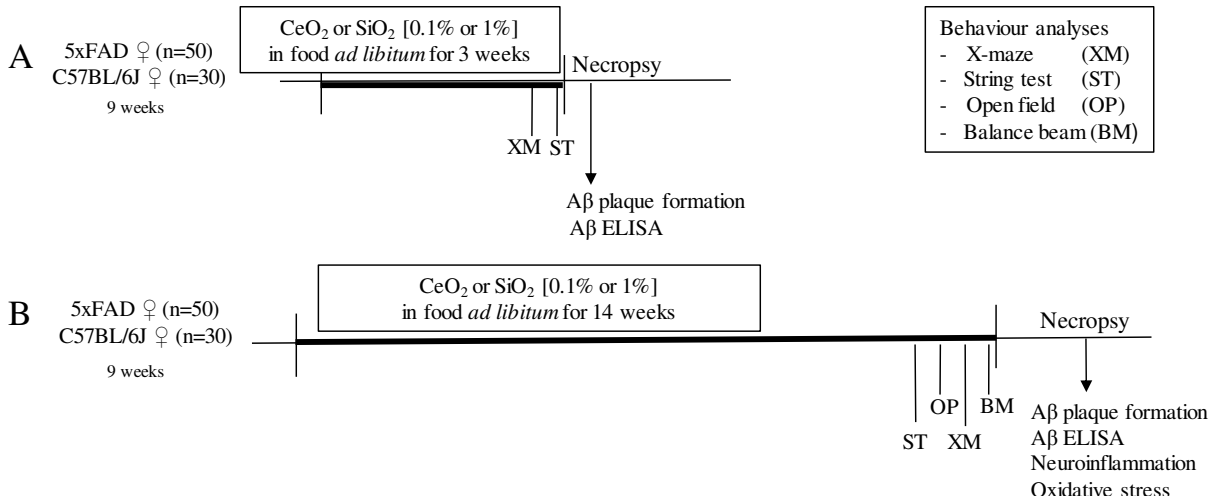

Figure 3.7. Study design. Nine weeks old female C57BL/6J or 5xFAD mice were exposed to 0.1 or 1% CeO_2 or SiO_2 [0.1 or 1%] nanomaterials (NMs) in feed pellets ad libitum for 3 weeks (A) or for 14 weeks (B). Motor function, memory and anxiety were determined in a series of behaviour tests performed in the weeks before the necropsies, as follows for the respective substudies: The X-maze test (XM) was performed on exposure day 19 (A) or 95 (B), the string test (ST) was performed on day 20 (A) or 88 (B), the open field test (OP) was performed on day 91 (B) and the balance beam test (BM) was performed on day 96 (B). Aβ plaque formation and Aβ ELISA (A, B) or markers of neuroinflammation and oxidative stress (B) were analysed in the brains of the mice after necropsy.

3.3.3 **Behavioural tests.**

In alignment with animal ethics, requirements and routine of our animal facility and previous studies [11, 14, 42] all behaviour tasks were performed during daytime, i.e. during the resting phase of the animals.

Motor function and grip strength were tested using the string suspension task, where mice are permitted to grab a string with their forepaws and allowed move to one of the platforms in between the string is suspended [37, 38]. To rate motor performance during 60 s trials, a scoring system from 0 to 7 was used which was adapted from [96] and described in detail in our previous work [14, 42]. Spatial working memory by spontaneous alternation behaviour was assessed using an open arm cross (X)-maze task as described in Jawhar and colleagues [37] and recent work of our studies [11, 14, 42]. During 5 min test sessions, spontaneous alternation was measured and defined as successful if a mouse visited all of the 4 arms alternately. An impairment in spatial working memory is defined by decrease in spontaneous alternation [97]. Anxiety and exploratory activity was measured using the open field test (Noldus, the Netherlands) [39] as previously described [14]. Increased anxiety was defined by spending less time in the open central area compared to the more hidden border during 5 min test sessions. The balance beam walking assay is used to test motor coordination and balance in rodents as previously described [37, 40]. Therefore, a 50 cm long wooden beam was suspended between two plastic platforms (9 cm x 15 cm) placed above two vertical poles at a height of 40 cm. The mice were released in the middle of the beam and released thereafter allowing the mice to traverse the beam. Performance on the walking assay is quantified by measuring the time it takes for the mouse to escape to one of the platforms during a 60 second trial. The trial was repeated three times in one day of testing. If an animal remains on the beam for whole 60 second and does not escape to one of the platforms, the maximum time of 60 seconds is recorded. All three trials are averaged. To avoid odour distraction, all behaviour tasks were cleaned between trials with 70% ethanol. Behaviour tests were recorded with an infrared camera and analysed with associated software (EthoVision XT 11, Noldus).

3.3.4 **Dissection, tissue preparations and histopathology**

The mice were sacrificed by cervical dislocation, followed by decapitation. Right brain hemispheres were stored in 4% paraformaldehyde (PFA) for immunohistochemistry. Left brain hemispheres were rapidly dissected into cortex, cerebellum and midbrain, snap frozen in liquid nitrogen, then stored at -80°C until processing for biochemical analyses. Liver, spleen and kidneys were removed and weighed. Small intestines and colons were removed, flushed with

saline and opened, subsequently analysed for weight and length and used to prepare Swiss-rolls. Histology analyses were performed according to routine procedures (fixation in 4% PFA and paraffine embedding). Sections of small and large intestines, liver and spleen were blindly evaluated by an experienced veterinary pathologist using Haematoxylin and Eosin (H&E) stained sections for these organs and additionally Periodic Acid Schiff (PAS) stained sections for small and large intestine. The slides were evaluated semi-quantitatively applying the following grading score: 0 = no findings; 1 = minimal; 2 = slight; 3 = moderate; 4 = severe; 5 = massive.

3.3.5 **Immunostaining of paraffin-embedded brain tissue sections**

After sacrificing the mice and careful dissection of the brains, the right hemisphere was fixated in 4% buffered paraformaldehyde at 4°C for a minimum of 24 hours for the following cutting in 3 µm paraffin-embedded sections on glass. For the immunostaining of Aβ 42, IBA-1 and GFAP the paraffin sections were deparaffinized in xylene and rehydrated in a series of ethanol baths. To block endogenous peroxidases, sections were pre-treated with 0.3% H_2O_2 in PBS. Antigen retrieval was generated by boiling slices in 10 mM citrate buffer followed by a 3 min incubation in 88% formic acid. A solution of 10% FCS and 4% milk powder in PBS was used to block unspecific antigens. Slices were incubated in primary antibody diluted (1:500 for IBA-1, 1:1000 for Aβ, 1:2000 for GFAP) in 0.01 M PBS and 10% FCS. GFAP and IBA-1 slices were incubated at 4°C while Aβ-immunostaining was incubated at RT overnight. Next day the sections were washed and incubated 1.5 hours at 37°C for Aβ and 45 min at RT for GFAP and IBA-1 with biotinylated secondary antibody, diluted 1:200 in 0.01 M PBS and 10% FCS. The counterstaining with Haematoxylin led to a blue staining of the nucleus. Positive antibody staining was visualized using the Avidin-Biotin-Complex-method (ABC) by Vectastain kit and diaminobenzidine (DAB) as chromogen which resulted in a brown colour. Images were taken with a Zeiss Axiophot light microscope equipped with AxioCam MRc (Carl Zeiss, Jena, Germany) and analysed using image analysis software by colour deconvolution algorithm of brown pixels (ZEN2011, Zeiss). The percentage of positive staining relative to the total area represents plaque, GFAP or IBA-1 load and was analysed in cortex and hippocampus.

3.3.6 **Aβ extraction from brain samples and ELISA**

Water-soluble Aβ levels were analysed by Enzyme Linked Immunosorbent Assay (ELISA) in cortical cytosolic fractions [98]. To evaluate soluble proteins, brain tissues were homogenized

in ~8 volumes of ice-cold PBS and supernatants were subsequently frozen at -80 °C until further analysis. The amount of Aβ 40 and Aβ 42 was determined using an ELISA kit from WAKO Chemicals according to the manufactures protocol and normalized to the total protein content in the respective sample [pmol g^{-1} tissue]. Total protein content was determined by PierceTM BCA Protein Assay Kit (Thermo Scientific) as described by the manufacturer.

3.3.7 **Oxidative stress markers**

Lipid peroxidation was determined in midbrain tissues by the reaction of MDA with thiobarbituric acid (TBA) to form a colorimetric (532 nm)/fluorometric (λ_{ex} = 532/ λ_{em} = 553 nm) product, proportional to the MDA present. The amount of MDA was evaluated with the MDA kit (Sigma-Aldrich) according to the manufactures protocol. The amount of total and oxidized glutathione was evaluated in cerebellum after homogenization in cold 100 mM phosphate buffer (pH 6.8), containing 0.1 mM EDTA. After centrifugation (10 000 g, 15 min, 4°C) the supernatants were deproteinized with an equal volume of 10% metaphosphoric acid and thereafter with a solution of 4 M triethanolamine to increase the pH of the sample. This assay is based on the catalytic reaction of GSH with 5,5'-dithio-bis (2-nitrobenzoic acid) (DTNB, also named as Ellman's reagent) that forms the yellow derivate 5-thionitrobenzoic acid (TNB). The concentration of GSH in a sample is proportional to the rate of formation of TNB, measured at 412 nm. The concentration of total glutathione was expressed as nmol tGSH per mg of protein. In addition, oxidized GSH (GSSG) was measured using 2-vinylpyridine for masking GSH which is rapidly reduced in two GSH by glutathione reductase and NADPH. The ratio of reduced glutathione to oxidized glutathione was expressed as (GSH/GSSG). Total protein content was determined by PierceTM BCA Protein Assay Kit (Thermo Scientific) as described by the manufacturer.

3.3.8 **Western blot analysis of IBA-1 and GFAP**

For the analysis of protein levels, cortex tissues were homogenized in ~8 volumes of ice-cold PBS in a potter tissue grinder. The homogenate was centrifuged in a microcentrifuge for 45 min at 12500 rpm and 4°C. The amount of protein in the supernatant was evaluated with the BCA kit (Thermo) according to the manufactures protocol. The samples were prepared with equal amounts of protein (40 µg) and loaded on a 4-12% precast NUPAGE gel (Invitrogen) and were separated at 180 V in a Mini-PROTEAN II tank (BIO-RAD). After electrophoresis the proteins were blotted on a 0.45 µm pore diameter nitrocellulose transfer membrane (Whatman,

Schleicher & Schuell) at 250 mA for 45 min in a Mini Trans-Blot tank (BIO-RAD). The membrane was blocked with 5% milk in PBS-T for 30 min. After the blocking, the membrane was incubated with the primary antibody (GFAP, IBA-1 1:1000) overnight at 4°C. Next day the membrane was washed with PBS-T and was incubated 1 h at room temperature with the horseradish peroxidase-conjugated secondary antibody and washed again 5 times with PBS-T. For the detection of the proteins the ECL solutions were applied (GE Healthcare), and the visualization was performed with the FluorChem 8900 (Biozym, Hessisch Oldendorf). Quantification of protein expression was done using the ImageJ software (National Institutes of Health, Bethesda, USA).

3.3.9 **Statistical analyses**

All data are shown as mean and standard error of mean (SEM) unless specified otherwise, with the number of animals indicated in the figure legends for each endpoint. Treatment related effects were analysed using one-way analysis of variance (ANOVA) followed by Dunnett's post hoc evaluation of control groups versus NMs- exposed groups. For the evaluation of ordinal data, indicated as scatterplots with median values, the Kruskal-Wallis test with Dunn-Bonferroni post hoc analysis was used. Analysis were performed using SPSS statistics (V25 IBM Corporation, USA).

3.4 Results

3.4.1 **Body and organ weight changes**

No effects on body weight gain were observed in the 5xFAD mice or their C57BL/6J littermates during 3 weeks of feeding with the SiO_2 or CeO_2 dosed feed pellets (see **Figure 3.1 and Table 3.1**). In the 5xFAD mice that were exposed for 14 weeks to 1% SiO_2, a reduction in body weight gain was observed from weeks 5 to 7 as well as from weeks 9 to 13 (Figure 3.1D). In the corresponding non-transgenic mice, the subchronic exposure to SiO_2 did not cause any significant reduction in body weight gain (Figure 3.1C).

In the C57BL/6J mice that were exposed for 14 weeks to 1% CeO_2 body weight gain and body weights at sacrifice were found to be significantly augmented in comparison to the corresponding control group (Table 3.1B). This effect was observed from exposure week 8 onwards (Figure 3.1C).

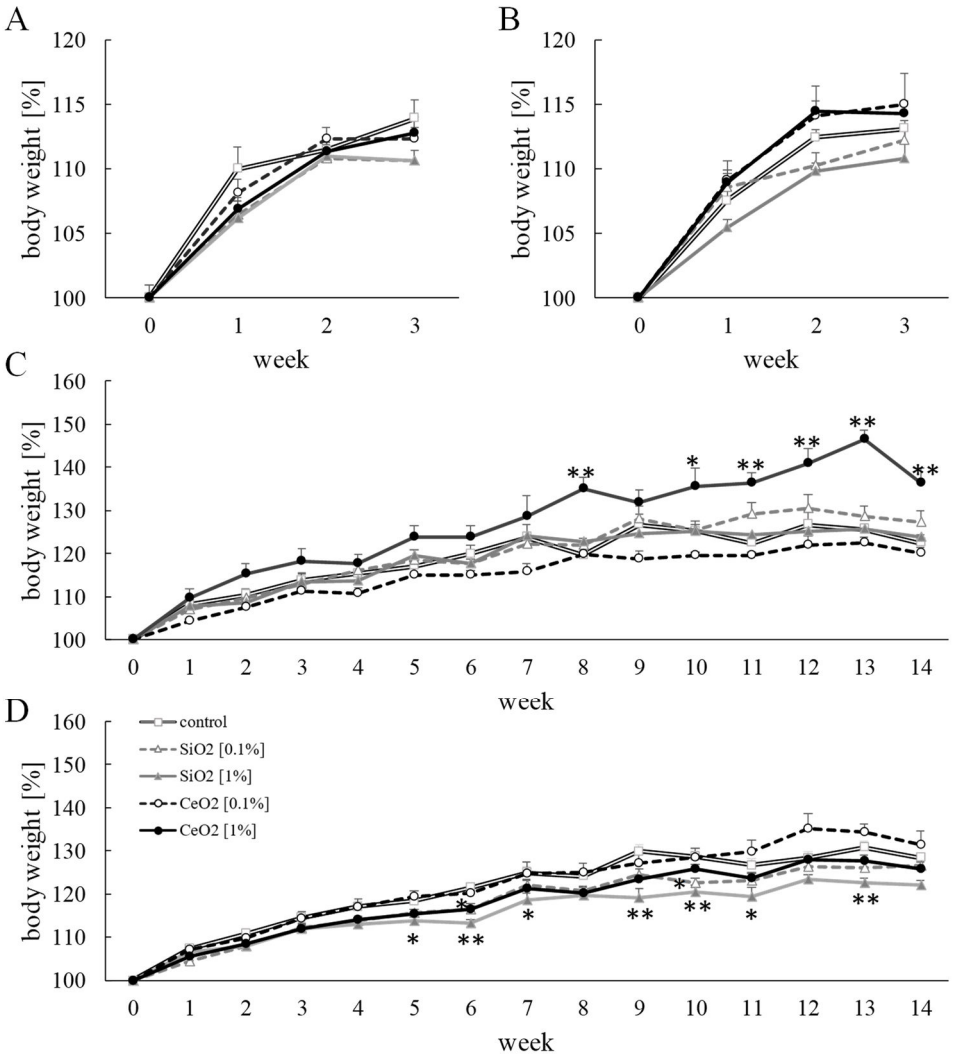

Figure 3.1. Body weight gain [%] of C57BL/6J (A, C) and 5xFAD (B, D) mice during 3 weeks (A, B) or 14 weeks (C, D) exposure to CeO_2 or SiO_2 [0.1% or 1%] in feed pellets *ad libitum*. Statistical analysis was performed using ANOVA followed by Dunnett evaluation; *$p < 0.05$ and **$p \leq 0.01$ versus mice exposed to control feed pellets.

We found no differences in the weights of liver, spleen, kidney, small intestine or colon of the 5xFAD and C57BL/6J mice after 3 weeks or 14 weeks exposure (**Table 3.2**). Treatment related effects on length and weight/length ratios of small intestine and colon were also not seen, with one exception: A reduced colon length was observed in the 5xFAD mice after 3 weeks exposure to 1% SiO_2 (Table 3.2A). However, colon weight and colon weight/length ratio were not significantly different in this group.

Table 3.1. Body and organ weights of C57BL/6J and 5xFAD mice after 3 weeks (A) or 14 weeks (B) exposure to CeO_2 or SiO_2 [0.1% or 1%] in feed pellets *ad libitum*

A	control		SiO_2 [0.1%]		SiO_2 [1%]		CeO_2 [0.1%]		CeO_2 [1%]	
	C57BL/6J	5xFAD	C57BL/6J	5xFAD	C57BL/6J	5xFAD	C57BL/6J	5xFAD	C57BL/6J	5xFAD
Body weight, sacrifice [g]	20.17 ± 1.32	19.15 ± 0.82	19.12 ± 1.03	18.78 ± 0.92	19.23 ± 0.67	18.58 ± 0.92	19.65 ± 1.51	19.23 ± 1.04	19.15 ± 0.91	19.20 ± 0.78
Body weight gain [g][a]	2.47 ± 0.66	2.21 ± 0.33	1.80 ± 0.47	2.03 ± 0.61	1.83 ± 0.35	1.79 ± 1.03	2.17 ± 0.52	2.46 ± 1.17	2.15 ± 0.42	2.38 ± 0.47
Liver/body weight [mg g^{-1}]	45.28 ± 8.89	44.71 ± 5.55	43.52 ± 4.78	47.36 ± 5.57	42.64 ± 6.70	45.27 ± 8.54	47.04 ± 2.06	44.50 ± 4.74	44.96 ± 3.04	44.08 ± 7.27
Spleen/body weight [mg g^{-1}]	4.07 ± 0.31	3.80 ± 0.40	4.31 ± 0.76	4.10 ± 0.51	3.66 ± 0.47	4.23 ± 0.65	3.92 ± 0.66	3.92 ± 0.38	3.82 ± 0.29	3.89 ± 0.69
Kidney/body weight [mg g^{-1}]	10.20 ± 3.01	8.99 ± 3.61	10.18 ± 3.22	8.60 ± 3.25	9.92 ± 2.62	8.60 ± 3.41	10.74 ± 3.82	8.60 ± 2.98	9.64 ± 2.83	9.22 ± 3.21
Colon/body weight [mg g^{-1}]	8.19 ± 0.81	8.39 ± 1.37	8.19 ± 1.03	8.15 ± 1.09	8.17 ± 0.91	8.69 ± 0.85	8.55 ± 0.78	8.91 ± 0.78	8.03 ± 1.23	8.79 ± 1.22
Small int./body weight [mg g^{-1}]	42.51 ± 6.00	42.38 ± 7.08	40.47 ± 6.60	46.40 ± 5.41	40.96 ± 7.20	40.89 ± 13.61	39.84 ± 7.16	44.34 ± 5.74	45.72 ± 1.55	46.69 ± 3.28

B	control		SiO_2 [0.1%]		SiO_2 [1%]		CeO_2 [0.1%]		CeO_2 [1%]	
	C57BL/6J	5xFAD	C57BL/6J	5xFAD	C57BL/6J	5xFAD	C57BL/6J	5xFAD	C57BL/6J	5xFAD
Body weight, sacrifice [g]	21.68 ± 1.36	22.56 ± 1.25	23.72 ± 1.53	22.32 ± 2.24	22.33 ± 1.39	21.60 ± 1.03	22.47 ± 1.05	22.92 ± 1.65	25.20* ± 2.14	21.92 ± 0.26
Body weight gain [g][a]	3.98 ± 0.80	4.96 ± 0.60	5.10 ± 1.19	4.72 ± 1.07	4.28 ± 1.28	3.88 ± 0.67	3.73 ± 0.69	5.45 ± 1.64	6.72* ± 1.59	4.47 ± 0.77
Liver/body weight [mg g^{-1}]	42.59 ± 2.92	42.20 ± 4.57	39.62 ± 2.99	42.97 ± 1.97	43.67 ± 3.97	43.47 ± 1.61	42.37 ± 5.91	43.80 ± 2.96	36.77 ± 3.20	43.83 ± 3.51
Spleen/body weight [mg g^{-1}]	3.61 ± 0.36	3.55 ± 0.27	3.46 ± 0.27	3.60 ± 0.45	4.09 ± 1.02	3.48 ± 0.44	3.44 ± 0.41	3.61 ± 0.52	3.05 ± 0.34	3.50 ± 0.39
Kidney/body weight [mg g^{-1}]	6.03 ± 0.47	6.07 ± 0.39	5.68 ± 0.64	5.99 ± 0.32	6.15 ± 0.88	6.26 ± 0.53	6.26 ± 0.42	6.07 ± 0.39	5.61 ± 0.73	5.52 ± 1.96
Colon/body weight [mg g^{-1}]	8.08 ± 1.05	8.25 ± 0.84	7.77 ± 0.86	8.36 ± 0.67	9.13 ± 1.09	8.38 ± 0.58	8.68 ± 1.01	8.50 ± 0.46	7.55 ± 0.41	8.84 ± 0.83
Small int./body weight [mg g^{-1}]	36.80 ± 1.84	36.39 ± 3.50	36.83 ± 5.11	38.14 ± 3.78	35.88 ± 3.88	36.89 ± 3.59	37.05 ± 4.18	36.19 ± 4.20	31.29 ± 2.33	36.65 ± 3.92

Data represent mean ± SD. Statistical analysis was performed using ANOVA with Dunnett evaluation; * *versus* control feed pellets exposed C57BL/6J mice, $p < 0.01$; [a] Body weight gain at time interval between exposure start and sacrifice

Table 3.2. Lengths and weight/length ratios of colon and small intestine of C57BL/6J and 5xFAD mice after 3 weeks (A) or 14 weeks (B) exposure to CeO_2 or SiO_2 [0.1% or 1%] in feed pellets *ad libitum*

A	control		SiO_2 [0.1%]		SiO_2 [1%]		CeO_2 [0.1%]		CeO_2 [1%]	
	C57BL/6J	5xFAD	C57BL/6J	5xFAD	C57BL/6J	5xFAD	C57BL/6J	5xFAD	C57BL/6J	5xFAD
Colon length [cm]	7.88 ± 0.66	7.77 ± 0.60	7.23 ± 0.65	7.41 ± 0.68	7.81 ± 0.53	6.97* ± 0.54	7.58 ± 0.56	8.00 ± 0.54	6.97 ± 0.89	7.56 ± 0.68
C. weight/length ratio [g cm^{-1}]	0.022 ± 0.002	0.021 ± 0.003	0.022 ± 0.002	0.021 ± 0.004	0.020 ± 0.003	0.023 ± 0.003	0.022 ± 0.003	0.022 ± 0.003	0.022 ± 0.003	0.022 ± 0.003
Small intestine length [cm]	31.30 ± 2.47	34.20 ± 2.55	31.48 ± 1.68	33.00 ± 2.66	32.34 ± 2.13	32.11 ± 2.52	31.95 ± 3.05	32.66 ± 2.83	31.55 ± 1.99	31.64 ± 2.43
S.I. weight/length ratio [g cm^{-1}]	0.028 ± 0.005	0.024 ± 0.005	0.025 ± 0.004	0.026 ± 0.003	0.024 ± 0.004	0.024 ± 0.008	0.024 ± 0.003	0.026 ± 0.003	0.028 ± 0.002	0.028 ± 0.003

B	control		SiO_2 [0.1%]		SiO_2 [1%]		CeO_2 [0.1%]		CeO_2 [1%]	
	C57BL/6J	5xFAD	C57BL/6J	5xFAD	C57BL/6J	5xFAD	C57BL/6J	5xFAD	C57BL/6J	5xFAD
Colon length [cm]	8.60 ± 0.85	8.16 ± 0.73	8.32 ± 0.65	8.36 ± 0.55	8.55 ± 0.27	8.16 ± 0.62	8.55 ± 0.43	8.19 ± 0.85	7.80 ± 0.76	8.00 ± 0.51
C. weight/length ratio [g cm^{-1}]	0.021 ± 0.004	0.023 ± 0.003	0.022 ± 0.003	0.022 ± 0.002	0.024 ± 0.002	0.022 ± 0.002	0.023 ± 0.003	0.024 ± 0.004	0.025 ± 0.003	0.024 ± 0.003
Small intestine length [cm]	31.88 ± 2.65	31.19 ± 3.08	34.77 ± 1.53	31.79 ± 3.51	31.50 ± 3.12	32.27 ± 1.61	32.47 ± 1.83	33.55 ± 1.36	30.68 ± 1.64	32.22 ± 1.39
S.I. weight/length ratio [g cm^{-1}]	0.025 ± 0.003	0.027 ± 0.004	0.025 ± 0.001	0.027 ± 0.003	0.025 ± 0.003	0.025 ± 0.002	0.026 ± 0.003	0.025 ± 0.004	0.026 ± 0.003	0.025 ± 0.003

Data represent mean ± standard deviation. C = Colon; S.I. = Small intestine. Statistical analysis was performed using ANOVA followed by Dunnett evaluation; * $p < 0.05$ *versus* 5xFAD mice exposed control feed pellet.

3.4.2 **Histopathology**

Table 3.3. Liver and spleen, small and large intestine histopathology of C57BL/6J mice that were exposed for 14 weeks to CeO_2 or SiO_2 [0.1% or 1%] in feed pellets *ad libitum.* Shown is the grading of the lesion and the number of animals in brackets. The following grading has been used: 0 = no findings, 1 = minimal, 2 = slight, 3 = moderate, 4 = severe, 5 = massive.

	control	**0.1% SiO_2**	**1% SiO_2**	**0.1% CeO_2**	**1% CeO_2**
Liver	n = 5	n = 6	n = 6	n = 6	n = 6
Focal inflammatory infiltrated	1 (5)	1 (4), 2(2)	1 (6)	1 (6)	1 (6)
Focal necrosis	1 (2)	1 (1)	1 (2)	0 (6)	0 (6)
Increased interstitial cells	0 (5)	2 (1)	1 (1)	1 (1)	1 (1)
Increased glycogen	0 (5)	0 (6)	0 (6)	2 (2), 3 (1)	0 (6)
Vacuolation	0 (5)	0 (6)	0 (6)	0 (6)	2 (3)
Spleen	n = 5	n = 6	n = 6	n = 5*	n = 6
Increased pigment	2 (1)	2 (3)	0 (6)	2 (2)	1 (1), 2 (1)
Congestion	0 (5)	2 (1)	0 (6)	0 (5)	0 (6)
Increased extramedullary hematopoiesis	0 (5)	0 (6)	3 (1)	1 (1)	2 (1)
Increased megakaryocytes	0 (5)	0 (6)	2 (1)	0 (5)	0 (6)
	* one sample not evaluable due to embedding artefacts				

Small & Large Intestine

Minimal focal inflammatory infiltrates (intra-mucosal) in all specimens.

In some cases, inflammatory infiltrates in adjacent tissue and pancreas with focal vacuolation (grade 2).

Clearly visible goblet cells in PAS stained slides (small intestine +; large intestine +++)

Partly mucus on surface. Gut associated lymphoid tissue (GALT) in almost all specimens detectable.

Histopathology was performed on liver and spleen, small and large intestine of C57BL/6J mice that were exposed for 14 weeks to evaluate potential treatment-related dose-dependent effects (**Table 3.3**). In the liver, increased glycogen was observed in 3 out of 6 mice exposed to 0.1% CeO_2 and periportal vacuolation in 3 out of 6 mice exposed to 1% CeO_2. In small and large intestine focal, minimal inflammatory infiltrates were seen, occasionally together with some focal irregular epithelial surface. These findings and all other findings seen in the organs evaluated are not assessed to be treatment-related adverse effects.

3.4.3 **Behaviour**

Early memory deficits, followed by successive reduction of other cognitive functions are major characteristics of AD. A battery of behavioural tests was performed to assess for functional neurotoxic effects resulting from the oral exposures to the SiO_2 and CeO_2 NMs in the 5xFAD and C57BL/6J littermate mice, as well as to correlate their outcomes with Aβ neuropathology. Results of the behaviour studies are show in **Figure 3.2**.

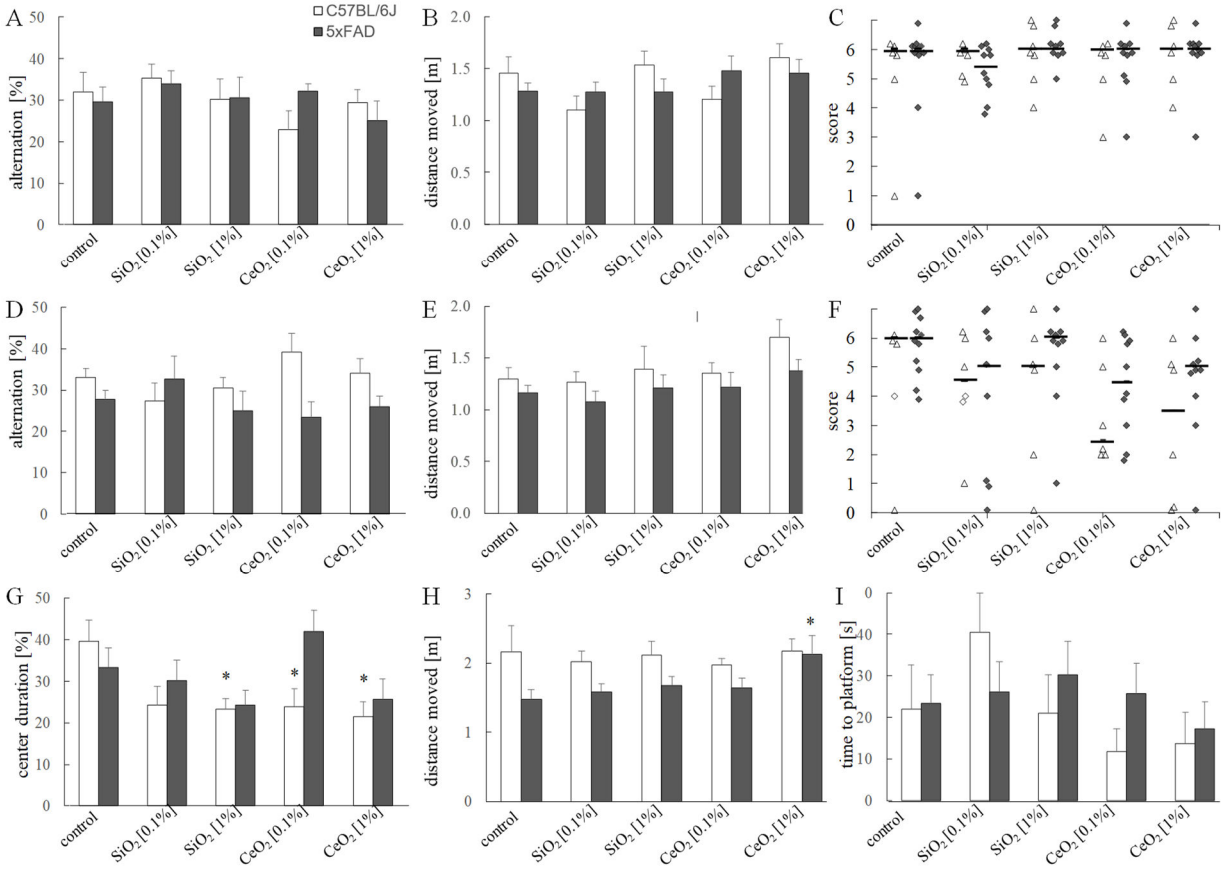

Figure 3.2. Behaviour tasks performances of C57BL/6J and 5xFAD mice. Mice were exposed for 3 weeks (A, B, C) or 14 weeks (D, E; F, G, H, I) to SiO_2 [0.1%, 1%] or CeO_2 [0.1%, 1%] nanomaterials in food pellets ad libitum. Data represent mean ± SEM of the % alternation and distance moved [m] in the X-maze task (A, B, D, E), the % centre duration and distance (m) moved in the open field task (G, H) and the time to reach the platform (s) of the balance beam test (I). String suspension task score data are indicated as scatterplots (C, F). Statistical analysis was performed using ANOVA followed by Dunnett post-hoc evaluation for X-maze, string and balance beam tests. Results of the string suspension task were evaluated by the Kruskal-Wallis test followed by Dunn-Bonferroni post hoc evaluation; * $p < 0.01$ versus corresponding C57BL/6J or 5xFAD mice exposed to control feed pellets. Number of animals per group: 3 weeks C67BL/6J control (n = 6); SiO_2 0.1% (n = 6); SiO_2 1% (n = 7); CeO_2 0.1% (n = 6). CeO_2 1% (n = 6); 5xFAD control (n = 10); SiO_2 0.1% (n = 10); SiO_2 1% (n = 9); CeO_2 0.1% (n = 10). CeO_2 1% (n = 10); 14 weeks C67BL/6J control (n = 5); SiO_2 0.1% (n = 6); SiO_2 1% (n = 6); CeO_2 0.1% (n = 11). CeO_2 1% (n = 6); 5xFAD control (n = 11); SiO_2 0.1% (n = 9); SiO_2 1% (n = 10); CeO_2 0.1% (n = 10). CeO_2 1% (n = 10).

The X-maze test was used to asses for decreased spontaneous alternation behaviour as an indicator of impaired spatial working memory [37]. Spontaneous alternation is based on the natural behaviour of rodents to explore new environments and thus to rotate in the entries of the arms of the maze. We observed no significant treatment-related effects on spatial working memory in the 3-week and 14-week sub-studies for SiO_2 and CeO_2 (Figure 3.2A and D). Total distance moved in the X-maze also did not differ between the treatment groups (Figure 3.2B and E). The string suspension task was performed to evaluate the agility and grip strength of the mice [38] using a score rating system as described in detail in the methods section. For this

test, also no significant differences were identified associated with the exposures to SiO_2 or CeO_2 (Figure 3.2C and F).

In addition to the aforementioned tests, in the 14-week sub-study the open field test [39] and the balance beam test were included. In the open field test a decreased proportion of time spent in the central versus the border regions of the arena has been proposed an indicator of increased anxiety. In this study, the WT mice that were exposed for the 14 weeks to 1% SiO_2 as well as those that were exposed to 0.1% and 1% CeO_2 spent significantly less time in the central region of the open field arena compared to the control mice (Figure 3.2G). In the 5xFAD mice, these treatment-related differences in centre residency times were not observed. However, the 5xFAD mice exposed to 1% CeO_2 were found to be significantly more active and travelled a greater distance compared to the 5xFAD control mice (1.48 ± 0.45 m for control vs 2.13 ± 0.87 m, $p = 0.030$) indicative of increased locomotor activity (Figure 3.2H). In the balance beam test, which was included as an independent indicator of motor coordination and balance [37, 40] the 14-week oral exposures to SiO_2 and CeO_2 revealed no significant differences, neither in the 5xFAD mice nor in the WT mice (Figure 3.2I).

3.4.4 **Plaque formation**

Amyloid β-containing senile plaques are present before clinical symptoms of AD appear [41]. Therefore, parasagittal brain slices of 5xFAD mice were stained with an antibody against human Aβ42 to investigate the impact of the oral exposure to CeO_2 or SiO_2 on Aβ plaque load in hippocampus and cortex of the 5xFAD mice. Results are shown in **Figure 3.3**. As observed in representative images, at younger age (i.e. 3-week exposure study) the 5xFAD mice display much less and smaller plaque formation (Figure 3.3A) compared to the older animals (i.e. 14-week exposure study) (Figure 3.3D). The relative extent of plaque formation detected in the control animals at the respective ages aligned well the described accelerating phenotype of the 5xFAD model [36] and findings in previous studies in our lab [11, 42]. In the mice that were exposed for 3 weeks to the lower concentrations (i.e. 0.1%) of SiO_2 and CeO_2 tended to show some lower plaque levels, in cortex as well as hippocampus, in comparison to the control mice. However, these differences were not statistically significant.

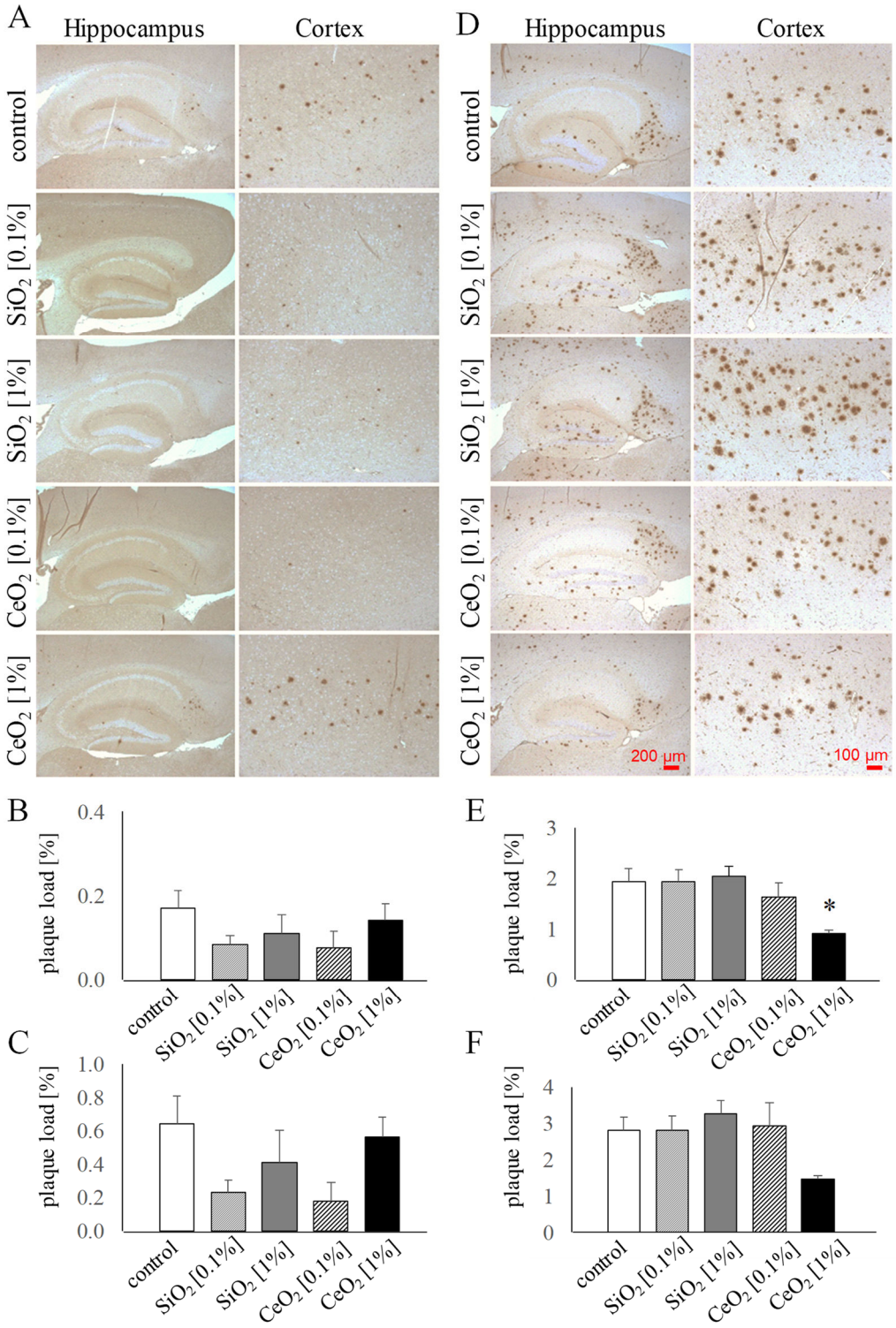

Figure 3.3: β-Amyloid pathology in 5xFAD transgenic mice. Accumulation of Aβ42 (brown staining) in cortex and hippocampus of 5xFAD mice exposed orally to SiO_2 [0.1%, 1%] and CeO_2 [0.1%, 1%] nanomaterials. Aβ42 was visualized by immunohistochemistry in 3 µm sections of paraffin-embedded brain hemispheres. Representative images of hippocampus (50-fold microscopic magnification) and cortex (100-fold microscopic magnification) are shown for each treatment after 3 weeks exposure (A) and after 14 weeks exposure (D). The graphs represent mean ± SEM of plaque load, determined using image analysis software and calculated as the percentage area occupied by Aβ immunostaining in hippocampus (B, E) and cortex (C, F) of mice after 3 weeks (B, C) and after 14 weeks exposure (E, F). Statistical analysis was performed using ANOVA with Dunnett post-hoc analysis; * $p < 0.01$ versus mice exposed to control feed pellets. Number of animals per group: 3 weeks 5xFAD control (n = 10); SiO2 0.1% (n = 10); SiO2 1% (n = 9); CeO2 0.1% (n = 10). CeO2 1% (n = 10); 5xFAD control (n = 11); SiO2 0.1% (n = 9); SiO2 1% (n = 10); CeO2 0.1% (n = 10). CeO2 1% (n = 10).

More importantly, the 14-week sub-study, plaque load tended to be decreased in dose-dependent fashion in the hippocampus of the CeO_2 exposed mice. In the hippocampus as well as in the cortex, plaque load in the 1% CeO_2 group was approximately half as abundant as in the control group, and statistically significant for hippocampus (ANOVA-Dunnett, $p<0.01$) but not cortex ($p=0.075$).

3.4.5 **Amyloid β levels**

To further evaluate effects of the oral exposures to the SiO_2 and CeO_2 NMs, cortex lysates were analysed for protein levels of Aβ40 and Aβ42 by ELISA (**Figure 3.4**).

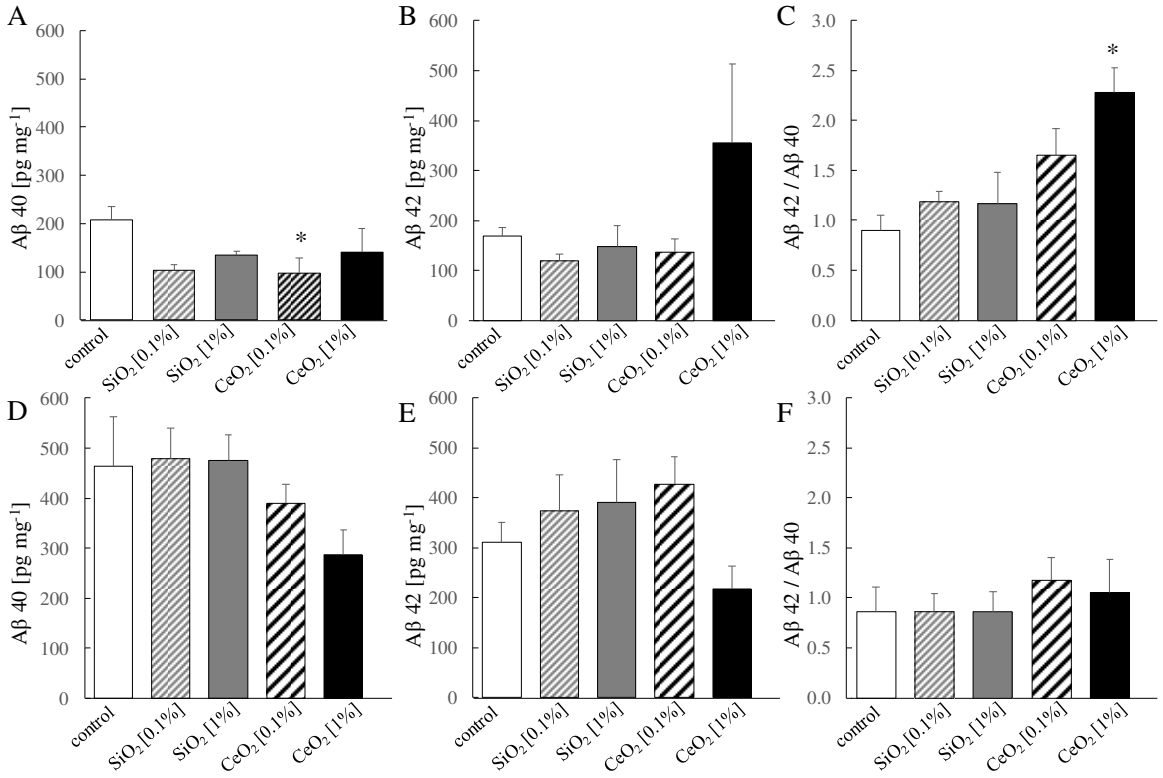

Figure 3.4: β-amyloid protein levels in 5xFAD transgenic mice exposed to different nanomaterials. Aβ40 (A, D) and Aβ42 (B, E) protein levels and Aβ42/Aβ40 ratio (C, F) were determined by ELISA in cortex brain homogenates of 5xFAD mice after oral exposure to SiO_2 and CeO_2 nanomaterials [0.1% and 1%] for 3 weeks (A, B, C) or 14 weeks (D, E, F). Statistical analysis was performed using ANOVA with Dunnett post-hoc analysis; * $p < 0.01$ versus mice exposed to control feed pellets. N = 6 animals per group for 3 weeks study and N = 7 for 14 weeks study.

In the tissues of the mice that were exposed for 3 weeks to the lower concentration of SiO_2 and CeO_2 NMs, protein levels of both Aβ40 and Aβ42 tended to be lowest, in alignment with the histopathological findings (see Figure 3.3). The levels of Aβ40 in the 0.1% CeO_2 group were significantly lower than the controls. Furthermore, the 1% CeO_2 exposed mice revealed a significantly increased Aβ42/Aβ40 ratio, which was mainly the result of the increased trend of

Aβ42 levels in this group. In the 14-week sub-study, levels of Aβ40 as well as Aβ42 were lowest in the cortex tissues of the 1% CeO_2 group. Although these differences were not significant, they aligned well with the Aβ plaque load findings (Figure 3.3). Differences in Aβ42/Aβ40 ratios were not observed at this time point.

3.4.6 **Oxidative stress**

Oxidative stress resulting from a disruption of pro- and antioxidant balance has been proposed as a major mechanism of neurotoxicity of NMs [43, 44, 45] and has also been connected to β-amyloidogenesis and AD pathology [46, 47, 48, 49]. To evaluate oxidative stress in the brains of the 5xFAD mice, we measured in the levels of glutathione (GSH) [50]. In addition, we determined the ratio of reduced to oxidized glutathione (GSH/GSSG), as reduced ratios have been observed in AD [51, 52]. Results are shown in **Figure 3.5**. The brain tissue levels of GSH were not affected following the subchronic oral exposures to SiO_2 or CeO_2. Also, no decreases in GSH/GSSG ratio were observed that would suggest increased oxidative stress in the brain by the nanomaterials. Interestingly, in the brains of the CeO_2 exposed animals, rather a trend for a dose-dependent increase in GSH/GSSG was noted. However, this effect was not statistically significant. As an independent indicator of oxidative stress, we analysed the levels of the lipid peroxidation marker malondialdehyde (MDA) in selected brain tissue samples (Figure 3.5). In alignment with the GSH findings, these results confirmed that neither SiO_2 nor CeO_2 cause sustained oxidative stress in the mouse brains.

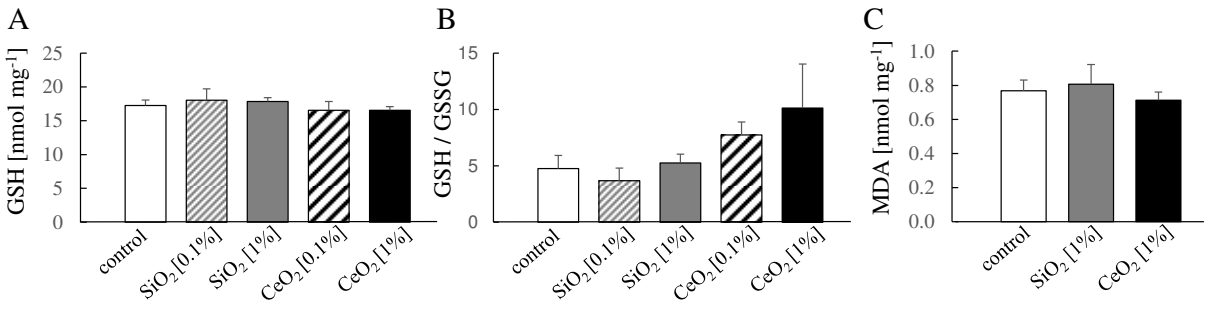

Figure 3.5: GSH concentrations, GSH/GSSG ratios and MDA concentration in 5xFAD transgenic mice. GSH concentrations (A), ratio of GSH/GSSG (B) (mean ± SEM, N = 6) in cerebellum after 14 weeks oral administration of SiO_2 [0.1%, 1%] and CeO_2 [0.1%, 1%] nanomaterials and MDA concentration (C) in midbrain (mean ± SEM, N = 5) after 14 weeks oral administration of SiO_2 [1%] and CeO_2 [1%] nanomaterials encapsulated in feed pellets.

3.4.7 **Neuroinflammation**

Neuroinflammation is a crucial pathological hallmark and mediator of neurodegenerative diseases including AD. We therefore evaluated the expression ionized calcium-binding adapter molecule 1 (IBA-1) and glial fibrillary acidic protein (GFAP) in the brains of the 5xFAD mice after the subchronic exposures to for SiO_2 and CeO_2.

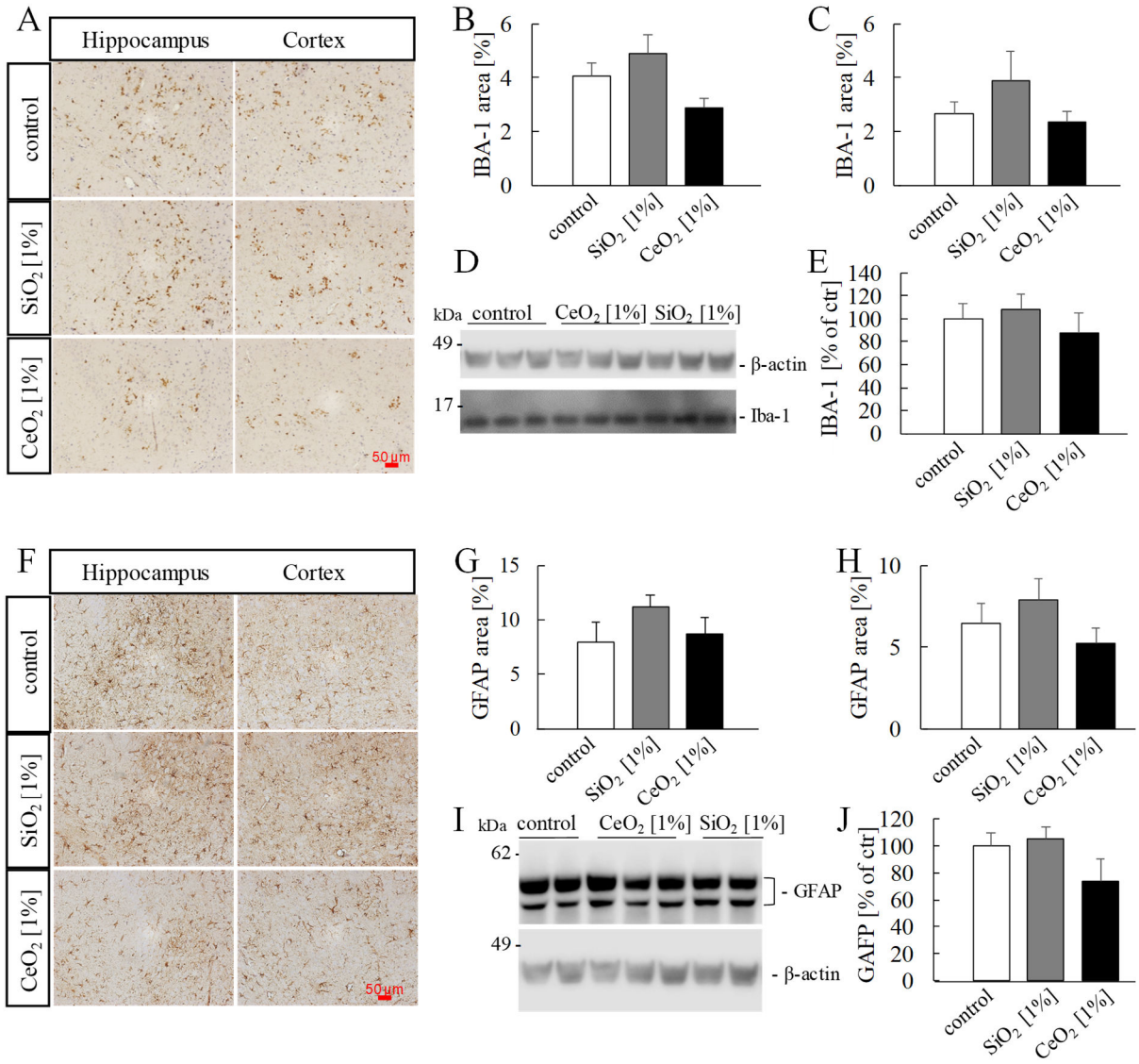

Figure 3.6: Ionized calcium-binding adapter molecule 1 (IBA-1) and glial fibrillary acidic protein (GFAP) pathology. Representative pictures of IBA-1 (A) and GFAP (F) (brown staining) in cortex and hippocampus of 5xFAD mice exposed orally to SiO_2 [1%] and CeO_2 [1%] nanomaterials. Analyses were performed using image analysis software (ZEN2011, Zeiss) at 200x magnification. The output of the analyses represents the percentage of positive staining relative to the total area of the cortex or hippocampus and is defined as IBA-1 load for positive stained microglia and GFAP load for positive stained astrocytes in hippocampus (B, G) and cortex (C, H). Number of animals per group: GFAP staining control (n = 10); SiO_2 1% (n = 8); CeO_2 1% (n = 8); IBA-1 staining: control (n = 10); SiO_2 1% (n = 3); CeO_2 1% (n = 10). IBA-1 and GFAP were also visualized by western blot using FluorChem Imager (D, I). Total IBA-1 or GFAP was detected in cortex and normalized to the respective control sample (E, J). Animal numbers: control (n = 10); SiO_2 1% (n = 9); CeO_2 1% (n = 10). Data represent mean ± SEM.

Increased IBA-1 expression is an indicator of activated microglia in the brain under conditions of inflammation [53] and therefore used as marker of neuroinflammation [54]. The expression of GFAP is upregulated in most forms of reactive astrogliosis [55]. The results of the IBA-1 and GFAP analyses are shown in **Figure 3.6**. As shown by representative immunohistochemical staining images from sections of paraffin-embedded brain hemispheres (Figure 3.6A), no significant effects of the oral exposures to the NMs on IBA-1 expression were found in hippocampus (Figure 3.6B) or cortex (Figure 3.6C). For the cortex region this was also confirmed using Western blot analysis (Figure 3.6D & 3.6E). Similarly, neither SiO_2 nor CeO_2 caused increased expression of GFAP. The expression of this astrocyte marker did not differ between the exposure groups as revealed by immunohistochemical analysis in hippocampus (Figure 3.6F & 3.6G) and cortex (Figure 3.6F & 3.6H) and independently by Western blot detection (Figure 3.6I & 3.6J). Taken together, in alignment with the findings on Aβ plaque formation, Aβ peptide levels and oxidative stress markers, neither SiO_2 nor CeO_2 caused neuroinflammation upon long-term oral exposure.

3.5 Discussion

The present work was undertaken to address if long-term oral exposure to two of the most commonly used NMs, SiO_2 and CeO_2 can cause neurotoxicity and promote AD. The findings suggest that long-term oral exposure to these NMs has no adverse health impact on the central nervous system but, by contrast, support a potential anti-amyloidogenic role of CeO_2 in Alzheimer's disease.

With regard to SiO_2, our findings are of main relevance in view of its use as a food additive. The amount of use of SiO_2 in food applications is limited to 2% by the US Food and Drug Administration (US FDA 2021), while the European Food Safety Authority (EFSA) authorizes the *quantum satis* use of E551 [56]. The latest evaluation by EFSA concluded that there is no indication of a risk when used as a food additive [22]. However, in a recent study in mice adverse effects were observed following 18 months exposure via drinking water [57]. In the present study, mice were exposed to SiO_2 incorporated in the food. This differs from exposure via drinking water and the most commonly used administration by repeated gavage, regarding the physicochemical interactions of the NMs with food and intestinal constituents [14, 58]. Based on an estimated daily feed consumption of 4 g and average mouse body weight of 20 g, the *ad libitum* exposure to the dosed feed pellets (0.1 and 1% w/w) result in a daily intake of about 0.2 and 2 $g \cdot kg^{-1}$ bodyweight (BW). Up to the highest 14-week cumulative dose, the dietary exposure to SiO_2 NMs did not cause accelerated plaque formation, oxidative stress,

neuroinflammation, spatial working memory deficits, locomotor activity changes or motor coordination impairments. Solely, for the wildtype C57BL/6J mice an effect in the open field test was observed for the 14-week 1% SiO_2 group. As this effect was not seen in 5xFAD mice and not accompanied with any further effects, it can be debated whether this reflects an adverse neurotoxic response. When applied in an unconditioned manner, the open field test has been suggested to reflect other effects than anxiety, like avoidance or natural preference responses [59].

The findings from our *in vivo* study in the 5xFAD model are in contrast to *in vitro* papers that suggest potential amyloidogenic effects of SiO_2 NMs [60, 61]. However, when investigating such direct effects of NMs on cells *in vitro,* it should be kept in mind that *in vivo* research has shown that the translocation and accumulation of SiO_2 into the brain following oral exposure is extremely low, if at all [62, 63]. Peripheral effects, including those in intestine, liver and spleen as major recognized target organs for ingested NMs, were also found to be mostly absent. However, a significantly diminished body weight gain was observed, exclusively, in the 5xFAD mice of the 1% SiO_2 group. This effect was first apparent at the 5th week of exposure but no longer present after week 14 as sacrifice. In association with this, a lower colon length was found in the 1% SiO_2 exposed 5xFAD mice after 3 weeks exposure, but not after 14 weeks. This may point towards a (transient) increase in susceptibility to local intestinal effects of SiO_2 NMs in the 5xFAD model compared to the C57BL/6J mice. Indeed, in support of this hypothesis, differences in intestinal gene expression, trypsin levels, faecal microbiota composition and associated weight changes have been shown between 5xFAD mice and their wildtype littermates [64, 65].

Similar to SiO_2, the oral exposure to the other NM that we chose to investigate, CeO_2, did not result in adverse neurotoxic and AD-promoting outcomes. On the contrary, a marked anti-amyloidogenic effect was found in the 5xFAD mouse model. Unlike SiO_2, CeO_2 presently finds no intentional application in the food sector. However, its potential use in disease prevention, therapy and diagnostics has been promoted in several recent oral exposure studies in rodents, for instance, in models of non-alcoholic fatty liver disease [66] and colitis [67, 68].

To the best of our knowledge, this study is the first to demonstrate an inhibition of AD-like pathology following long-term oral exposure to CeO_2 NMs. Specifically, in the 14-weeks exposed mice, the Aβ plaque load was approximately 50% lower in both hippocampus and cortex of the 1% CeO_2 fed 5xFAD mice compared to the corresponding control group. In alignment with these pronounced immunohistopathology findings, cortical protein levels of Aβ40 and Aβ42 tended to be markedly lower in the 1% CeO_2 group as well, albeit not

statistically significant. Since our study was *a priori* designed to address the potential adverse effects of long-term oral exposures to NMs, we can only speculate about underlying mechanisms of the observed beneficial effects of the CeO_2 feeding. While amyloid pathology in AD has been linked to oxidative stress and inflammation [69, 70, 71, 72], the reduced plaque burden in the 1% CeO_2 exposed mice was not accompanied by significant changes in oxidative stress or neuroinflammation. Yet, it was interesting to observe the highest GSH/GSSG ratio in the brains of the 1% CeO_2 group. Lower GSH/GSSG ratios have been observed in AD [51, 52] and an increase might thus reflect a compensatory improved antioxidant status in the CeO_2 fed 5xFAD mice. Notably, the lower amyloid plaque burden was apparent after the 14-week cumulative exposure to CeO_2 despite the aggressive phenotype of the 5xFAD model. In a previous study, we demonstrated a rapid acceleration of plaque formation in 5xFAD mice following a 3-week inhalation exposure to diesel exhaust, representing a dominant contributor of nano-size air pollution particles in urban environments [11]. At 13-weeks exposure, the plaque promoting effect of the diesel exhaust was no longer present, most likely due to the strong age-dependent progressive nature of the 5xFAD model [11]. In our present study, a beneficial effect of the CeO_2 was not yet observed after 3 weeks, which could be due to the low absolute plaque load in cortex and hippocampus at this young age. Interestingly, however, at this time point a significant increase in Aβ42/Aβ40 ratio was detected in the 1% CeO_2 exposed 5xFAD mice, mainly as a result of the relatively higher levels of the more toxic and aggregation prone Aβ42 protein [73, 74]. Whether and how this seemingly contrasting finding at early exposure could relate to the lower formation of plaques at the later 14-week exposure needs further research. In another recent study, we investigated the neurotoxic and AD-promoting effects of CeO_2 NMs doped with varying amount of zirconium (ZrO_2) in a 4-week inhalation design in 5xFAD mice [42]. Here, unlike diesel exhaust, these CeO_2 containing NMs did not lead to an aggravate plaque formation following inhalation exposure and, unlike our current oral exposure study, also did not inhibit plaque formation in 5xFAD mice. While this may be explained by differences in levels and duration of exposure, it also demonstrates the likely importance of the route of exposure.

As a redox-sensitive nanomaterial, CeO_2 has been long recognized for its free radical scavenging properties and, therefore, is widely studied for its potential as antioxidant and anti-inflammatory agent in the field of nanomedicine [75, 76, 77, 78, 79]. Several research groups have already investigated the neuroprotective properties of CeO_2 NMs and explored their potential therapeutic use in brain diseases [75, 76, 77, 78, 80]. In a rat model of Parkinson's disease, intrastriatal injection of CeO_2 NMs could attenuate neurobehavioral impairments [81].

In a mouse model of multiple sclerosis, intravenous administration of citrate/EDTA-stabilized CeO_2 ameliorated motor function deficits [82]. Interestingly, Kwon and co-workers [83] revealed therapeutic promise for triphenylphosphonium-conjugated CeO_2 in AD by showing a suppression of reactive gliosis and mitochondria damage in 5xFAD mice upon stereotactic injection. However, in contrast to our findings, they did not observe a significant attenuation of plaque load in these mice.

While increasingly complex nanomedicine-based strategies are being proposed and developed for AD [80, 84], it was striking to observe the effects in our study (1) with pristine, non-stabilized/conjugated CeO_2, and (2) by a mere dietary exposure instead of a forced intravenous or intracranial administration. It is tempting to conclude that the effects observed with the CeO_2-fed mice resulted from direct redox-restoring effects of these NMs, as suggested from *in vitro* investigations. Indeed, CeO_2 NMs were shown to reduce ROS generation in neuronal cell cultures and to block mitochondrial fragmentation produced by Aβ [85]. Hybrid nanoparticles composed of ceria and polyoxometalate were shown to degrade Aβ aggregates and reduce intracellular ROS in PC12 cells [86]. As our study did not include a pharmacokinetic design, it is not known to what extent the CeO_2 NMs may have reached and accumulated in the brain of the mice. Major progress in this specific research area has been achieved previously by Yokel and colleagues. Using CeO_2 NMs of different primary size, they demonstrated that liver and spleen are major target organs in rat after a single intravenous administration, while only a small proportion of the dose enters the brain [87, 88, 89]. More recently, they demonstrated that translocation of CeO_2 NMs from the lung to the rest of the body is less than 1% of the deposited dose and that translocation from the gastrointestinal is even lower [90]. However, they also observed that the organ burdens of the translocated fractions persisted for at least months, suggesting very slow clearance rates. Several other groups have confirmed the minimal to absent absorption of CeO_2 NMs from the gastrointestinal tract of rats [91] and mice [92, 93].

In our study, indications of peripheral adverse effects of the CeO_2 NMs were merely detected in the C57BL/6J mice. As a main finding, in these wildtype animals, a significant increase on body weight gain was observed during the 14 weeks with the 1% dosed pellets. Subsequent histopathology analysis revealed increased glycogen in 3 out of 6 animals of the 0.1% CeO_2 group and periportal vacuolation in 3 out of 6 animals of the 1% CeO_2 group. Changes in the weights of liver, spleen and kidney, as well as weights, lengths and weight/length ratios of colon and small intestine were absent. The observed histological findings in the livers of the CeO_2 fed mice are likely features of increased glycogen storage are therefore considered to be of no toxicologic significance. In contrast to our study, Yokel and

co-workers recently found no increased liver vacuolization in C57BL/6 mice after a single intraperitoneal injection of CeO_2 NMs, and even a decreased vacuolation in BALB/c mice [94]. In the behavioural studies, the only statistically significant effect observed in the C57BL/6J mice with CeO_2 NMs at 0.1% and 1% was a diminished time spent in the centre of the open field arena.

As opposed to the C57BL/6J mice, in the 5xFAD mice that were fed with 0.1% or 1% CeO_2 NMs for up to 14 weeks no significant changes in body weights were found. Histopathology was not evaluated in these transgenic animals, but differences in organ weights, including length and weight/length ratios of small intestine and colon were not observed. This suggests that the beneficial plaque inhibiting effect occurred in the absence of any substantial peripheral toxicity. Moreover, behavioural changes were absent in all tests at both time points of investigation (i.e. week 3 and 14), except for the open field test. Here, the 1% CeO_2 exposed 5xFAD mice at week 14 were found to be much more active compared to the corresponding 5xFAD controls. Interestingly, the distance covered in the open field test by the CeO_2 fed 5xFAD animals was highly similar with that of the C57BL/6J controls (i.e. 2.13 ± 0.87 m versus 2.16 ± 0.84 m). Accordingly, it can be suggested that this activity change reflects an improved behaviour as a result of the inhibited plaque load following CeO_2 exposure. Recently, the 5xFAD model has been proposed as a useful model to study motor dysfunction in AD [95]. Indeed, in line with our investigations, 5xFAD mice travel shorter distances in the open field test than WT mice with increasing age.

Conclusions

Our present study was designed to test the hypothesis that long-term oral exposure to NMs can cause neurotoxicity and aggravate the pathogenesis of AD. It was demonstrated that neither synthetic amorphous SiO_2 nor CeO_2 increases amyloid-β plaque formation, neuroinflammation and oxidative stress in 5xFAD Alzheimer model mice in a subchronic dietary exposure design. Behavioural analyses also revealed absence of spatial working memory deficits and motor coordination impairments. Surprisingly, the subchronic exposure to 1% CeO_2 containing feed pellets resulted in a marked inhibition of plaque burden in the 5xFAD mice and increased locomotor activity. Summarizing the results, the findings from the present study suggest that long-term oral exposure to synthetic amorphous silica NMs, which find wide applications in the food sector, has no major adverse health impact on the central nervous system, specifically regarding the development or progression of the neurodegenerative Alzheimer's disease. The

observations with CeO_2 warrant further investigations to explore if long-term dietary administration of this redox-active NM could have beneficial effects in AD.

Declarations

Funding

The work leading to these results has received funding from the European Union Seventh Framework Programme (FP7/2007-2013) under grant agreement n° NMP4-LA-2013-310451 (NanoMILE) and the German Federal Ministry of Education and Research (BMBF/ZonMW project N3rvousSystem, FKZ 031L0020).

Authors' contributions

AS participated in the coordination of the study, the interpretation of results, carried out the behaviour studies, the brain tissue sectioning, plaque load quantification and amyloid beta ELISAs, provided advice regarding GSH analyses, performed MDA, GFAP and IBA-1 analyses, and drafted the manuscript. TW participated in the planning and coordination of the study, carried out the behaviour studies, supervised brain tissue sectioning and processing, provided advice regarding brain tissue analyses for plaque load quantification, amyloid beta ELISA, participated in the interpretation of the results and has been involved in critically revising the manuscript. JK participated in conceiving the study and participated in the tissue dissection and body and organ weight analyses. HJH participated in the coordination of the study and brain tissue sectioning. BS carried out scanning electron microscope (SEM) analyses and the interpretation of the results. MR carried out the histopathology analysis and the interpretation of the results. CA participated in the design, planning and coordination of the study, supervised tissue sectioning and processing. PFRS devised and coordinated the project, participated in the design and planning of the study, organ weight analyses, interpretation and the statistical analyses of the results, is co-writer and corresponding author of the manuscript. All authors have read, reviewed, commented and approved the final version of the manuscript.

Ethics approval

The mice were handled according to guidelines of the Society for Laboratory Animals Science (GV-SOLAS). The study was approved by the Landesamt für Natur, Umwelt und Verbraucherschutz (LANUV, NRW, Germany; Ref. no. 84-02.04.2013.A443).

Consent for publication

Not applicable (no human data presented).

Competing interests

The authors declare that they have no competing interests.

Acknowledgements

The authors thank Waluree Thongkam, Miriam G. Hovest, Paul M. Peeters, Kathrin Hampel, Christel Weishaupt, Gabriele Wick and Petra Gross for technical support.

3.6 Supplementary Material

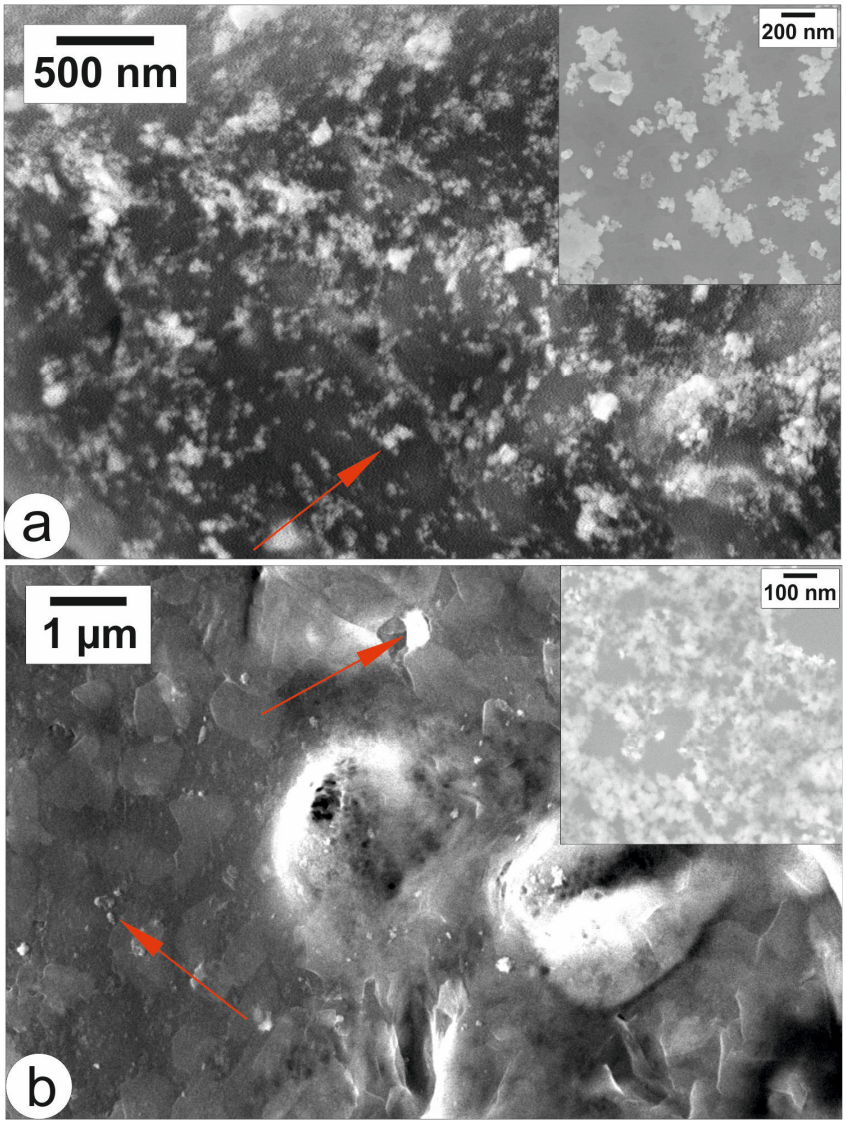

Figure S1. Scanning electron microscope images of feed pellets loaded with a) CeO_2 NM and b) SiO_2 NM. The red arrows exemplarily point to the particles visible by their brighter contrast. The inserts show the pristine NMs in a higher magnification.

Method: To analyse the added NMs and the feed pellets high resolution scanning electron microscope (SEM) images were obtained. For the pristine NMs a JEOL 7500F high resolution SEM (JEOL (Germany) GmbH) was used. The NMs were dispersed in deionized water and applied onto single crystalline silicon wafer pieces. After drying the SEM images were obtained at an acceleration voltage of 5 kV (see Sofranko et al., 2021[1]). The SEM investigations of the feed pellets were conducted on the pellets with the 1% NMs using a Tescan CLARA RISE (Tescan GmbH, Dortmund, Germany) high-resolution scanning electron microscope at an acceleration voltage of 15 kV. The feed pellets were not covered with a conductive layer due to the size of the nanoparticles. The images shown in Figure S5 were obtained by using the 4-quadrant backscatter detector revealing the elemental composition of the sample (z-contrast), thus emphasizing the added nanoparticles. The composition was cross-checked by applying energy dispersive x-ray analysis (EDAX Octane Elect detector, AMETEK GmbH, Wiesbaden, Germany) verifying the presence of Cerium and silicon, respectively. The SEM images show that the added NMs are distributed over the surface of the feed pellet ingredients both at the surface of the pellets as well as inside the pellets. The nanoparticles are usually well dispersed with only a few agglomeration areas present.

[1] Sofranko, A.; Wahle, T.; Heusinkveld, H. J.; Stahlmecke, B.; Dronov, M.; Pijnenburg, D.; Hilhorst, R.; Lamann, K.; Albrecht, C.; Schins, R. P. F., NeuroToxicology 2021, 84, 155-171.

3.7 References

1. Stone V, Miller MR, Clift MJD, Elder A, Mills NL, Moller P, et al. Nanomaterials Versus Ambient Ultrafine Particles: An Opportunity to Exchange Toxicology Knowledge. Environ Health Perspect. 2017;125 10:106002;
2. Boyes WK, van Thriel C. Neurotoxicology of Nanomaterials. Chem Res Toxicol. 2020;33 5:1121-44; doi: 10.1021/acs.chemrestox.0c00050.
3. Heusinkveld HJ, Wahle T, Campbell A, Westerink RHS, Tran L, Johnston H, et al. Neurodegenerative and neurological disorders by small inhaled particles. NeuroToxicology. 2016;56:94-106;
4. Block ML, Calderon-Garciduenas L. Air pollution: mechanisms of neuroinflammation and CNS disease. Trends in neurosciences. 2009;32 9:506-16;
5. Weuve J. Invited Commentary: How Exposure to Air Pollution May Shape Dementia Risk, and What Epidemiology Can Say About It. American Journal of Epidemiology. 2014;180 4:367-71;
6. Selkoe DJ. Alzheimer's disease: genes, proteins, and therapy. Physiol Rev. 2001;81 2:741-66;
7. Selkoe DJ, Hardy J. The amyloid hypothesis of Alzheimer's disease at 25 years. EMBO Molecular Medicine. 2016;8 6:595-608;
8. Chin-Chan M, Navarro-Yepes J, Quintanilla-Vega B. Environmental pollutants as risk factors for neurodegenerative disorders: Alzheimer and Parkinson diseases. Front Cell Neurosci. 2015;9:124-;
9. Schmidt R, Kienbacher E, Benke T, Dal-Bianco P, Delazer M, Ladurner G, et al. [Sex differences in Alzheimer's disease]. Neuropsychiatrie : Klinik, Diagnostik, Therapie und Rehabilitation : Organ der Gesellschaft Osterreichischer Nervenarzte und Psychiater. 2008;22 1:1-15.
10. Zhang Y-w, Thompson R, Zhang H, Xu H. APP processing in Alzheimer's disease. Molecular brain. 2011;4:3-;
11. Hullmann M, Albrecht C, van Berlo D, Gerlofs-Nijland ME, Wahle T, Boots AW, et al. Diesel engine exhaust accelerates plaque formation in a mouse model of Alzheimer's disease. Particle and fibre toxicology. 2017;14:35;
12. Hadrup N, Lam HR. Oral toxicity of silver ions, silver nanoparticles and colloidal silver – A review. Regulatory Toxicology and Pharmacology. 2014;68 1:1-7;
13. Skalska J, Dabrowska-Bouta B, Struzynska L. Oxidative stress in rat brain but not in liver following oral administration of a low dose of nanoparticulate silver. Food and chemical toxicology : an international journal published for the British Industrial Biological Research Association. 2016;97:307-15; doi: 10.1016/j.fct.2016.09.026.
14. Sofranko A, Wahle T, Heusinkveld HJ, Stahlmecke B, Dronov M, Pijnenburg D, et al. Evaluation of the neurotoxic effects of engineered nanomaterials in C57BL/6J mice in 28-day oral exposure studies. NeuroToxicology. 2021;84:155-71;
15. Liang H, Chen A, Lai X, Liu J, Wu J, Kang Y, et al. Neuroinflammation is induced by tongue-instilled ZnO nanoparticles via the Ca2+-dependent NF-κB and MAPK pathways. Particle and fibre toxicology. 2018;15 1:39;
16. Chen J, Zhang S, Chen C, Jiang X, Qiu J, Qiu Y, et al. Crosstalk of gut microbiota and serum/hippocampus metabolites in neurobehavioral impairments induced by zinc oxide nanoparticles. Nanoscale. 2020;12 41:21429-39;
17. Zhang S, Jiang X, Cheng S, Fan J, Qin X, Wang T, et al. Titanium dioxide nanoparticles via oral exposure leads to adverse disturbance of gut microecology and locomotor activity in adult mice. Archives of Toxicology. 2020;94 4:1173-90;
18. Manickam V, Dhakshinamoorthy V, Perumal E. Iron Oxide Nanoparticles Affects Behaviour and Monoamine Levels in Mice. Neurochemical research. 2019;44 7:1533-48;

19. Napierska D, Thomassen LCJ, Lison D, Martens JA, Hoet PH. The nanosilica hazard: another variable entity. Particle and fibre toxicology. 2010;7 1:39-;
20. Murugadoss S, Lison D, Godderis L, Van Den Brule S, Mast J, Brassinne F, et al. Toxicology of silica nanoparticles: an update. Archives of toxicology. 2017;91 9:2967-3010;
21. Brinch A, Hansen SF, Hartmann NB, Baun A. EU Regulation of Nanobiocides: Challenges in Implementing the Biocidal Product Regulation (BPR). Nanomaterials (Basel, Switzerland). 2016;6 2:33;
22. Additives EPanel oF, Nutrient Sources added to F, Younes M, Aggett P, Aguilar F, Crebelli R, et al. Re-evaluation of silicon dioxide (E 551) as a food additive. EFSA Journal. 2018;16 1:e05088;
23. Dahle JT, Arai Y. Environmental Geochemistry of Cerium: Applications and Toxicology of Cerium Oxide Nanoparticles. International Journal of Environmental Research and Public Health. 2015;12 2:1253-78;
24. Cassee FR, van Balen EC, Singh C, Green D, Muijser H, Weinstein J, et al. Exposure, Health and Ecological Effects Review of Engineered Nanoscale Cerium and Cerium Oxide Associated with its Use as a Fuel Additive. Critical Reviews in Toxicology. 2011;41 3:213-29;
25. Mittal D, Kaur G, Singh P, Yadav K, Ali SA. Nanoparticle-Based Sustainable Agriculture and Food Science: Recent Advances and Future Outlook. Frontiers in Nanotechnology. 2020;2 10;
26. Gomez A, Narayan M, Zhao L, Jia X, Bernal RA, Lopez-Moreno ML, et al. Effects of nano-enabled agricultural strategies on food quality: Current knowledge and future research needs. Journal of hazardous materials. 2021;401:123385;
27. Rico CM, Majumdar S, Duarte-Gardea M, Peralta-Videa JR, Gardea-Torresdey JL. Interaction of Nanoparticles with Edible Plants and Their Possible Implications in the Food Chain. Journal of agricultural and food chemistry. 2011;59 8:3485-98;
28. Ma Y, Yao Y, Yang J, He X, Ding Y, Zhang P, et al. Trophic Transfer and Transformation of CeO2 Nanoparticles along a Terrestrial Food Chain: Influence of Exposure Routes. Environmental Science & Technology. 2018;52 14:7921-7;
29. Zhang J, Nazarenko Y, Zhang L, Calderon L, Lee K-B, Garfunkel E, et al. Impacts of a Nanosized Ceria Additive on Diesel Engine Emissions of Particulate and Gaseous Pollutants. Environmental Science & Technology. 2013;47 22:13077-85;
30. Zamankhan F, Pirouzfar V, Ommi F, Valihesari M. Investigating the effect of MgO and CeO2 metal nanoparticle on the gasoline fuel properties: empirical modeling and process optimization by surface methodology. Environmental Science and Pollution Research. 2018;25 23:22889-902;
31. Heyder J, Gebhart J, Rudolf G, Schiller CF, Stahlhofen W. Deposition of particles in the human respiratory tract in the size range 0.005–15 μm. Journal of Aerosol Science. 1986;17 5:811-25;
32. Oberdörster G, Oberdörster E, Oberdörster J. Nanotoxicology: an emerging discipline evolving from studies of ultrafine particles. Environmental health perspectives. 2005;113 7:823-39;
33. Semmler-Behnke M, Takenaka S, Fertsch S, Wenk A, Seitz J, Mayer P, et al. Efficient elimination of inhaled nanoparticles from the alveolar region: evidence for interstitial uptake and subsequent reentrainment onto airways epithelium. Environmental health perspectives. 2007;115 5:728-33; d
34. Nelson BC, Johnson ME, Walker ML, Riley KR, Sims CM. Antioxidant Cerium Oxide Nanoparticles in Biology and Medicine. Antioxidants. 2016;5 2;

35. Casals E, Zeng M, Parra-Robert M, Fernández-Varo G, Morales-Ruiz M, Jiménez W, et al. Cerium Oxide Nanoparticles: Advances in Biodistribution, Toxicity, and Preclinical Exploration. Small. 2020;16 20:e1907322;
36. Oakley H, Cole SL, Logan S, Maus E, Shao P, Craft J, et al. Intraneuronal beta-amyloid aggregates, neurodegeneration, and neuron loss in transgenic mice with five familial Alzheimer's disease mutations: potential factors in amyloid plaque formation. The Journal of neuroscience : the official journal of the Society for Neuroscience. 2006;26 40:10129-40;
37. Jawhar S, Trawicka A, Jenneckens C, Bayer TA, Wirths O. Motor deficits, neuron loss, and reduced anxiety coinciding with axonal degeneration and intraneuronal Abeta aggregation in the 5XFAD mouse model of Alzheimer's disease. Neurobiol Aging. 2012;33 1:196.e29-40;
38. Miquel J, Blasco M. A simple technique for evaluation of vitality loss in aging mice, by testing their muscular coordination and vigor. Experimental Gerontology. 1978;13 6:389-96;
39. Hall C, Ballachey EL. A study of the rat's behavior in a field. A contribution to method in comparative psychology. University of California Publications in Psychology. 1932;6:1-12.
40. Richard BC, Kurdakova A, Baches S, Bayer TA, Weggen S, Wirths O. Gene Dosage Dependent Aggravation of the Neurological Phenotype in the 5XFAD Mouse Model of Alzheimer's Disease. Journal of Alzheimer's disease : JAD. 2015;45 4:1223-36;
41. Lippa CF NL, Mori H, George-Hyslop P. Abeta-42 deposition precedes other changes in PS-1 Alzheimer´s disease. Lancet 352. 1998:1117-8.
42. Wahle T, Sofranko A, Dekkers S, Miller MR, Heusinkveld HJ, Albrecht C, et al. Evaluation of neurological effects of cerium dioxide nanoparticles doped with different amounts of zirconium following inhalation exposure in mouse models of Alzheimer's and vascular disease. Neurochemistry International. 2020;138:104755;
43. Feng X, Chen A, Zhang Y, Wang J, Shao L, Wei L. Central nervous system toxicity of metallic nanoparticles. International journal of nanomedicine. 2015;10:4321-40;
44. Boyes WK, van Thriel C. Neurotoxicology of Nanomaterials. Chemical Research in Toxicology. 2020;33 5:1121-44;
45. Song B, Zhou T, Liu J, Shao L. Involvement of Programmed Cell Death in Neurotoxicity of Metallic Nanoparticles: Recent Advances and Future Perspectives. Nanoscale research letters. 2016;11 1:484;
46. Tramutola A, Lanzillotta C, Perluigi M, Butterfield DA. Oxidative stress, protein modification and Alzheimer disease. Brain Res Bull. 2017;133:88-96;
47. Gardener SL, Rainey-Smith SR, Martins RN. Diet and Inflammation in Alzheimer's Disease and Related Chronic Diseases: A Review. Journal of Alzheimer's disease : JAD. 2016;50 2:301-34;
48. Heppner FL, Ransohoff RM, Becher B. Immune attack: the role of inflammation in Alzheimer disease. Nature reviews Neuroscience. 2015;16 6:358-72;
49. Islam MT. Oxidative stress and mitochondrial dysfunction-linked neurodegenerative disorders. Neurological research. 2017;39 1:73-82;
50. Pastore A, Federici G, Bertini E, Piemonte F. Analysis of glutathione: implication in redox and detoxification. Clin Chim Acta. 2003;333 1:19-39;
51. Owen JB, Butterfield DA. Measurement of Oxidized/Reduced Glutathione Ratio. In: Bross P, Gregersen N, editors. Protein Misfolding and Cellular Stress in Disease and Aging: Concepts and Protocols. Totowa, NJ: Humana Press; 2010. p. 269-77.
52. Zhang C, Rodriguez C, Spaulding J, Aw TY, Feng J. Age-Dependent and Tissue-Related Glutathione Redox Status in a Mouse Model of Alzheimer's Disease. Journal of Alzheimer's Disease. 2012;28:655-66;

53. Ransohoff RM. How neuroinflammation contributes to neurodegeneration. Science (New York, NY). 2016;353 6301:777-83;
54. Kovacs GG. Cellular reactions of the central nervous system. Handbook of clinical neurology. 2017;145:13-23;
55. Sofroniew MV, Vinters HV. Astrocytes: biology and pathology. Acta neuropathologica. 2010;119 1:7-35;
56. Committee ES, Hardy A, Benford D, Halldorsson T, Jeger MJ, Knutsen HK, et al. Guidance on risk assessment of the application of nanoscience and nanotechnologies in the food and feed chain: Part 1, human and animal health. EFSA Journal. 2018;16 7:e05327;
57. Boudard D, Aureli F, Laurent B, Sturm N, Raggi A, Antier E, et al. Chronic Oral Exposure to Synthetic Amorphous Silica (NM-200) Results in Renal and Liver Lesions in Mice. Kidney Int Rep. 2019;4 10:1463-71;
58. Riedle S, Wills JW, Miniter M, Otter DE, Singh H, Brown AP, et al. A Murine Oral-Exposure Model for Nano- and Micro-Particulates: Demonstrating Human Relevance with Food-Grade Titanium Dioxide. Small. 2020;16 21:2000486;
59. Ennaceur A, Chazot PL. Preclinical animal anxiety research - flaws and prejudices. Pharmacol Res Perspect. 2016;4 2:e00223-e;
60. Yang X, He C, Li J, Chen H, Ma Q, Sui X, et al. Uptake of silica nanoparticles: neurotoxicity and Alzheimer-like pathology in human SK-N-SH and mouse neuro2a neuroblastoma cells. Toxicology letters. 2014;229 1:240-9;
61. Arnoldussen YJ, Kringlen Ervik T, Baarnes Eriksen M, Kero I, Skaug V, Zienolddiny S. Cellular Responses of Industrially Relevant Silica Dust on Human Glial Cells In Vitro. International Journal of Molecular Sciences. 2019;20 2;
62. Lee J KM, Paek H, Kim Y, Kim M, Lee JK, Jeong J, Choi S. Tissue distribution and excretion kinetics of orally administered silica nanoparticles in rats. Int J Nanomedicine. 2014;
63. Shim KH JK, Bae SO, Kang MO, Maeng E, Choi C, Kim Y, Hulme J, Lee EK, Kim M, An SSA. Assessment of ZnO and SiO2 nanoparticle permeability through and toxicity to the blood–brain barrier using Evans blue and TEM. International journal of nanomedicine. 2014;9(Supplement 2):225-233;
64. Brandscheid C, Schuck F, Reinhardt S, Schäfer KH, Pietrzik CU, Grimm M, et al. Altered Gut Microbiome Composition and Tryptic Activity of the 5xFAD Alzheimer's Mouse Model. Journal of Alzheimer's disease : JAD. 2017;56 2:775-88;
65. Stoye NM, dos Santos Guilherme M, Endres K. Alzheimer's disease in the gut—Major changes in the gut of 5xFAD model mice with ApoA1 as potential key player. The FASEB Journal. 2020;34 9:11883-99;
66. Kobyliak N, Virchenko O, Falalyeyeva T, Kondro M, Beregova T, Bodnar P, et al. Cerium dioxide nanoparticles possess anti-inflammatory properties in the conditions of the obesity-associated NAFLD in rats. Biomed Pharmacother. 2017;90:608-14;
67. Asgharzadeh F, Hashemzadeh A, Rahmani F, Yaghoubi A, Nazari SE, Avan A, et al. Cerium oxide nanoparticles acts as a novel therapeutic agent for ulcerative colitis through anti-oxidative mechanism. Life sciences. 2021;278:119500;
68. Naha PC, Hsu JC, Kim J, Shah S, Bouché M, Si-Mohamed S, et al. Dextran-Coated Cerium Oxide Nanoparticles: A Computed Tomography Contrast Agent for Imaging the Gastrointestinal Tract and Inflammatory Bowel Disease. ACS nano. 2020;14 8:10187-97;
69. Mattson MP. Pathways towards and away from Alzheimer's disease. Nature. 2004;430 7000:631-9;

70. Guglielmotto M, Tamagno E, Danni O. Oxidative stress and hypoxia contribute to Alzheimer's disease pathogenesis: two sides of the same coin. TheScientificWorldJournal. 2009;9:781-91;
71. Tong Y, Zhou W, Fung V, Christensen MA, Qing H, Sun X, et al. Oxidative stress potentiates BACE1 gene expression and Abeta generation. Journal of neural transmission (Vienna, Austria : 1996). 2005;112 3:455-69;
72. Alvarino R, Alonso E, Lacret R, Oves-Costales D, Genilloud O, Reyes F, et al. Caniferolide A, a Macrolide from Streptomyces caniferus, Attenuates Neuroinflammation, Oxidative Stress, Amyloid-Beta, and Tau Pathology in Vitro. Molecular pharmaceutics. 2019;
73. Bernstein SL, Dupuis NF, Lazo ND, Wyttenbach T, Condron MM, Bitan G, et al. Amyloid-β protein oligomerization and the importance of tetramers and dodecamers in the aetiology of Alzheimer's disease. Nature Chemistry. 2009;1 4:326-31;
74. Chakraborty D, Straub JE, Thirumalai D. Differences in the free energies between the excited states of Aβ40 and Aβ42 monomers encode their aggregation propensities. Proc Natl Acad Sci U S A. 2020;117 33:19926-37;
75. Estevez AY, Pritchard S, Harper K, Aston JW, Lynch A, Lucky JJ, et al. Neuroprotective mechanisms of cerium oxide nanoparticles in a mouse hippocampal brain slice model of ischemia. Free Radic Biol Med. 2011;51 6:1155-63;
76. Esch F, Fabris S, Zhou L, Montini T, Africh C, Fornasiero P, et al. Electron localization determines defect formation on ceria substrates. Science (New York, NY). 2005;309 5735:752-5;
77. Coppede F, Migliore L. Evidence linking genetics, environment, and epigenetics to impaired DNA repair in Alzheimer's disease. Journal of Alzheimer's disease : JAD. 2010;20 4:953-66;
78. Rzigalinski BA, Carfagna CS, Ehrich M. Cerium oxide nanoparticles in neuroprotection and considerations for efficacy and safety. Wiley interdisciplinary reviews Nanomedicine and nanobiotechnology. 2017;9 4:10.1002/wnan.444;
79. Hirst SM, Karakoti AS, Tyler RD, Sriranganathan N, Seal S, Reilly CM. Anti-inflammatory Properties of Cerium Oxide Nanoparticles. Small. 2009;5 24:2848-56;
80. Eleftheriadou D, Kesidou D, Moura F, Felli E, Song W. Redox-Responsive Nanobiomaterials-Based Therapeutics for Neurodegenerative Diseases. Small. 2020;16 43:e1907308;
81. Hegazy MA, Maklad HM, Samy DM, Abdelmonsif DA, El Sabaa BM, Elnozahy FY. Cerium oxide nanoparticles could ameliorate behavioral and neurochemical impairments in 6-hydroxydopamine induced Parkinson's disease in rats. Neurochem Int. 2017;108:361-71;
82. Heckman KL, DeCoteau W, Estevez A, Reed KJ, Costanzo W, Sanford D, et al. Custom Cerium Oxide Nanoparticles Protect against a Free Radical Mediated Autoimmune Degenerative Disease in the Brain. ACS nano. 2013;7 12:10582-96;
83. Kwon HJ, Cha M-Y, Kim D, Kim DK, Soh M, Shin K, et al. Mitochondria-Targeting Ceria Nanoparticles as Antioxidants for Alzheimer’s Disease. ACS nano. 2016;10 2:2860-70;.
84. Gregori M, Masserini M, Mancini S. Nanomedicine for the treatment of Alzheimer's disease. Nanomedicine. 2015;10 7:1203-18;
85. Dowding JM, Dosani T, Kumar A, Seal S, Self WT. Cerium oxide nanoparticles scavenge nitric oxide radical (NO). Chemical communications (Cambridge, England). 2012;48 40:4896-8;
86. Guan Y, Li M, Dong K, Gao N, Ren J, Zheng Y, et al. Ceria/POMs hybrid nanoparticles as a mimicking metallopeptidase for treatment of neurotoxicity of amyloid-β peptide. Biomaterials. 2016;98:92-102;

87. Wu J, Wang C, Sun J, Xue Y. Neurotoxicity of silica nanoparticles: brain localization and dopaminergic neurons damage pathways. ACS nano. 2011;5 6:4476-89;
88. Liu D, Lin B, Shao W, Zhu Z, Ji T, Yang C. In vitro and in vivo studies on the transport of PEGylated silica nanoparticles across the blood-brain barrier. ACS applied materials & interfaces. 2014;6 3:2131-6;
89. Yokel RA, Tseng MT, Dan M, Unrine JM, Graham UM, Wu P, et al. Biodistribution and biopersistence of ceria engineered nanomaterials: size dependence. Nanomedicine : nanotechnology, biology, and medicine. 2013;9 3:398-407;
90. Yokel RA, Hussain S, Garantziotis S, Demokritou P, Castranova V, Cassee FR. The Yin: An adverse health perspective of nanoceria: uptake, distribution, accumulation, and mechanisms of its toxicity. Environmental science Nano. 2014;1 5:406-28;
91. Park K, Park J, Lee H, Choi J, Yu W-J, Lee J. Toxicity and tissue distribution of cerium oxide nanoparticles in rats by two different routes: single intravenous injection and single oral administration. Archives of Pharmacal Research. 2018;41 11:1108-16;
92. Hirst SM, Karakoti A, Singh S, Self W, Tyler R, Seal S, et al. Bio-distribution and in vivo antioxidant effects of cerium oxide nanoparticles in mice. Environmental Toxicology. 2013;28 2:107-18;
93. Modrzynska J, Berthing T, Ravn-Haren G, Kling K, Mortensen A, Rasmussen RR, et al. In vivo-induced size transformation of cerium oxide nanoparticles in both lung and liver does not affect long-term hepatic accumulation following pulmonary exposure. PLOS ONE. 2018;13 8:e0202477;
94. Yokel RA, Tseng MT, Butterfield DA, Hancock ML, Grulke EA, Unrine JM, et al. Nanoceria distribution and effects are mouse-strain dependent. Nanotoxicology. 2020;14 6:827-46; doi: 10.1080/17435390.2020.1770887.
95. O'Leary TP, Mantolino HM, Stover KR, Brown RE. Age-related deterioration of motor function in male and female 5xFAD mice from 3 to 16 months of age. Genes, Brain and Behavior. 2020;19 3:e12538;
96. Moran PM, Higgins LS, Cordell B, Moser PC. Age-related learning deficits in transgenic mice expressing the 751-amino acid isoform of human beta-amyloid precursor protein. Proc Natl Acad Sci U S A. 1995;92 12:5341-5;
97. Holcomb LA, Gordon MN, Jantzen P, Hsiao K, Duff K, Morgan D. Behavioral changes in transgenic mice expressing both amyloid precursor protein and presenilin-1 mutations: lack of association with amyloid deposits. Behav Genet. 1999;29 3:177-85;
98. Hirsch-Reinshagen V, Maia LF, Burgess BL, Blain JF, Naus KE, McIsaac SA, et al. The absence of ABCA1 decreases soluble ApoE levels but does not diminish amyloid deposition in two murine models of Alzheimer disease. The Journal of biological chemistry. 2005;280 52:43243-56;

4 Neurological effects of inhaled nano-sized cerium dioxide in a mouse model of Alzheimer´s Disease

Tina Wahle[1,*], Adriana Sofranko[1,*], Susan Dekkers[2], Mark R. Miller[3], Harm J. Heusinkveld[1,2], Catrin Albrecht[1], Flemming R. Cassee[2,4], Roel P.F. Schins[1]

[1]IUF - Leibniz Research Institute for Environmental Medicine, Düsseldorf, Germany; [2]National Institute for Public Health and the Environment, Bilthoven, The Netherlands; [3]Centre for Cardiovascular Science & Centre for Inflammation Research, University of Edinburgh, Edinburgh, United Kingdom; [4]Institute for Risk Assessment Sciences, Faculty of Science, Utrecht University, Utrecht, The Netherlands

* These authors contributed equally to this work.

Neurochemistry International, Volume 138, September 2020, 104755

DOI: 10.1016/j.neuint.2020.104755

Author contribution: The author of this dissertation examined immunhistochemical analyses of amyloid plaque burden and IBA-1 load, performed GFAP, IBA-1, HO-1 and Nrf2 western blot analyses, made the graphs of these assays, reviewed and discussed the results of the whole manuscript. Relative contribution: about 40%.

4.1 Abstract

Increasing evidence from toxicological and epidemiological studies indicates that the brain is an important target for ambient (ultrafine) particles. Disturbance of redox-homeostasis and inflammation in the brain are proposed as possible mechanisms that can contribute to neurotoxic and neurodegenerative effects. Whether and how engineered nanoparticles (NPs) may cause neurotoxicity and promote neurodegenerative diseases such as Alzheimer´s disease (AD) is largely unstudied.

We have assessed the neurological effects of subacute inhalation exposures (4 mg/m^3 for 3 h/day, 5 days/week for 4 weeks) to cerium dioxide (CeO_2) NPs doped with different amounts of zirconium (Zr, 0%, 27% and 78%), to address the influence of particle redox-activity in the 5xFAD transgenic mouse model of AD. Four weeks post-exposure, effects on behaviour were evaluated and brain tissues were analysed for amyloid-β plaque formation and reactive microglia (Iba-1 staining). Behaviour was also evaluated in concurrently exposed non-transgenic C57BL/6J littermates, as well as in Western diet-fed apolipoprotein E-deficient ($ApoE^{-/-}$) mice as a model of vascular disease. Markers of inflammation and oxidative stress were evaluated in brain cortex.

The brains of the NP-exposed 5xFAD mice revealed no accelerated amyloid-β plaque formation. No significant treatment-related behaviour impairments were observed in the healthy C57BL/6J mice. In the 5xFAD and $ApoE^{-/-}$ models, the NP inhalation exposures did not affect the alternation score in the X-maze indicating absence of spatial working memory deficits. However, following inhalation exposure to the 78% Zr-doped CeO_2 NPs changes in forced motor performance (string suspension) and exploratory motor activity (X-maze) were observed in $ApoE^{-/-}$ and 5xFAD mice, respectively. Exposure to the 78% doped NPs also caused increased cortical expression of glial fibrillary acidic protein (GFAP) in the C57BL/6J mice. No significant treatment-related changes neuroinflammation and oxidative stress were observed in the 5xFAD and $ApoE^{-/-}$ mice.

Our study findings reveal that subacute inhalation exposure to CeO_2 NPs does not accelerate the AD-like phenotype of the 5xFAD model. Further investigation is warranted to unravel whether the redox-activity dependent effects on motor activity as observed in the mouse models of AD and vascular disease result from specific neurotoxic effects of these NPs.

4.2 Introduction

Several research groups have postulated that ultrafine air pollution particles are an important environmental risk factor for neurotoxicity and, more specifically, may potentiate the risk of

neurodegenerative disorders, like Alzheimer's Disease (AD) (reviewed in (Heusinkveld et al. 2016). In relation to this, concerns have been raised about the potential neurotoxic and neurodegenerative effects of engineered nanoparticles (NPs). However, despite great progress in nanotechnologies, comparatively little is known to date on the potential adverse effects that exposure to manufactured NPs may have on the human brain, including the potential induction of pathways leading to neurodegeneration (Cupaioli et al. 2014). Indeed, NPs can enter the human body through several routes, e.g. via inhalation, absorption from the digestive tract, or following injection into the blood in nanomedical applications. With regard to potential adverse impacts on the brain, uptake and retrograde axonal transport of NPs via the olfactory nerve has been demonstrated in rodent inhalation studies (Oberdorster et al. 2004; Elder et al. 2006; Elder and Oberdorster 2006). Besides, NPs may reach the central nervous system via the blood–brain barrier (BBB), where they have been suspected to impair several molecular pathways and contribute to neurodegeneration (Iqbal et al. 2013; Cupaioli et al. 2014). The ability to generate reactive oxygen species and associated inflammation is considered one of the key mechanisms of nanomaterials´ toxicity to the respiratory tract and cardiovascular system (Unfried et al. 2008; Miller, Shaw, and Langrish 2012; Stone et al. 2017) and thus could also play a major role in their neurotoxic and neurodegenerative effects. Indeed, oxidative stress and neuroinflammation have long been recognised in neurotoxicity and neurodegenerative diseases including AD (Heneka et al. 2015; Zhao and Zhao 2013).

Among the various types of NPs, cerium oxide NPs (CeO_2 NPs) have been subjected to various toxicological investigations in relation to inhalation exposure (Cassee et al. 2011a; Demokritou et al. 2013). CeO_2 NPs are widely used as catalysts in industrial applications. They are used as additive to diesel fuels in order to reduce the amount of emitted pollutants after their combustion. Because of their radical-scavenging properties, CeO_2 NPs have gained strong interest in the field of nanomedicine (reviewed in (Das et al. 2013)). The antioxidant properties of CeO_2 NPs are accomplished through its ability to switch from the 3+ to the 4+ valence state (Hirst et al. 2009). It has been shown that the antioxidant efficacy of CeO_2 NPs can be affected by incorporation of zirconium (Zr) in the CeO_2 lattice (Tsai et al. 2008). However, whilst research has been devoted since many years to elaborate on neuroprotective and potential anti-neurodegenerative effects of CeO_2 (Singh, Cohen, and Rzigalinski 2007), adverse effects on the brain should also be considered for this type of nanoparticles as indicated e.g. from intravenous application studies in rats (Hardas et al. 2010; Hardas et al. 2014) and *in vitro* neuronal activity experiments with primary rat cortex cultures (Strickland et al. 2016).

Given that free radicals play a prominent role in the pathology of many neurological diseases, we explored the neurotoxicity of CeO_2 NPs doped with varying amounts of Zr following inhalation exposure in three different mouse models, i.e. C57BL/6J, 5xFAD and $ApoE^{-/-}$ mice. The 5xFAD transgenic mice were used in this study as a model for AD. The 5xFAD mouse model was used in a previous study, in which we have demonstrated that inhalation exposure to diesel engine exhaust results in an accelerated formation of Aβ-plaques as well as motor function impairment (Hullmann et al. 2017a). Diesel engine exhaust represents a major source of unintentionally generated NPs in most urban environments and therefore supports the selection of the 5xFAD model for the investigation of the neurological effects of engineered NPs after inhalation. The nontransgenic littermate controls of the 5xFAD mice (C57BL/6J background) were used as a healthy mouse model. Finally, apolipoprotein E-deficient ($ApoE^{-/-}$) mice, subjected to a high-fat diet, were included in present study. $ApoE^{-/-}$ mice represent a well-established model for the study of atherosclerosis, a disease characterized by the build-up of lipid- and inflammatory cell-rich plaques within arteries, which underlies the majority of cardiovascular diseases (Cassee et al. 2012; Miller et al. 2013). Since this ApoE deficiency compromises the blood brain barrier (Methia et al. 2001) this model could also be useful to study the susceptibility to NP-induced neurological effects. The adverse cardiovascular effects of diesel exhaust particles as well as specific types of engineered NPs have been clearly demonstrated in $ApoE^{-/-}$ mice in several studies (Hansen et al. 2007; Kang et al. 2011; Miller et al. 2013). Interestingly, a comparative inhalation study with engine exhausts generated using fuels with or without added CeO_2 NPs in $ApoE^{-/-}$ mice revealed differences in atherosclerotic plaque formation but also in pro-inflammatory responses in (Nelson et al.)cortical brain regions (Cassee et al. 2012; Lung et al. 2014), which could reflect a direct effect of these redox active NPs on the central nervous system.

The aim of the current study was to evaluate the potential neurotoxic and neurodegenerative effects of CeO_2 NPs in mice following a four-week inhalation exposure and to assess the influence of redox activity by the concurrent evaluation of CeO_2 NPs with different Zr-doping grades. The investigations formed part of a large study conducted in to explore the (patho)physiological effects of NP exposure on multiple organ systems in various mouse models (Dekkers et al. 2017; Dekkers et al. 2018).

4.3 Materials and Methods

4.3.1 **Animals.**

In this study, three different mouse models were used. The 5xFAD transgenic mice were used as a model for AD. Only the female mice were used for the study in view of the reported sex-specific differences in age- and treatment related Aβ development (Devi et al. 2010). The 5xFAD mice overexpress the 695 amino acid isoform of the human amyloid precursor protein (APP695) carrying Swedish (K670N), London (V717I) and Florida (I716V) mutations as well as the human PS1 (M146L; L286V) mutations (Oakley et al. 2006; Ohno et al. 2004). The mice develop a specific phenotype that includes high APP expression levels, amyloid deposition (beginning at two months of age) and memory impairments and motor deficits (Oakley et al. 2006; Jawhar et al. 2012). The breeding was performed by mating heterozygote transgenic founders with C57BL/6J wild-type mice. The nontransgenic female littermates were used as model of healthy mice in this study. The 5xFAD and C57BL/6J mice originated from Jackson Laboratories. For the study, female 5xFAD mice (n=64) and female cross bred C57BL/6J littermates (n= 40) were used at the age of 8-11 weeks. As a third model, $ApoE^{-/-}$ mice were used. Female $ApoE^{-/-}$ mice (n=32) were obtained from Taconic, Denmark at age 10–12 weeks at the beginning of the study. The four-week inhalation exposure protocol in the $ApoE^{-/-}$ mice was integrated into an 8-week high-fat (Western diet) feeding regime (Purified Diet Western 4021.06, ABdiets, Woerden, The Netherlands), which has been shown to generate complex atherosclerotic plaques with many of the hallmarks of the human disease in specific arterial locations (Cassee et al. 2012; Miller et al. 2013; Dekkers et al. 2017). All mice were barrier maintained and housed in a single room in macrolon cages. Temperature and relative humidity were controlled at 22±2°C and at 40-70%, respectively. Lighting was artificial with a sequence of 12 hours light (during daytime) and 12 hours dark (at night). Feed and drinking water were provided *ad libitum* from the arrival of the mice until the end of the study, except during exposure. The study was conducted at Intravacc (Bilthoven, The Netherlands) under a protocol approved by the Ethics Committee for Animal Experiments of the RIVM and performed according to applicable national and EU regulations.

4.3.2 **Inhalation study design.**

The mice were exposed via nose only inhalation to CeO_2 NPs with varying amounts of Zr-doping (0%, 27% or 78% Zr) or clean air, respectively, over a four-week period (4 mg/m^3 for 3 h/day, 5 days/week). The number of animals per treatment group designed for the present

study was n=10 for the C57BL/6J mice, n=16 for the 5xFAD mice and n=8 for the $ApE^{-/-}$ mice. For three mice data could not be obtained because of their early removal from the study for humane reasons not related to the toxicity of the NP exposure. Combined with the genotyping verification, this resulted in the following animal numbers per group: $ApoE^{-/-}$: control (n=8); CeO_2 (n=7); 27% ZrO_2-doped CeO_2 (n=8); 78% ZrO_2-doped CeO_2 (n=8). 5XFAD: control (n=16); CeO_2 (n=14); 27% ZrO_2-doped CeO_2 (n=16); 78% ZrO_2-doped CeO_2 (n=16). Wt: control (n=10); CeO_2 (n=10); 27% ZrO_2-doped CeO_2 (n=10); 78% ZrO_2-doped CeO_2 (n=10). On day 52 and day 53 after the first exposure day behaviour tests were performed with the mice to assess for exposure-related neurotoxic effects. The animals were killed on day 57. The 4-week post-exposure period was included in the study design to address persistency of the effects and for the compromised mouse models to develop their respective disease phenotypes, i.e. Aβ formation in the brains of the 5xFAD mice and the atherosclerotic plaques in the $ApoE^{-/-}$ mice.

4.3.3 **Nanomaterial production, characterization and inhalation exposure.**

Production and detailed characterization of CeO_2 NPs doped with different amounts of ZrO_2 (ZrO_2 contents in the doped NPs were 0 mol%, 27 mol% and 78 mol%) is described elsewhere (Dekkers et al. 2017). Approximately one week before the four-week exposure period, 20 samples of each NP (one for each day) were prepared at a concentration of 1 mg/mL from the stock dispersions (20, 20 or 29 mg/mL for 0%, 27% and 78% ZrO_2-doped CeO_2 NPs, respectively) by diluting with ultrapure water. Before use, stock and sample dispersions were sonicated for 5 minutes in an ultrasonic bath (Branson CPX2800, 40 kHz, 110W) before use to re-disperse any possible agglomerates. Aerosols of NPs were freshly generated using a spray nozzle technique, diluted with pressurized, clean and particle-free air, and heated to 24-25°C (for detailed description see (Dekkers et al. 2017). Control animals were exposed to 3-h filtered air under the same exposure conditions (i.e. nose-only tubes) for the same amount of time. Prior to the day of exposure start all animals were trained to get used to the nose-only inhalation tubes.

4.3.4 **Behaviour tests.**

At day 52 and 53 (i.e. 24 and 25 days after the last exposure day) the mice were examined by means of behavioural tests. At least 1 hour before behavioural testing, mice were placed in the test room for acclimatisation. All tests were performed in dim red light. All test equipment and mazes were cleaned with 70% ethanol prior to each test to avoid odour recognition. On day 52,

a string suspension test was performed: as a test of agility and grip strength (Miquel and Blasco 1978), a 3 mm thick, 35 cm long cotton string was stretched between two escape platforms on top of two vertical poles. The mice were permitted to grasp the central part of the string by their forepaws, released immediately thereafter and allowed to escape to one of the platforms. A rating system from 0 to 7 was used during a single 60 seconds trial to assess each animals´ performance (Moran et al. 1995) with the following modifications. Score: 0, unable to hang on the string; score 1, hangs only by forepaws; score 2, attempting to climb the string; score 3, climbing the string with four paws successfully; score 4, moving laterally along the string; score 5, escaping to the end of the string; score 6, falls while trying to climb the platform, score 7, reaches the platform.

On day 53, the X-maze task was performed to reflect activity and spatial working memory of mice by spontaneous alternation. Spontaneous alternation in rodents is based on the willingness to explore; a mouse tends to rotate in their entries between the four arms arranged in 90° position extending from a central space, which makes it more discriminative (arm sizes: 30 cm length, 8 cm width and 15 cm height). During 5 min test sessions, each mouse was placed in one arm and was allowed to move freely through the maze. The total number of arm entries was recorded using an infrared beam video camera during the 5 min interval to evaluate exploratory motor activity and this was then combined with the alternation to assess spatial working memory. Alternation was defined as successive entries into the four arms in overlapping quadruple sets (for example 1, 2, 3, 4 or 2, 3, 4, 1 but not 3, 2, 1, 3). Mice with impaired working memory will not remember visited arms leading to a decrease in spontaneous alternation (Holcomb et al. 1999). A successful entry was defined as a mouse entering one arm with all four paws. The alternation percentage was calculated as % of the actual alternations to the possible arm entries.

4.3.5 **Necropsy and immunohistochemical analyses of paraffin embedded slices.**

At day 57, the mice were anesthetized with a mixture of ketamine and xylazine. The right brain hemispheres of 5xFAD mice were stored in 4% PFA for later processing for immunohistochemistry. The left brain hemispheres of C57/BL6, ApoE$^{-/-}$ and 5xFAD animals were rapidly dissected into cortex, olfactory bulb, cerebellum and midbrain. All brain regions were immediately transferred in liquid nitrogen and stored at -80°C until further processing for Western blotting (see below). Dehydration was performed in a series of ethanol concentrations, followed by a transfer into xylene. Subsequently, the brains were embedded in paraffin. Four µm thick paraffin sections were cut using a sliding microtome and transferred on Superfrost

Ultra Plus object slides (Thermo Scientific) and dried over night at 40°C. Subsequently, sections were deparaffinised in xylene, followed by rehydration in a series of ethanol (100%, 96%, 70%) and blocking of endogenous peroxidase by treatment with 0.3% H_2O_2 in PBS. Antigen retrieval was performed by boiling sections in 10 mM citrate buffer, pH 6.0 followed by incubation for 3 min in 88% formic acid. Non-specific antibody binding was blocked via incubation in 10% fetal calf serum (FCS) and 4% skimmed milk in 0.01 M PBS. Thereafter, slides were incubated overnight with primary anti human Aβ 42 antibody (clone G2-11, Cat.N0. MABN12, Merck Millipore, Darmstadt, Germany diluted 1:1000 in 0.01 M PBS and 10% FCS in a humid chamber at room temperature. After washing slices were incubated with a biotinylated anti-mouse secondary antibody (dilution 1:200 in 0.01M PBS and 10% FCS), and the signal was visualised avidin-biotin-complex-method (ABC) by a Vectastain kit (Vectorlabs, Burlingame, USA) using diaminobenzidine (DAB, Sigma-Aldrich, Deisenhofen, Germany)) as chromogen and Hematoxylin for nuclear counterstaining. Light microscope images from cortex and hippocampus were taken with 100x or 50x magnification, respectively, using a Zeiss Axiophot microscope equipped with AxioCam MRc (Carl Zeiss, Jena, Germany). Quantitative Aβ42 plaque analyses were performed via calculation of the percentage of total amyloid plaque load in the analysed area of the section. Plaque load was determined using ZEN 2011 image processing software (Zeiss) after a fixed adjustment of contrast threshold for stained Aβ42 plaques. Plaque load was interactively determined in the whole hippocampal area as well as in a defined cortex region. From each animal, three brain slides with an interspace of approximately 30 µm were analysed. For the immunostaining of ionized calcium-binding adapter molecule 1 (Iba-1), brain sections were incubated overnight with Iba-1 antibody (Cat No. GTX100042, GeneTex; dilution 1:1000 in 0.01 M PBS and 10% FCS) at 4°C. The next day, slides were washed and incubated for 45 min at RT with biotinylated secondary antibody (dilution 1:200 in 0.01M PBS and 10% FCS. Staining was visualized using the ABC Vectastain kit (Vectorlabs, Burlingame, USA) and diaminobenzidine (DAB, Sigma-Aldrich, Deisenhofen, Germany)) as chromogen and Hematoxylin for nuclear counterstaining. Light microscope images from cortex and hippocampus were taken with 200x magnification using a Zeiss Axiophot microscope equipped with AxioCam MRc (Carl Zeiss, Jena, Germany). Iba-1 area (%) was quantified using ZEN 2011 image processing software (Zeiss) via calculation of the positive stained microglia (brown colour) in the defined cortical and hippocampal area.

4.3.6 **Western blot analyses.**

Protein expression of Iba-1, glial fibrillary acidic protein (GFAP), nuclear factor E2-related factor 2 (Nrf2) and heme oxygenase-1 (HO-1) was evaluated by Western blot to address whether the exposures to the CeO_2 NPs resulted in neuroinflammation and oxidative stress. Iba-1 and GFAP represent well-established markers of activated microglia (Kovacs 2017; Sasaki et al. 2001) and mature astrocytes in neuroinflammation (Li et al. 2020; Sofroniew and Vinters 2010), respectively. The transcription factor Nrf2 is a master regulator of cellular responses to oxidants via its activation of oxidative stress response genes including HO-1. Both Nrf2 and HO-1 are implicated in neurotoxicity and neurodegenerative diseases including AD (Kanninen et al. 2009; Sandberg et al. 2014; Schipper et al. 2019). For the analysis of these markers, cortex brain tissues were homogenized in ~5 volumes of ice-cold RIPA buffer for 2 h in a potter tissue grinder. The total protein level was evaluated with the BCA kit (Thermo) according to the manufactures protocol. Equal amounts of protein (50 µg) were loaded on a 4-12% precast NUPAGE gel (Invitrogen) and separated at 180 V in a Mini-PROTEAN II tank (BIO-RAD). The proteins were blotted at 250 mA for 45 min in a Mini Trans-Blot tank (BIO-RAD) on a 0.45 µm pore diameter nitrocellulose transfer membrane (Whatman, Schleicher & Schuell). With 5% milk in PBS-T (0.01 M PBS and 0.05 % Tween-20) unspecific protein bounds were blocked for 60 min. After the blocking, the membrane was incubated with the primary antibody: GFAP (Cat No. ab7260, Abcam, 1:5000), Iba-1 (Cat No. GTX100042, Gentex, 1:1000), HO-1 (Cat No. AB1284, Merck, 1:1000), Nrf2 (C-20) (Cat No. sc-722, Santa Cruz,1:500) overnight at 4°C. Next day, secondary hrp-conjugated antibody and β-Actin-hrp (AC-15) (Cat No. A384, Sigma,1:50000) was incubated for 1 h at room temperature. Detection of proteins was performed with ECL solution (GE Healthcare) and visualized with CHEMI Premium Imager (VWR). With the use of ImageJ software (National Institutes of Health, Bethesda, USA) quantification of protein expression was evaluated relative to β-actin protein level.

4.3.7 **Statistical analyses.**

Data were analysed using IBM-SPSS (version 22) and are expressed as mean ± SEM unless stated otherwise. Data were evaluated by one-way analysis of variance (ANOVA) with Dunnett post-hoc analysis using the air exposed animals as statistical control group. Differences were considered statistically significant at $p < 0.05$.

4.4 Results

4.4.1 Exposure conditions.

Detailed characteristics of NPs and their particle size distributions, mass and number exposure concentrations as well as lung deposited dose estimations for the inhalations are described in detail elsewhere (Dekkers et al. 2017; Dekkers et al. 2018). Briefly, the different CeO_2 particles had a primary particle size of 4.7 ± 1.4 nm. The gravimetric mass concentrations and size distribution of the aerosols were almost identical for the exposures to the CeO_2, 27% Zr-doped CeO_2 and 78% Zr-doped CeO_2 NPs.

4.4.2 Effects on motor activity and cognitive function.

The effect of exposure to redox-modified CeO_2 NPs on the behaviour of the mice was determined using the string suspension test and the X-maze test. The string suspension task was used to assess for motor activity, where mice were allowed to grasp a cotton string stretched between two vertical poles and the ability of the animals to cling on and move to one of the platforms on top of the poles within 60 seconds was measured and scored. Results are shown in Figure 4.1.

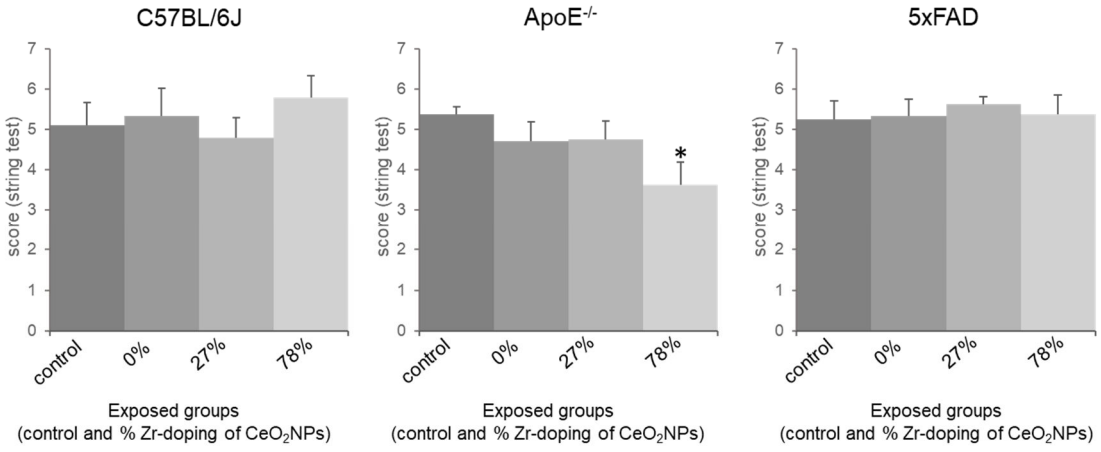

Figure 4.1: Effects of redox-modified CeO_2 on performance in the string suspension task. Female C57BL/6J (A), ApoE-/- (B) and 5xFAD (C) mice were exposed to clean air (control) or CeO_2 and 27% ZrO_2-doped CeO_2 or 78% ZrO_2-doped CeO_2 NPs via inhalation. The ability of the mice to escape to a platform within 60 seconds was measured and transferred to a rating system from 0 to 7 whereby a higher score represents a better performance. Data are expressed in mean ± SEM, *statistical significantly different from the respective control in Dunnet post-hoc test following one-way ANOVA with $p<0.05$. Number of animals per group: $ApoE^{-/-}$: control (n=8); CeO_2 (n=7); 27% ZrO_2-doped CeO_2 (n=8); 78% ZrO_2-doped CeO_2 (n=8). 5XFAD: control (n=16); CeO_2 (n=14); 27% ZrO_2-doped CeO_2 (n=16); 78% ZrO_2-doped CeO_2 (n=16). C57/Bl6J control (n=10); CeO_2 (n=10); 27% ZrO_2-doped CeO_2 (n=10); 78% ZrO_2-doped CeO_2 (n=10).

There was no significant difference in test performance between the controls (clean air exposed mice) of the three different strains. Exposure of the mice with the distinct CeO_2 NPs did not affect the performance of the C57BL/6J mice and the 5xFAD transgenic mice in the string suspension task. However, among the $ApoE^{-/-}$ mice the string suspension test performance was diminished in the group that was exposed to the 78% Zr-doped CeO_2 NPs compared to controls, indicative of an adverse impact on the motor function (Fig. 4.1). The inhalation exposures to the CeO_2 NPs that contained less (27%) or no (0%) Zr did not significantly alter the behaviour of the $ApoE^{-/-}$ mice in the string suspension test in comparison to the clean air exposed animals.

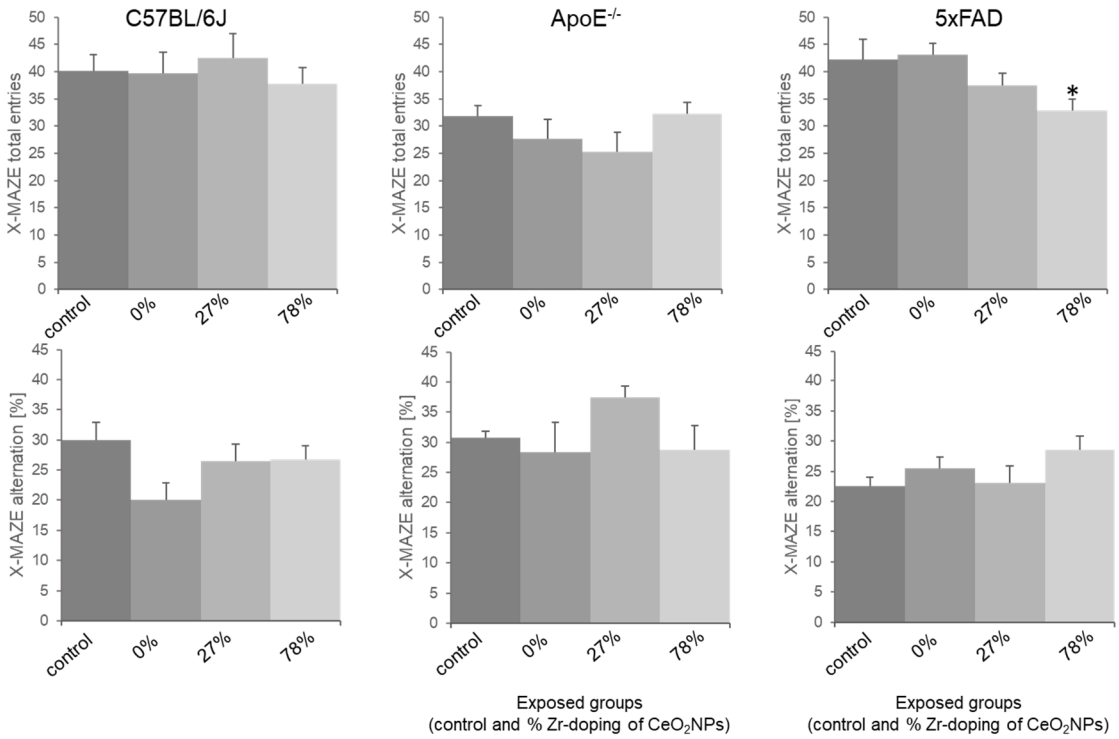

Figure 4.2: Effects of redox-modified CeO2 on performance in the X-maze task. Female C57BL/6J (A, D), ApoE-/- (B, E) and 5xFAD (C, F) mice were exposed to clean air (control) or CeO_2 and 27% ZrO_2-doped CeO_2 or 78% ZrO_2-doped CeO_2 NPs via inhalation. After this treatment, the differently exposed groups were subjected to the X-maze task. Mice were place in the maze for 5 minutes. The behavioural parameters analysed were total arm entries (A, B, C) and alternation (D, E, F) and expressed in mean ± SEM. *Statistical significance different from the respective control in Dunnet post-hoc test following one-way ANOVA with $p<0.05$. Number of animals per group: ApoE-/-: control (n=8); CeO_2 (n=7); 27% ZrO_2-doped CeO_2 (n=8); 78% ZrO_2-doped CeO_2 (n=8). 5XFAD: control (n=16); CeO2 (n=15); 27% ZrO_2-doped CeO_2 (n=16); 78% ZrO_2-doped CeO_2 (n=16). C57/Bl6J: control (n=10); CeO_2 (n=10); 27% ZrO_2-doped CeO_2 (n=10); 78% ZrO_2-doped CeO_2 (n=10).

The X-maze task was performed to assess for locomotor activity and spatial working memory of the mice in relation to the different inhalation exposures. The results of these investigations are shown in Figure 4.2. In contrast to the string suspension test, for this task some differences were already noted between the controls (clean air) of the different mouse models. On the one hand, for the $ApoE^{-/-}$ control group the total number of arm entries tended to be lower than for

the C57BL/6J and 5xFAD controls. On the other hand, the alternation (%) in the test tended to be lower for the 5xFAD control mice in comparison to the C57BL/6J and ApoE$^{-/-}$ controls. However, in both cases the observed differences were not statistically significant.

In concordance with the string suspension task, the X-maze test also revealed a significant effect on behaviour following inhalation exposure to the 78% Zr-doped CeO_2 NPs, whereas the other types of NPs showed no effects. In this case, however, the effect was seen in the 5xFAD mouse model: The 5xFAD mice that had been exposed to the 78% Zr-doped CeO_2 NPs showed a significantly reduced number of total arm entries compared to the control 5xFAD mice, indicative of a decreased exploratory motor activity for this treatment group (Figure 4.2). However, the alternation in the X-maze task, which is an indicator of the spatial working memory of mice, did not differ between these groups. In fact, the alternation percentage among the 5xFAD groups tended to be highest in the 78% Zr-doped CeO_2 NPs. In the ApoE$^{-/-}$ and C57BL/6J mice, no significant treatment-related effects on locomotor activity and spatial working memory were found with the X-maze testing.

4.4.3 **Effects on Aβ plaque formation and markers of neuroinflammation and oxidative stress**

Histopathologically, AD is characterized by the presence of extracellular senile plaques and intracellular neurofibrillary tangles (Beyreuther and Masters 1991; Selkoe 2001b). To investigate the impact of the exposure to different redox-modified CeO_2 NPs on the level of Aβ plaque formation, parasagittal brain slices of the 5xFAD mice were stained with an antibody against human Aβ42, and the Aβ plaque load was determined in hippocampus and cortex. The results of this analysis are shown in Figure 4.3. There were no significant differences in plaque formation between the different treatment groups: the inhalation exposures to NPs, irrespective of their redox modification, did not result in an acceleration of the Aβ plaque formation in this transgenic mouse model of AD.

To determine whether the inhalation of redox-modified CeO_2 NPs affect the level of neuroinflammation in the brains of the 5xFAD mice, the amount of Iba-1 positive microglia cells was assessed in the same brain regions using immunohistochemical analysis. Compared to the clean air exposed 5xFAD mice, the number of activated Iba1-positive microglia cells was not significantly altered in the brain of NPs treated 5xFAD mice (Fig. 4.4).

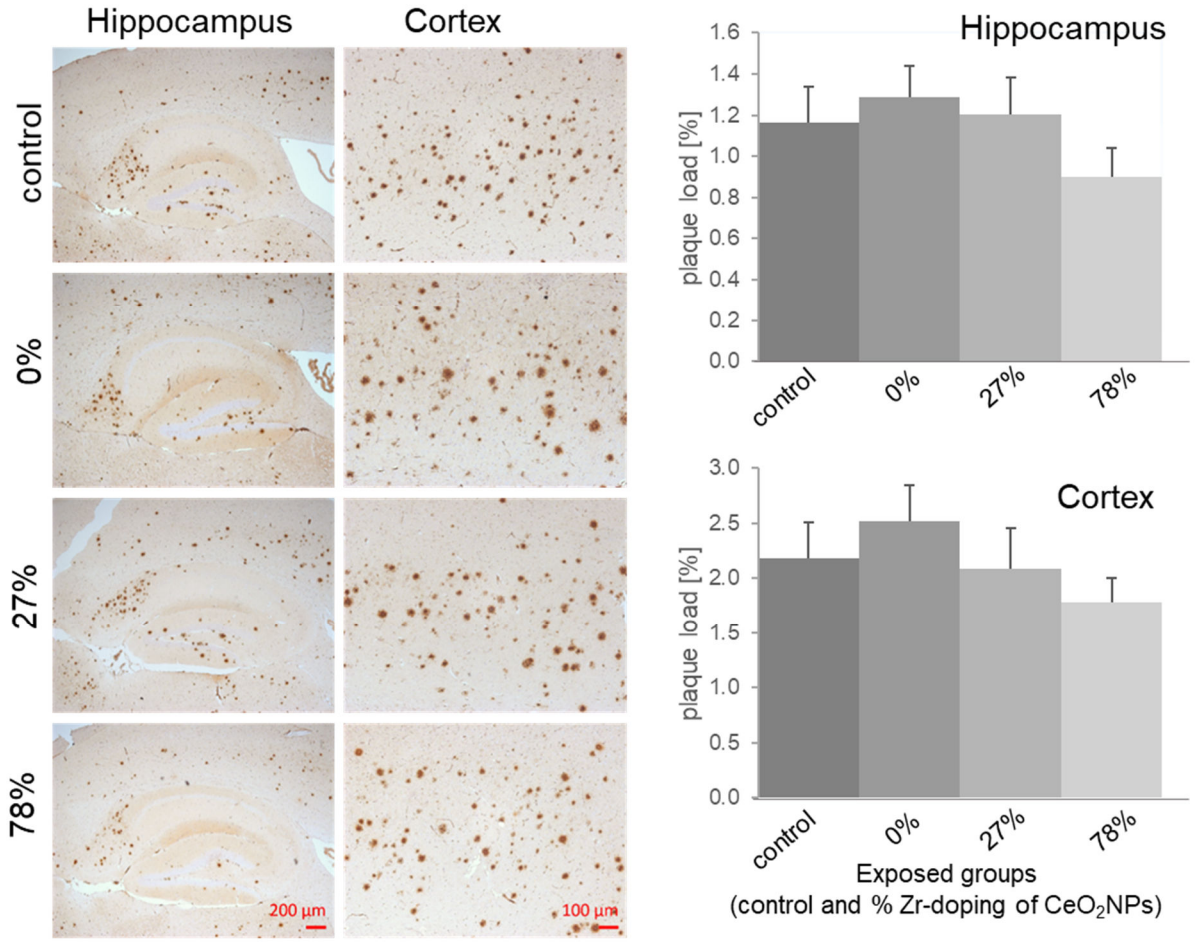

Figure 4.3: Effect of redox-modified CeO_2 NPs inhalation on β-Amyloid pathology in 5xFAD mice. Aβ plaque load was determined in parasagittal brain slices of 5xFAD mice after exposure to clean air (control n=16), CeO_2 (n=15), 27% ZrO_2-doped CeO_2 (n=16) or 78% ZrO_2-doped CeO_2 (n=16) NPs. Aβ42 was visualized by IHC in 4 µm sections of paraffin-embedded brain hemispheres (Representative pictures are shown in A). For quantification, plaque load was determined in the hippocampus (B) and in the cortex (C) using image analysis software and calculated as the percentage area occupied by Aβ immunostaining expressed in mean ± SEM. For determination of plaques in the cortex, whole image sections were evaluated while the hippocampus regions were defined by hand to evaluate only the hippocampus. A trend was observed of reduced Aβ plaques in the brains of mice exposed to the 78% Zr-doped CeO2 NPs, but this effect was not statistically significant.

To further evaluate the potential effect of the different redox-modified CeO_2 NPs on neuroinflammation and oxidative stress, cortical brain tissues of all three mouse models were analysed by Western blotting for the expression of Iba-1 and GFAP as well as Nrf2 and HO-1, respectively. Results for Iba-1 and GFAP are shown in Figure 4.5.

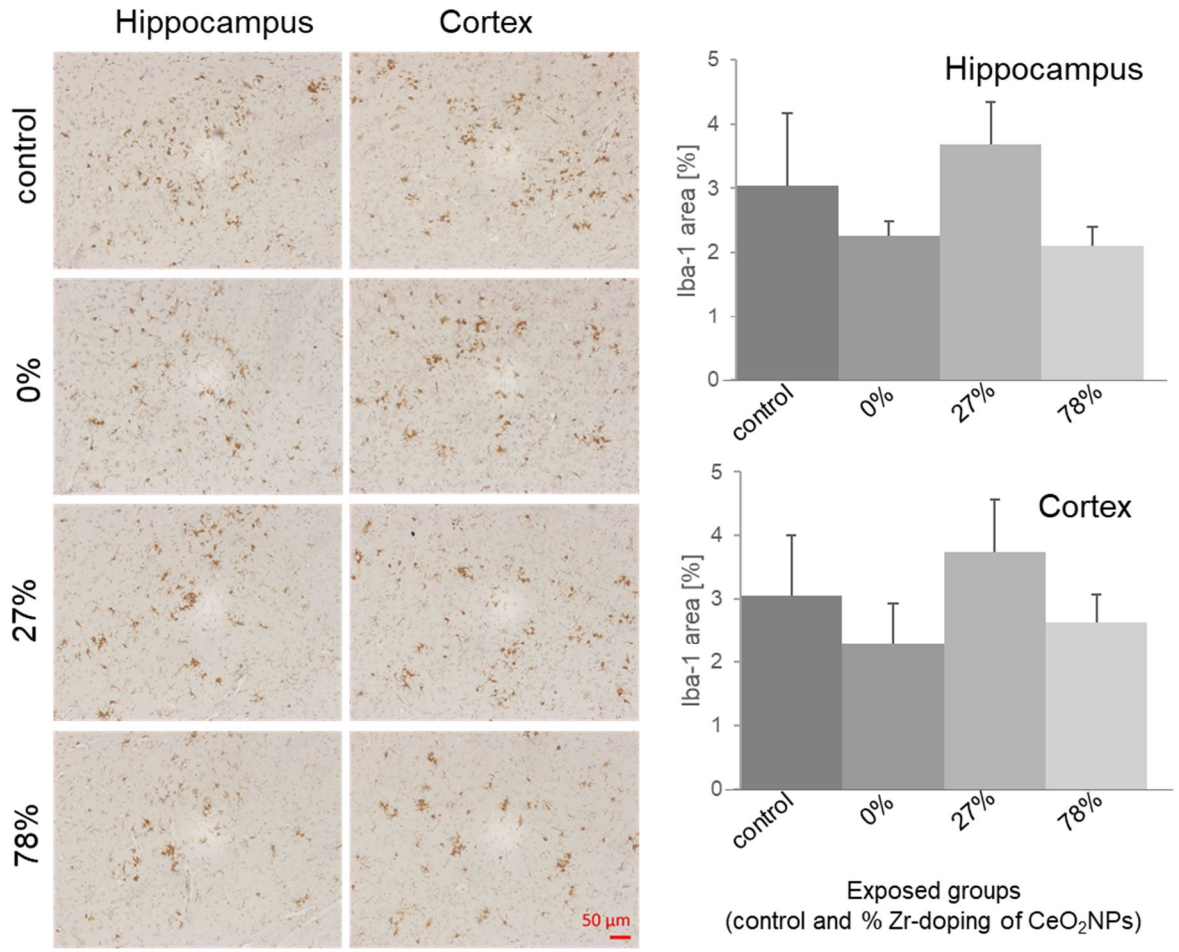

Figure 4.4: Effect of redox-modified CeO_2 NP inhalation on Iba-1 immunostaining in hippocampus and cortex of 5xFAD mice. Parasagittal brain slices of 5xFAD mice exposed to clean air of CeO_2 NPs with different doping of Zr (n=6 per group), were stained with an antibody against Iba-1 to detect activated microglia (representative pictures are shown in A). For quantification, Iba-1 stain was determined in (B) CA1/subiculum of the hippocampus (200-fold microscopic magnification) and (C) cortex layer 5 (200-fold microscopic magnification) using image analysis software and calculated as the percentage area occupied by Iba-1 immunostaining and expressed in mean ± SEM.

As can be seen in the Figure, the Western blot analyses for Iba-1 confirmed the absence of treatment-related changes in abundance of Iba-1 positive microglia cells in the 5xFAD mice by immunohistochemistry: No significant differences Iba-1 protein levels were detected in the 5xFAD mice in association with the CeO_2 inhalation exposures. Likewise, the protein levels of Iba-1 were not significantly altered in the brains of the C57BL/6J and ApoE$^{-/-}$ mice. Next, the protein level of the astrocyte marker GFAP was analysed. In the ApoE$^{-/-}$ and 5xFAD mice, no treatment related effects on GFAP protein level could be observed. Interestingly, however, the C57BL/6J mice exposed to the 78% Zr-doped CeO_2 NPs displayed significant higher GFAP levels whereas inhalation of both other types of NPs showed no effect.

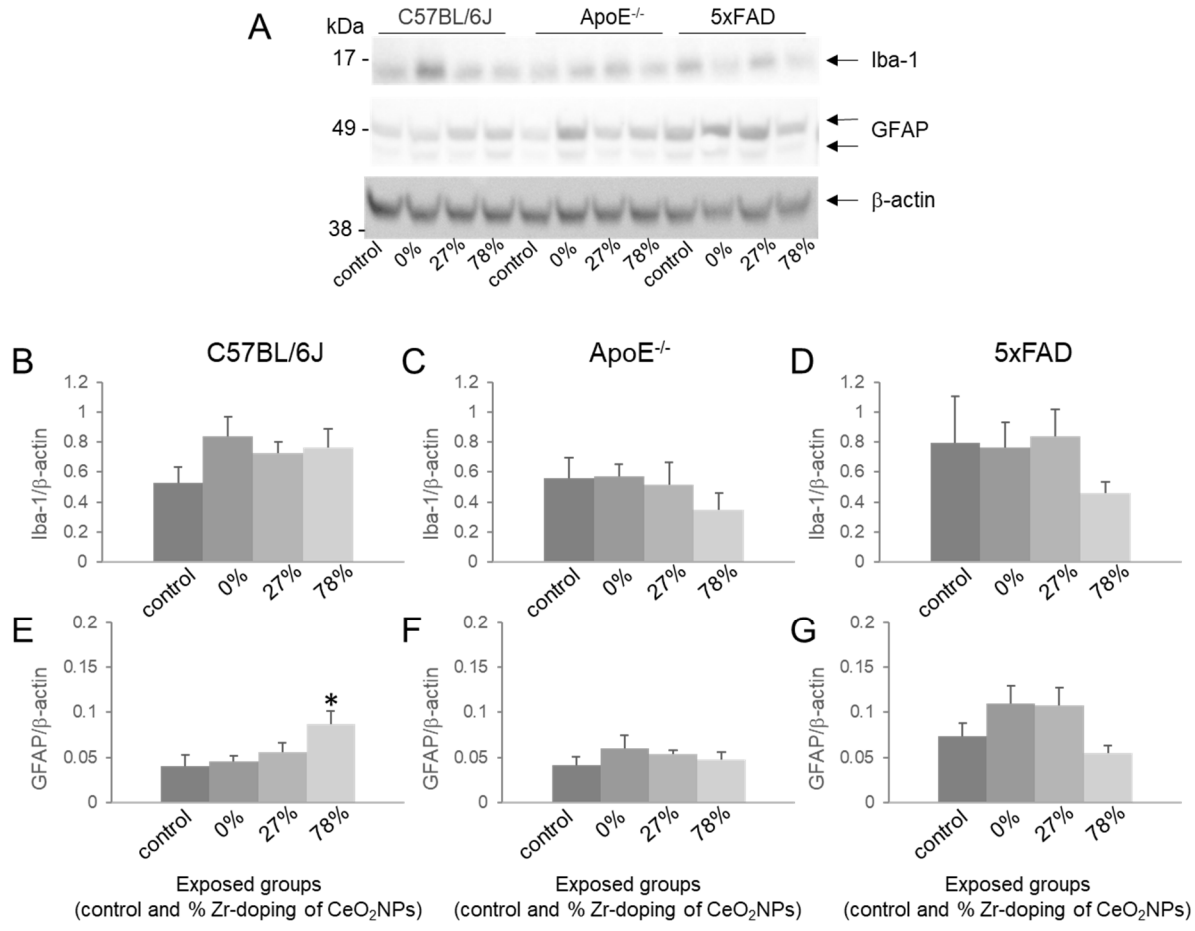

Figure 4.5: Effect of redox-modified CeO_2 NP inhalation on Iba-1 and GFAP protein levels. Levels of Iba-1 (B, C, D) and GFAP (E, F, G) were assessed by Western blot analysis in lysates of the cortex of female C57BL/6J (B, E), ApoE-/- (C, F) and 5xFAD (D, G) exposed to clean air or CeO_2 NPs with different doping of Zr (representative blots are shown in A). Data were normalized to the level of β-actin and expressed in mean ± SEM. * Statistical significance different from the respective control in Dunnet post-hoc test following one-way ANOVA with $p<0.05$. Number of animals per group: ApoE$^{-/-}$: control (n=5); CeO_2 (n=5); 27% ZrO_2-doped CeO_2 (n=5); 78% ZrO_2-doped CeO_2 (n=4). 5XFAD: control (n=4); CeO_2 (n=4); 27% ZrO_2-doped CeO_2 (n=4); 78% ZrO_2-doped CeO_2 (n=4). C57/Bl6J: control (n=5); CeO_2 (n=5); 27% ZrO_2-doped CeO_2 (n=5); 78% ZrO_2-doped CeO_2 (n=5).

The effect of exposure to redox-modified CeO_2 NPs on the protein expressions of Nrf2 and its downstream target HO-1 are shown in Figure 4.6. Inhalation exposure to the NPs, irrespective of their redox-modification, did not affect the level of Nrf2 or HO-1 in the brains of C57BL/6J, $ApoE^{-/-}$ and 5xFAD mice (Fig. 4.6). In the 5xFAD mice, a tendency of increasing Nrf2 protein levels with increased Zr-doping was noted suggestive of increasing oxidative stress response. However, the observed differences were not statistically significant and were also not further substantiated by the HO-1 findings for the same mice.

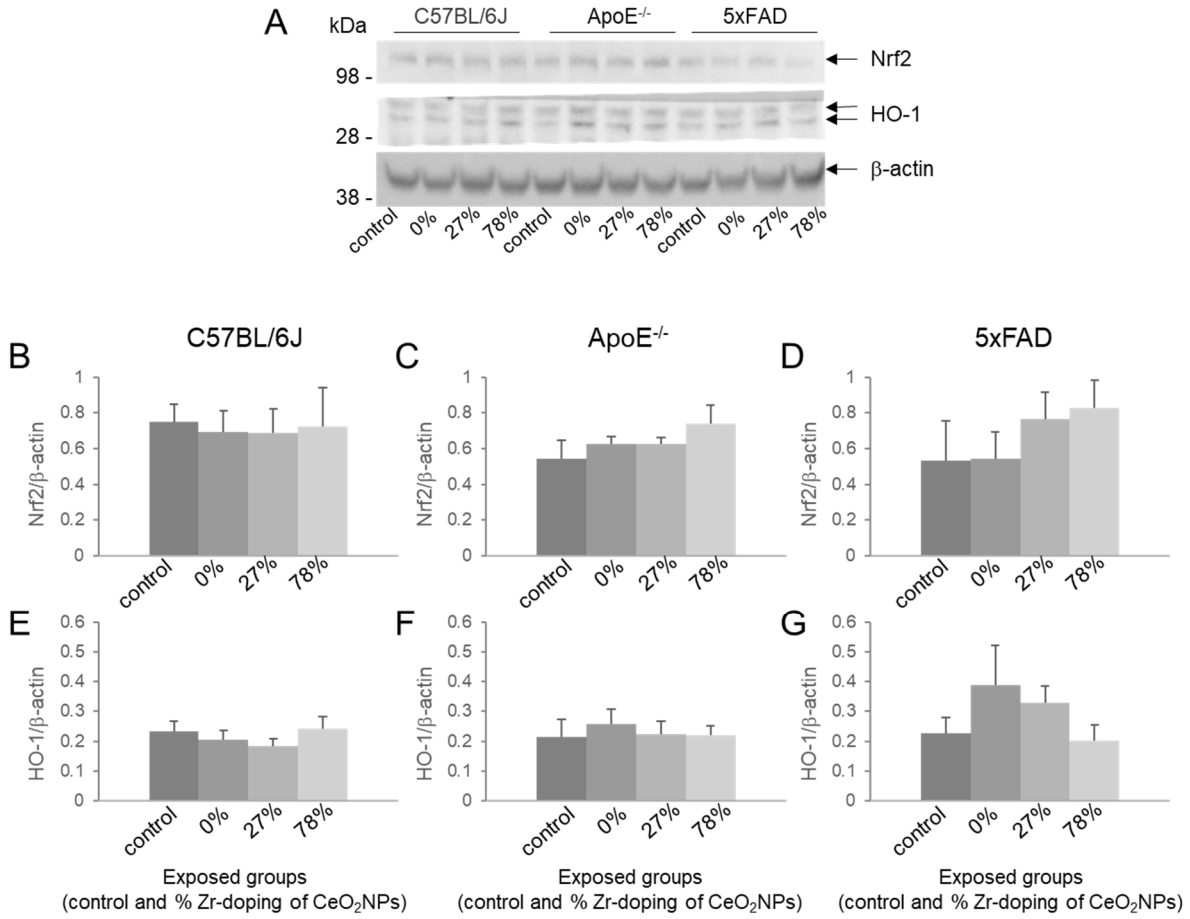

Figure 4.6: Effect of redox-modified CeO_2 NP inhalation on Nrf2 and HO-1 protein levels. Lysates of the cortex of C57BL/6J (B, E), ApoE-/- (C, F) and 5xFAD (D, G) mice exposed to clean air or CeO_2 NPs with different doping of Zr were subjected to Western Blot analysis. Levels of Nrf2 (B, C, D) and HO-1 (E, F, G) were normalized to the level of β-actin and expressed in mean ± SEM. Representative blots are shown in A. Number of animals per group: $ApoE^{-/-}$: control (n=5); CeO_2 (n=5); 27% ZrO_2-doped CeO_2 (n=5); 78% ZrO_2-doped CeO_2 (n=4). 5XFAD: control (n=4); CeO_2 (n=4); 27% ZrO_2-doped CeO_2 (n=4); 78% ZrO_2-doped CeO_2 (n=4). C57/Bl6J: control (n=5); CeO_2 (n=5); 27% ZrO_2-doped CeO_2 (n=5); 78% ZrO_2-doped CeO_2 (n=5).

4.5 Discussion

The experiments performed in this study formed part of a large study to assess the influence of redox activity on the toxicity of inhaled CeO_2 NPs in mice, by comparison of the effects of different quantities of Zr-doping. Detailed physicochemical and exposure characteristics of the

NPs as well as the pulmonary and cardiovascular findings in the exposed mice have been published in a separate paper (Dekkers et al. 2017). In all three mouse models (C57BL/6J, 5xFAD, ApoE$^{-/-}$) the four-week inhalation exposures were without any major toxicological effects in the lungs. In the ApoE$^{-/-}$ mouse model of vascular disease, the inhalation exposures to the NPs did not cause a statistically significant change in the overall size of atherosclerotic plaques. However, there was a trend towards an increased inflammatory cell content (i.e. macrophage-derived foam cells) in the plaques with the inhalation of CeO_2 NPs with increasing ZrO_2 content (Dekkers et al. 2017).

In the present study, we evaluated whether inhalation exposure to these NPs could also cause neurotoxicity and promote AD. Therefore, mouse behaviour tests were performed in all the three mouse models to explore effects on motor activity and cognitive function. Brain tissue protein levels of HO-1, Nrf2, Iba-1 and GFAP were measured to address the role of oxidative stress and neuroinflammation. The potential effects of the inhaled CeO_2 NPs on amyloid-β plaque formation were assed in the 5xFAD mouse model. In this study, we could observe specific effects that were dependent on the mouse model as well as the NP modification. While the behaviour effects were observed in both compromised mouse models, increase protein levels of GFAP were found only in the healthy C57BL/6J mice. These significant effects were observed exclusively for the CeO_2 NPs that were doped with the highest amount of Zr (78%). In the ApoE$^{-/-}$ mice, the four-week inhalation exposure to these specific NPs resulted in a significantly diminished performance in the string suspension test. Such effect could be an indication of a greater susceptibility to an impaired forced motor performance in this mouse model of vascular disease. In the 5xFAD mice, the exposure to the 78% Zr-doped CeO_2 NPs resulted in a significant reduction of the total of arm entries in the X-maze task. This latter effect suggests a possible reduction in explorative locomotor activity for this mouse model of AD. However, alternation behaviour in the X-maze test, which is an indicator of cognitive performance, was not impaired in same treatment group.

Interestingly, while the motor performance effects on behaviour were observed with the two disease models, no behavioural effects were seen in the healthy (C57BL/6J) mice. Rodent models of susceptibility and disease are being increasingly used in toxicological studies exploring air pollution to better understand the underlying mechanisms (Oberdorster, Oberdorster, and Oberdorster 2005; Stone et al. 2017). In line with our present findings with the Zr-doped CeO_2 NPs, impaired motor performance was observed following diesel engine exhaust inhalation exposure in 5xFAD mice but not in their wildtype littermates (Hullmann et al. 2017a). Studies with diesel exhaust particles in high-fat fed ApoE deficient mice have also

demonstrated the value of this susceptibility model over wildtype mice to support the epidemiological evidence that links exposure to airborne particles to cardiovascular disease (Miller et al. 2013). Interestingly, the behaviour changes in the two compromised mouse models were exclusively seen with the highest Zr-doped CeO_2, indicating that these effects appear to depend on the redox-activity of the inhaled NPs. The introduction of Zr into the crystalline structure of CeO_2 NPs is considered to enhance their antioxidant properties (Tsai et al. 2008). As such, one would have expected a possibly protective effect for the undoped CeO_2 NPs. However, our present findings are in line with the previously reported effects of the inhalation exposures on the inflammatory content of atherosclerotic plaques in the $ApoE^{-/-}$ mice, which revealed an increased presence of macrophage-derived foam cells for CeO_2 NPs with increasing Zr content (Dekkers et al. 2017).

Behaviour tests form an important component of neurotoxicity testing (Moser 2011; OECD 1997). It is therefore tempting to speculate that the observed motor performance effects in the $ApoE^{-/-}$ and 5xFAD mice result from a direct neurotoxic effect of the high Zr-doped CeO_2 NPs. Indeed, several studies that have explored the pulmonary toxicity of NPs, including CeO_2, indicate that their adverse effects are driven by oxidative stress and inflammation (Unfried et al. 2008; Morimoto et al. 2016; Stone et al. 2017; Schwotzer et al. 2018). However, in our present inhalation study we found no significant treatment related changes in HO-1 or Nrf2 for all three mouse models. In contrast, Hardas and colleagues observed increased HO-1 in rat brain upon intravenous administration of CeO_2 NPs (Hardas et al. 2014). The fundamental differences in exposure route and dose offer a plausible explanation for these contrasts. The brains of $ApoE^{-/-}$ and 5xFAD mice in our inhalation study also did not display significant treatment related changes in protein levels of Iba-1 and GFAP, even for the groups that were exposed to the 78% Zr-doped CeO_2 NPs. Taken together, this suggests that the motor function effects which we observed in both compromised mouse models were not mediated by local oxidative stress and neuroinflammation.

Surprisingly, however, increased protein levels of GFAP were observed in the cortex of the healthy C57BL/6J mice, the only mouse model that did not show significant changes in (motor function) behaviour. On the one hand, this adds further support to the absence of a mechanistic link between neuroinflammation and motor activity changes for inhaled CeO_2 NPs. On the other hand, the finding again indicates the importance of the redox-properties of CeO_2 NPs, as the effect on GFAP was only seen with the particles that were doped with the highest amount of Zr (78%). Increased GFAP levels were previously also found in rat brain following repeated inhalation exposures to steel welding fumes (Antonini et al. 2009). In contrast to our

findings, increased GFAP levels were observed in ApoE$^{-/-}$ mice after long term inhalation of ambient ultrafine particles (Kleinman et al. 2008). In another study with in C57BL/6 mice, the long term inhalation of fine (µm size mode) ambient particulate matter ($PM_{2.5}$) did not cause significant changes in brain levels of GFAP and Iba-1 (Bhatt et al. 2015).

The ApoE$^{-/-}$ mice were selected *a priori* for the investigation of cardiovascular effects following NP inhalation exposure, however, due to the logistical requirements of the extensive tissue collection, we were unable the further evaluate the brain tissue from these mice by immunohistochemistry (Dekkers et al. 2017). However, the brains of the 5xFAD mice were prioritised to address the potential impact of (undoped and Zr-doped) CeO_2 NPs on the development of the neurodegenerative processes. Previously, we demonstrated an accelerated amyloid plaque load formation (whole brain Aβ42 protein levels) in 15 week old female 5xFAD mice following a three-week diesel engine exhaust inhalation exposure (0.95 mg/m^3, 6 h/day, 5 days/week) (Hullmann et al. 2017a). In the present study, however, we did not observe a significant alteration in the β-amyloid pathology in the brains of 5xFAD animals following four-week inhalation exposure to the (Zr-doped) CeO_2 NPs (4 mg/m^3 for 3 h/day, 5 days/week). Moreover, in alignment with the Western blot findings, the brains of the 5xFAD mice did not reveal significant differences in immunostaining of Iba-1. Combined with the observed absence of (cognitive) behaviour changes in the 5xFAD mice, these data argue against the hypothesis that CeO_2 NPs may promote AD pathology in association with their redox-activity. The motor performance changes observed to NPs in the ApoE$^{-/-}$ and 5xFAD mice may not necessarily be related to a direct neurotoxic effect in isolation, but instead due to indirect effects, or alternatively, a result of an interaction between the exposure and increased susceptibility of both disease models. Age related changes in motor performance are well-described in the 5xFAD mouse model (Jawhar et al. 2012; O'Leary, Mantolino, et al. 2018) and have also been reported for the ApoE$^{-/-}$ mice (Raber et al. 2000; Zerbi et al. 2014). Importantly, however, we did not observe statistically significant differences in behaviour test performance of the (clean air exposed) control mice between the three different mouse modes. This indicates that there was no major behaviour impairment *per se* in the two mouse disease models, and also suggests that it is unlikely that the effects of NPs on ApoE$^{-/-}$ mice were principally due to the high-fat diet fed to the mice. Further research is needed to verify the potential adverse impact of inhaled CeO_2 NPs on motor function and to unravel the mechanism that could explain the redox-involvement for these metal oxide NPs.

Up to now, there is only very limited data about the potential neurotoxic effects of CeO_2 NPs in association with inhalation exposure. A recent study showed that female ICR mice

exposed to CeO_2 particles (intranasal instillation, daily dose of 40 mg/kg body weight) of varying sizes (i.e. 35 nm, 300 nm and >1 μm) displayed significantly increased GFAP expression in the hippocampus and olfactory bulb. The authors claim that intranasal instillation of CeO_2 particles induced damage within the olfactory bulb and hippocampus, but that particle size does not play a major role in the observed adverse responses (Liu et al. 2016). Nemmar and colleagues reported increased levels of the inflammatory cytokine Tumor Necrosis Factor-α, reactive oxygen species and DNA damage in the brains of mice by CeO_2 NPs, 24 hours after a single intratracheal instillation (0.5 mg/kg) (Nemmar et al. 2017). However, for the aforementioned studies the observed effects require perspective on the method and site of administration in the respiratory tract for the CeO_2 particles, when compared to the outcomes of our present controlled inhalation exposure study. This relates to the obvious differences in dose and dose-rate of the NPs (i.e. bolus application *versus* inhalation) as well as to the regional deposition in the respiratory tract organ (i.e. nasal *versus* alveolar).

Conclusions. We have investigated the neurological effects of redox-modified CeO_2 NPs using varying levels of Zr-doping (0 %, 27% and 78%), after four-week inhalation exposures in three different mouse models. Our study findings reveal that the subacute inhalation exposure to CeO_2 NPs did not cause major cognitive behavioural impairments in mice or promote amyloid-β plaque formation and neuroinflammation in the 5xFAD transgenic mouse model of AD. However, motor performance changes were observed both in the 5xFAD and $ApoE^{-/-}$ mice for the CeO_2 NPs that were doped with the highest amount of Zr. In healthy C57BL/6J mice, the same particles caused increased GFAP levels in the absence of behaviour changes. The observed behavioural effects in the two compromised models were not substantiated further by changes in markers of neuroinflammation and oxidative stress. Therefore, further investigations are warranted to unravel the mechanism whereby inhaled CeO_2 NPs can affect motor activity in a redox activity dependent manner.

ACKNOWLEDGEMENTS

We thank Mike Russ and Promethean Particles Ltd, Nottingham, United Kingdom with regard to the preparation of the nanoparticles used in this study and Julia Kolling, Christel Weishaupt, Gabriele Wick and Petra Gross (IUF Düsseldorf) as well as John A. Boere, Paul H. Fokkens and Daan L.A.C. Leseman (RIVM) for technical support. We also thank Éva Valsami-Jones (University of Birmingham, UK; coordinator of the NanoMILE project) and Wim De Jong (RIVM) for their fruitful scientific discussions and support.

FUNDING

The work leading to these results has received funding from the European Union Seventh Framework Programme for research, technology development and demonstration [grant agreement no. 310451 (NanoMILE)] and the Netherlands Food and Consumer Product Safety Authority (NVWA). MRM is supported by the British Heart Foundation [SP/15/8/31575; CH/09/002].

4.6 References

Alvarino, R., E. Alonso, R. Lacret, D. Oves-Costales, O. Genilloud, F. Reyes, A. Alfonso, and L. M. Botana. 2019. 'Caniferolide A, a Macrolide from Streptomyces caniferus, Attenuates Neuroinflammation, Oxidative Stress, Amyloid-Beta, and Tau Pathology in Vitro', *Mol Pharm*.

Antonini, James M., Krishnan Sriram, Stanley A. Benkovic, Jenny R. Roberts, Samuel Stone, Bean T. Chen, Diane Schwegler-Berry, Amy M. Jefferson, Brenda K. Billig, Christopher M. Felton, Mary Ann Hammer, Fang Ma, David G. Frazer, James P. O'Callaghan, and Diane B. Miller. 2009. 'Mild steel welding fume causes manganese accumulation and subtle neuroinflammatory changes but not overt neuronal damage in discrete brain regions of rats after short-term inhalation exposure', *NeuroToxicology*, 30: 915-25.

Arnaiz, E., and O. Almkvist. 2003. 'Neuropsychological features of mild cognitive impairment and preclinical Alzheimer's disease', *Acta Neurol Scand Suppl*, 179: 34-41.

Arnold S, Hyman B, Flory J, Damasio A, Van Hoesen G. 1991. 'The topographical and neuroanatomical distribution of neurofibrillary tangles and neuritc plaques in the cerebral cortex of patients with Alzheimer´s disease', *Cereb Cortex*: 103-06.

Baghirov, H., D. Karaman, T. Viitala, A. Duchanoy, Y. R. Lou, V. Mamaeva, E. Pryazhnikov, L. Khiroug, C. de Lange Davies, C. Sahlgren, and J. M. Rosenholm. 2016. 'Feasibility Study of the Permeability and Uptake of Mesoporous Silica Nanoparticles across the Blood-Brain Barrier', *PLoS ONE*, 11: e0160705.

Beyreuther, K., and C. L. Masters. 1991. 'Amyloid precursor protein (APP) and beta A4 amyloid in the etiology of Alzheimer's disease: precursor-product relationships in the derangement of neuronal function', *Brain Pathol*, 1: 241-51.

Bhatt, Dhaval P., Kendra L. Puig, Matthew W. Gorr, Loren E. Wold, and Colin K. Combs. 2015. 'A pilot study to assess effects of long-term inhalation of airborne particulate matter on early Alzheimer-like changes in the mouse brain', *PLoS ONE*, 10: e0127102-e02.

Block, M. L. 2008. 'NADPH oxidase as a therapeutic target in Alzheimer's disease', *BMC Neurosci*, 9 Suppl 2: S8.

Block, M. L., and L. Calderon-Garciduenas. 2009. 'Air pollution: mechanisms of neuroinflammation and CNS disease', *Trends Neurosci*, 32: 506-16.

Blyth, Brian J., Arash Farhavar, Christopher Gee, Brendan Hawthorn, Hua He, Akshata Nayak, Veit Stöcklein, and Jeffrey J. Bazarian. 2009. 'Validation of serum markers for blood-brain barrier disruption in traumatic brain injury', *Journal of neurotrauma*, 26: 1497-507.

Bouwmeester, H., S. Dekkers, M. Y. Noordam, W. I. Hagens, A. S. Bulder, C. de Heer, S. E. ten Voorde, S. W. Wijnhoven, H. J. Marvin, and A. J. Sips. 2009. 'Review of health safety aspects of nanotechnologies in food production', *Regul Toxicol Pharmacol*, 53: 52-62.

Brinch, Anna, Steffen Foss Hansen, Nanna B. Hartmann, and Anders Baun. 2016. 'EU Regulation of Nanobiocides: Challenges in Implementing the Biocidal Product Regulation (BPR)', *Nanomaterials (Basel, Switzerland)*, 6: 33.

Calzolai, L., D. Gilliland, and F. Rossi. 2012. 'Measuring nanoparticles size distribution in food and consumer products: a review', *Food Addit Contam Part A Chem Anal Control Expo Risk Assess*, 29: 1183-93.

Cassee, F. R., A. Campbell, A. J. Boere, S. G. McLean, R. Duffin, P. Krystek, I. Gosens, and M. R. Miller. 2012. 'The biological effects of subacute inhalation of diesel exhaust

following addition of cerium oxide nanoparticles in atherosclerosis-prone mice', *Environ Res*, 115: 1-10.

Cassee, F. R., E. C. van Balen, C. Singh, D. Green, H. Muijser, J. Weinstein, and K. Dreher. 2011a. 'Exposure, health and ecological effects review of engineered nanoscale cerium and cerium oxide associated with its use as a fuel additive', *Crit Rev Toxicol*, 41: 213-29.

Cassee, Flemming R., Erna C. van Balen, Charanjeet Singh, David Green, Hans Muijser, Jason Weinstein, and Kevin Dreher. 2011b. 'Exposure, Health and Ecological Effects Review of Engineered Nanoscale Cerium and Cerium Oxide Associated with its Use as a Fuel Additive', *Critical Reviews in Toxicology*, 41: 213-29.

Chin-Chan, Miguel, Juliana Navarro-Yepes, and Betzabet Quintanilla-Vega. 2015. 'Environmental pollutants as risk factors for neurodegenerative disorders: Alzheimer and Parkinson diseases', *Frontiers in cellular neuroscience*, 9: 124-24.

Coppede, F., and L. Migliore. 2010. 'Evidence linking genetics, environment, and epigenetics to impaired DNA repair in Alzheimer's disease', *J Alzheimers Dis*, 20: 953-66.

Cupaioli, F. A., F. A. Zucca, D. Boraschi, and L. Zecca. 2014. 'Engineered nanoparticles. How brain friendly is this new guest?', *Prog Neurobiol*, 119-120: 20-38.

Dahle, Jessica T., and Yuji Arai. 2015. 'Environmental Geochemistry of Cerium: Applications and Toxicology of Cerium Oxide Nanoparticles', *International Journal of Environmental Research and Public Health*, 12: 1253-78.

Das, S., J. M. Dowding, K. E. Klump, J. F. McGinnis, W. Self, and S. Seal. 2013. 'Cerium oxide nanoparticles: applications and prospects in nanomedicine', *Nanomedicine (Lond)*, 8: 1483-508.

Dekkers, S., L. Ma-Hock, I. Lynch, M. Russ, M. R. Miller, R. P. F. Schins, J. Keller, I. Romer, K. Kuttler, V. Strauss, W. H. De Jong, R. Landsiedel, and F. R. Cassee. 2018. 'Differences in the toxicity of cerium dioxide nanomaterials after inhalation can be explained by lung deposition, animal species and nanoforms', *Inhal Toxicol*, 30: 273-86.

Dekkers, S., M. R. Miller, R. P. F. Schins, I. Romer, M. Russ, R. J. Vandebriel, I. Lynch, M. F. Belinga-Desaunay, E. Valsami-Jones, S. P. Connell, I. P. Smith, R. Duffin, J. A. F. Boere, H. J. Heusinkveld, C. Albrecht, W. H. de Jong, and F. R. Cassee. 2017. 'The effect of zirconium doping of cerium dioxide nanoparticles on pulmonary and cardiovascular toxicity and biodistribution in mice after inhalation', *Nanotoxicology*, 11: 794-808.

Demokritou, Philip, Samuel Gass, Georgios Pyrgiotakis, Joel M. Cohen, William Goldsmith, Walt McKinney, David Frazer, Jane Ma, Diane Schwegler-Berry, Joseph Brain, and Vincent Castranova. 2013. 'An in vivo and in vitro toxicological characterisation of realistic nanoscale CeO2 inhalation exposures', *Nanotoxicology*, 7: 1338-50.

Devi, L., M. J. Alldred, S. D. Ginsberg, and M. Ohno. 2010. 'Sex- and brain region-specific acceleration of beta-amyloidogenesis following behavioral stress in a mouse model of Alzheimer's disease', *Mol Brain*, 3: 34.

Dowding, J. M., T. Dosani, A. Kumar, S. Seal, and W. T. Self. 2012. 'Cerium oxide nanoparticles scavenge nitric oxide radical (NO)', *Chem Commun (Camb)*, 48: 4896-8.

Elder, A., R. Gelein, V. Silva, T. Feikert, L. Opanashuk, J. Carter, R. Potter, A. Maynard, Y. Ito, J. Finkelstein, and G. Oberdorster. 2006. 'Translocation of inhaled ultrafine manganese oxide particles to the central nervous system', *Environ Health Perspect*, 114: 1172-8.

Elder, A., and G. Oberdorster. 2006. 'Translocation and effects of ultrafine particles outside of the lung', *Clin Occup Environ Med*, 5: 785-96.

Esch, F., S. Fabris, L. Zhou, T. Montini, C. Africh, P. Fornasiero, G. Comelli, and R. Rosei. 2005. 'Electron localization determines defect formation on ceria substrates', *Science*, 309: 752-5.

Estevez, A. Y., S. Pritchard, K. Harper, J. W. Aston, A. Lynch, J. J. Lucky, J. S. Ludington, P. Chatani, W. P. Mosenthal, J. C. Leiter, S. Andreescu, and J. S. Erlichman. 2011. 'Neuroprotective mechanisms of cerium oxide nanoparticles in a mouse hippocampal brain slice model of ischemia', *Free Radic Biol Med*, 51: 1155-63.

Fandrich, M. 2012. 'Oligomeric intermediates in amyloid formation: structure determination and mechanisms of toxicity', *J Mol Biol*, 421: 427-40.

Flanigan, T. J., Y. Xue, S. Kishan Rao, A. Dhanushkodi, and M. P. McDonald. 2014. 'Abnormal vibrissa-related behavior and loss of barrel field inhibitory neurons in 5xFAD transgenics', *Genes, brain, and behavior*, 13: 488-500.

Forstl, H., and A. Kurz. 1999. 'Clinical features of Alzheimer's disease', *Eur Arch Psychiatry Clin Neurosci*, 249: 288-90.

Gardener, S. L., S. R. Rainey-Smith, and R. N. Martins. 2016. 'Diet and Inflammation in Alzheimer's Disease and Related Chronic Diseases: A Review', *J Alzheimers Dis*, 50: 301-34.

Guan, Yijia, Meng Li, Kai Dong, Nan Gao, Jinsong Ren, Yongchen Zheng, and Xiaogang Qu. 2016. 'Ceria/POMs hybrid nanoparticles as a mimicking metallopeptidase for treatment of neurotoxicity of amyloid-β peptide', *Biomaterials*, 98: 92-102.

Guglielmotto, M., E. Tamagno, and O. Danni. 2009. 'Oxidative stress and hypoxia contribute to Alzheimer's disease pathogenesis: two sides of the same coin', *ScientificWorldJournal*, 9: 781-91.

Hansen, C. S., M. Sheykhzade, P. Moller, J. K. Folkmann, O. Amtorp, T. Jonassen, and S. Loft. 2007. 'Diesel exhaust particles induce endothelial dysfunction in apoE-/- mice', *Toxicol Appl Pharmacol*, 219: 24-32.

Hardas, Sarita S., David Allan Butterfield, Rukhsana Sultana, Michael T. Tseng, Mo Dan, Rebecca L. Florence, Jason M. Unrine, Uschi M. Graham, Peng Wu, Eric A. Grulke, and Robert A. Yokel. 2010. 'Brain Distribution and Toxicological Evaluation of a Systemically Delivered Engineered Nanoscale Ceria', *Toxicological Sciences*, 116: 562-76.

Hardas, Sarita S., Rukhsana Sultana, Govind Warrier, Mo Dan, Peng Wu, Eric A. Grulke, Michael T. Tseng, Jason M. Unrine, Uschi M. Graham, Robert A. Yokel, and D. Allan Butterfield. 2014. 'Rat hippocampal responses up to 90 days after a single nanoceria dose extends a hierarchical oxidative stress model for nanoparticle toxicity', *Nanotoxicology*, 8: 155-66.

He, M. L., and W. A. Rambeck. 2000. 'Rare earth elements--a new generation of growth promoters for pigs?', *Arch Tierernahr*, 53: 323-34.

Heneka, Michael T., Monica J. Carson, Joseph El Khoury, Gary E. Landreth, Frederic Brosseron, Douglas L. Feinstein, Andreas H. Jacobs, Tony Wyss-Coray, Javier Vitorica, Richard M. Ransohoff, Karl Herrup, Sally A. Frautschy, Bente Finsen, Guy C. Brown, Alexei Verkhratsky, Koji Yamanaka, Jari Koistinaho, Eicke Latz, Annett Halle, Gabor C. Petzold, Terrence Town, Dave Morgan, Mari L. Shinohara, V. Hugh Perry, Clive Holmes, Nicolas G. Bazan, David J. Brooks, Stéphane Hunot, Bertrand Joseph, Nikolaus Deigendesch, Olga Garaschuk, Erik Boddeke, Charles A. Dinarello, John C. Breitner, Greg M. Cole, Douglas T. Golenbock, and Markus P. Kummer. 2015. 'Neuroinflammation in Alzheimer's disease', *The Lancet. Neurology*, 14: 388-405.

Heppner, F. L., R. M. Ransohoff, and B. Becher. 2015. 'Immune attack: the role of inflammation in Alzheimer disease', *Nat Rev Neurosci*, 16: 358-72.

Heusinkveld, Harm J., Tina Wahle, Arezoo Campbell, Remco H. S. Westerink, Lang Tran, Helinor Johnston, Vicki Stone, Flemming R. Cassee, and Roel P. F. Schins. 2016.

'Neurodegenerative and neurological disorders by small inhaled particles', *NeuroToxicology*, 56: 94-106.

Hirst, S. M., A. S. Karakoti, R. D. Tyler, N. Sriranganathan, S. Seal, and C. M. Reilly. 2009. 'Anti-inflammatory properties of cerium oxide nanoparticles', *Small*, 5: 2848-56.

Holcomb, L. A., M. N. Gordon, P. Jantzen, K. Hsiao, K. Duff, and D. Morgan. 1999. 'Behavioral changes in transgenic mice expressing both amyloid precursor protein and presenilin-1 mutations: lack of association with amyloid deposits', *Behav Genet*, 29: 177-85.

Hullmann, M., C. Albrecht, D. van Berlo, M. E. Gerlofs-Nijland, T. Wahle, A. W. Boots, J. Krutmann, F. R. Cassee, T. A. Bayer, and R. P. F. Schins. 2017a. 'Diesel engine exhaust accelerates plaque formation in a mouse model of Alzheimer's disease', *Part Fibre Toxicol*, 14: 35.

Hullmann, Maja, Catrin Albrecht, Damiën van Berlo, Miriam E. Gerlofs-Nijland, Tina Wahle, Agnes W. Boots, Jean Krutmann, Flemming R. Cassee, Thomas A. Bayer, and Roel P. F. Schins. 2017b. 'Diesel engine exhaust accelerates plaque formation in a mouse model of Alzheimer's disease', *Part Fibre Toxicol*, 14: 35.

Hüttenrauch, M., A. Brauß, A. Kurdakova, H. Borgers, F. Klinker, D. Liebetanz, G. Salinas-Riester, J. Wiltfang, H. W. Klafki, and O. Wirths. 2016. 'Physical activity delays hippocampal neurodegeneration and rescues memory deficits in an Alzheimer disease mouse model', *Translational psychiatry*, 6: e800-e00.

Iqbal, A., I. Ahmad, M. H. Khalid, M. S. Nawaz, S. H. Gan, and M. A. Kamal. 2013. 'Nanoneurotoxicity to nanoneuroprotection using biological and computational approaches', *J Environ Sci Health C Environ Carcinog Ecotoxicol Rev*, 31: 256-84.

Islam, M. T. 2017. 'Oxidative stress and mitochondrial dysfunction-linked neurodegenerative disorders', *Neurol Res*, 39: 73-82.

Jawhar, S., A. Trawicka, C. Jenneckens, T. A. Bayer, and O. Wirths. 2012. 'Motor deficits, neuron loss, and reduced anxiety coinciding with axonal degeneration and intraneuronal Abeta aggregation in the 5XFAD mouse model of Alzheimer's disease', *Neurobiol Aging*, 33: 196.e29-40.

Kang, G. S., P. A. Gillespie, A. Gunnison, A. L. Moreira, K. M. Tchou-Wong, and L. C. Chen. 2011. 'Long-term inhalation exposure to nickel nanoparticles exacerbated atherosclerosis in a susceptible mouse model', *Environ Health Perspect*, 119: 176-81.

Kanninen, Katja, Riikka Heikkinen, Tarja Malm, Taisia Rolova, Susanna Kuhmonen, Hanna Leinonen, Seppo Ylä-Herttuala, Heikki Tanila, Anna-Liisa Levonen, Milla Koistinaho, and Jari Koistinaho. 2009. 'Intrahippocampal injection of a lentiviral vector expressing Nrf2 improves spatial learning in a mouse model of Alzheimer's disease', *Proceedings of the National Academy of Sciences of the United States of America*, 106: 16505-10.

Kleinman, M. T., J. A. Araujo, A. Nel, C. Sioutas, A. Campbell, P. Q. Cong, H. Li, and S. C. Bondy. 2008. 'Inhaled ultrafine particulate matter affects CNS inflammatory processes and may act via MAP kinase signaling pathways', *Toxicol Lett*, 178: 127-30.

Kook, S. Y., K. M. Lee, Y. Kim, M. Y. Cha, S. Kang, S. H. Baik, H. Lee, R. Park, and I. Mook-Jung. 2014. 'High-dose of vitamin C supplementation reduces amyloid plaque burden and ameliorates pathological changes in the brain of 5XFAD mice', *Cell Death & Disease*, 5: e1083.

Kovacs, G. G. 2017. 'Cellular reactions of the central nervous system', *Handb Clin Neurol*, 145: 13-23.

Lazarov, O., J. Robinson, Y. P. Tang, I. S. Hairston, Z. Korade-Mirnics, V. M. Lee, L. B. Hersh, R. M. Sapolsky, K. Mirnics, and S. S. Sisodia. 2005. 'Environmental enrichment reduces Abeta levels and amyloid deposition in transgenic mice', *Cell*, 120: 701-13.

Li, Dongyang, Xiaoyu Liu, Tianming Liu, Haitao Liu, Li Tong, Shuwei Jia, and Yu-Feng Wang. 2020. 'Neurochemical regulation of the expression and function of glial fibrillary acidic protein in astrocytes', *Glia*, 68: 878-97.

Lippa CF, Nee LE, Mori H, George-Hyslop P. 1998. 'Abeta-42 deposition precedes other changes in PS-1 Alzheimer´s disease', *Lancet 352*: 1117-18.

Liu, D., B. Lin, W. Shao, Z. Zhu, T. Ji, and C. Yang. 2014. 'In vitro and in vivo studies on the transport of PEGylated silica nanoparticles across the blood-brain barrier', *ACS Appl Mater Interfaces*, 6: 2131-6.

Liu, Y., Y. Li, T. Yang, J. Yang, H. Wang, and G. Wu. 2016. 'Acute changes in murine hippocampus and olfactory bulb after nasal instillation of varying size cerium dioxide particles', *J Toxicol Environ Health A*, 79: 869-77.

Lung, S., F. R. Cassee, I. Gosens, and A. Campbell. 2014. 'Brain suppression of AP-1 by inhaled diesel exhaust and reversal by cerium oxide nanoparticles', *Inhal Toxicol*, 26: 636-41.

Martin, E. M., R. S. Wilson, R. D. Penn, J. H. Fox, R. A. Clasen, and S. M. Savoy. 1987. 'Cortical biopsy results in Alzheimer's disease: correlation with cognitive deficits', *Neurology*, 37: 1201-4.

Masters, C. L., and K. Beyreuther. 1991. 'Alzheimer's disease: molecular basis of structural lesions', *Brain Pathol*, 1: 226-7.

Mattson, M. P. 2004. 'Pathways towards and away from Alzheimer's disease', *Nature*, 430: 631-9.

Maurer-Jones, Melissa A., Ian L. Gunsolus, Catherine J. Murphy, and Christy L. Haynes. 2013. 'Toxicity of Engineered Nanoparticles in the Environment', *Analytical chemistry*, 85: 3036-49.

Methia, N., P. Andre, A. Hafezi-Moghadam, M. Economopoulos, K. L. Thomas, and D. D. Wagner. 2001. 'ApoE deficiency compromises the blood brain barrier especially after injury', *Mol Med*, 7: 810-5.

Miller, M. R., S. G. McLean, R. Duffin, A. O. Lawal, J. A. Araujo, C. A. Shaw, N. L. Mills, K. Donaldson, D. E. Newby, and P. W. Hadoke. 2013. 'Diesel exhaust particulate increases the size and complexity of lesions in atherosclerotic mice', *Part Fibre Toxicol*, 10: 61.

Miller, M. R., C. A. Shaw, and J. P. Langrish. 2012. 'From particles to patients: oxidative stress and the cardiovascular effects of air pollution', *Future Cardiol*, 8: 577-602.

Miller, Mark R. 2014. 'The role of oxidative stress in the cardiovascular actions of particulate air pollution', *Biochemical Society Transactions*, 42: 1006.

Miquel, Jaime, and Margarita Blasco. 1978. 'A simple technique for evaluation of vitality loss in aging mice, by testing their muscular coordination and vigor', *Experimental Gerontology*, 13: 389-96.

Moran, P. M., L. S. Higgins, B. Cordell, and P. C. Moser. 1995. 'Age-related learning deficits in transgenic mice expressing the 751-amino acid isoform of human beta-amyloid precursor protein', *Proc Natl Acad Sci U S A*, 92: 5341-5.

Morimoto, Yasuo, Hiroto Izumi, Yukiko Yoshiura, Taisuke Tomonaga, Takako Oyabu, Toshihiko Myojo, Kazuaki Kawai, Kazuhiro Yatera, Manabu Shimada, Masaru Kubo, Kazuhiro Yamamoto, Shinichi Kitajima, Etsushi Kuroda, Kenji Kawaguchi, and Takeshi Sasaki. 2016. 'Evaluation of Pulmonary Toxicity of Zinc Oxide Nanoparticles Following Inhalation and Intratracheal Instillation', *International Journal of Molecular Sciences*, 17: 1241.

Moser, V. C. 2011. 'Functional assays for neurotoxicity testing', *Toxicol Pathol*, 39: 36-45.

Murugadoss, S., D. Lison, L. Godderis, S. Van Den Brule, J. Mast, F. Brassinne, N. Sebaihi, and P. H. Hoet. 2017a. 'Toxicology of silica nanoparticles: an update', *Arch Toxicol*, 91: 2967-3010.

Murugadoss, Sivakumar, Dominique Lison, Lode Godderis, Sybille Van Den Brule, Jan Mast, Frederic Brassinne, Noham Sebaihi, and Peter H. Hoet. 2017b. 'Toxicology of silica nanoparticles: an update', *Archives of toxicology*, 91: 2967-3010.

Napierska, D., L. C. Thomassen, D. Lison, J. A. Martens, and P. H. Hoet. 2010a. 'The nanosilica hazard: another variable entity', *Part Fibre Toxicol*, 7: 39.

Napierska, Dorota, Leen C. J. Thomassen, Dominique Lison, Johan A. Martens, and Peter H. Hoet. 2010b. 'The nanosilica hazard: another variable entity', *Part Fibre Toxicol*, 7: 39-39.

Nelson, Peter T., Irina Alafuzoff, Eileen H. Bigio, Constantin Bouras, Heiko Braak, Nigel J. Cairns, Rudolph J. Castellani, Barbara J. Crain, Peter Davies, Kelly Del Tredici, Charles Duyckaerts, Matthew P. Frosch, Vahram Haroutunian, Patrick R. Hof, Christine M. Hulette, Bradley T. Hyman, Takeshi Iwatsubo, Kurt A. Jellinger, Gregory A. Jicha, Enikö Kövari, Walter A. Kukull, James B. Leverenz, Seth Love, Ian R. Mackenzie, David M. Mann, Eliezer Masliah, Ann C. McKee, Thomas J. Montine, John C. Morris, Julie A. Schneider, Joshua A. Sonnen, Dietmar R. Thal, John Q. Trojanowski, Juan C. Troncoso, Thomas Wisniewski, Randall L. Woltjer, and Thomas G. Beach. 2012. 'Correlation of Alzheimer Disease Neuropathologic Changes With Cognitive Status: A Review of the Literature', *Journal of neuropathology and experimental neurology*, 71: 362-81.

Nemmar, A., P. Yuvaraju, S. Beegam, M. A. Fahim, and B. H. Ali. 2017. 'Cerium Oxide Nanoparticles in Lung Acutely Induce Oxidative Stress, Inflammation, and DNA Damage in Various Organs of Mice', *Oxid Med Cell Longev*, 2017: 9639035.

Newby, David E., Pier M. Mannucci, Grethe S. Tell, Andrea A. Baccarelli, Robert D. Brook, Ken Donaldson, Francesco Forastiere, Massimo Franchini, Oscar H. Franco, Ian Graham, Gerard Hoek, Barbara Hoffmann, Marc F. Hoylaerts, Nino Künzli, Nicholas Mills, Juha Pekkanen, Annette Peters, Massimo F. Piepoli, Sanjay Rajagopalan, Robert F. Storey, European Association for Cardiovascular Prevention Esc Working Group on Thrombosis, Rehabilitation, and E. S. C. Heart Failure Association. 2015. 'Expert position paper on air pollution and cardiovascular disease', *European heart journal*, 36: 83-93b.

Niu, Jianli, Kangkai Wang, and Pappachan E. Kolattukudy. 2011. 'Cerium Oxide Nanoparticles Inhibits Oxidative Stress and Nuclear Factor-κB Activation in H9c2 Cardiomyocytes Exposed to Cigarette Smoke Extract', *J Pharmacol Exp Ther*, 338: 53-61.

O'Leary, T. P., H. M. Mantolino, K. R. Stover, and R. E. Brown. 2018. 'Age-related deterioration of motor function in male and female 5xFAD mice from 3 to 16 months of age', *Genes Brain Behav*: e12538.

O'Leary, T. P., A. Robertson, P. H. Chipman, V. F. Rafuse, and R. E. Brown. 2018. 'Motor function deficits in the 12 month-old female 5xFAD mouse model of Alzheimer's disease', *Behav Brain Res*, 337: 256-63.

O'Leary, T. P., A. Robertson, P. H. Chipman, V. F. Rafuse, and R. E. Brown. 2018. 'Motor function deficits in the 12 month-old female 5xFAD mouse model of Alzheimer's disease', *Behav Brain Res*, 337: 256-63.

Oakley, H., S. L. Cole, S. Logan, E. Maus, P. Shao, J. Craft, A. Guillozet-Bongaarts, M. Ohno, J. Disterhoft, L. Van Eldik, R. Berry, and R. Vassar. 2006. 'Intraneuronal beta-amyloid aggregates, neurodegeneration, and neuron loss in transgenic mice with five familial Alzheimer's disease mutations: potential factors in amyloid plaque formation', *J Neurosci*, 26: 10129-40.

Oberdorster, G., E. Oberdorster, and J. Oberdorster. 2005. 'Nanotoxicology: an emerging discipline evolving from studies of ultrafine particles', *Environ Health Perspect*, 113: 823-39.

Oberdorster, G., Z. Sharp, V. Atudorei, A. Elder, R. Gelein, W. Kreyling, and C. Cox. 2004. 'Translocation of inhaled ultrafine particles to the brain', *Inhal Toxicol*, 16: 437-45.

Oberdörster, Günter, Alison Elder, and Amber Rinderknecht. 2009. 'Nanoparticles and the Brain: Cause for Concern?', *J Nanosci Nanotechnol*, 9: 4996-5007.

Oberdörster, Günter, Eva Oberdörster, and Jan Oberdörster. 2005. 'Nanotoxicology: an emerging discipline evolving from studies of ultrafine particles', *Environmental Health Perspectives*, 113: 823-39.

OECD. 1997. *Test No. 424: Neurotoxicity Study in Rodents*.

Ohno, M., E. A. Sametsky, L. H. Younkin, H. Oakley, S. G. Younkin, M. Citron, R. Vassar, and J. F. Disterhoft. 2004. 'BACE1 deficiency rescues memory deficits and cholinergic dysfunction in a mouse model of Alzheimer's disease', *Neuron*, 41: 27-33.

Park, E. J., and K. Park. 2009. 'Oxidative stress and pro-inflammatory responses induced by silica nanoparticles in vivo and in vitro', *Toxicol Lett*, 184: 18-25.

Phyu, Moe Pwint, and Jitbanjong Tangpong. 2014. 'Neuroprotective effects of xanthone derivative of Garcinia mangostana against lead-induced acetylcholinesterase dysfunction and cognitive impairment', *Food and Chemical Toxicology*, 70: 151-56.

Power, Melinda C., Marc G. Weisskopf, Stacey E. Alexeeff, Brent A. Coull, Avron Spiro, 3rd, and Joel Schwartz. 2011. 'Traffic-related air pollution and cognitive function in a cohort of older men', *Environmental Health Perspectives*, 119: 682-87.

Raber, J., D. Wong, G. Q. Yu, M. Buttini, R. W. Mahley, R. E. Pitas, and L. Mucke. 2000. 'Apolipoprotein E and cognitive performance', *Nature*, 404: 352-4.

Ransohoff, R. M. 2016. 'How neuroinflammation contributes to neurodegeneration', *Science*, 353: 777-83.

Reiss, A. B., H. A. Arain, M. M. Stecker, N. M. Siegart, and L. J. Kasselman. 2018. 'Amyloid toxicity in Alzheimer's disease', *Rev Neurosci*, 29: 613-27.

Repar, Neza, Hao Li, Jose S. Aguilar, Qingshun Quinn Li, Damjana Drobne, and Yiling Hong. 2018. 'Silver nanoparticles induce neurotoxicity in a human embryonic stem cell-derived neuron and astrocyte network', *Nanotoxicology*, 12: 104-16.

Rzigalinski, Beverly A., Charles S. Carfagna, and Marion Ehrich. 2017. 'Cerium oxide nanoparticles in neuroprotection and considerations for efficacy and safety', *Wiley Interdiscip Rev Nanomed Nanobiotechnol*, 9: 10.1002/wnan.444.

Sandberg, Mats, Jaspal Patil, Barbara D'Angelo, Stephen G. Weber, and Carina Mallard. 2014. 'NRF2-regulation in brain health and disease: implication of cerebral inflammation', *Neuropharmacology*, 79: 298-306.

Sasaki, Yo, Keiko Ohsawa, Hiroko Kanazawa, Shinichi Kohsaka, and Yoshinori Imai. 2001. 'Iba1 Is an Actin-Cross-Linking Protein in Macrophages/Microglia', *Biochemical and Biophysical Research Communications*, 286: 292-97.

Schipper, Hyman M., Wei Song, Ayda Tavitian, and Marisa Cressatti. 2019. 'The sinister face of heme oxygenase-1 in brain aging and disease', *Progress in Neurobiology*, 172: 40-70.

Schmidt, R., E. Kienbacher, T. Benke, P. Dal-Bianco, M. Delazer, G. Ladurner, K. Jellinger, J. Marksteiner, G. Ransmayr, H. Schmidt, E. Stogmann, J. Friedrich, and C. Wehringer. 2008. '[Sex differences in Alzheimer's disease]', *Neuropsychiatr*, 22: 1-15.

Schwotzer, Daniela, Monika Niehof, Dirk Schaudien, Heiko Kock, Tanja Hansen, Clemens Dasenbrock, and Otto Creutzenberg. 2018. 'Cerium oxide and barium sulfate nanoparticle inhalation affects gene expression in alveolar epithelial cells type II', *Journal of nanobiotechnology*, 16: 16.

Selkoe, D. J. 2001a. 'Alzheimer's disease results from the cerebral accumulation and cytotoxicity of amyloid beta-protein', *J Alzheimers Dis*, 3: 75-80.

———. 2001b. 'Alzheimer's disease: genes, proteins, and therapy', *Physiol Rev*, 81: 741-66.

Sharma, H. S., D. F. Muresanu, R. Patnaik, and A. Sharma. 2013. 'Exacerbation of brain pathology after partial restraint in hypertensive rats following SiO(2) nanoparticles exposure at high ambient temperature', *Mol Neurobiol*, 48: 368-79.

Singh, Neeraj, Courtney A. Cohen, and Beverly A. Rzigalinski. 2007. 'Treatment of Neurodegenerative Disorders with Radical Nanomedicine', *Annals of the New York Academy of Sciences*, 1122: 219-30.

Singh, Sanjay, Amit Kumar, Ajay Karakoti, Sudipta Seal, and William T. Self. 2010. 'Unveiling the mechanism of uptake and sub-cellular distribution of cerium oxide nanoparticles', *Molecular bioSystems*, 6: 1813-20.

Sofroniew, Michael V., and Harry V. Vinters. 2010. 'Astrocytes: biology and pathology', *Acta Neuropathol*, 119: 7-35.

Stone, V., M. R. Miller, M. J. D. Clift, A. Elder, N. L. Mills, P. Moller, R. P. F. Schins, U. Vogel, W. G. Kreyling, K. Alstrup Jensen, T. A. J. Kuhlbusch, P. E. Schwarze, P. Hoet, A. Pietroiusti, A. De Vizcaya-Ruiz, A. Baeza-Squiban, J. P. Teixeira, C. L. Tran, and F. R. Cassee. 2017. 'Nanomaterials Versus Ambient Ultrafine Particles: An Opportunity to Exchange Toxicology Knowledge', *Environ Health Perspect*, 125: 106002.

Strickland, Jenna D., William R. Lefew, James Crooks, Diana Hall, Jayna N. R. Ortenzio, Kevin Dreher, and Timothy J. Shafer. 2016. 'In vitro screening of metal oxide nanoparticles for effects on neural function using cortical networks on microelectrode arrays', *Nanotoxicology*, 10: 619-28.

Tong, Y., W. Zhou, V. Fung, M. A. Christensen, H. Qing, X. Sun, and W. Song. 2005. 'Oxidative stress potentiates BACE1 gene expression and Abeta generation', *J Neural Transm (Vienna)*, 112: 455-69.

Tramutola, A., C. Lanzillotta, M. Perluigi, and D. A. Butterfield. 2017. 'Oxidative stress, protein modification and Alzheimer disease', *Brain Res Bull*, 133: 88-96.

Tsai, Y. Y., J. Oca-Cossio, S. M. Lin, K. Woan, P. C. Yu, and W. Sigmund. 2008. 'Reactive oxygen species scavenging properties of ZrO2-CeO2 solid solution nanoparticles', *Nanomedicine (Lond)*, 3: 637-45.

Tuppo, E. E., and H. R. Arias. 2005. 'The role of inflammation in Alzheimer's disease', *Int J Biochem Cell Biol*, 37: 289-305.

Unfried, K., U. Sydlik, K. Bierhals, A. Weissenberg, and J. Abel. 2008. 'Carbon nanoparticle-induced lung epithelial cell proliferation is mediated by receptor-dependent Akt activation', *Am J Physiol Lung Cell Mol Physiol*, 294: L358-67.

Węsierska, M., K. Dziendzikowska, J. Gromadzka-Ostrowska, J. Dudek, H. Polkowska-Motrenko, J. N. Audinot, A. C. Gutleb, A. Lankoff, and M. Kruszewski. 2018. 'Silver ions are responsible for memory impairment induced by oral administration of silver nanoparticles', *Toxicol Lett*, 290: 133-44.

Weuve, Jennifer. 2014. 'Invited Commentary: How Exposure to Air Pollution May Shape Dementia Risk, and What Epidemiology Can Say About It', *American Journal of Epidemiology*, 180: 367-71.

Wittnam, J. L., E. Portelius, H. Zetterberg, M. K. Gustavsson, S. Schilling, B. Koch, H. U. Demuth, K. Blennow, O. Wirths, and T. A. Bayer. 2012. 'Pyroglutamate amyloid beta (Abeta) aggravates behavioral deficits in transgenic amyloid mouse model for Alzheimer disease', *J Biol Chem*, 287: 8154-62.

Wu, J., C. Wang, J. Sun, and Y. Xue. 2011. 'Neurotoxicity of silica nanoparticles: brain localization and dopaminergic neurons damage pathways', *ACS Nano*, 5: 4476-89.

Yang, T., S. Li, H. Xu, D. M. Walsh, and D. J. Selkoe. 2017. 'Large Soluble Oligomers of Amyloid beta-Protein from Alzheimer Brain Are Far Less Neuroactive Than the Smaller Oligomers to Which They Dissociate', *J Neurosci*, 37: 152-63.

Yang, X., C. He, J. Li, H. Chen, Q. Ma, X. Sui, S. Tian, M. Ying, Q. Zhang, Y. Luo, Z. Zhuang, and J. Liu. 2014. 'Uptake of silica nanoparticles: neurotoxicity and Alzheimer-like

pathology in human SK-N-SH and mouse neuro2a neuroblastoma cells', *Toxicol Lett*, 229: 240-9.

Yokel, R. A., M. T. Tseng, M. Dan, J. M. Unrine, U. M. Graham, P. Wu, and E. A. Grulke. 2013. 'Biodistribution and biopersistence of ceria engineered nanomaterials: size dependence', *Nanomedicine*, 9: 398-407.

Yokel, Robert A., Salik Hussain, Stavros Garantziotis, Philip Demokritou, Vincent Castranova, and Flemming R. Cassee. 2014. 'The Yin: An adverse health perspective of nanoceria: uptake, distribution, accumulation, and mechanisms of its toxicity', *Environmental science. Nano*, 1: 406-28.

You, Ran, Yuen-Shan Ho, Clara Hiu-Ling Hung, Yan Liu, Chun-Xia Huang, Hei-Nga Chan, See-Lok Ho, Sheung-Yeung Lui, Hung-Wing Li, and Raymond Chuen-Chung Chang. 2018. 'Silica nanoparticles induce neurodegeneration-like changes in behavior, neuropathology, and affect synapse through MAPK activation', *Part Fibre Toxicol*, 15: 28-28.

Zerbi, V., M. Wiesmann, T. L. Emmerzaal, D. Jansen, M. Van Beek, M. P. Mutsaers, C. F. Beckmann, A. Heerschap, and A. J. Kiliaan. 2014. 'Resting-state functional connectivity changes in aging apoE4 and apoE-KO mice', *J Neurosci*, 34: 13963-75.

Zhang, Yun-wu, Robert Thompson, Han Zhang, and Huaxi Xu. 2011. 'APP processing in Alzheimer's disease', *Molecular brain*, 4: 3-3.

Zhao, Yan, and Baolu Zhao. 2013. 'Oxidative stress and the pathogenesis of Alzheimer's disease', *Oxidative medicine and cellular longevity*, 2013: 316523-23.

5 Publications beyond the scope of the dissertation

During her doctorate, the author of this dissertation contributed to several additional publications which are not included to this work because they are beyond the scope of this dissertation.

5.1 Model Complexity as Determining Factor for In Vitro Nanosafety Studies: Effects of Silver and Titanium Dioxide Nanomaterials in Intestinal Models

Angela A M Kämpfer[1], Mathias Busch[1], Veronika Büttner[1], Gerrit Bredeck[1], Burkhard Stahlmecke[2], Bryan Hellack[2 3], Isabelle Masson[1], Adriana Sofranko[1], Catrin Albrecht[1], Roel P F Schins[1]

[1]IUF - Leibniz Research Institute for Environmental Medicine, Auf'm Hennekamp 50, Düsseldorf, 40225, Germany. [2]IUTA - Institute of Energy and Environmental Technology, Bliersheimer Str. 58-60, Duisburg, 47229, Germany. [3]UBA - German Environment Agency, Paul-Ehrlich-Str. 29, Langen, 63225, Germany.

Small. 2021 Apr;17(15):e2004223
DOI: 10.1002/smll.202004223

Author contribution: The author of this dissertation contributed to the *in vivo* study design, weighed and handled the mice in the animal facility during the whole study and discussed the results. Relative contribution: about 5%.

5.2 Effects of dietary exposure to the engineered nanomaterials CeO_2, SiO_2, Ag, and TiO_2 on the murine gut microbiome

Bredeck G, Kämpfer AAM, Sofranko A, Wahle T, Lison D, Ambroise J, Stahlmecke B, Albrecht C, Schins RPF

[1]IUF - Leibniz Research Institute for Environmental Medicine, Auf'm Hennekamp 50, Düsseldorf, 40225, Germany. [2]IUTA - Institute of Energy and Environmental Technology, Bliersheimer Str. 58-60, Duisburg, 47229, Germany. [3]UBA - German Environment Agency, Paul-Ehrlich-Str. 29, Langen, 63225, Germany.

Nanotoxicology 15(7): 934-950, 2021

Doi: 10.1080/17435390.2021.1940339

Author contribution: The author of this dissertation contributed to the *in vivo* study design, weighed and handled the mice in the animal facility and discussed the results. Relative contribution: about 10%.

5.3 Ingested Engineered Nanomaterials Affect the Expression of Mucin Genes—An In Vitro-In Vivo Comparison

Gerrit Bredeck, Angela A. M. Kämpfer, Adriana Sofranko, Tina Wahle, Veronika Büttner, Catrin Albrecht and Roel P. F. Schins
IUF - Leibniz Research Institute for Environmental Medicine, Düsseldorf, Germany

Nanomaterials 2021, 11(10), 2621
DOI: 10.3390/nano11102621

Author contribution: The author of this dissertation contributed to the *in vivo* study design, weighed and handled the mice in the animal facility during the whole study and discussed the results. Relative contribution: about 5%.

5.4 Discussion on Existing Standards and Quality Criteria in Nanosafety Research - Summary of the NanoS-QM Expert Workshop

Kunigunde Binder[1], Christian Bonatto Minella[1], Linda Elberskirch[2], AnnetteKraegeloh[2], Julia Liebing[4], Christiane Petzold[2], Matthias Razum[1], Norbert Riefler[5], Roel Schins[3], Adriana Sofranko[3], Christoph van Thriel[4], Klaus Unfried[3]

[1]FIZ Karlsruhe – Leibniz Institute for Information Infrastructure, Hermann-von-Helmholtz-Platz 1, 76133 Eggenstein-Leopoldshafen, Germany; [2]INM – Leibniz-Institute for New Materials, Campus D2 2, 66123 Saarbrücken,Germany; [3]IUF – Leibniz Research Institute for Environmental Medicine, Auf'm Hennekamp50, 40225 Düsseldorf, Germany; [4]IfADo – Leibniz Research Centre for Working Environment and Human Factors,Ardeystraße 67, 44139 Dortmund. Germany; [5]Leibniz Institute for Materials Engineering – IWT, Badgasteiner Str. 3, 28359Bremen, Germany

Zenodo, March 10, 2021

DOI: 10.5281/zenodo.4584790

Author contribution: The author of this dissertation contributed to the planning of the workshop, was involved in writing and discussion of the results. Relative contribution: about 8%.

5.5 Digital Research Data: From analysis of existing standards to a scientific foundation for a modular metadata schema in Nanosafety

Linda Elberskirch[1†], Kunigunde Binder[2†], Norbert Riefler[3], Adriana Sofranko[4], Julia Liebing[5], Christian Bonatto Minella[2], Lutz Mädler[3], Matthias Razum[2], Christoph van Thriel[5], Klaus Unfried[4], Roel P.F. Schins[4], Annette Kraegeloh[1]

[1]INM - Leibniz Institute for New Materials, Campus D2 2, 66123 Saarbrücken; [2]FIZ Karl ruhe – Leibniz Institute for Information Infrastructure, Hermann-von-Helmholtz-Platz 1, 76133 Eggenstein-Leopoldshafen; [3]IWT - Leibniz-Institut für Werkstofforientierte Technologien, Badgasteiner Str. 3, 28359 Bremen; [4]IUF - Leibniz Research Institute for Environmental Medicine, Auf'm Hennekamp 50, 40225 Düsseldorf; [5]IfADo - Leibniz Research Centre for Working Environment and Human Factors, Ardeystraße 67, 44139 Dortmund

† Contributed equally

Manuscript under revision in Particle and Fibre Toxicology.

Author contribution: The author of this dissertation contributed to the writing, reviewing and discussion of the manuscript. Relative contribution: about 10%.

5.6 Evaluation of the benchmark dose approach from neurobehavioural data in C57BL/6J mice exposed to engineered nanoparticles orally for 28 days

Adriana Sofranko[1], Tina Wahle[1], Harm J. Heusinkveld[2,3], Catrin Albrecht[1], Roel P.F. Schins[1]

[1]IUF - Leibniz Research Institute for Environmental Medicine, Düsseldorf, Germany; [2]National Institute for Public Health and the Environment (RIVM), Bilthoven, The Netherlands; [3]Utrecht University, Utrecht, The Netherlands

Manuscript in preparation

Author contribution: The author of this dissertation wrote the manuscript, planned the study design, performed the behaviour tests, dissected brain tissues, performed the biochemical experiments, analysed the data, made all graphs and discussed the results. Relative contribution: about 70%.

6 General Discussion

Due to their beneficial properties, NMs are used in various medical and industrial applications as well as in daily-life consumer products. Beyond the lung, which is the entrance organ for inhaled NMs, and thus considered as the most crucial primary target organ, there is an increasing concern about the safety of specific NMs on the brain as target organ [1]. Translocation to the brain and subsequent induction of oxidative stress and neuroinflammation has been postulated as a major mode of action of NM-induced neurotoxicity and neurodegeneration [2-5]. Neurodegeneration is defined as a slow and progressive pathological condition in which neurons lose their function, structure until cell death [6, 7]. These processes are the main pathological features of neurodegenerative diseases like AD, which builds with 60-80% the major cause of dementia and its progression is age-related, but not everyone who ages will develop this disease [8, 9]. AD is mainly induced sporadic and associated with various etiological factors from which the most are still unidentified [10, 11]. Recent studies from Calderon-Carciduenas and co-workers could demonstrate that residents of highly polluted cities had a significantly higher accumulation of Aβ42 and increased neuroinflammation as well as measurable levels of iron-rich, highly oxidative and combustion derived NMs in the brain of every examined resident living in Mexico City [12-14]. However, it is mostly unknown whether and how specific types of NMs at which doses and via which exposure routes might contribute to neurotoxicity or the initiation of AD. Currently, available literature suggests that specific types of engineered nanoparticles have neurotoxic effects and as such, might contribute to the development and progression of neurodegenerative diseases. However, contrasting data have been reported in the literature regarding the neurotoxicity of NMs especially following oral exposure, possibly due to differences in study design.

The aim of the experiments carried out in the framework of this thesis was to determine the effects of NMs on neurotoxicity and/or on AD-related features following inhalation or dietary exposure. For this purpose, the four most widely used and investigated NMs, TiO_2, Ag, CeO_2 and SiO_2 were selected. For the oral exposure studies, we choose 1% mass in the food as highest for the dietary fed TiO_2, CeO_2 and SiO_2 as it represents the highest permitted dose recognized as safe for TiO_2 in food by the Food and Drug Administration [15]. A fivefold lower dose for the Ag NM was chosen based on its higher toxicity and due to its ability to release silver ions [16]. For the experiments with the Zr-doped CeO_2 NMs, mice were exposed to 4 mg/m^3 in alignment with typical exposure levels in particle inhalation toxicology studies.

In the first experimental study (**Chapter 2**), a broad spectrum of neurotoxic endpoints following subacute dietary oral exposure to TiO_2 and Ag NMs, including a 2-week post-exposure period, were investigated in male and female C57BL/6J mice [17]. The oral exposure studies were performed in alignment with the OECD guideline 424 for neurotoxicity testing in rodents [18]. The neurotoxicological endpoints included several neurobehavioural tests, neuroinflammatory, oxidative stress and BBB integrity markers, as well as a tyrosine and serine/threonine protein kinases activity assay. While neurotoxicity was absent in TiO_2 NM exposed male and female mice, decreased motor coordination and increased tyrosine kinase activity was observed in Ag NM exposed female mice. An upstream kinase analysis indicated increased activity of, among others, Src family kinases, which are involved in the regulation of neuronal activity through glutamatergic NMDA receptors [19]. Very recently, an *in vivo* study in rats confirmed previous *in vitro* investigations of the involvement of NMDA receptors in Ag NM-induced neurotoxicity [20, 21]. The main findings of our study suggest that subacute exposure to foodborne Ag NM causes sex-dependent neurobehavioural effects in female mice and that the observed impairments in motor coordination may be due to an increased tyrosine kinase activity. In concordance with our study outcome, sex-related differences in oxidative stress parameters in mice were recently also found after subacute intraperitoneal exposure to Ag NMs [22]. Furthermore, the study investigated sex-related differences in Ag accumulation in the brain that could explain the observed sex-dependent response in our study. Our kinetics study was designed for one mouse sex only due to animal ethical restrictions and thus, unfortunately, we were not able to verify such sex-dependent accumulation. However, we examined a rapid and persistent accumulation of Ag in various organs, including the brain, over the post-exposure period. Further studies are needed to evaluate neurotoxicological endpoints of foodborne Ag NM at lower doses to establish a no-observed adverse effect level (NOAEL). Therefore, in a subsequent study, we evaluated dose-dependent effects of dietary Ag NM using a benchmark dose approach study design (Sofranko et al. in preparation).

In the second experimental study (**Chapter 3**), the hypothesis that long-term exposure to NMs can cause neurotoxicity and progress the pathogenesis of AD was tested for dietary fed CeO_2 and SiO_2 NMs in 5xFAD mice and their C57BL/6J littermates. The amyloid cascade hypothesis suggests that an abnormal extracellular accumulation of Aβ peptides in the brain is a crucial contributor to the pathogenesis of the disease [23]. The 5xFAD transgenic mice are a valuable model for studying AD-related pathology. They rapidly display massive Aβ42 levels, gliosis and amyloid plaque formation by expressing a total of five familiar AD-linked mutations: three

mutations in APP and two mutations in PS1 [24]. Contrary to our hypothesis, it was demonstrated that long-term dietary exposure to both NMs did not result in a progression of AD-related pathology. Neurobehavioural impairments were absent, accelerated amyloid-β plaque formation was not observed, and neuroinflammation and oxidative stress were not induced. Unexpectedly, the dietary exposure to 1% of the pristine CeO_2 for 14 weeks significantly decreased amyloid plaque formation in the hippocampus and improved motor function in 5xFAD mice compared to the untreated control group. CeO_2 NM is known for its antioxidant and free radical scavenger properties, and numerous research groups have already investigated the neuroprotective properties of CeO_2 NMs in neurodegenerative diseases, which are associated with high levels of oxidative stress like AD [25-29]. The effects observed in our study with the CeO_2-fed mice may be the result of direct redox-restoring effects, although we did not observe significant changes in oxidative stress response. Interestingly, in contrast to the neuroprotective effects at late exposure, a significant increase in neurotoxic Aβ42/Aβ40 ratio due to higher Aβ42 protein levels was detected in the 1% CeO_2 exposed 5xFAD mice at early exposure. Therefore, additional research is needed to identify the exact underlying mechanism of dietary fed CeO_2 NM on Aβ42 generation and amyloid plaque formation.

To evaluate the influence of redox activity of CeO_2 NMs on AD-related pathology (**Chapter 4**), a subacute inhalation study in C57BL/6J, 5xFAD and $ApoE^{-/-}$ mice using CeO_2 NMs coated with varying amounts of Zr (0 %, 27% and 78%) formed the third study of this thesis [30]. It has been demonstrated in previous studies that the redox activity and thermal stability of CeO_2 NM can be enhanced by mixing them with Zr [31]. $ApoE^{-/-}$ mice were included in this study because a mutation in the APOE4 gene is the most important known genetic risk factor for developing AD. It also enabled testing of the potential susceptibility to NM-induced effects in a compromised mouse model of delayed lipoprotein clearance, hyperlipidemia and atherosclerosis with BBB leakage [32, 33]. Here, inhalation exposure to these CeO_2 NMs did not lead to an aggravated plaque formation. This was in contrast to a previous inhalation exposure study to diesel engine exhaust [34]. Moreover, unlike the oral exposure study (**Chapter 3**), inhalation exposure to CeO_2 NMs did not inhibit plaque formation in the 5xFAD mice. While this may be explained by differences in levels and duration of exposure, it also demonstrates the likely importance of the route of exposure. In contrast, exposure to the highest Zr-doped CeO_2 initiated motor performance changes in the 5xFAD and $ApoE^{-/-}$ mice. Also, in C57BL/6J mice, the identical particles increased neuroinflammation but did not affect motor coordination. Taken together, the study outcome of the third study indicates that neurotoxic

effects depend on the redox-activity of the inhaled CeO_2 NMs, although the endpoints varied among the healthy and the compromised mouse models. A future study is needed to identify the exact mechanism of inhaled CeO_2 NMs on motor performance and neuroinflammation. As it seems that the neurotoxic effects are strongly dependent on the redox state of the same NM following inhalation, it could be relevant to evaluate the potential neurotoxic effects of other types of NMs that are redox reactive, such as iron oxide (FeO_2), TiO_2, gold (Au), Ag, selenium (Se), or various nanoscale carbon NMs [35].

Translocation of NMs to the brain is considered as a critical event to understand potential neurotoxicity. The main findings of this thesis may be the result of direct NM effects on the CNS. Indeed, we were able to demonstrate Ag accumulation and slow clearance in mouse brain (**Chapter 2**), which is in accordance with a recently published study in male CD-1 (ICR) mice and 28 days of oral administration of Ag NM [36]. However, it must be emphasized that the Ag was detected by ICP-MS, a method that cannot distinguish soluble elemental Ag from nanoparticulate Ag. Moreover, as our study did not include a pharmacokinetic design for the other NMs, it is also not known to what extent these other types of NMs or their ions may have reached and accumulated in the brain of the mice. Yokel and colleagues demonstrated in a review that less than 0.1% of the deposited dose could be found in the brain following intravenous injection of various metal-based NMs like nanoceria, nanosilica and nanotitania [4] and more recently, they showed that less than 1% of inhaled NMs translocated from the lung to the rest the body and even less from the gastrointestinal tract [37]. Following oral exposure, NMs have to cross a series of biological barriers, including the gastric and intestinal milieu, the mucus barrier, the epithelial cells of the gastrointestinal tract, and finally, the BBB [38, 39]. Further toxicokinetic studies are needed to study the translocation and accumulation of NMs into the CNS, especially after the physiologically relevant exposure via food. The use of new techniques like ToF-SIMS (**Chapter 2**) should also be encouraged in such studies as an independent confirmation of the conventional methods like ICP-MS. Such new techniques could also be used to identify subregions within the brain that have increased accumulation and thus potentially display stronger toxic outcomes.

Moreover, NM neurotoxicity through indirect effects may be of importance as well. In recent years, research targeting the gut-brain axis is gaining interest [40, 41]. Thus, we further analyzed the feces of the mice from the first study (**Chapter 2**) to assess impacts on the gut microbiome and found that dietary Ag NMs can disturb the gut microbiota in a sex-dependent

manner [42]. Furthermore, a review of Liu et al. 2021 summarized that gut microbiota-derived products can disrupt BBB integrity and enter the brain and may even progress AD [43]. Thus, future studies evaluating neurotoxic or neurodegenerative endpoints upon oral exposure to NMs should consider possible effects of NMs on the gut microbiome homeostasis.

In terms of hazard and risk assessment, the main findings of this thesis indicate that TiO_2, SiO_2, or CeO_2 NMs at concentrations of up to 1% in food may not have an adverse health impact on the CNS (**Chapter 2 and 3**). In contrast, our findings with Ag NM indicate that long-term dietary exposures to this NM at 0.2% concentration in food may cause adverse effects on the CNS in a sex-dependent manner. These findings are in accordance with the literature that there are substantial differences in the toxicity of different types of NMs. As most experimental oral exposure studies were mainly performed with artificial oral gavage techniques, and the doses reported to be neurotoxic may be much higher than actual human exposure levels [1], a further study with dietary fed Ag NM at lower doses was conducted to obtain data of more realistic scenarios for risk assessment (Sofranko et al., in preparation).

Finally, in contrast to absence or neurotoxic effects, further findings of this thesis even indicated neuroprotective effects depending on the type of the NM. Surprisingly, beneficial effects on AD progression were seen in the mice fed with CeO_2 NM containing feed pellets at a concentration of 1% for 14 weeks. This exposure condition resulted in a reduced amyloid plaque accumulation and improved locomotor activity (**Chapter 3**). In contrast, CeO_2 NMs that were inhaled at an exposure concentration of 4 mg/m^3 for five days per week during a 4-week interval had no beneficial effects on AD pathology in 5xFAD mice (**Chapter 4**). While this may be explained by the duration of exposure and the dosing, it demonstrates the likely importance of the route of exposure as well. The observations with CeO_2 warrant further mechanistic studies to identify the exact underlying mechanism of dietary fed CeO_2 on amyloid plaque pathology and to unravel whether the chemical composition, the exposure route, or the duration is responsible for the absence of beneficial AD-related effects from the previous study.

In conclusion, the *in vivo* neurotoxicity studies that were performed in the framework of the thesis clearly demonstrated that neurotoxicity induced by NMs is dependent on: (1) the type of NM including physicochemical properties of the same NM, e.g., the redox state of CeO_2 NM, (2) the dose and exposure time, (3) the route of exposure, inhalation vs. oral and dietary exposure vs. gavage, (4) susceptibility of sexes and disease mouse models (see Figure 6.1). Currently, there is still a lack in neurotoxicity data of NMs, but the understanding, characterization and evaluation of the potential neurotoxicological properties of NMs are essential for human health risk assessment. The generated data of this thesis clearly indicates the need for long-term exposure studies with more realistic exposure scenarios as well as the inclusion of both sexes to identify NM-dependent neurotoxicity pathways.

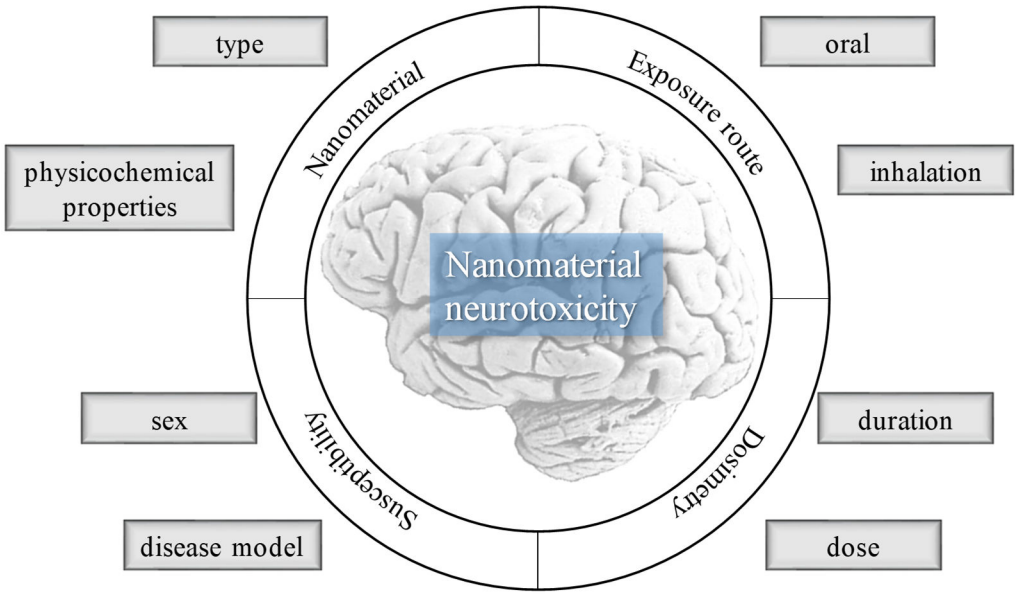

Figure 6.1: Nanomaterial (NM) neurotoxicity dependency. The results of this dissertation demonstrated that NM-induced neurotoxicity is dependent on: (1) the type of NM including physicochemical properties, (2) the exposure route, (3) the exposure dose and duration, and (4) the susceptibility of sex and disease models.

6.1 References

1. Boyes, W.K. and C. van Thriel, *Neurotoxicology of Nanomaterials.* Chemical research in toxicology, 2020. **33**(5): p. 1121-1144.
2. Wu, J., et al., *Neurotoxicity of Silica Nanoparticles: Brain Localization and Dopaminergic Neurons Damage Pathways.* ACS Nano, 2011. **5**(6): p. 4476-4489.
3. Liu, Y., et al., *Oxidative stress and acute changes in murine brain tissues after nasal instillation of copper particles with different sizes.* J Nanosci Nanotechnol, 2014. **14**(6): p. 4534-40.
4. Yokel, R., E. Grulke, and R. MacPhail, *Metal-based nanoparticle interactions with the nervous system: the challenge of brain entry and the risk of retention in the organism.* Wiley Interdiscip Rev Nanomed Nanobiotechnol, 2013. **5**(4): p. 346-73.
5. Bencsik, A., P. Lestaevel, and I. Guseva Canu, *Nano- and neurotoxicology: An emerging discipline.* Progress in Neurobiology, 2018. **160**: p. 45-63.
6. Rubinsztein, D.C., *The roles of intracellular protein-degradation pathways in neurodegeneration.* Nature, 2006. **443**(7113): p. 780-6.
7. Bredesen, D.E., R.V. Rao, and P. Mehlen, *Cell death in the nervous system.* Nature, 2006. **443**(7113): p. 796-802.
8. *2020 Alzheimer's disease facts and figures.* Alzheimer's & Dementia, 2020. **16**(3): p. 391-460.
9. Sharma, V.K., et al., *Apoptotic Pathways and Alzheimer's Disease: Probing Therapeutic Potential.* Neurochemical Research, 2021.
10. Calderón-Garcidueñas, L., et al., *Early Alzheimer's and Parkinson's Disease Pathology in Urban Children: Friend versus Foe Responses—It Is Time to Face the Evidence.* BioMed Research International, 2013. **2013**: p. 161687.
11. Serrano-Pozo, A. and J.H. Growdon, *Is Alzheimer's Disease Risk Modifiable?* Journal of Alzheimer's disease : JAD, 2019. **67**(3): p. 795-819.
12. Calderón-Garcidueñas, L., et al., *Brain inflammation and Alzheimer's-like pathology in individuals exposed to severe air pollution.* Toxicol Pathol, 2004. **32**(6): p. 650-8.
13. Calderón-Garcidueñas, L., et al., *Reduced repressive epigenetic marks, increased DNA damage and Alzheimer's disease hallmarks in the brain of humans and mice exposed to particulate urban air pollution.* Environmental Research, 2020. **183**: p. 109226.
14. Calderón-Garcidueñas, L., et al., *Alzheimer disease starts in childhood in polluted Metropolitan Mexico City. A major health crisis in progress.* Environmental Research, 2020. **183**: p. 109137.
15. FDA, *Title 21 - Food and Drugs, Part 73: LISTING OF COLOR ADDITIVES EXEMPT FROM CERTIFICATION*, U.S.F.a.D. Administration, Editor. 2020: https://www.govinfo.gov/content/pkg/CFR-2020-title21-vol1/pdf/CFR-2020-title21-vol1-sec73-575.pdf. p. 447-448.
16. Additives, E.P.o.F. and F. Nutrient Sources added to, *Scientific opinion on the re-evaluation of silver (E 174) as food additive.* EFSA Journal, 2016. **14**(1): p. 4364.
17. Sofranko, A., et al., *Evaluation of the neurotoxic effects of engineered nanomaterials in C57BL/6J mice in 28-day oral exposure studies.* NeuroToxicology, 2021. **84**: p. 155-171.
18. OECD, *Test No. 424: Neurotoxicity Study in Rodents*. 1997.
19. Grosshans, D.R. and M.D. Browning, *Protein kinase C activation induces tyrosine phosphorylation of the NR2A and NR2B subunits of the NMDA receptor.* J Neurochem, 2001. **76**(3): p. 737-44.
20. Ziemińska, E., A. Stafiej, and L. Strużyńska, *The role of the glutamatergic NMDA receptor in nanosilver-evoked neurotoxicity in primary cultures of cerebellar granule cells.* Toxicology, 2014. **315**: p. 38-48.

21. Dąbrowska-Bouta, B., et al., *Early and Delayed Impact of Nanosilver on the Glutamatergic NMDA Receptor Complex in Immature Rat Brain.* Int J Mol Sci, 2021. **22**(6).
22. Tariba Lovaković, B., et al., *Sex-related response in mice after sub-acute intraperitoneal exposure to silver nanoparticles.* NanoImpact, 2021. **23**: p. 100340.
23. Hardy, J.A. and G.A. Higgins, *Alzheimer's disease: the amyloid cascade hypothesis.* Science, 1992. **256**(5054): p. 184-5.
24. Oakley, H., et al., *Intraneuronal beta-amyloid aggregates, neurodegeneration, and neuron loss in transgenic mice with five familial Alzheimer's disease mutations: potential factors in amyloid plaque formation.* J Neurosci, 2006. **26**(40): p. 10129-40.
25. Sultana, R. and D.A. Butterfield, *Role of oxidative stress in the progression of Alzheimer's disease.* J Alzheimers Dis, 2010. **19**(1): p. 341-53.
26. Esch, F., et al., *Electron Localization Determines Defect Formation on Ceria Substrates.* Science, 2005. **309**(5735): p. 752-755.
27. Estevez, A.Y., et al., *Neuroprotective mechanisms of cerium oxide nanoparticles in a mouse hippocampal brain slice model of ischemia.* Free Radic Biol Med, 2011. **51**(6): p. 1155-63.
28. Rzigalinski, B.A., C.S. Carfagna, and M. Ehrich, *Cerium oxide nanoparticles in neuroprotection and considerations for efficacy and safety.* Wiley interdisciplinary reviews. Nanomedicine and nanobiotechnology, 2017. **9**(4): p. 10.1002/wnan.1444.
29. Eleftheriadou, D., et al., *Redox-Responsive Nanobiomaterials-Based Therapeutics for Neurodegenerative Diseases.* Small, 2020. **16**(43): p. e1907308.
30. Wahle, T., et al., *Evaluation of neurological effects of cerium dioxide nanoparticles doped with different amounts of zirconium following inhalation exposure in mouse models of Alzheimer's and vascular disease.* Neurochemistry International, 2020. **138**: p. 104755.
31. Devaraju, M.K., et al., *Solvothermal synthesis and characterization of ceria-zirconia mixed oxides for catalytic applications.* Nanotechnology, 2009. **20**(40): p. 405606.
32. Methia, N., et al., *ApoE deficiency compromises the blood brain barrier especially after injury.* Mol Med, 2001. **7**(12): p. 810-5.
33. Verghese, P.B., J.M. Castellano, and D.M. Holtzman, *Apolipoprotein E in Alzheimer's disease and other neurological disorders.* The Lancet Neurology, 2011. **10**(3): p. 241-252.
34. Hullmann, M., et al., *Diesel engine exhaust accelerates plaque formation in a mouse model of Alzheimer's disease.* Particle and Fibre Toxicology, 2017. **14**: p. 35.
35. Sims, C.M., et al., *Redox-active nanomaterials for nanomedicine applications.* Nanoscale, 2017. **9**(40): p. 15226-15251.
36. Recordati, C., et al., *Repeated oral administration of low doses of silver in mice: tissue distribution and effects on central nervous system.* Particle and Fibre Toxicology, 2021. **18**(1): p. 23.
37. Yokel, R.A., et al., *The Yin: An adverse health perspective of nanoceria: uptake, distribution, accumulation, and mechanisms of its toxicity.* Environmental science. Nano, 2014. **1**(5): p. 406-428.
38. Oberdörster, G., E. Oberdörster, and J. Oberdörster, *Concepts of nanoparticle dose metric and response metric.* Environ Health Perspect, 2007. **115**(6): p. A290.
39. Kreyling, W.G., et al., *Age-Dependent Rat Lung Deposition Patterns of Inhaled 20 Nanometer Gold Nanoparticles and their Quantitative Biokinetics in Adult Rats.* ACS Nano, 2018. **12**(8): p. 7771-7790.
40. Zhang, S., et al., *Titanium dioxide nanoparticles via oral exposure leads to adverse disturbance of gut microecology and locomotor activity in adult mice.* Archives of Toxicology, 2020. **94**(4): p. 1173-1190.

41. Morais, L.H., H.L.t. Schreiber, and S.K. Mazmanian, *The gut microbiota-brain axis in behaviour and brain disorders.* Nat Rev Microbiol, 2021. **19**(4): p. 241-255.
42. Bredeck, G., et al., *Effects of dietary exposure to the engineered nanomaterials CeO(2), SiO(2), Ag, and TiO(2) on the murine gut microbiome.* Nanotoxicology, 2021. **15**(7): p. 934-950.
43. Liu, S., et al., *Microbiota-gut-brain axis and Alzheimer's disease: implications of the blood-brain barrier as an intervention target.* Mech Ageing Dev, 2021: p. 111560.

7 Eidesstattliche Erklärung

Ich versichere an Eides Statt, dass die Dissertation von mir selbständig und ohne unzulässige fremde Hilfe unter Beachtung der „Grundsätze zur Sicherung guter wissenschaftlicher Praxis an der Heinrich-Heine-Universität Düsseldorf“ erstellt worden ist. Die vorliegende Arbeit wurde von mir selbständig verfasst und keine anderen als die angegebenen Hilfsmittel verwendet. Alle wörtlich oder inhaltlich übernommenen Stellen habe ich als solche gekennzeichnet. Zudem versichere ich, dass ich die vorliegende Dissertation nur in diesem und keinem anderen Promotionsverfahren eingereicht habe und diesem kein früheres Promotionsverfahren vorausgegangen ist.

Düsseldorf, im Oktober 2021

_____

Adriana Sofranko